PEOPLE, INSTITUIONS, AND PIXELS: LINKING REMOTE SENSING AND SOCIAL SCIENCE TO UNDERSTAND SOCIAL ADAPTATION TO ENVIRONMENTAL CHANGE

by

Jun Wang

A dissertation submitted in partial fulfillment
of the requirements for the degree of
Doctoral of Philosophy
(Natural Resources and Environment)
in The University of Michigan
2013

Doctoral Committee:

Professor Daniel G. Brown, Chair
Professor Arun Agrawal
Associate Research Scientist Kathleen M. Bergen
Professor Scott E. Page
Associate Research Scientist Rick L. Riolo

Dedication

To the memory of my grandfathers

Acknowledgements

The maple trees outside my office window have had their four phenologic cycles since I moved here. It is time that makes me grow, and I have been getting confident intellectually through learning, thinking, and working day and night over the past four years. The completion of the doctoral degree is built on the support and help from many people. I am grateful to my advisor Dr. Daniel Brown, who provided a broad platform for me to play on and challenged and mentored me over the years. Dr. Brown always tried to train me to be a professional scholar and scientist, and he trained me in every way.

I also deeply appreciate the mentoring and help from my dissertation committee advisors: Dr. Arun Agrawal, Dr. Rick Riolo, Dr. Scott Page, and Dr. Kathleen Bergen. Dr. Agrawal made me understand more about institutions and human dimensions of environmental problems. His sage comments in every meeting I will always remember. Dr. Riolo introduced me to the field of complex adaptive systems. His patience and generosity to students and his insightful comments and advice I will always appreciate. I read the three books written by Dr. Page, which made me finally understand complex adaptive systems. His sharp and constructive comments in every committee meeting made me to rethink my work and improve the quality of my dissertation. Dr. Bergen helped me understand more about remote sensing. Her seriousness to science and dedication to research always made me admire.

I would like to thank Dorit Hammerling, a good classmate. She is almost a doctor now. Dorit helped me finally understand geostatistics. Dr. Vineet Yadav also helped me solve some technical problems in geostatistics. I also would like to acknowledge people in the Environmental Spatial Analysis Lab at the School of Natural Resources and Environment, and they helped me to grow up intellectually and socially. Some of my work wouldn't have been possible without contributions from them. I will always appreciate this. Many people on the NASA funded Mongolian project helped me to finish my work, and some of them I do not even

know their names. I would like to acknowledge the help from Dr. Yongfei Bai from the Institute of Botany, Chinese Academy of Sciences, Professor Qi Xing from the Inner Mongolian Grassland Survey and Design Institute, and grassland scientists from the Institute of Botany, Mongolian Academy of Sciences. They made great contributions to field data collections for the project.

It has been 23 years since the day my mother took me to the pre-school. I have never been out of school since then. Many things could happen in 23 years, but sometimes I feel it was just like yesterday. This dissertation is dedicated to the memory of my grandfathers. I always feel disappointed that they were not able to see me graduate with my final degree. Their love, encouragement, and expectation will be with me forever. Finally, I would like to thank my professors and mentors in China. They led me to the field of Geography. Their words sometimes like a light beam in the dark when I feel I lose my way. My years at the University of Michigan, Ann Arbor, are memories that will be cherished by me forever.

Table of Contents

Dedication……..ii
Acknowledgements……...iii
List of Tables……...……ix
List of Figures……...……x
Abstract……...……xiii

PART I — INTROCUTION……...1

Chapter One

Analyzing Sustainability of Social-Ecological Systems on the Mongolian Plateau: An Interdisciplinary Approach……2

1.1 Research Motivation……...……2
1.2 Frameworks, Theories, and Methods……...……4
1.3 Research Objectives and Dissertation Outline……7

PART II — REMOTE SENSING OF GRASSLAND ECOSYSTEMS……11

Chapter Two

Dynamics of Net Primary Productivity in the Mongolian Grasslands (1982−2009) in Response to Climate Variability and Change.....12

Abstract……...……12
2.1 Introduction……...……13
2.2 Study Area and Data……..14
2.2.1 Study Area……14
2.2.2 Remotely Sensed Data……...15
2.2.3 Ecological and Climate Data……16
2.3 Methods……...……17
2.3.1 Integrating GIMMS AVHRR NDVI and Terra MODIS NDVI……...……17
2.3.2 Estimating Annual NPP of the Mongolian Grasslands (1982-2009)……18
2.3.3 Spatial Predictions of Grassland NPP by Universal Kriging……23
2.3.4 Analyzing the Changes of NPP and Their Relationships with Climate……26
2.4 Results……27
2.4.1 Evaluations of the Estimated Grassland NPP……...…27
2.4.2 The Interannual Variability of Grassland NPP……...……29
2.4.3 The Temporal Trends of Grassland NPP……...……30
2.4.4 The Relationship between NPP and Climate……32
2.5 Discussion……..33
Acknowledgements……..35

Chapter Three

Estimating the Quantity and Quality of Grassland Communities across an Ecological Gradient of the Inner Mongolian Grasslands with *In Situ* Hyperspectral Remote Sensing……...…….36

Abstract……...…….36
3.1 Introduction……...…….37
3.2 Study Area and Data……..40
3.2.1 Study Area……....40
3.2.2 Field Data Collection……41
3.3 Methods……..42
3.3.1 Preprocessing *In Situ* Hyperspectral Data……42
3.3.2 Vegetation Indices, Red-Edge Inflection Points, and Aboveground Biomass Prediction…….43
3.4 Results……...…….47
3.4.1 Ecological Variables of the Investigated Plant Communities ……..……47
3.4.2 Canopy Reflectance Curves of the Investigated Plant Communities ……...49
3.4.3 Optimal Narrowband Vegetation Indices……..53
3.4.4 Linear Relationships between Hyperspectral Indices and Aboveground Biomass……...56
3.5 Discussion……...57
3.6 Conclusions……59
Acknowledgements……..60

PART III — INTERPRETATIONS OF GRASSLAND DYNAMICS…….61

Chapter Four

Sustainable Governance of the Mongolian Grasslands: Comparing Ecological and Social-Institutional Changes in Mongolia and Inner Mongolia, China……62

Abstract……...……62
4.1 Introduction……63
4.2 Explanatory Models of Grassland Dynamics……65
4.3 Analyses and Results……67
4.3.1 Collectivization of Pastures and Livestock……69
4.3.2 Privatization and Market Incentives……..72
4.3.3 Recentralization of Grassland Management in IMAR, China……...74
4.3.4 Changing Roles of the State, Market, and Community for Grassland Management…….75
4.3.5 Climate Variability and Change: History and Future……...…….76
4.4 Discussion……..77
4.5 Conclusions……81
Acknowledgements……..……82

Chapter Five

Drivers of the Dynamics in Net Primary Productivity across Agro-Ecological Zones of Mongolia and Inner Mongolia, China……...83

Abstract……...……83
5.1 Introduction……84
5.2 Study Area and Data……..88
5.2.1 Study Area……88
5.2.2 Time-series of Annual NPP……...……89

5.2.3 Climate and Socioeconomic Data……..…90
5.3 Methods……..90
5.3.1 Mapping Agro-ecological Zones of the Mongolian Grasslands……...…….90
5.3.2 Modeling the Drivers of NPP Dynamics with Spatial Panel Data Models……...……91
5.4 Results……...…….95
5.4.1 Correlations between NPP and Explanatory Variables…….95
5.4.2 Drivers of NPP Dynamics across Agro-ecological Zones…….98
5.5 Discussion……101
Acknowledgements……104

PART IV — SOCIAL ADAPTATION TO ENVIRONMENTAL CHANGE……...105

Chapter Six

Climate Adaptation, Local Institutions, and Rural Livelihoods: A Comparative Study of Herder Communities in Mongolia and Inner Mongolia, China……106

Abstract……..……106
6.1 Introduction……..107
6.2 Study Area and Data……110
6.2.1 Study Area……...110
6.2.2 Household Survey……112
6.3 Methods……114
6.3.1 Descriptive Analyses of Livelihood Adaptation Strategies……114
6.3.2 Modeling Fodder Purchasing Behaviors of Herders……114
6.4 Results……..119
6.4.1 Local Institutions and Climate Adaptation……..119
6.4.2 Determinants of Fodder Purchasing Behaviors……...……124
6.5 Discussion……...…….129
Acknowledgements……...……132

Chapter Seven

Exploring the Role of Local Institutions in Adaptation to Environmental Change in the Semiarid and Arid Mongolian Grasslands: An Agent-Based Modeling Approach……..……..…133

Abstract……..133
7.1 Introduction……..134
7.2 Empirical Background……137
7.3 The Conceptual Agent-Based Model……...…139
7.3.1 The Agent Landscape and Agents……...……139
7.3.2 Sedentary Grazing…….……...142
7.3.3 Pasture Rental Markets……143
7.3.4 Reciprocal Use of Pastures……..144
7.3.5 The Free-Rider Problem in Cooperation……145
7.4 Computational Experiments……146
7.4.1 The Social-Ecological Performance of Alternative Resource Institutions……..146
7.4.2 Social Mechanisms for Promoting Cooperation……..147
7.4.3 Social Mechanisms for Maintaining Cooperation……...148
7.5 Results……..……149
7.5.1 The Importance of Cooperation in Climate Adaptation…….……....149

7.5.2 Effects of Agent Diversity and Social Norms on Promoting Cooperation……..151
7.5.3 Solving the Free-Rider Problem in Cooperation……153
7.6 Discussion……154
7.7 Conclusions……..156
Acknowledgements……..……156

PART V — CONCLUSIONS……..157

Chapter Eight

Synthesis……..……158
8.1 Conclusions……..159
8.1.1 Remote Sensing of the Mongolian Grasslands……...…….159
8.1.2 Interpretations of Grassland Dynamics……160
8.1.3 Social Adaptation to Climate Change and Grassland Degradation……162
8.2 Research Limitations and Future Directions……163
8.2.1 Remote Sensing of Grassland Ecosystems……..163
8.2.2 People, Institutions, and Pixels……164
8.2.3 Modeling Sustainability of Social-Ecological Systems……...165
8.2.4 Scale, Uncertainty, and Error Propagations…….……166

Appendix A: Geostatistical Inverse Modeling for Super-Resolution Mapping of Continuous Spatial Processes……...168

References……..194

List of Tables

Table 2.1 The coefficients of the linear regressions used for adjusting AVHRR NDVI (1982-1999) to MODIS NDVI……..18

Table 2.2 The proportions of the six land-covers over the five time periods……..20

Table 2.3 The comparisons of grassland NPP in Inner Mongolia estimated in this study with the results of other studies…….34

Table 3.1 Dominant plant species of the investigated plant communities ……48

Table 3.2 Descriptive statistics of the ecological parameters for the investigated plant communities…...48

Table 3.3 The REIP of reflectance for the sites in meadow steppe with fenced and grazed plot pairs…..53

Table 3.4 The optimal red and NIR band combinations for predicting AGB in meadow, typical, and desert steppes……...56

Table 3.5 The results of linear regressions between hyperspectral indices and AGB in meadow, typical, and desert steppes…….57

Table 4.1 Amounts of grassland area reclaimed in IMAR (1949–2005) (Unit: 1,000,000 hectares)…….72

Table 5.1 Variables for the static and dynamic spatial panel data models…….....95

Table 5.2 Static spatial panel data models for NPP dynamics using normalized variables……99

Table 5.3 Dynamic spatial panel data models for NPP dynamics using normalized variables……100

Table 5.4 Pseudo-R^2 values of static spatial panel data models for NPP dynamics: iteratively removing the independent variables to show their explanatory power……..100

Table 5.5 Pseudo-R^2 values of dynamic spatial panel data models for NPP dynamics: iteratively removing the independent variables to show their explanatory power……..101

Table 6.1 The socioeconomic and biophysical variables measured at the household and village/soum levels…….…117

Table 6.2 The livelihood adaptation strategies of the surveyed herder households in Mongolia and IMAR, China (2000−2009)……122

Table 6.3 The estimates of the effects of biophysical and socioeconomic variables on the percentage of degraded pastures within the surveyed villages/soums……..125

Table 6.4 The estimations of the determinants for the livelihood adaptation behaviors of purchasing fodder and hay……128

Table 7.1 The values of the major parameters of the agent-based model…….141

List of Figures

Fig. 2.1 The study area. Note: the background image is the 1-km resolution MODIS NDVI in the second half of August, 2009. IMGERS is the abbreviation of the Inner Mongolian Grassland Ecosystem Research Station, China……...15

Fig. 2.2 The field ecological sampling sites and the vegetation maps of 2009: (a) Ewenke county, meadow steppe; (b) Xilinhot county, typical steppe; (c) Wulatezhong county, desert steppe. The three sites are corresponding to sites A, B, and C in Fig. 2.1……...17

Fig. 2.3 The major land-cover types on the Mongolian plateau. The vegetation maps of IMAR (1990s) and Mongolia (1980s) were provided by the Institutes of Botany in China and Mongolia, respectively. The original scale of the two vegetation maps is 1:1,000,000. The ecological sampling sites in IMAR are the long-term ecological observation sites, which are managed by Chinese Academy of Sciences……...21

Fig. 2.4 The comparisons between estimated NPP by the LUE model and spatially predicted NPP by UK in the three evaluation sites of IMAR: (a) Ewenke county, meadow steppe; (b) Xilinhot county, typical steppe; (c) Wulatezhong county, desert steppe……28

Fig. 2.5 The comparisons between the estimated annual NPP ($g \cdot C \cdot m^{-2} \cdot year^{-1}$) by the light-use efficiency (LUE) model and ground measured biomass ($g \cdot C \cdot m^{-2}$) at IMGERS (1982−2003)…….29

Fig. 2.6 (a) mean annual NPP ($g \cdot C \cdot m^{-2} \cdot year^{-1}$) (1982−2009); (b) the interannual variability of NPP in Period 1 (1982−1990); (c) the interannual variability of NPP in Period 2 (1991−1999); and (d) the interannual variability of NPP in Period 3 (2000−2009)…….30

Fig. 2.7 Temporal trends of NPP ($g \cdot C \cdot m^{-2} \cdot year^{-1}$) (1982−2009) in (a) spring, (b) summer, (c) overall growing season, and (d) three grassland types of IMAR and Mongolia; IMAR_M, IMAR_T, IMAR_D, Mongolia_M, Mongolia_T, and Mongolia_D denote meadow, typical, and desert steppes in IMAR and Mongolia, respectively…….31

Fig. 2.8 Relationships between the interannual variability of NPP (NPP-CV) and precipitation: **a** NPP-CV and the mean precipitation per half-annum (MPHA); **b** NPP-CV and the interannual variability of precipitation (precipitation-CV)……...32

Fig. 2.9 The correlations between NPP and climate: (a) NPP−temperature and (b) NPP−precipitation (January-July; 1982−2009)……..33

Fig. 3.1 Field sampling sites across the ecological gradient of the Inner Mongolian grasslands. The vegetation map of Inner Mongolia, China, was provided by the Institute of Botany, China. It was made in the 1990s with an original scale of 1:1,000,000……..41

Fig. 3.2 The normalized canopy reflectance curves and their first-order derivatives of the investigated grassland communities: (a), (c), and (e) are the normalized reflectance curves in meadow, typical, and desert steppes; (b), (d), and (f) are the first-order derivatives of (a), (c), and (e). In each plot, there were measurements from at least 12 subplots (120 measurements) used for spectral averaging. In order to make the reflectance curves more readable, standard deviation bars were not added on the plots……...50

Fig. 3.3 The normalized canopy reflectance curves and their first-order derivatives of the field sites with fenced and grazed plot pairs: (a), (c), and (e) are the normalized reflectance curves; (b), (d), and (f) are the first-order derivatives of (a), (c), and (e). In each plot, there were measurements from at least 12 subplots (120 measurements) used for spectral averaging. In order to make the reflectance curves more readable, standard deviation bars were not added on the plots……...52

Fig. 3.4 The correlation plots representing the coefficient of determination (R^2) of the linear relationships between VI and AGB, calculated from all possible combinations spread across red and NIR bands: (a), (b), and (c) are the R^2 for the regressions between SR and AGB in meadow, typical, and desert steppes, respectively; (d), (e), and (f) are the R^2 values for the regressions between NDVI and AGB in meadow, typical, and desert steppes, respectively; and (g), (h), and (i) are the R^2 for the regressions between SAVI and AGB in meadow, typical, and desert steppes, respectively……..56

Fig. 4.1 Spatial distributions of the major vegetation types on the Mongolian plateau. Source: vegetation maps of IMAR and Mongolia were respectively provided by the Institute of Botany, China, and the Institute of Botany, Mongolia. They were made respectively in the 1990s and 1980s. The original scale of the two vegetation maps is 1:1,000,000……...68

Fig. 4.2 Changes of the average grassland biomass of IMAR and Mongolia over the past fifty years. Source: the data of IMAR was provided by the Inner Mongolian Institute of Grassland Survey and Design (IMIGSD, 2011) and the data of Mongolia was reconstructed from Olonbayar, 2010……...68

Fig. 4.3 Changes of livestock numbers in IMAR, China, (a) and Mongolia (b) (1961–2009) (Unit: 10,000). Source: Annual census books of IMAR, China, and Mongolia (ACBIMAR, 2005, 2010; ACBM, 1990, 2010)……70

Fig. 4.4 Demographic changes in IMAR, China, (a) and Mongolia (b) (1961–2009) (Unit: 10,000). Source: Annual census books of IMAR, China, and Mongolia (ACBIMAR, 2005, 2010; ACBM, 1990, 2010)……71

Fig. 4.5 Changes of the prices of livestock products in IMAR (Unit: 1000 Yuan/Tonne) (a) and Mongolia (Unit: 1000 MNT/Tonne) (b) (1991–2007). The historical prices from the Food and Agriculture Organization (FAO) were adjusted to constant 1991 currency. Source: FAO price statistics database (FAO, 2011)……....73

Fig. 4.6 The temporal variability of annual mean temperature (Unit: °C) (a) and annual precipitation (Unit: mm) (b) in IMAR and Mongolia with multi-year means and five-year moving averages (1961–2009). Source: national standard climate stations of IMAR, China, and Mongolia (CIMAR, 2011; CM, 2011)..77

Fig. 5.1 Spatial distributions of the major land-cover types on the Mongolian plateau. Source: vegetation maps of IMAR and Mongolia were respectively provided by the Institute of Botany, China, and the Institute of Botany, Mongolia. They were made in the 1990s and 1980s, respectively. The original scale of the two vegetation maps was 1:1,000,000……...89

Fig. 5.2 Spatial heterogeneity of grassland social-ecological systems in Mongolia and IMAR, China…..91

Fig. 5.3 Temporal correlations between NPP and explanatory variables in counties of IMAR (1986−2007) and provinces of Mongolia (1995−2009): (a) NPP–temperature in Mongolia; (b) NPP–precipitation in Mongolia; (c) NPP–livestock populations in Mongolia; (d) NPP–human populations in Mongolia; (e) NPP–temperature in IMAR; (f) NPP–precipitation in IMAR; (g) NPP–livestock populations in IMAR; (h) NPP–grain output in IMAR; (i) NPP–human populations in IMAR……...97

Fig. 5.4 Values of the spatial fixed effects for the static spatial panel data models of NPP dynamics: (a) Mongolia; (b) IMAR……99

Fig. 6.1 The framework of adaptation, institutions, and livelihoods (adapted from Agrawal, 2009)…...108

Fig. 6.2 The major vegetation types on the Mongolian plateau (shaded colors) and the locations of surveyed herder households (red dots). The vegetation maps of Mongolia and IMAR were made by the Institute of Botany, Mongolia (1980s), and the Institute of Botany, China (1990s), respectively. The original scale of the two vegetation maps was 1:1,000,000……...112

Fig. 6.3 Income (a) and expenditure (b) structures of IMAR and Mongolia. IM_M, IM_T, IM_D, MG_M, MG_T, and MG_D means the study sites in meadow, typical, and desert steppes of IMAR and Mongolia, respectively……124

Fig. 6.4 A Landsat-5 satellite image covering the border between China and Mongolia. The area covers one of the six case study sites for the household surveys (the site in northeastern Mongolia; Fig. 6.2). Lakes are black and dark blue. Areas with the most vegetation are red. Greens and grays indicate intermediate amount of vegetation, and pale and white areas are sandy and bare earth……125

Fig. 7.1 Major vegetation types (shaded color) and the surveyed herder households (red dots) in the Mongolian grasslands. Vegetation maps of Mongolia and Inner Mongolia were made by the Institutes of Botany, Mongolia (1980s) and China (1990s), respectively……139

Fig. 7.2 The conceptual agent-based model of resource institutions……142

Fig. 7.3 Snapshots of the experiments for the three institutional scenarios. (a) sedentary grazing. (b) pasture rental markets. (c) reciprocal use of pastures. The green blocks were the parcels not hit by drought; the blue blocks in (a) were the parcels hit by drought; the blue blocks in (b) were the parcels hit by drought, and the agents did not find parcels to migrate to; the red blocks in (b) were the parcels hit by drought, and the agents found parcels to migrate to; the red blocks in (c) were cooperators……150

Fig. 7.4 The social-ecological performance of four institutional scenarios under different conditions of drought probability. (a) the average net benefit of agents. (b) the number of undegraded parcels……...150

Fig. 7.5 Sensitivity analyses of the parameters related to the organization cost of cooperation and the increasing rate of cooperation benefit for the institutional scenario of reciprocal use of pastures. (a) the average net benefit of agents; and (b) the number of undegraded parcels in the agent world……...151

Fig. 7.6 The social-ecological performance of reciprocal use of pastures with agent diversity and neighborhood effects included in the model. (a) the average net benefit of agents. (b) the number of undegraded parcels. Baseline means the baseline scenario; Diversity means the scenario of agent diversity; and for the scenarios related to neighborhood effects, the neighborhood parameter was changed from 75% (N_75%) to 50% (N_50%) and 25% (N_25%). The error bars represent one standard deviation……152

Fig. 7.7 Sensitivity analyses of the parameters related to the organization cost of cooperation and the increasing rate of cooperation benefit for the institutional scenario of reciprocal use of pastures with the mechanism of agent diversity included in the model. (a) the average net benefit of agents; and (b) the number of undegraded parcels in the agent world……152

Fig. 7.8 The social-ecological performance of reciprocal use of pasture with the kinship mechanism included in the model. (a) the average net benefit of agents. (b) the number of undegraded parcels. The error bars represent one standard deviation……...153

Fig. 7.9 The social-ecological performance of reciprocal use of pasture with the punishment mechanism included in the model. (a) the average net benefit of agents. (b) the number of undegraded parcels. The error bars represent one standard deviation……...154

Abstract

Understanding social-ecological systems precedes studying solutions to natural resource problems. This research presents an interdisciplinary approach, which links theories from grassland ecology and institutional economics and methods from remote sensing, field ecological measurements, household survey, statistical modeling, and agent-based computational modeling, to study the dynamics of grassland social-ecological systems on the Mongolian plateau, including Mongolia and Inner Mongolia Autonomous Region, China, and social adaptation to climate change and ecosystem degradation. A range of research questions in the fields of remote sensing of vegetation, drivers and mechanisms of resource dynamics, and societal adaptation to environmental change were addressed at regional and local scales.

This dissertation includes three research objectives: (1) monitoring grassland ecosystems at regional and local scales using remote sensing; (2) interpreting the dynamics of grassland productivity on the Mongolian plateau; and (3) studying social adaptation to climate change and grassland degradation. First, using a remote sensing based light-use efficiency model, I estimated annual grassland net primary productivity on the Mongolian plateau over the past three decades and analyzed the spatial-temporal dynamics of grassland net primary productivity in response to climate variability and change. In order to account for the insufficiency of using multispectral coarse resolution images to monitor grassland dynamics, especially grassland degradation, I analyzed the potential for using hyperspectral remote sensing to detect the quantity and quality of dominant grassland communities across ecological gradients of the Inner Mongolian grasslands, based on a sampling of field conditions across a large geographic area.

Second, I linked the patterns of the dynamics in grassland productivity with biophysical and social variables. I drew on theories from grassland ecology and institutional economics to interpret the broad determinants of dynamics in grassland productivity, and used a hybrid state-market-community framework to present a new interpretation of differences in the dynamics of

grassland productivity over the past five decades in China and Mongolia, based on grassland, demographic, socioeconomic, and climate data. In addition to qualitative analyses, I used spatial panel data models to identify the biophysical and socioeconomic factors driving the interannual dynamics of grassland net primary productivity across agro-ecological zones on the Mongolian plateau over the past three decades. The results showed that the major drivers of NPP dynamics vary across agro-ecological zones and between the two political regions. The heterogeneous drivers indicated the necessity of institutional diversity for sustainable governance of grassland resources.

Third, social adaptation to environmental change was studied at both the household and community levels. The documented increases in climate variability and the deterioration of grassland productivity have increased livelihood vulnerability of the natural resource dependent herders on the Mongolian plateau. A household survey was designed to understand livelihood adaptation strategies adopted by local herders over the past ten years, and implemented in each of three grassland types in Mongolia (210 households in seven soums/towns) and China (541 households in 15 villages). Based on the rich field data, I analyzed livelihood adaptation strategies of the surveyed herder households and associated local institutions, which facilitated herders' livelihood adaptation behaviors. Hierarchical linear models, which I used to diagnose the determinants of fodder-purchasing behavior as a frequently cited adaptation, revealed that resource institutional factors, climate variability, and household financial capital were the dominant factors associated with livelihood adaptation strategies of the surveyed households.

Local institutions played the central role in shaping and facilitating livelihood adaptation behaviors of herders in the Mongolian grasslands. Based on an agent-based model informed by empirical studies, I analyzed the social-ecological performance of alternative resource institutions and their combinations. I also explored effective social mechanisms for promoting and maintaining cooperation among herders. The results showed that under certain conditions resource institutions that can facilitate cooperative use of pastures generated better social-ecological performance than the performance of sedentary grazing. Agent diversity and social norms were important for promoting cooperation among herders. Social structures and governmental regulations were important for solving the free-rider problem and maintaining

cooperation. The results implied that relaxing state-control related management strategies and allowing herders to form cooperative arrangements are effective ways to improve social-ecological outcomes of pasture-use; and governmental support is also important for promoting and maintaining self-organized resource institutions.

PART I

INTRODUCTION

Chapter One

Analyzing Sustainability of Social-Ecological Systems on the Mongolian Plateau: An Interdisciplinary Approach

1.1 Research Motivation

Terrestrial vegetation performs pivotal roles in socio-ecological systems. Grasslands occupy about 40% of the earth's terrestrial surface (and 38% of the Asian continent) and are generally characterized by single-stratum vegetation structures dominated by grasses and other herbaceous plants (Brown and Thorpe, 2008). Livestock graze on nearly all available grasslands, and managed grazing occupies about 25% of the terrestrial surface (Asner et al., 2004). The Mongolian plateau is part of the larger central Asian plateau, covering approximately 2.6 million km^2. It is occupied by Mongolia in the northwest and Inner Mongolian Autonomous Region (IMAR), China, in the southeast. Grasslands are the dominant ecosystem types there. About 66% of the total land in IMAR (0.78 million km^2) is classified as grasslands, which is a quarter of all Chinese grasslands (Zhang, 1992). Nearly 84% of the total territory in Mongolia (1.26 million km^2) is covered by grasslands (Angerer et al., 2008). As relatively intact terrestrial ecosystems, they play significant roles in sequestrating carbon dioxide, conserving biodiversity, and providing livelihood benefits to herders (Chapter Four).

The Mongolian grasslands have supported millions of pastoralists over the past thousands of years, and it is expected to provide goods and services for regional development as well as exports. Recent studies show that grasslands in IMAR and Mongolia have degraded to varying degrees; the degradation status in IMAR is more serious than in Mongolia (Angerer et al., 2008; Jiang et al., 2006). From the early 1960s to 2010, the average grassland biomass productivities in IMAR and Mongolia had decreased from 1871 to 900 kg/ha and from 804 to 369 kg/ha, respectively (IMIGSD, 2011; IOB, Mongolia, 2011). Grassland degradation has undermined ecosystem services they generated and endangered the livelihoods of local herders. The

sustainability of grassland social-ecological systems has become a major ecological, economic, and social issue on there, especially in the context of climate change.

Climate on the Mongolian plateau is continental with extremely cold winters and warm summers. Droughts and heavy winter snowstorms (*Dzuds*) are the two major climate disasters there. Over the past half century, climate there has become warmer and drier (Chapter Four). The number of droughts increased significantly in Mongolia over the last 60 years, particularly in the last decade (NCRM, 2009). The worst *Dzuds* that Mongolia experienced recently were in the consecutive summers and winters of 1999, 2000, 2001, and 2002, which affected 50–70% of the territory. About 35% (12 million) of livestock population perished in that period. The 2010 *Dzud* was the worst ever, resulting in the death of about 8.5 million livestock or 20% of the 2009 national livestock population in Mongolia (Vernooy, 2011). The adverse climate affects grassland productivity as well as grassland degradation. Studies have shown that in Mongolia, grassland productivity in areas in which grazing is not allowed has decreased by 20–30% over the past 40 years (Angerer et al., 2008). Until recently, the major rural income sources in Mongolia and IMAR were still from herding (Olonbayar, 2010; Waldron et al., 2010). Climate change and grassland degradation have endangered the livelihoods of herders on the Mongolian plateau.

In the semiarid and arid grasslands of Inner Asia (Southern Russia, Mongolia, and Northern China), local herders used to migrate in large geographic distances to adapt to the high spatio-temporal variability of precipitation and vegetation productivity (Humphrey and Sneath, 1999). Flexible property boundaries and reciprocal use of pastures allow herders to use grassland resources efficiently and to cope with frequent climate hazards (Fernandez-Gimenez, 1997). Those institutions have evolved over thousands of years and can well fit the biophysical characteristics of local ecological systems. However, over the past 50 years, the social-institutional changes have undermined the traditional resource institutions and replaced them with a series of alternative systems. Since the mid-1980s and the early 1990s, IMAR and Mongolia have been transforming from centrally planned to market economies. Pastures there have been privatizing to individual households since then, and livestock was privatized at the beginning of their economic transforms. In IMAR, most pastures have been contracted to

individual households and fenced. In Mongolia, due to the lack of effective resource institutions, pastures have become open-access resources. The grazing sedentarization process has almost been completed in IMAR, China (Humphrey and Sneath, 1999). In Mongolia, poor families, who could not afford long distance migrations, migrated less frequently or became sedentary grazers around water points or fertile pastures (Olonbayar, 2010). Along with grazing sedentarization, the social norms of reciprocal use of pastures that the traditional nomadism was relied on have been disappearing (Li and Huntsinger, 2011; Upton, 2009). Migration, used to be the major adaptation strategy for herders on the Mongolian plateau to cope with uncertainties in precipitation and forage becomes less feasible. Therefore, social-institutional changes have increased the vulnerability of livelihoods for natural resource dependent herders on the Mongolian plateau.

In this dissertation the dynamics of grassland productivity on the Mongolian plateau since the early 1960s was systematically investigated, by combining multiple datasets derived from satellite remote sensing and field measurements and drawing on theories from grassland ecology and institutional economics and methods from remote sensing, household survey, statistical modeling, and agent-based modeling. Current resource institutions and polices implemented in IMAR and Mongolia for governing grassland resources were analyzed and assessed. Diverse resource policy and institutional recommendations across ecological gradients and between IMAR and Mongolia were discussed. Social adaptation to climate change and grassland degradation was studies at household and community levels, i.e., changing herder livelihood choices and adjusting resource institutions. Taken as a whole, my dissertation provides knowledge that can support the development of policy and management strategies within the Mongolian plateau to produce more sustainable use of the grassland resources in the context of climate change.

1.2 Frameworks, Theories, and Methods

A social-ecological system is an ecological system intricately linked with and affected by one or more social systems (Anderies et al., 2004). All natural resources are embedded in social-ecological systems. Social-ecological systems are composed of multiple subsystems and internal

variables within these subsystems at multiple levels analogous to organisms composed of organs, organs of tissues, tissues of cells, cells of proteins, etc. (Ostrom, 2009). Due to complexity in social-ecological systems, a single theory cannot explain phenomena that emerge from the interactions of social and ecological sub-systems. In addition, without a common framework to organize findings, isolated knowledge about social-ecological systems does not accumulate (Ostrom, 2009). A general framework helps us to identify the components and the relationships among those components in the studied systems.

Several frameworks have been developed to analyze and harness complex adaptive social-ecological systems. Ostrom developed two frameworks for understanding institutional diversity and analyzing complex social-ecological systems, i.e., the Institutional Analysis and Development (IAD) framework (Ostrom, 2005) and the diagnostic framework for analyzing sustainability of social-ecological systems (Ostrom, 2009). Lemos and Agrawal (2006) proposed a governance framework that recognizes the importance of hybrid arrangements for sustainable environmental governance. Such hybrid arrangements connect the state, market, and community. Agrawal (2009) developed an analytical framework to examine the interactions among climate-related vulnerability, local institutions, and livelihood adaptation practices. In this integrated research, the above analytical frameworks were used in multiple analysis and modeling settings to address the complex interactions between environment and social dynamics affecting adaptation to environmental change on the Mongolian plateau.

Theories are sets of logics that are used to explain phenomena and predict outcomes. The development and use of theories enable the analyst to specify which components of a framework are relevant for certain kinds of questions (Ostrom, 2005). Several theories can be compatible within a framework. For example, in the diagnostic framework for analyzing sustainability of social-ecological systems (Ostrom, 2009), multiple social science theories, such as theories of institutions, institutional change, public choice, and common-pool resources, are all compatible within the framework. In this study of Mongolian grassland social-ecological systems, I mainly draw on theories from grassland ecology (Ellis and Swift, 1988) and institutional economics (North, 1990, 2005; Ostrom, 1990; 2005). Specifically, equilibrium and non-equilibrium ecosystem theories from grassland ecology and theories of institutions, institutional change, and

institutional diversity from institutional economics were used to generate hypotheses and explain phenomena for this integrated study. In addition, the concepts and analytical frameworks from complex adaptive systems (Miller and Page, 2007) were used in analyzing and modeling agent interactions, adaptations, and emergence in the Mongolian grassland social-ecological systems.

Understanding the dynamics of social-ecological systems requires an interdisciplinary approach and methodological pluralism. Focusing on a single research method used in one academic discipline will not lead to holistic and multi-scale comprehensions of natural resource management problems (Ostrom and Nagendra, 2006). This doctoral research analyzes satellite images, conducts social-ecological measurements on the ground, and explores social-ecological performances of alternative resource institutions by an agent-based computational model. Time-series of satellite images were used to track regional-scale grassland dynamics within different management regimes overtime. Satellite remote sensing is the one of the most frequently used techniques for mapping changes in natural resources. By combining satellite data with on-the-ground observations, I investigated the biophysical and social-institutional mechanisms that drive the dynamics of grassland productivity.

Household surveys and interviews with local resource users helped me to understand the major biophysical and social-economic factors, such as climate variability, household capital, and local institutions, which were closely related to the livelihood adaptation practices of local inhabitants. Statistical models (e.g. spatial panel data models and hierarchical linear models) were used for identifying the major drivers of the dynamics in grassland NPP across ecological zones of the Mongolian plateau and the factors that determine livelihood adaptation strategies of herder households. Agent-based models are computational platforms for exploring the dynamics of socio-ecological systems, and they are process-based models that can be used to explain empirical phenomena, to help design and choose institutions, and to generate alternative scenarios of agent actions and interactions. Agent heterogeneity, learning and adaptation, and social interactions can be easily incorporated in the model. They are flexible enough to represent and model various real world phenomena, compared with equilibrium-based analytical models (e.g. game theoretical models). In this integrated research, they were used for modeling the social-ecological outcomes of pasture-use under alternative resource institutional scenarios.

1.3 Research Objectives and Dissertation Outline

The overall objective of this research was to quantify the dynamics of grassland productivity on the Mongolian plateau over the past half century, analyze the drivers and mechanisms of the dynamics in grassland productivity, and understand social adaptation to climate change and grassland degradation. I advance the understanding of grassland dynamics on the Mongolian plateau and social adaptation to environmental change through monitoring, interpretation, and modeling. An interdisciplinary approach, which combines remote sensing, field ecological measurements, household survey, and agent-based modeling, enabled me better understand the dynamics of the Mongolian grassland social-ecological systems. The strengths of remote sensing and social science were combined advance understanding of coupled human and natural dynamics. Linking the estimated grassland NPP from remotely sensed data with field social-ecological measurements enabled me to interpret the dynamics of grassland NPP. Moreover, the linkages between the results of household surveys and the interpreted degradation status of grasslands from remotely sensed data are useful to understand the consequences of different land-use and management behaviors (e.g. grazing intensity) and the environmental effects on livelihood adaptation choices of herder households.

This dissertation includes three- research objectives: (1) monitoring grassland ecosystems using remote sensing, (2) interpreting the dynamics of grassland productivity on the Mongolian plateau; (3) studying social adaptation to climate change and ecosystem degradation. The research questions and methodologies for each of the three research objectives are presented in the following.

Objective One: monitoring grassland ecosystems using remote sensing

The major research questions behind this objective are: (1) what is the spatio-temporal variability of grassland annual NPP since the early 1980s?; and (2) what are the advantages and constraints of using hyperspectral remote sensing to monitor grassland ecosystems? The main advantage of the remote sensing technology, compared with traditional ecological samplings, in mapping grassland quantity and quality are that it can repeatedly monitor large-scale grassland

ecosystems in relatively low cost. In Chapter two, I sought to improve the availability of long term, spatially explicit, and regionally extensive record of grassland productivity dynamics with remote sensing. This research addresses lack of a long-term record of these dynamics that is needed for study of human-environment dynamics. It also relates those dynamics to climate variables to explore the variability and strength of those relationships before diving into the human-environment interactions in the next section

In order to uncover vegetation patterns that may be masked due to the coarse spatial and spectral resolution of the foregoing analysis, I explored the use of hyperspectral remote sensing to measure vegetation productivity. Hyperspectral remote sensing with hundreds of spectral bands has the potential to measure specific ecological variables of grassland ecosystems that were difficult to measure using traditional multispectral sensors. In Chapter three, I analyzed the potential for using hyperspectral remote sensing to detect the quantity and quality of dominant grassland communities across ecological gradients of the Inner Mongolian grasslands, based on a sampling of field conditions across a large geographic area. Though based on measurements taken in the field, the work provides a basis for developing methods to improve our ability to detect changes in vegetation productivity from space

Objective Two: interpreting the dynamics of grassland productivity

The major research question behind this objective is: how well do changes in resource policies and institutions, populations of livestock and humans, climate factors, and human land-use activities explain the dynamics of grassland productivity since the early 1960s? Understanding the drivers and mechanisms of the dynamics in grassland productivity is prerequisite for studying effective resource policies and institutions that can govern grassland resources sustainably. Mongolia and IMAR share similar ecological gradients of climate, vegetation, and soils, and they have undergone significant social-institutional and ecological transformations over the past half century. However, the two regions are different in their demographic, ethnic, cultural, economic, and political contexts.

In Chapter four, I focused on human dimensions of grassland degradation on the Mongolian plateau since the early 1960s. I adopted a hybrid state-market-community framework to analyze the dynamics of social-ecological systems on Mongolian plateau over the past 50 years based on grassland, socioeconomic, and climate data, collected in the field. In Chapter five, I presented a diagnostic analysis of the major drivers of the dynamics in grassland NPP across agro-ecological zones of the Mongolian plateau, using spatial panel data models. The dynamics of grassland NPP was modeled as a function of climatic and socioeconomic datasets. The time-series of grassland NPP estimated in Chapter two were used as inputs for the spatial panel data models. The Mongolian grasslands were first divided into six sub-regions based on the agro-ecological conditions. Then, spatial panel data models were run in each of the six agro-ecological zones in order to identify the major drivers of the dynamics in grassland annual NPP.

Objective Three: studying social adaptation to climate change and grassland degradation

The major research questions behind this objective are: (1) what were the major livelihood adaptation strategies adopted by herders on the Mongolian plateau to cope with climate change and grassland degradation?; (2) what kinds of local institutions were those livelihood adaptation strategies facilitated by?; (3) what were the determinants of variations in livelihood adaptation choices?; (4) what are the efficient resource institutions that can improve social-ecological outcomes of pasture-use in the semiarid and arid Mongolian grasslands in the context of climate change?

In Chapter six, social adaptation to climate change and grassland degradation were studied at the household level. A household survey was designed based on the adaptation, institutions, and livelihoods framework (Agrawal, 2009), and it was implemented across ecological gradients (meadow, typical, and desert steppes) of IMAR and Mongolia. I first analyzed the livelihood adaptation choices adopted by herder households over the past ten years. Then, a hierarchical linear model was applied to diagnose the factors at household and village levels that determined fodder purchasing behaviors of herder households. In Chapter seven, I presented an agent-based modeling approach to explore the social-ecological performance of alternative resource institutions (i.e., sedentary grazing, pasture rental markets, and reciprocal use of pastures) and

their combinations. Model parameters were set based on empirical data from household survey and literature review. I hypothesized resource institutions that can facilitate cooperative use of pastures can generate better social-ecological performance than the performance of sedentary grazing without cooperation. Based on the agent-based model informed by empirical studies in the Mongolian grasslands, I tested this hypothesis and explored effective social mechanisms for promoting and maintaining cooperation among herders.

PART II

REMOTE SENSING OF GRASSLAND ECOSYSTEMS

Chapter Two

Dynamics of Net Primary Productivity in the Mongolian Grasslands (1982−2009) in Response to Climate Variability and Change

Abstract

In order to understand the dynamics of grassland productivity on the Mongolian plateau over the past three decades, we used a remote-sensing-based light-use efficiency model to estimate annual net primary productivity (NPP) of the Mongolian grasslands from 1982 to 2009. We also analyzed the response of grassland NPP to climate variability and change. The estimated NPP was evaluated with the results of two empirically based methods. The results indicated that the interannual variability of grassland NPP generally increased over the study period, especially for desert steppe. The temporal trends of NPP varied across spring and summer seasons. Spring NPP increased in northern Mongolia, where climate was cold and humid, and decreased in desert steppe of Mongolia and eastern Inner Mongolia, China. Summer NPP increased in southern Inner Mongolia, mainly covered by cropland, and decreased in central Mongolia. Annual NPP increased significantly in northern Mongolia and southern Inner Mongolia, and decreased in some parts of desert and typical steppes of the Mongolian grasslands. In order to interpret the interannual variability of NPP and the temporal trends of NPP, we analyzed the relationships between NPP and climate. The results showed that the interannual variability of NPP decreases with the increase of precipitation (January-July), and the interannual variability of NPP increases with the increase of the interannual variability of precipitation (January-July). Based on correlation analyses between NPP and climate, NPP was more strongly associated with precipitation than with temperature, especially in desert and typical steppes.

Keywords: Grassland dynamics; net primary productivity; light-use efficiency; remote sensing; climate variability and change; Mongolian grasslands

---

Wang, J., Brown, D. G., and Chen, J. Dynamics of net primary productivity in the Mongolian grasslands (1982−2009) in response to climate variability and change. Manuscript submitted for review.

2.1 Introduction

The Mongolian grasslands, including Mongolia and Inner Mongolia Autonomous Region (IMAR), China, has supported millions of pastoralists over thousands of years. Local herders continue to expect the grassland to provide goods and services for regional development as well as exports. However, climate variability and intensified human land-use activities have interacted to significantly alter the grassland ecosystems over the past 50 years (Chapter Four). Grassland sustainability has become a major ecological, economic, and social issue there. Quantifying grassland productivity is prerequisite for understanding grassland dynamics on the Mongolian plateau. Estimating grassland net primary productivity (NPP) is also of interest in better understanding the role of the Mongolian grasslands in global carbon budget and the provision of other ecosystem services. Studies based on satellite derived data indicate that vegetation NPP has been increasing in the northern middle and high latitudes since the early 1980s (Fang et al., 2003; Hicke et al., 2002; Piao et al., 2009; Potter et al., 1999; Slayback et al., 2003; Tucker et al., 2001). However, the temporal trends of vegetation NPP may vary geographically due to the spatial heterogeneity of climate variability and change and the intensity of human land-use activities. Estimates of NPP over large geographic areas and long-time frames are needed to explore their spatio-temporal patterns and responses to climate variability and change.

Vegetation NPP with global coverage, such as the Advanced Very High Resolution Radiometer (AVHRR) Global Production Efficiency Model (GLOPEM) NPP (1981-2000) (Goetz et al., 1999, Prince and Goward, 1995) and the Moderate Resolution Imaging Spectroradiometer (MODIS) NPP (2000-present) (Heinsch et al., 2003; Running et al., 1999) have been developed for studying global vegetation dynamics. Although the models used for estimating GLOPEM NPP and MODIS NPP are both based on the light-use efficiency (LUE) model (Monteith, 1972; 1977), the model parameterization processes and spatial resolutions are different. Normalized difference vegetation index (NDVI) is one of the major inputs for these remote-sensing-based LUE models for NPP estimation (Field et al., 1995; Running et al., 2004; Seaquist et al., 2003). NDVI can provide important information on spatial complexity and temporal dynamics of biophysical properties of the Earth Surface. However, NDVI products derived from different sensors have different spatial resolutions, compositing schedules, and

image processing streams (e.g., differences in atmospheric corrections) (Brown et al., 2006). For example, AVHRR and MODIS image systems are different in their spectral, spatial, and radiometric resolutions and off-nadir view-angles (Tarnavsky et al., 2008). Therefore, NDVI values derived from the two sensors are different. In this work, we used a spatial degradation and linear-regression adjustment approach to integrate 8-km resolution GIMMS AVHRR NDVI (1982-1999) with 1-km resolution MODIS NDVI (2000-2009) and to build a spatially consistent and temporally continuous NDVI time-series used for estimating long-term grassland NPP.

The primary goal of this work was to build a spatially consistent and temporally continuous NPP time-series (1982-2009), covering the whole Mongolian grasslands, based on the integrated NDVI time-series processed through the LUE model. Then, we used the NPP time-series to explore: (1) the interannual variability and the temporal trends of NPP (1982-2009); and (2) the relationships between NPP and climate. We hypothesized that in the Mongolian grasslands, precipitation played a dominant role in influencing the interannual variability of NPP, and the long-term trends of NPP were also strongly affected by human land-use activities. Following this introduction, Section 2.2 provides a brief description of the study area and the datasets used in this study. Section 2.3 introduces the methods for estimating NPP, evaluating the estimated NPP, and analyzing the changes of NPP and their relationships with climate. Section 2.4 presents the results. In Section 2.5, we compare the estimated NPP with the results of other studies and discuss the drivers of the interannual variability and the temporal trends of NPP.

2.2 Study Area and Data

2.2.1 Study Area

The Mongolian plateau exhibits gradients of vegetation cover and density (Fig. 2.1). Grassland is the dominant ecosystem type there. About 66% of the total land area in Inner Mongolia (0.78 million km^2) is classified as grassland, comprising a quarter of all Chinese grassland (Zhang, 1992). Nearly 84% of the total territory in Mongolia (1.26 million km^2) is covered by grassland (Angerer et al., 2008). Climate on the Mongolian plateau is continental. Droughts and winter snowstorms are the two main types of climate disasters. Over the past half

century, climate there has been getting warmer and drier, and the frequencies of climate hazards have also increased (Chapter Four). Climate variability and change is likely affecting grassland productivity as well as grassland degradation. Besides climate, socioeconomic factors, such as increasing populations of human and livestock, human land-use intensification, and inefficient resource institutions have been identified as the major drivers of the dynamics in grassland productivity (Chapter Four; John et al., 2009).

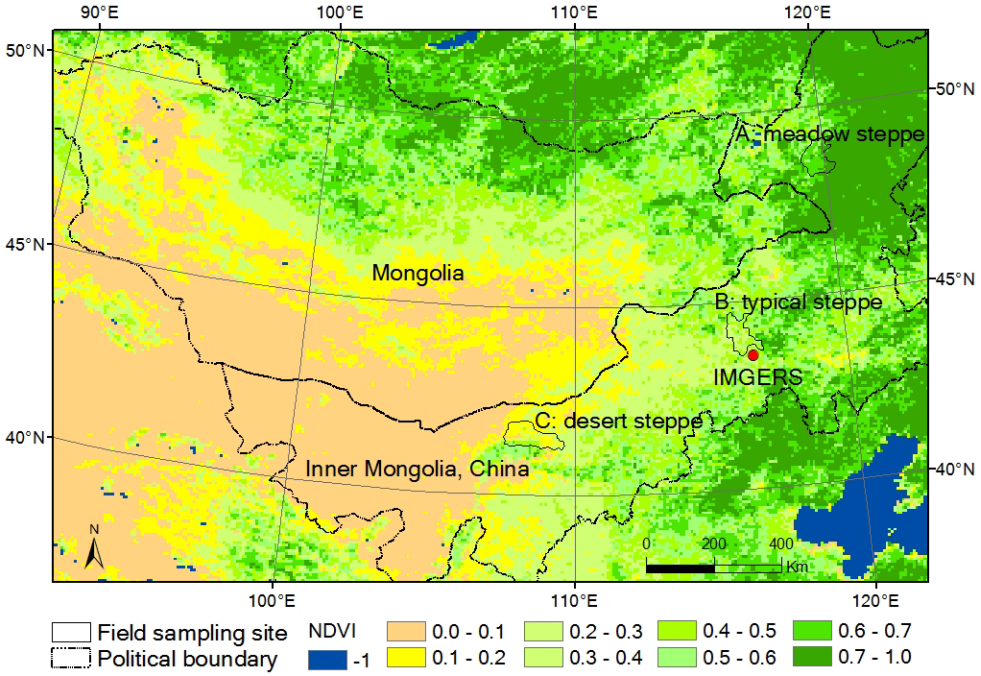

Fig. 2.1 The study area. Note: the background image is the 1-km resolution MODIS NDVI in the second half of August, 2009. IMGERS is the abbreviation of the Inner Mongolian Grassland Ecosystem Research Station, China.

2.2.2 Remotely Sensed Data

In this study, we used three NDVI datasets. The first dataset is GIMMS AVHRR NDVI, which are 15-day maximum value composite images (MVC) with 8-km spatial resolution. GIMMS AVHRR NDVI has been corrected for sensor degradation, cloud contamination, viewing-angle effects due to satellite drift, volcanic aerosols, and low signal-to-noise ratios due to sub-pixel cloud contamination and water vapor (Fensholt et al., 2009; Tarnavsky et al., 2008). GIMMS AVHRR NDVI has been demonstrated to be more stable than other AVHRR NDVI products (Slayback et al., 2003). We acquired twenty-five years of GIMMS AVHRR NDVI

images (1982-2006) from the Global Land Cover Facility (GLCF). We also acquired two MODIS NDVI products (2000-2009): MOD13Q1 and MOD13A2. Their spatial resolutions were 250-m and 1-km, respectively. The two MODIS NDVI products were acquired from the NASA Reverb database. Monthly mean surface incident shortwave radiation (1982-2009) with spatial resolution of 1.0° × 1.0° was acquired from the Goddard Earth Sciences (GES) Data and Information Services Center (DISC). Advanced space-borne thermal emission and reflection radiometer (ASTER) DEM data, covering the three field sites in Inner Mongolia (Figs. 2.1 and 2.2), were also acquired from the NASA Reverb database.

2.2.3 Ecological and Climate Data

Regional-scale vegetation maps of Mongolia and Inner Mongolia were collected and used for establishing the parameter values of the LUE model. The two maps were made by the Institutes of Botany in Mongolia and China, in the 1980s and 1990s, respectively. The two vegetation maps were created based on large-scale field campaigns and samplings. The original scale of the vegetation maps was 1:1,000,000. The field sampled aboveground biomass in the summer (i.e., from mid-August to early September) of 2009 were used to validate the NPP estimated by the LUE model. These data were collected by our collaborators, the Inner Mongolian Grassland Survey and Design Institute and used for assessing grassland quality and mapping vegetation distribution. In this study, we only used the field measured aboveground biomass of three counties, distributed in meadow, typical, and desert steppes (Figs. 2.1 and 2.2). The numbers of field samples in the three counties were 107, 80, and 114, respectively. In the sampling process, each 1 × 1 m field plot was randomly selected within relatively homogeneous sites with a size of 100 × 100 m. For the purpose of evaluating the estimated NPP, we also used the detailed vegetation maps for the three counties (Fig. 2.2). These vegetation maps were made based on visual interpretations of Landsat TM 5 images in 2009, assisted by detailed field campaigns.

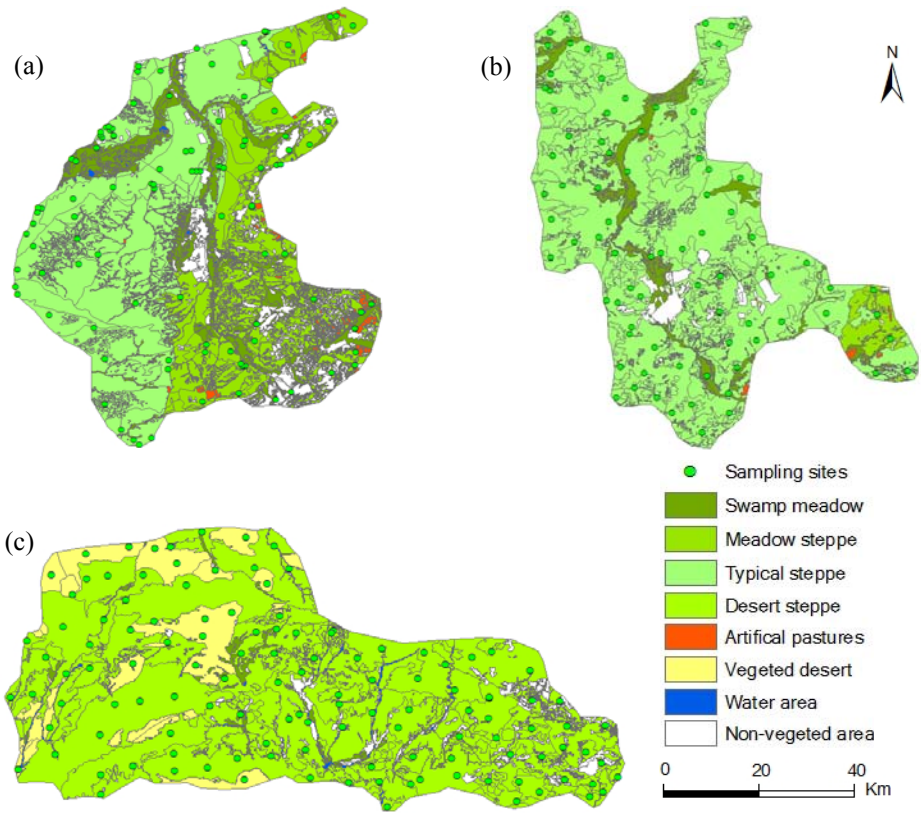

Fig. 2.2 The field ecological sampling sites and the vegetation maps of 2009: (a) Ewenke county, meadow steppe; (b) Xilinhot county, typical steppe; (c) Wulatezhong county, desert steppe. The three sites are corresponding to sites A, B, and C in Fig. 2.1.

Monthly precipitation and temperature (1982-2009) were collected from 17 and 47 national standard climate stations in Mongolia and Inner Mongolia, respectively. Monthly total precipitation and monthly mean temperature were spatially interpolated to 8-km resolution using the universal kriging model for consistency with the spatial resolution of GIMMS AVHRR NDVI. Spatial coordinates of the climate stations were used as the secondary information for incorporating the spatial trends of temperature and precipitation into the spatial predictions.

2.3 Methods

2.3.1 Integrating GIMMS AVHRR NDVI and Terra MODIS NDVI

The process of integrating 8-km resolution GIMMS AVHRR NDVI and 1-km resolution MODIS NDVI proceeded as follows. First, in order to put the two NDVI datasets at the same

spatial resolution, 1-km MODIS NDVI were spatially degraded to 8-km by averaging all 64 1-km pixels within each 8-km pixel. Second, regression analyses were performed to relate AVHRR NDVI and MODIS NDVI during the period in which both were operating (i.e., from the second half of May to September, 2000-2006) (Ji et al., 2008). Ten thousand regularly distributed sample points were generated to cover the study area and used to extract the values of AVHRR NDVI and MODIS NDVI. The coefficients of the linear regression models used for calculating MODIS NDVI as a function of AVHRR NDVI were estimated in the software package MATLAB (Mathworks Inc., Natick, Massachusetts, USA). In order to test the stability of the regression coefficients over time, we built linear regression models between AVHRR NDVI and MODIS NDVI for all biweekly intervals between 2000 and 2006. T-tests showed that all regression coefficients were significant at $p < 0.01$. The regression coefficients and intercepts exhibited periodic or seasonal variations, with seasonal variations being larger. Therefore, we averaged the regression coefficients and intercepts across years for each biweekly interval to represent the values of regression coefficients and intercepts in that seasonal period (Table 2.1).

Table 2.1 The coefficients of the linear regressions used for adjusting AVHRR NDVI (1982-1999) to MODIS NDVI

Biweekly Period	Intercept	Slope	R^2	*p*
April_Period 2	0.0046	1.0256	0.9285	< 0.01
May_Period 1	0.0003	1.1532	0.9034	< 0.01
May_ Period 2	0.0060	1.0808	0.9163	< 0.01
June_ Period 1	0.0156	1.0413	0.9230	< 0.01
June_ Period 2	0.0293	1.0366	0.9276	< 0.01
July_ Period 1	0.0305	1.0053	0.9361	< 0.01
July_ Period 2	0.0423	0.9574	0.9237	< 0.01
August_ Period 1	0.0413	0.9086	0.9150	< 0.01
August_ Period 2	0.0292	0.8582	0.8895	< 0.01
September_ Period 1	0.0374	0.7250	0.8827	< 0.01
September_ Period 2	0.0424	0.6546	0.8704	< 0.01

2.3.2 Estimating Annual NPP of the Mongolian grasslands (1982-2009)

The light-use efficiency (LUE) approach for estimating vegetation productivity assumes that biological production is proportional to the amount of absorbed photosynthetically active radiation (APAR). APAR itself is the product of the incident photosynthetically active radiation (PAR) and the reflectance properties expressed through vegetation indices (e.g., NDVI)

(Running et al., 1999). The maximum biological efficiency of converting PAR to dry matter in units of carbon ($g \cdot C \cdot MJ^{-1}$), known as LUE, is constrained by environmental factors (e.g., precipitation and temperature). LUE varies not only between biomes but also between species, and even across leaves within a plant (Brogaard et al., 2005). Gross primary productivity (GPP; $g \cdot C \cdot day^{-1} \cdot m^{-2}$) represents the amount of solar energy converted through photosynthesis. NPP subtracts from this energy used for the maintenance and growth respiration, and represents the mass of dry plant matter produced (i.e., allocated in roots, shoot, leaves, and seeds). Annual NPP was accumulated in the vegetation growing season. For the LUE model, we defined that the growing season of the Mongolian grasslands was from the second half of April to September. Annual NPP was estimated by the following equations.

$$NPP_j = N \times \varepsilon_{i,j} \times PAR_j \times FPAR_j \tag{2-1}$$

$$ANPP_j = \sum_{k=1}^{11} NPP_{j,k} \tag{2-2}$$

where $ANPP_j$ is the annual NPP of pixel j. For a given biweekly period, NPP in pixel j (NPP_j) is estimated based on the LUE of biome type i at pixel j ($\varepsilon_{i,j}$), the PAR received at pixel j (PAR_j), and the proportion of PAR absorbed at pixel j ($FPAR_j$). N is the number of days over which the maximum NDVI images were produced (Equation (2-1)); for GIMMS AVHRR NDVI (1982-1999) and MODIS NDVI (2000-2009), the values of N are 15 and 16, respectively. Annual NPP of pixel j ($ANPP_j$) is estimated as the sum of eleven ($k = 1, 2, \cdots, 11$) biweekly NPP values over the growing season (Equation (2-2)).

To parameterize the LUE model, we first defined land-cover types for each pixel. There are three main types of grassland on the Mongolian plateau: meadow, typical, and desert steppes. Over the past thousands of years, some of the grassland has been converted to cropland. Cropland is mainly distributed in the ecological zones that were originally covered by meadow and typical steppes. Besides the three types of grassland, forests, desert/bare-rock mountains, and lakes are the other main land-cover types in the study area. In order to diagnose the changes of land-cover types over the study period (1982-2009), we classified the land-cover types over five time periods (i.e., 1982-1987, 1988-1993, 1994-1999, 2000-2004, and 2005-2009) using the

integrated NDVI time-series. NDVI values in each biweekly period were averaged over the number of years in each time period to minimize the influences of climate variability on NDVI values. The differentiation of land-cover types was based on the differences in their phenologic curves. The preliminary analyses of the phenologic curves, represented by biweekly NDVI values, indicated that typical steppe and cropland cannot be differentiated clearly because their phenologic curves were largely overlapping. Therefore, we combined cropland into typical steppe.

We used the K-means unsupervised classification method for image classification. The classification process was assisted by the K-means clustering functions in MATLAB. In order to make the classification results comparable over the five time periods, we first pooled the NDVI data of the five time periods by averaging the NDVI values in each biweekly period between 1982 and 2009 to calculate the cluster centers. The extracted cluster centers were used for image classification in the five time periods. The land-cover clusters were labeled and combined into six land-cover types: forests, forest/meadow steppe, cropland/typical steppe, desert steppe, desert and bare-rock mountains, and lakes. There should be a certain amount of misclassified pixels because we used the coarse resolution NDVI images for land-cover classifications. In order to assess the classification accuracy over the five time periods, we compared the results of land-cover classification with the vegetation maps of Mongolia and Inner Mongolia. The proportions for most land-cover types in most time periods were reasonably consistent with the vegetation maps with slight differences (Table 2.2). Considering the uncertainties associated with the land-cover classifications, we used the vegetation maps of Mongolia and Inner Mongolia to assign land-cover types for each pixel. In this study, we focused only on studying the dynamics of grassland productivity, so other land-cover types were taken out of the study area.

Table 2.2 The proportions of the six land-covers over the five time periods.

Vegetation Type	1982−1987	1988−1993	1994−1999	2000−2004	2005−2009	Vegetation Map
Forests	8.97%	9.15%	8.87%	8.30%	8.47%	8.64%
Forest/Meadow steppe	17.54%	17.30%	17.15%	16.88%	16.40%	17.65%
Cropland/Typical steppe	30.87%	31.95%	33.67%	34.10%	34.72%	32.98%
Desert steppe	18.40%	17.33%	15.76%	13.89%	14.80%	17.02%
Desert and bare mountains	23.89%	23.86%	24.12%	26.49%	25.32%	23.39%
Lakes	0.33%	0.41%	0.43%	0.34%	0.29%	0.31%

In the second step, we calculated the values of LUE for meadow, typical, and desert steppes. We used the values of NPP, PAR, and FPAR for selected field sites to solve Equation (2-1) in order to calculate LUE. Here, we used annual maximum grassland biomass to represent annual NPP. The annual biomass was calculated based on the aboveground biomass measured in the field and the established ratios of belowground to aboveground biomass. In this process, we used the long-term field measurements of annual aboveground biomass observed from 16 field sites: five in meadow steppe, eight in typical steppe, and three in desert steppe (Fig. 2.3). Aboveground live biomass was sampled in the mid-August of each year. This was because the biomass of grassland communities in Inner Mongolia reached the annual peak in the mid-August. Aboveground biomass of the sampled grassland communities was dried at 65 °C for 48h before weighting. The lengths of records for these sites range from 8 years to 24 years. For 14 of the 16 sites, the size of the study plots was 250 × 40 m, and the size of the other two plots was 500 × 500 m. Detailed descriptions of the ecological dataset are provided in Bai et al. (2008).

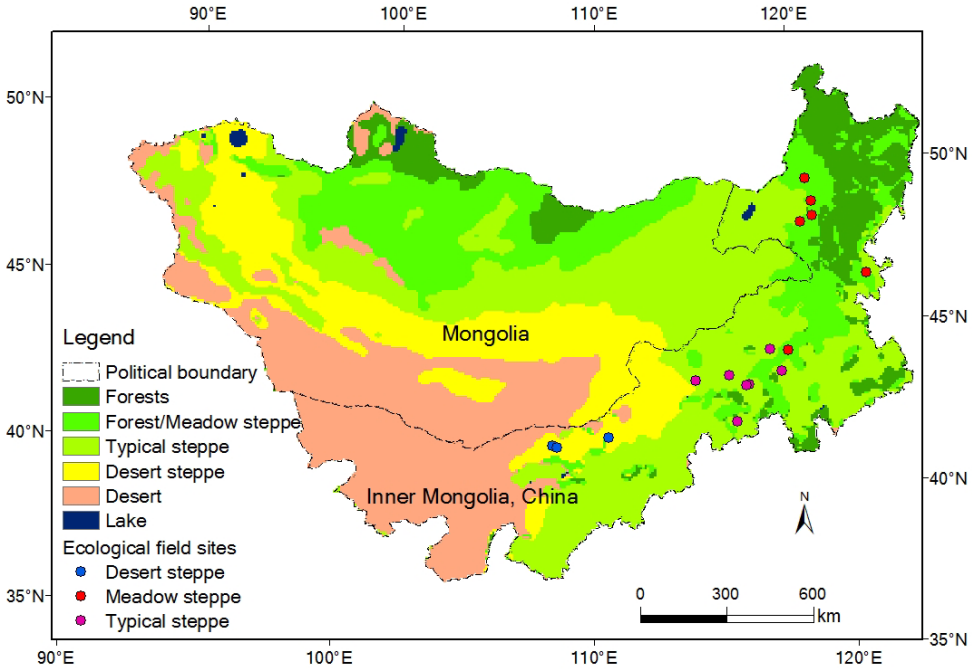

Fig. 2.3 The major land-cover types on the Mongolian plateau. The vegetation maps of IMAR (1990s) and Mongolia (1980s) were provided by the Institutes of Botany in China and Mongolia, respectively. The original scale of the two vegetation maps is 1:1,000,000. The ecological sampling sites in IMAR are the long-term ecological observation sites, which are managed by Chinese Academy of Sciences.

We estimated belowground biomass based on the empirical ratios between aboveground and belowground biomass. The approach of using aboveground to belowground biomass ratio has been the most common method for estimating belowground biomass at local to landscape, regional, and biome scales (Mokany et al., 2006). Physiologically the ratio is explained as reflecting the differential investment of photosynthates between aboveground and belowground organs (Mokany et al., 2006; Titlyanova et al., 1999). In this study, the ratios of belowground to aboveground biomass for meadow, typical and desert steppes were drawn from other field studies including 113 field sites in Inner Mongolia (i.e., 18 in meadow steppe, 55 in typical steppe, and 40 in desert steppe) at which both aboveground and belowground live biomass were measured (Ma et al., 2008). The belowground to aboveground biomass ratios for meadow, typical, and desert steppes of the study area were set to 6.90, 5.16, and 5.32, respectively. The multi-year mean of aboveground biomass was converted to total live biomass by multiplying the established ratios. Then, total live biomass ($g \cdot m^{-2}$) was converted to units of carbon measurements ($g \cdot C \cdot m^{-2}$) by multiplying the empirical ratio 0.45 (Lieth and Whittaker, 1975).

PAR (2000-2006) was calculated based on monthly mean incident shortwave radiation ($J \cdot sec^{-1} \cdot m^{-2}$) multiplied by a scalar 0.45 (i.e., the photosynthetically active proportion of the total incident shortwave electromagnetic radiation) and 24 hours in units of seconds (Zhao et al., 2007). FPAR (2000-2006) was calculated using an empirical MODIS NDVI-FPAR look-up table (Knyazikhin et al., 1999). Moreover, in order to minimize the scale-mismatch between the sizes of field plots (i.e., 14 plots were with a size of 250 × 40 m; two were with a size of 500 × 500 m) and the size of remote sensing pixels, we chose the 250-m MODIS NDVI dataset in calculating LUE. We estimated absorbed photosynthetically active radiation (APAR) by multiplying the incident solar radiation in photosynthetically active wavelengths with FPAR (Running et al., 2004). Annual APAR was summarized over the eleven biweekly periods of a given year. We averaged annual APAR between 2000 and 2006 to represent the multi-year mean APAR. Finally, we calculated the values of LUE for the 16 field sites based on APAR and NPP. The LUE values and their standard deviations (i.e., among the number of sites in each type) for meadow, typical, and desert steppes were 0.78 $g \cdot C \cdot MJ^{-1}$ (0.14), 0.60 $g \cdot C \cdot MJ^{-1}$ (0.10), and 0.51 $g \cdot C \cdot MJ^{-1}$ (0.15), respectively. The calculated LUE values are relatively consistent with the field measured grassland LUE by Turner et al. (2003).

Finally, biweekly FPAR (1982-2009) for the LUE model was also calculated using the empirical MODIS NDVI-FPAR look-up table. Monthly mean PAR (1982-2009) was calculated using the same method for PAR processing as described in calculating LUE. Then, we calculated biweekly NPP based on the values of PAR, FPAR, and LUE for each pixel. In the end, annual NPP was summarized over the eleven biweekly growing-season periods in a given year.

In the above process, any uncertainties associated with land-cover type, LUE, PAR, and FPAR can influence the accuracy of the NPP estimates. First, biweekly NPP was calculated assuming NDVI was constant over the 15- or 16-day period. However, NDVI changes all the time due to changes in plant phenology, incident solar radiation, and cloud cover. Second, in calculating FPAR, we used the empirical MODIS NDVI-FPAR look-up table that was developed based on simulated data from the NOAA-11 AVHRR sensor. This might affect the magnitude of our estimated annual NPP in a systematic way (Zhao et al., 2007). Third, the land-cover types used for assigning the LUE values for each pixel can introduce errors. Although the spatial distributions of the three broad grassland types were fairly stable over the study period, some changes may have occurred that influence the accuracy of LUE parameter. Fourth, the LUE calculation process may introduce errors. We used multi-year mean aboveground biomass for calculating LUE, and we cannot diagnose the interannual variability of LUE due to the lack of field data over time. Moreover, we used one empirical ratio of belowground to aboveground biomass for each of the three broad grassland types. Field studies have shown that these empirical ratios vary within each of the three grassland types (Ma et al., 2008). In addition, the coarse resolution images used in this study can also decrease the spatial variability of LUE (Tuner et al., 2002). Finally, any errors associated with the monthly mean incident solar radiation dataset can systematically influence the accuracy of the estimated annual NPP because PAR is one of the major inputs for the LUE model.

2.3.3 Spatial Predictions of Grassland NPP by Universal Kriging

In order to evaluate the estimated NPP by the LUE model, we compared the NPP estimates with the results of a geostatistical model used for predicting NPP with field measurements and

auxiliary variables for the three evaluation sites (Fig. 2.2). Geostatistical methods, such as universal kriging and co-kriging, have been used for spatially predicting vegetation quantities (Dungan, 1998; Sales et al., 2007). Here, we used the universal kriging (UK) model for spatially predicting NPP. UK is a commonly used geostatistical interpolation method. It can incorporate auxiliary variables to provide additional information about the spatial distributions of predictions. Auxiliary variables in the UK model are similar to the regression covariates in multiple linear regression models (MLR). Compared with MLR, UK can also account for the spatial structure of predictions and can reproduce measurements (Chilès and Delfiner, 2012). UK has been applied in combining remote sensing data with field biomass measurements (Berterretche et al., 2005; Chatterjee et al., 2010). Detailed discussions about UK are provided in Chilès and Delfiner (2012). Only a few key equations are described here.

UK splits the random function into a linear combination of a deterministic function, known at any location of the prediction field, and a random component, which is the function of random residuals. The prediction problem can be expressed as

$$s = X_s\beta + \nu \tag{2-3}$$

where s is an $m \times 1$ vector of predictions, X_s is an $m \times p$ matrix representing the model of the trend, β is a $p \times 1$ vector of drift coefficients representing the weights assigned to the p auxiliary variables. ν is the function of random residuals. The matrix form of the solution is

$$\begin{bmatrix} Q_{zz} & X_z \\ X_z^T & 0 \end{bmatrix} \begin{bmatrix} \lambda^T \\ M \end{bmatrix} = \begin{bmatrix} Q_{zs} \\ X_s^T \end{bmatrix} \tag{2-4}$$

where Q_{zz} is an $n \times n$ size matrix representing the covariance of observations, X_z is an $n \times p$ size matrix of auxiliary variables representing the spatial trend of observations, X_s is an $m \times p$ size matrix representing the trend of predictions. Q_{zs} is an $n \times m$ matrix representing covariance between predictions and observations, λ is an $m \times n$ matrix of weights assigned to related observations, and M is a $p \times m$ matrix of Lagrange multipliers. The best predictions of NPP and their variances are produced by

$$\hat{s} = \lambda z \tag{2-5}$$

$$V_{\hat{s}} = Q_{ss} - \lambda^T Q_{zs} - X_s M \tag{2-6}$$

Field sampled aboveground biomass in the three evaluation sites are used as the measurements for spatial prediction (Fig. 2.2). We used the 2009 vegetation maps, 1-km MODIS NDVI, and 30-m ASTER DEM as auxiliary information. Vegetation maps were rasterized to 1-km resolution grids. Each vegetation type was set as an independent layer. The spatial distribution of each vegetation type was coded as binary variables for each independent layer. 30-m DEM was aggregated to 1-km resolution by averaging all 30-m elevation values within each 1-km pixel. NDVI, elevation, and vegetation types represent the deterministic part of the UK model. The spatial resolution of the prediction field was set as 1-km. We used the restricted maximum likelihood (REML) method to estimate the values of covariance parameters. REML can detrend observations and estimate the covariance parameters simultaneously. Exponential covariance function was used in the UK framework. The objective function of RMEL is (Gourdji et al., 2010)

$$L = \frac{1}{2}\ln|Q_{zz}| + \frac{1}{2}\ln\left|X_z^T Q_{zz}^{-1} X_z\right| + \frac{1}{2}\left[s^T (Q_{zz}^{-1} - Q_{zz}^{-1} X_z (X_z^T Q_{zz}^{-1} X_z)^{-1} X_z^T Q_{zz}^{-1}) s\right] \tag{2-7}$$

The covariance parameters (sill, range, and nugget) can be derived by minimizing the objective function. We used the unconstrained nonlinear optimization routine for parameter optimization, provided in MATLAB. The UK method and the REML algorithm were coded by the authors in MATLAB. The total live biomass in the prediction field was calculated based on the spatially predicted aboveground biomass and the ratios of belowground to aboveground biomass for the three grassland types, which were used for calculating LUE. Then, we aggregated the 1-km resolution total live biomass to 8-km resolution by averaging the 1-km resolution values. The total live biomass ($g \cdot m^{-2}$) was converted to units of carbon ($g \cdot C \cdot m^{-2}$) by multiplying the empirical ratio 0.45. Finally, the spatially predicted grassland NPP of 2009 was compared with the estimated NPP by the LUE model.

2.3.4 Analyzing the Changes of NPP and Their Relationships with Climate

First, we analyzed the changes of the interannual variability of NPP over the study period. We divided the study period (1982-2009) into three sub-periods (i.e., 1982-1990, 1991-1999, and 2000-2009) and calculated the interannual variability of NPP, represented by the coefficient variance of NPP (NPP-CV), in each sub-period. Second, we calculated the changes of NPP in spring (from mid-April to June) and summer (from July to September) seasons, along with the changes of annual NPP, in each pixel. The changes of NPP were classified as significant increase or decrease if the linear regressions were significant at $p < 0.05$. Due to the spatial autocorrelation of NPP and the multiple-testing problem, some of the pixels may be falsely labeled as significant increase or decrease. Therefore, we adopted the false discovery rate (FDR) control procedure (Benjamini and Hochberg, 1995) to exclude the pixels that may be labeled falsely. In this study, we used the common approach and defined the threshold value of FDR as the same with the *p* value (0.05). Detailed discussions about the FDR control procedure are provided in Benjamini and Hochberg (1995).

In order to understand the spatial patterns of the interannual variability of NPP and the temporal trends of NPP, we analyzed the relationships between NPP and climate. Previous studies based on long-term field measurements indicated that grassland aboveground NPP in Inner Mongolia were sensitive to precipitation between January and July (Bai et al., 2008). Therefore, in this study, we only used precipitation data between January and July. First, we calculated the variations of NPP-CV, along the gradient of the mean precipitation per half-annum (MPHA; January-July, 1982-2009). We also binned the values of NPP-CV in every 50 mm by calculating averages and standard deviations. Second, we analyzed the relationships between NPP-CV and the interannual variability of precipitation, represented by the coefficient of variation of precipitation (precipitation-CV). In addition, we calculated the correlation coefficients between NPP and climate variables (January-July) for each pixel (1982-2009). If the correlation coefficient was significant at $p < 0.05$, we labeled the correlation as significantly positive or negative. We also used the FDR control procedure to exclude the pixels that were labels falsely as significantly positive or negative. Here, the threshold value of FDR was set as same with the *p* value.

2.4 Results

2.4.1 Evaluation of the Estimated Grassland NPP

The estimated grassland NPP by the LUE model was evaluated with the results of two empirically based methods. First, we compared the estimated NPP of 2009 with the spatially predicted NPP using the UK model in that year at the three evaluation sites in meadow, typical, and desert steppes of Inner Mongolia (Figs. 2.1 and 2.2). The estimated NPP values were plotted against the spatially predicted NPP (Fig. 2.4). For the three evaluation sites, the NPP values estimated by the LUE model were roughly consistent with the NPP values predicted by the UK model. For the three sites in meadow, typical, and desert steppes, the root mean square errors (RMSEs) between the two NPP datasets were 25.17 $g \cdot C \cdot m^{-2} \cdot year^{-1}$, 11.60 $g \cdot C \cdot m^{-2} \cdot year^{-1}$, and 6.89 $g \cdot C \cdot m^{-2} \cdot year^{-1}$, respectively.

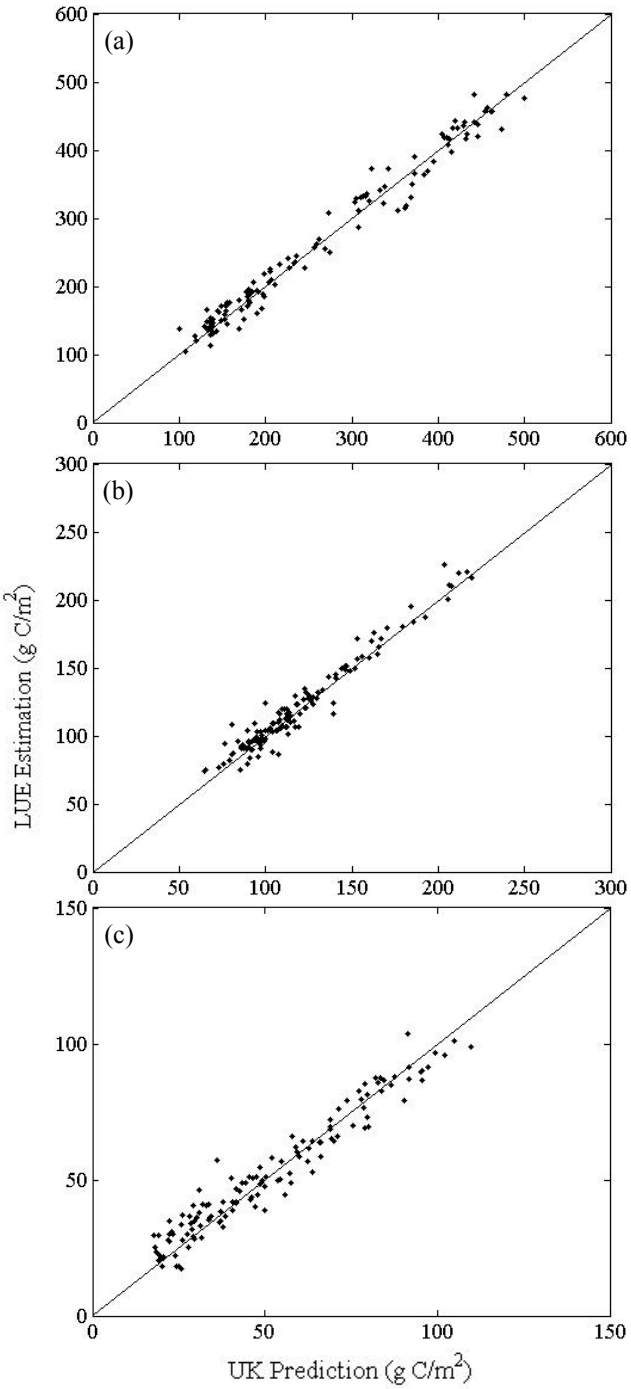

Fig. 2.4 The comparisons between estimated NPP by the LUE model and spatially predicted NPP by UK in the three evaluation sites of IMAR: (a) Ewenke county, meadow steppe; (b) Xilinhot county, typical steppe; (c) Wulatezhong county, desert steppe.

Second, we compared the estimated NPP by the LUE model with the field measurements at IMGERS (Fig. 2.1) (1982-2003) (Ma et al., 2010) for evaluating the NPP estimates over time. The plot size of the fenced experimental site at IMGERS was 500 × 500 m, which was smaller

than the pixel size of the estimated NPP. The measured aboveground biomass was first converted to total live biomass by multiplying the empirical ratio of belowground to aboveground biomass in typical steppe. Then, we converted the total live biomass ($g \cdot m^{-2}$) to units of carbon ($g \cdot C \cdot m^{-2}$) by multiplying the coefficient 0.45. The calculated NPP values based on field measurements were compared with the estimated annual NPP in the corresponding pixel, assuming that the field measured biomass taken at the end of the growing season can represent annual NPP. The calculated NPP based on field measurements were higher than the estimated NPP by the LUE model. The lower NPP estimated by the LUE model might be explained by grazing activities, which were excluded from IMGERS. The calculated NPP based on field measurements also had higher interannual variability (Fig. 2.5). This could be explained by the fact that the LUE model did not include the interannual variability of climate variables directly. In addition, the estimated NPP using coarse resolution remote sensing data also had the smoothing effect. The correlation coefficient between the two NPP time-series was 0.82 ($p < 0.01$).

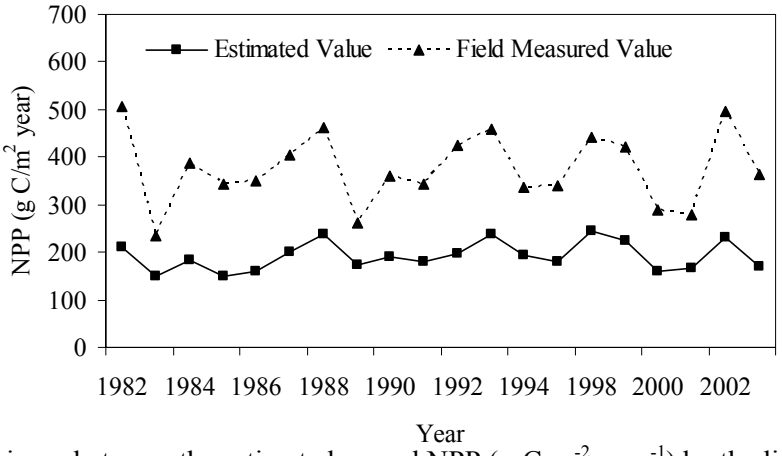

Fig. 2.5 The comparisons between the estimated annual NPP ($g \cdot C \cdot m^{-2} \cdot year^{-1}$) by the light-use efficiency (LUE) model and ground measured biomass ($g \cdot C \cdot m^{-2}$) at IMGERS (1982−2003).

2.4.2 The Interannual Variability of Grassland NPP

The spatial patterns of mean annual NPP (1982-2009) and the interannual variability of NPP in the three sub-periods follow the general trends observed in the vegetation map of the study area (Fig. 2.6). By statistics, mean annual NPP and their standard deviations for meadow, typical, and desert steppes were: 316.09 $g \cdot C \cdot m^{-2} \cdot year^{-1}$ (118.03), 164.27 $g \cdot C \cdot m^{-2} \cdot year^{-1}$ (87.14), and

85.70 g·C·m^{-2}·year^{-1} (35.86). For the three sub-periods, the interannual variability of grassland NPP (NPP-CV) decreased from desert to typical and meadow steppes. The spatial patterns of NPP-CV also varied over the three sub-periods. Over study period (1982-2009), the values of NPP-CV of the Mongolian grasslands generally increased, especially for desert steppe.

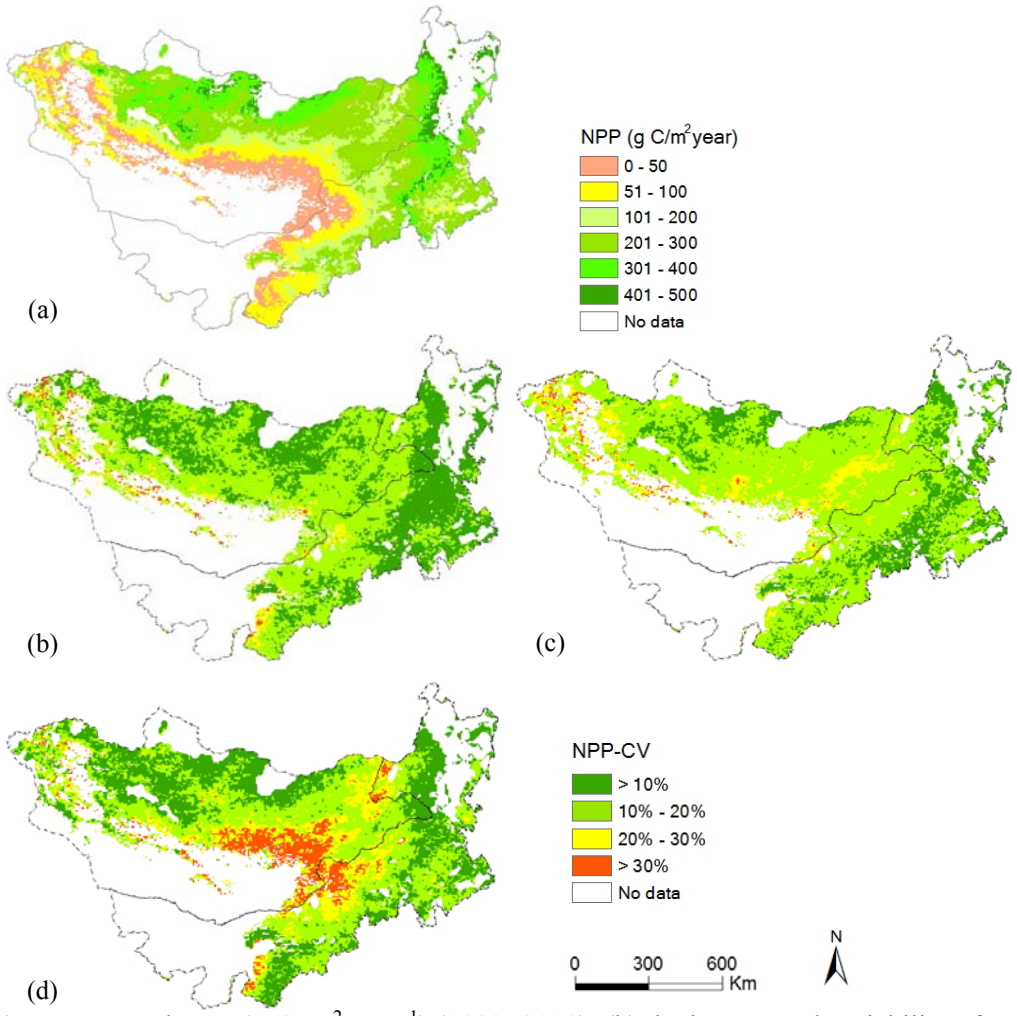

Fig. 2.6 (a) mean annual NPP (g·C·m^{-2}·year^{-1}) (1982−2009); (b) the interannual variability of NPP in Period 1 (1982−1990); (c) the interannual variability of NPP in Period 2 (1991−1999); and (d) the interannual variability of NPP in Period 3 (2000−2009).

2.4.3 The Temporal Trends of Grassland NPP

The temporal trends of grassland NPP vary across spring and summer seasons. Spring NPP increased in northern Mongolia, where climate was cold and humid, and decreased in desert steppe of Mongolia and eastern Inner Mongolia (Fig. 2.7a). Summer NPP increased in southern

Inner Mongolia, which is mainly covered by cropland, and decreased in the central part of Mongolia (Fig. 2.7b). Annual NPP increased significantly in northern Mongolia and southern Inner Mongolia, and decreased in some parts of desert and typical steppes of the Mongolian grasslands (Fig. 2.7c). The significant increase of annual NPP in southern Inner Mongolia indicated that human land-use activities strongly affected the long-term trend of grassland NPP. Over the study period, most of the aggregated temporal trends of NPP for meadow, typical, and desert steppes did not change significantly at $p < 0.05$, except for the significant decreasing trend in meadow steppe of Mongolia (Fig. 2.7d).

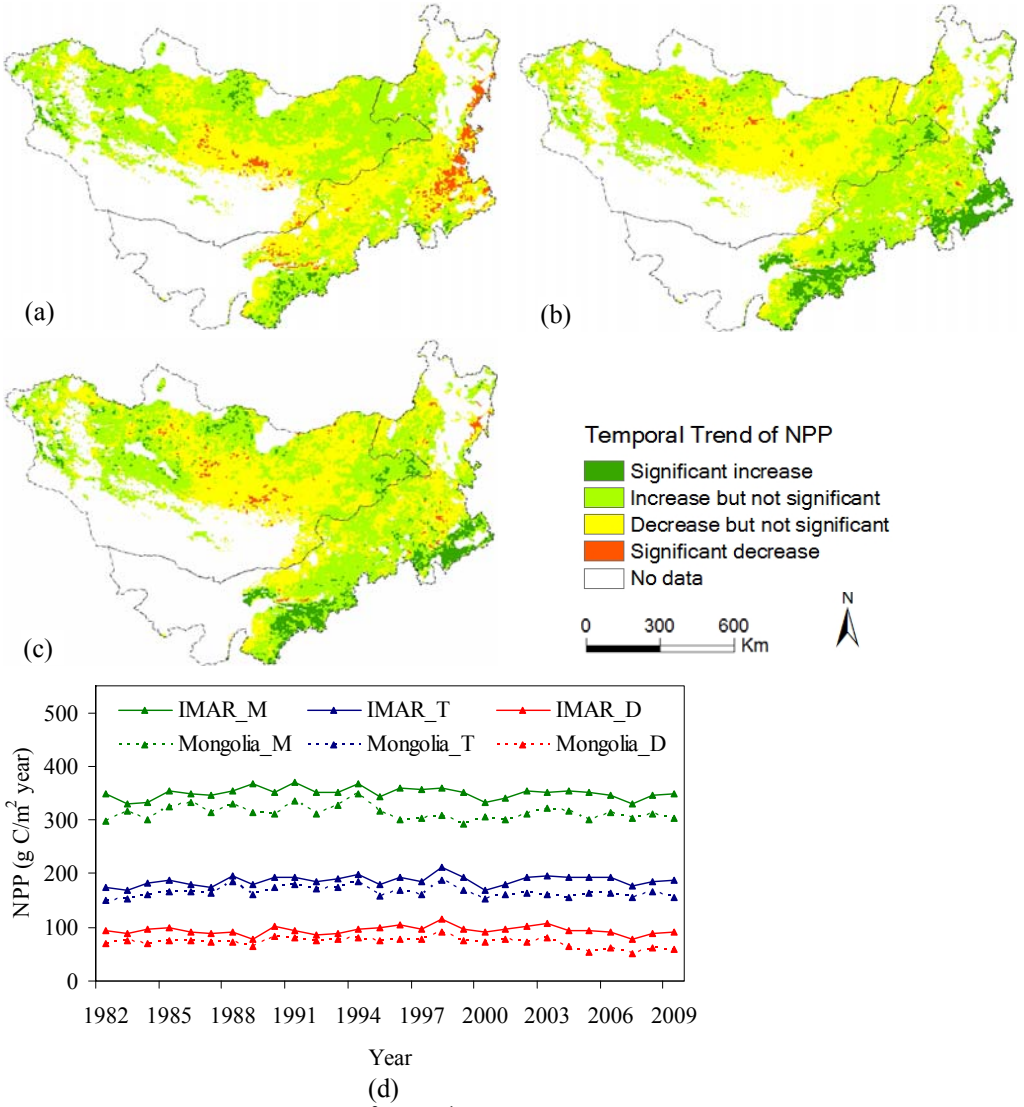

Fig. 2.7 Temporal trends of NPP ($g \cdot C \cdot m^{-2} \cdot year^{-1}$) (1982−2009) in (a) spring, (b) summer, (c) overall growing season, and (d) three grassland types of IMAR and Mongolia; IMAR_M, IMAR_T, IMAR_D,

Mongolia_M, Mongolia_T, and Mongolia_D denote meadow, typical, and desert steppes in IMAR and Mongolia, respectively.

2.4.4 The Relationships between NPP and Climate

The interannual variability of NPP (NPP-CV) decreases with increases of the mean precipitation per half-annum (MPHA), and the standard deviations of NPP-CV are higher where the values of MPHA are between 50 and 200 mm (Fig. 2.8a). Within this precipitation region, mainly covered by desert steppe, vegetation is sparsely distributed. The spatial heterogeneity of vegetation density in this region is higher than typical and meadow steppes. The values of NPP-CV increase with the increase of the interannual variability of precipitation (Fig. 2.8b).

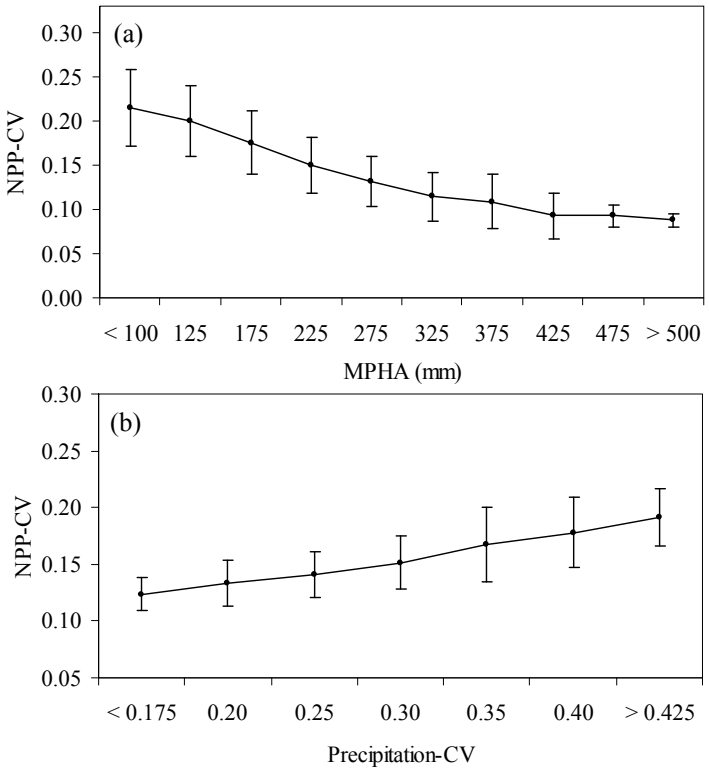

Fig. 2.8 Relationships between the interannual variability of NPP (NPP-CV) and precipitation: **a** NPP-CV and the mean precipitation per half-annum (MPHA); **b** NPP-CV and the interannual variability of precipitation (precipitation-CV).

The correlations between NPP and temperature were significantly negative in central Mongolia and eastern Inner Mongolia; and significantly positive in southern Inner Mongolia and western Mongolia (Fig. 2.9a). Southern Inner Mongolia is mainly covered by cropland, and

western Mongolia is the mountainous region with cold and wet climate. Our analyses of the temporal trends of temperature and precipitation (January-July; 1982-2009) indicated that temperature increased significantly in most parts of the Mongolian grasslands, except some parts of eastern Mongolia. However, precipitation had insignificant increasing or decreasing trends for most parts of the Mongolian grasslands. The significantly increased temperature may be one of the reasons for the decreased NPP in some parts of desert and typical steppes, and the increased NPP in the wet and cold mountainous region and the cropland region of Inner Mongolia. The increased temperature can either decrease water availability for plant growth in the arid and semi-arid region or increase plant activity in the cold and wet mountainous region, and in the cropland region without water constraints. Compared with the influence of temperature, precipitation played a more important role in influencing the interannual variability of NPP. The correlations between NPP and precipitation were significantly positive in most parts of the Mongolian grasslands, especially in desert and typical steppes (Fig. 2.9b).

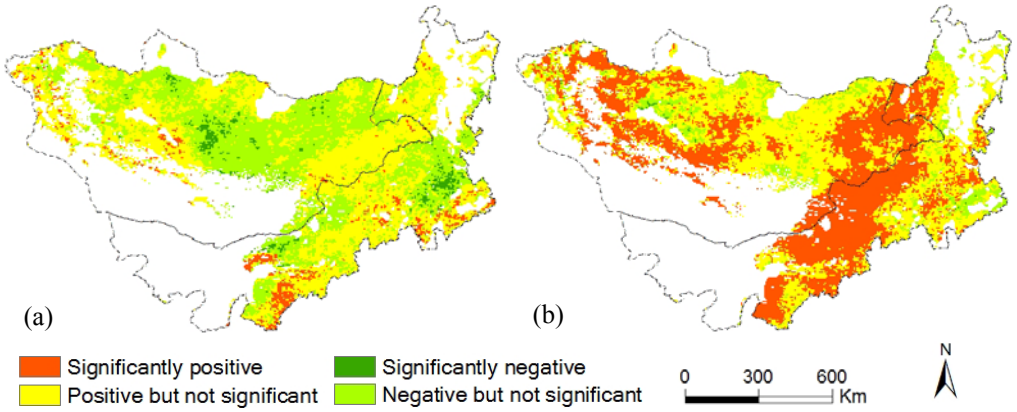

Fig. 2.9 The correlations between NPP and climate: (a) NPP−temperature and (b) NPP−precipitation (January-July; 1982−2009).

2.5 Discussion

Grassland NPP estimated by the LUE model was also evaluated by comparisons with the results of other studies. In this study, we only evaluated the NPP estimates in Inner Mongolia, based on the availability of references on NPP estimations of the Mongolian grasslands (Table 2.3). Our estimated NPP were slightly higher than MODIS NPP, but they were lower than the grassland NPP estimated by Ma et al. (2010), which were calculated based on the regression

analyses between field measured biomass and AVHRR GIMMS NDVI data. Moreover, our NPP estimates were slightly higher than the grassland NPP estimated by Xing et al. (2010), which were also calculated using the LUE model but with different model parameterization processes. Despite various uncertainties associated with our NPP estimates, the evaluations of the estimated NPP by two empirical methods and by comparisons with other studies indicated that the estimated grassland NPP by the LUE model was sufficient for assessing the dynamics of grassland NPP on the Mongolian plateau.

Table 2.3 The comparisons of grassland NPP in Inner Mongolia estimated in this study with the results of other studies.

Grassland NPP in Inner Mongolia ($g \cdot C \cdot m^{-2} \cdot year^{-1}$)				Source	
Meadow	Typical	Desert	Overall	Time period	References
330.17	172.63	93.81	198.87	2002-2006	This study
314.63	169.70	88.52	190.95	2002-2006	MODIS NPP
593.50	350.60	212.30	385.47	2002-2006	Ma et al. 2010
N/A	N/A	N/A	187.91	2000-2005	Xing et al. 2010

Estimating region-scale vegetation productivity over time and across heterogeneous landscapes has been an important research focus in recent years. This is driven by the demands from both basic (e.g., ecosystem function at broader spatial scales) and applied (e.g., carbon credit among countries) communities. The remote-sensing-based LUE model provided a useful tool to evaluate the dynamics of grassland productivity on the Mongolian plateau over the past three decades. Mean annual NPP and the interannual variability of NPP (NPP-CV) varied across ecological gradients characterized by the vegetation types. NPP-CV increased significantly over the study period, especially in desert steppe. Despite the rapid increase of livestock population in the Mongolian grasslands, especially in Inner Mongolia (Chapter Four), NPP only showed significant decrease in meadow steppe of Mongolia. Annual NPP increased in the high latitudes with cold and humid climate (i.e., northern and western Mongolia) and in the cropland-intensive region (i.e., southern Inner Mongolia). The significantly warming temperature may be one of the major reasons for the phenomena. The warming temperature may also be one of the major reasons for the decreased NPP in some parts of desert and typical steppes. The temporal trends of NPP varied across spring and summer seasons. The interannual variability of NPP was strongly affected by the mean precipitation per half-annum (January-July) and the interannual variability

of precipitation. The correlation analyses between NPP and climate indicated that NPP dynamics was strongly correlated with precipitation than with temperature.

Besides climate variability and change, human land-use activities, such as livestock grazing intensity and agricultural and mineral developments, also affected NPP dynamics, especially the long-term trend of NPP (Neupert, 1999; Olonbayar, 2009). Our analyses also showed that NPP increased significantly in southern Inner Mongolia (i.e., cropland-intensive region). In this study, the estimated NPP included the productivity of cropland. This was because we were not able to exclude cropland from the study area using the coarse resolution AVHRR and MODIS NDVI images. In Inner Mongolia, during 1985-2005, 20.3% (23.9 million hectares) of the total land had been reclaimed for grain production (13.14%, 15.5 million hectares), fodder production (5.93%, 7.0 million hectares), and other uses (1.19%, 1.4 million hectares; Chapter Four). Moreover, census data indicated that the total area of cropland increased about 40% from 1982 to 2009 (ACBIMAR, 2005, 2010). The quantitative interpretations of NPP dynamics driven by climate and socioeconomic variables across ecological zones of Inner Mongolia and Mongolia is presented in another piece of our work (Chapter Five).

Acknowledgments

This work was conducted with financial support from the NASA Land-Cover and Land-Use Change Program (NNX09AK87G). The authors would like to thank Professor Xing Qi from the Inner Mongolian Institute of Grassland Survey and Design, for field data collection. The authors also thank the NASA Global Inventory Modeling and Mapping Studies (GIMMS) group and the MODIS Land Discipline group for producing and sharing GIMMS AVHRR NDVI and MODIS NDVI products. The incident surface solar radiation data used in this study were acquired from the Goddard Earth Sciences (GES) Data and Information Services Center (DISC).

Chapter Three

Estimating the Quantity and Quality of Grassland Communities across an Ecological Gradient of the Inner Mongolian Grasslands with *In Situ* Hyperspectral Remote Sensing

Abstract

Grassland degradation, including the deterioration grassland productivity, has been evident in Inner Mongolia, China, over the past few decades. Hyperspectral remote sensing has the potential for monitoring and measuring ecological variables of grassland ecosystems that have been difficult to measure using multispectral sensors. In this study, we analyzed the spectral reflectance of the representative grassland communities and explored the relationships between hyperspectral indices and aboveground biomass of grassland communities across an ecological gradient of the Inner Mongolian grasslands, based on field samples across a large geographic area. The results showed that the ecological variables of grassland communities generally decreased from meadow to typical and desert steppes. The spectral reflectance curves of different types of grassland ecosystems were generally differentiable. In the three sites with fenced and grazed plot pairs, the fenced plots had lower reflectance in the visible bands and higher reflectance in the near infrared bands. The grazed plots showed a shift of the red-edge inflection points toward shorter wavelengths (i.e., "blue-shift"). The predictive power of vegetation indices (VI) for aboveground biomass generally decreased from desert to typical and meadow steppes. All narrowband VI tended to saturate at the study sites with high vegetation densities. The REIP produced better prediction accuracies than VI in meadow and typical steppes, but it was not a good predictor of aboveground biomass in desert steppe.

Keywords: *In situ* hyperspectral remote sensing; grassland communities; canopy reflectance curves; hyperspectral indices; ecological variables; Inner Mongolian grasslands

---

Wang, J., Brown, D. G., Bai, Y., and Xie, Y. Estimating the quantity and quality of grassland communities across an ecological gradient of the Inner Mongolian grasslands with *In Situ* hyperspectral remote sensing. Manuscript submitted for review.

3.1 Introduction

Grasslands are the dominant ecosystem types on the Mongolian plateau, including the Inner Mongolia Autonomous Region (IMAR), China. In IMAR, the average grassland productivity decreased from 1871 to 900 kg/ha over the past 50 years (1961−2010), and 90% of grasslands are in various stages of degradation (Chapter Four). Grassland degradation has significant impacts on herder livelihoods, carbon sequestration, and biodiversity conservation. Sustainable governance of the Inner Mongolian grassland resources requires a thorough understanding of grassland productivity and the up-to-date information about spatial distributions of grassland communities.

The main advantage of remote sensing technology in mapping grassland quantity and quality, compared with traditional large-scale ecological field approaches, are that it can repeatedly monitor large-scale grassland ecosystems at relatively low cost. Accurate spatial monitoring and assessment of terrestrial vegetation are increasingly critical for ecological conservation and restoration purposes, e.g., dealing with grassland degradation. Satellite images derived from broadband sensors have been used for studying biophysical properties of vegetation for decades. A major limitation of multispectral image data is their coarse spectral resolutions, which could mask the detailed reflectance features of vegetation canopies (Thenkabail et al., 2000). In addition, our previous work of mapping grassland types and their qualities in the Inner Mongolian grasslands was mainly based on visual interpretations of Landsat images, which was tedious and could introduce errors because interpreters were with different field experience and image interpretation skills. Because of its greater spectral dimensionality, hyperspectral data provide more detailed information on structural, biochemical, and biophysical properties of vegetation cover (Blackburn, 1998; Cho, 2007; Darvishzadeh et al., 2008; Hansen and Schjoerring, 2003; Treitz and Howarth, 1998). Therefore, hyperspectral remote sensing provides the potential for accurately and efficiently mapping grassland types and their degradation status in the Inner Mongolian grasslands.

There are essentially two approaches to estimating aboveground biomass of vegetation using hyperspectral data: statistical models (Cho, 2007; Darvishzadeh, 2008; Todd, 1988) and radiative

transfer models (Jacquemoud et al., 1995, 2009). In this chapter, we focused on using empirical-statistical methods for predicting aboveground biomass of grassland communities in IMAR. For this type of methods, a number of indices derived from spectral reflectance curves, such as spectral vegetation indices (VI) and red-edge inflection points (REIP), have been developed and used for predicting ecological variables of vegetation. VI are usually calculated from the linear combinations of reflectance in the red and near infrared (NIR) portions of the spectrum, and they exploit the contrast between low reflectance in the red band due to chlorophyll absorption and high reflectance in the NIR band related to multiple scattering effects. The frequently used VI include simple spectral ratio (SR) (Jordan, 1969), normalized difference vegetation index (NDVI) (Rouse et al., 1974), soil adjusted vegetation index (SAVI) (Huete, 1988), modified soil adjusted vegetation index (MSAVI) (Qi et al., 1994), and triangle vegetation index (TVI) (Broge and Leblane, 2000). The major limitation of using VI to study ecological variables of vegetation is that their values approach a saturation level above a certain level of biomass density (Gao et al., 2000; Hurcom and Harrison, 1998; Tucker, 1977). Hyperspectral remote sensing with hundreds of narrowbands provides an opportunity to develop new VI and refine conventional approaches for studying ecological variables of vegetation. A typical approach to identify the optimal VI is to calculate all possible linear combinations of two narrowbands and identify a band combination that has the highest fitness with ecological variables (Thenkabail et al., 2000; Thenkabail et al., 2004).

Besides VI, the REIP are the other type of frequently used hyperspectral indices for studying ecological variables of vegetation. The red-edge of the reflectance curve for green vegetation denotes a region of transition from the strong chlorophyll absorption in the red bands to the strong NIR reflectance. The REIP is usually found at wavelengths between 680 nm and 740 nm (i.e., around 720 nm), and it has been used to estimate vegetation nutritional status, based on the relationship between chlorophyll concentration and plant productivity (Cho, 2007). Several methods have been developed to calculate the REIP, such as maximum first-order derivative of spectra (Dawson and Curran, 1998), four-point linear interpolation (Guyot and Baret, 1998), the inverted Gaussian method (Bonham-Carter, 1988), polynomial curve fitting (Pu et al., 2003), and linear extrapolation method (Cho and Skidmore, 2006).

Plant communities of grassland ecosystems are usually composed by diverse sets of plant species. The heterogeneous canopies of plant communities create a challenge for using remote sensing data to estimate grassland quantity and quality. Hyperspectral remote sensing, with hundreds of narrow spectral bands, has the potential to improve our study of heterogeneous grassland communities. The potential of hyperspectral remote sensing for estimating the quantity and quality of grassland communities has been evaluated at laboratory, field, and airborne imaging scales (Adam and Mutanga, 2009; Cho, 2007; Darvishzadeh, 2008; Mutanga, 2004; Schmidt and Skidmore, 2001; Shen et al., 2008). Although VI and REIP are useful for measuring grasslands, grasslands with different biophysical characteristics (e.g., species composition) may produce similar index values if they have similar biomass and canopy cover percentages. Therefore, investigating spectral reflectance characteristics of various grassland communities is also important for mapping grassland types and their qualities. Besides the hyperspectral studies of grassland ecosystems in Europe (Cho, 2007; Darvishzadeh, 2008) and Africa (Adam and Mutanga, 2009; Mutanga, 2004; Schmidt and Skidmore, 2001), hyperspectral remote sensing also has been used for investigating spectral reflectance characteristics of grassland communities and predicting grassland aboveground biomass in the Inner Mongolian grasslands (Gao et al., 2012; Ren et al., 2011; Yamano et al., 2003). However, the above studies were implemented in only one of the major types of grassland ecosystems (i.e., meadow, typical, and desert steppes) of the Inner Mongolian grasslands. A comparative study of the spectral reflectance characteristics of grassland communities across different types of grassland ecosystems in the Inner Mongolian grasslands is still missing.

In this study, we used *in situ* hyperspectral remote sensing to estimate the quantity and quality of the representative grassland communities across an ecological gradient of the Inner Mongolian grasslands. We aimed to investigate (1) the spectral reflectance characteristics of the representative grassland communities across different types of grassland communities; (2) the differences in the spectral reflectance of the grazed and fenced grassland communities; (3) the performance of using multiple hyperspectral indices for predicting aboveground biomass of the representative grassland communities. We expected that the spectral library of the representative grassland communities built through this study and the explorations between spectral characteristics and ecological variables of grassland communities across the major types of

grassland ecosystems could be used to provide the foundations for future large-scale efforts of monitoring grassland communities in Inner Mongolia using either airborne or space-borne imaging spectroradiometers. Following this introduction, in Section 3.2, we briefly introduce the Inner Mongolian grasslands and field data collection procedures and the methods used for processing field data and linking hyperspectral and ecological data. The results and discussion are presented in Sections 3.4 and 3.5. Finally, we summarize the major findings of this work.

3.2 Study Area and Data

3.2.1 Study Area

The study area is located in the Inner Mongolia Autonomous Region (IMAR), China, which is part of the Mongolian plateau (Fig. 3.1). Grasslands are the dominant ecosystem types in IMAR, covering about 66% (0.78 million km^2) of the total territory (Angerer et al., 2008; Zhang, 1992). Vegetation types vary from forests, meadow steppe, typical steppe, and desert steppe to desert along an ecological gradient from east to west of IMAR. In order to investigate spectral and ecological characteristics of the representative grassland communities across the Inner Mongolian grasslands, field sampling sites were selected along an ecological gradient (e.g., from wet to dry areas) and covering meadow, typical, and desert steppes (Fig. 3.1).

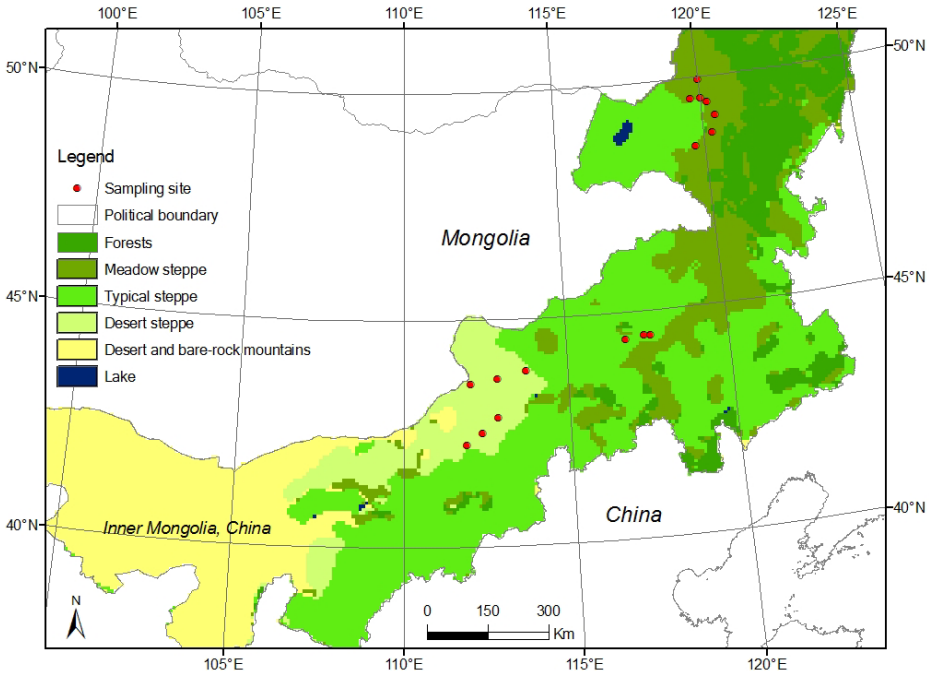

Fig. 3.1 Field sampling sites across the ecological gradient of the Inner Mongolian grasslands. The vegetation map of Inner Mongolia, China, was provided by the Institute of Botany, China. It was made in the 1990s with an original scale of 1:1,000,000.

3.2.2 Field Data Collection

In situ canopy spectral reflectance of the representative grassland communities across an ecological gradient of the Inner Mongolian grasslands were collected using Analytical Spectral Devices (ASD) FieldSpec 3 spectrometer, which has a wavelength ranging from 350 to 2500 nm with a sampling interval of 1.4 nm for the spectral region 350−1000 nm, 2 nm for the spectral region 1000−2500 nm, and a spectral resolution of 3−10 nm. The sampled spectra were then interpolated by the ASD software to produce readings at every 1 nm (ASD Inc., Boulder, Colorado, USA). The field campaign was carried out in August of 2010 (i.e., from August 1st to August 22th) using stratified random sampling with clustering. The study area was first stratified into meadow, typical, and desert steppes using the vegetation map of IMAR (Fig. 3.1). Then, seven field sites in meadow steppe; three sites in typical steppe; and six sites in desert steppe were selected. The field site selection was mainly based on the representativeness of local grassland communities, but the travel distance was also a consideration. For most of these sampling sites, three replicate plots were selected. The plot size was 30 m × 30 m, and the plot size was set to resemble the pixel size of EO-Hyperion images. The replicated plots of each site

were selected to account for the spatial variability of local biophysical environment. In meadow steppe, we had three sites with grazed and fenced (i.e., permanent exclosures) plot pairs. For these three sites, six plots were sampled: three plots were in the exclosures; and three plots were outside of the exclosures. In total, we sampled 57 field plots across meadow, typical, and desert steppes.

In order to account for the spatial variability of grassland communities in one field plot, 16 spectral samples and nine ecological samples were taken along the diagonals of each plot. The spectral and ecological subplots within each plot were set with equal distances. The spectral samples were taken between 10:00 am−14:00 pm under sunny and cloudless conditions. The field of view (FOV) of the sensor was 25°. Scans were taken from a height of 1.5 m looking towards the nadir so that the field of view at the ground was 1.4 m in diameter. Care was taken to avoid including shadows or equipment within the field of view. Each of 16 measurements in one plot was sampled ten times to account for random measurement errors. The sensor was calibrated with white reference Spectralon panel after every eight measurements to offset any changes in solar illuminations and weather conditions. The radiances recorded by the sensor were then converted to reflectance by the software package ViewSpecPro (ASD Inc., Boulder, Colorado, USA). For each plot, ecological samples of grassland communities were taken right after spectral samplings. The size of each subplot was 1 m × 1 m. The aboveground biomass (AGB) was harvested using the traditional agronomic methods. The standing senesced biomass and litter were excluded from the measurement of AGB, and only live biomass was collected. Moreover, canopy height (cm), canopy cover percentage (%), and the number of plant species were also measured at each subplot. GPS was used to locate the sampled plots in the field.

3.3 Methods

3.3.1 Preprocessing In Situ Hyperspectral Data

The analyses of spectral reflectance characteristics of grassland communities and the linear relationships between spectral and ecological measurements were conducted at plot level. Measurement errors in the field spectra, identified as any individual measurement among the ten

repeated measurements that deviated highly from the means, were removed from calculating the mean values of the spectral reflectance. Then, all measurements in one plot were averaged to represent the spectral reflectance for that plot. In this step, any of the 16 samples in one field plot that had more than five of their individual measurements identified as errors were removed from the averaging process. In order to reduce the background effects from soil, we normalized all of the averaged field spectra by dividing by the mean spectral reflectance for each plot (Gong et al., 2001). The normalized spectra were then smoothed using the Savitsky-Golay least-squares method (Tsai and Philpot, 1998) to reduce sensor noise. In this study, we only used the visible and NIR portions (350−900 nm) of the field spectra. Other spectral bands were removed, and this was mainly due to the noises caused by atmospheric water absorption. In addition to spectral reflectance curves, we also used spectral derivatives to characterize the key spectral features of the investigated grassland communities. Considering the higher order (i.e., second or higher) spectral derivative processing is very sensitive to data noise (Pu, 2012), only the first-order derivative analysis was conducted in this study. Grassland AGB, canopy height, canopy cover percentage, and the number of plant species in each plot was averaged from the nine subplots.

3.3.2 Vegetation Indices, Red-Edge Inflection Points, and Aboveground Biomass Prediction

In this study, we selected four frequently used VI (i.e., SR, NDVI, SAVI, and TVI) to predict AGB of grassland communities in meadow, typical, and desert steppes of the Inner Mongolian grasslands. Our field sites were selected across a large geographic area, which were with different percentages of vegetation cover. Therefore, SAVI was used since this index can account for soil background effects. However, due to lack of field data to calibrate the L parameter in SAVI across the field sites with different biophysical conditions. L was set as 0.5 because this value can be used for a wide range of vegetation conditions (Huete, 1988). TVI was created to describe the radiative energy absorbed by the pigments as a function of the relative difference between red and near-infrared reflectance in conjunction with the magnitude of reflectance in the green region (Broge and Leblane, 2000). TVI was calculated as the area of the triangle defined by the green peak, the chlorophyll absorption minimum (i.e. red valley), and the NIR shoulder in the spectral space.

$$SR = R_{NIR} / R_{red} \tag{3-1}$$

$$NDVI = (R_{NIR} - R_{red}) / (R_{NIR} - R_{red}) \tag{3-2}$$

$$SAVI = (R_{NIR} - R_{red})(1 + L) / (R_{NIR} + R_{red} + L), \quad L = 0.5 \tag{3-3}$$

$$TVI = [120 \times (R_{750} - R_{550}) - 200 \times (R_{670} - R_{550})] \times 0.5 \tag{3-4}$$

where R_{550}, R_{670}, and R_{750} are the spectral reflectance at the wavelengths of 550 nm (green), 670 nm (red), and 750 nm (NIR), respectively. The constants 0.5, 120, and 200 in Equation 3-4 are empirical values.

In order to determine the optimal red and NIR band combinations of VI (i.e., SR, NDVI, and SAVI) for predicting AGB, we calculated all two-band combinations between red (630−690 nm) and NIR (760−900 nm) portions of the reflectance spectrum. we ran linear regression between narrowband VI and AGB to identify the spectral bands that were more sensitive to AGB. The narrowband combinations with the highest values of the coefficient of determination (R^2) were selected for further analyses. Considering the spatial variations of biophysical conditions across meadow, typical, and desert steppes, we ran linear regression models for each of these types of grassland ecosystems and explored the spatial variability of the linear relationships.

In this study, we explored whether the REIP of grassland communities with livestock grazing showed the “blue-shift” phenomena, compared with the REIP of grassland communities with permanent exclosures. “Blue-shift” (i.e., a shift of the REIP towards shorter wavelengths) and “red-shift” (i.e., a shift towards longer wavelengths) are related to plant growth conditions. “Blue-shift” is associated with a decrease in green vegetation density, and “red-shift” is associated with an increase in chlorophyll concentration (Mutanga, 2004). Moreover, we also used the REIP as another set of predictors for predicting AGB of grassland communities. We applied five frequently used methods for calculating the REIP, including maximum first-order derivative, four-point linear interpolation, the inverted Gaussian method, polynomial curve fitting, and linear extrapolation.

The maximum first-order derivative of reflectance defines the REIP as the wavelength where the first-order derivative of the spectral reflectance curve reaches its maximum value. The first-order derivative of spectral reflectance calculates the slope values from the spectral reflectance (Dawson and Curran, 1998)

$$FDiff_{\lambda(i)} = (R_{\lambda(j+1)} - R_{\lambda(j)}) / \Delta_{\lambda} \tag{3-5}$$

$$REIP_{FDiff} = \lambda_{\max(FDiff)} \tag{3-6}$$

where $FDiff_{\lambda(i)}$ is the first-order derivative at a wavelength i midpoint between wavebands j and $j+1$. $R_{\lambda(j)}$ and $R_{\lambda(j+1)}$ are reflectance at j and $j+1$ wavebands, respectively; Δ_{λ} is the difference in wavelengths between j and $j+1$.

The four-point linear interpolation method assumes that the spectral reflectance at the red-edge can be simplified to a straight line centered at a midpoint between the reflectance in the NIR shoulder (i.e., around 780 nm) and the minimum reflectance in the red bands (i.e., around 670 nm). The reflectance value is first estimated at the inflection point (Equation 3-7). Then, a linear interpolation is applied for the spectral reflectance at 700 nm and 740 nm for estimating the wavelength corresponding to the estimated reflectance at the inflection point (Equation 3-8) (Guyot and Baret, 1998)

$$R_{red-edge} = (R_{670} + R_{780}) / 2 \tag{3-7}$$

$$REIP = 700 + 40 \times (R_{red-edge} - R_{700}) / (R_{740} - R_{700}) \tag{3-8}$$

where the constants 700 and 40 result from interpolation between 700 nm and 740 nm intervals, and R_{670}, R_{700}, R_{740}, and R_{780} are the reflectance values at 670 nm, 700 nm, 740 nm, and 780 nm, respectively.

The inverted Gaussian method explains the variations in reflectance as a function of wavelength (λ) at the REIP as (Bonham-Carter, 1988)

$$R_{\lambda} = R_s - (R_s - R_o)\exp(-(\lambda_0 - \lambda)^2 / 2\sigma^2) \tag{3-9}$$

$$REIP = \lambda_0 + \sigma \tag{3-10}$$

where R_s is the maximum shoulder reflectance, R_o and λ_0 are the minimum spectral reflectance and corresponding wavelengths, and σ is the variance of the Gaussian function.

For the polynomial curve fitting method, a red-edge reflectance curve between the wavelengths corresponding to the minimum reflectance in red (i.e., red valley) and the maximum NIR shoulder reflectance are fitted with a fifth-order polynomial equation as (Pu et al., 2003)

$$R_\lambda = a_0 + \sum_{i=1}^{5} a_i \lambda^i \tag{3-11}$$

where λ represents the wavebands in the red-edge, a_0 and a_i are the regression coefficients. The REIP is determined from the maximum first-order derivative spectrum. The first-order derivative was calculated using a first difference transformation of the reflectance obtained from the polynomial fit.

The linear extrapolation method is based on the linear extrapolation of two straight lines through two points on the far-red (680−700 nm) and two points on the NIR (725−760 nm) flank of the first-order derivative reflectance spectrum of the red-edge region (Cho and Skidmore, 2006). The REIP is defined by the wavelength value at the intersection of the straight lines (Equation 3-14)

Far-red line: $FDR_1 = m_1\lambda + c_1$ (3-12)

NIR line: $FDR_2 = m_2\lambda + c_2$ (3-13)

$$REIP = -(c_1 - c_2)/(m_1 - m_2) \tag{3-14}$$

where FDR_1 and FDR_2 are the first-order derivatives of reflectance, m_1 and m_2 are the slopes, c_1 and c_2 are the intercepts, and λ is the wavelength.

The independent data test and the cross-validation method are the two frequently used methods for validating regressions between hyperspectral indices and ecological variables of vegetation. Studies have demonstrated that the results of the two methods in terms of R^2 and root mean square error (RMSE) were similar (Darvishzadeh et al., 2008; Selige et al., 2006). In this

study, due to the limited number of field samplings relative to the large geographic area of the Inner Mongolian grasslands, we applied the cross-validation method, which is also called the leave-one-out method, to validate all of the linear regression models. In cross-validations, each sample was iteratively taken out and predicted by the remaining samples. As the predicted samples were not the same as the samples used to build the regression models, the cross-validated root mean square error ($RMSE_{CV}$) was selected as the accuracy indicator of the regression models in predicting unknown samples. Cross-validation can detect outliers and provide nearly unbiased estimations of the prediction error (Schlerf et al., 2005).

3.4 Results

3.4.1 Ecological Variables of the Investigated Plant Communities

The dominant plant species of the investigated grassland communities in meadow, typical, and desert steppes of the Inner Mongolian grasslands are shown in Table 3.1. *Stipa baicalensis*, *Stipa krylovii*, and Carex *pediformis* were the dominant plant species in meadow steppe; *Leymus chinensis* and *Stipa grandis* were the dominant plant species in typical steppe; *Artemisia frigid*, *Salsola collinsa*, *Stipa klemenzii*, and *Allium polyrhizum* were the dominant plant species in desert steppe. For the three sites with permanent exclosures, the dominant plant species varied between the fenced and grazed plots. This indicated that livestock grazing affected species compositions of the grassland communities. The descriptive statistics of the ecological variables for the investigated grassland communities are shown in Table 3.2. Overall, AGB, canopy cover percentage, canopy height, and species diversity decreased in values from meadow to typical and desert steppes. In meadow steppe, the fenced plots had higher AGB, canopy cover percentage, canopy height, and species diversity than the grazed plots. For these three sites, AGB and canopy height decreased more rapidly than canopy cover percentage and species diversity from the fenced to grazed plots. In this study, we only focused on predicting AGB of grassland communities using hyperspectral indices. However, other four ecological variables also could affect the spectral reflectance of the investigated grassland communities. The results of linear regression analyses between AGB and the other four ecological variables showed that AGB was

a good predictor of canopy height and canopy cover percentage ($R^2 > 0.7$, $p < 0.01$), but it was not a good predictor of species diversity ($R^2 < 0.3$, $p < 0.01$).

Table 3.1 Dominant plant species of the investigated plant communities.

Grassland type	Field site	Dominant plant species
Meadow steppe	1	*Carex pediformis+Filifolium sibiricum*
	2	*Carex pediformis*
	3	*Koeleria cristata+Stipa krylovii+Festuca ovina*
	4	*Filifolium sibiricum+Bupleurum+Stipa baicalensis*
	5_Fenced	*Stipa baicalensis+Filifolium sibiricum+Leymus chinensis*
	5_Grazed	*Stipa baicalensis+Leymus chinensis+Carex pediformis*
	6_Fenced	*Carex pediformis+Leymus chinensis*
	6_Grazed	*Carex pediformis+Agropyron cristatum*
	7_Fenced	*Leymus chinensis*
	7_Grazed	*Taraxacum mongolicum+Plantago depressa+Carex duriuscula*
Typical steppe	8	*Leymus chinensis+Stipa grandis+Anemarrhena asphodeloides*
	9	*Stipa grandis*
	10	*Stipa grandis*
Desert steppe	11	*Carex duriuscula+Kochia prostrata+Artemisia frigida*
	12	*Allium polyrhizum+Ceratoides latens+Salsola collinsa*
	13	*Stipa klemenzii*
	14	*Cleistogenes songorica+Stipa breviflora+Allium polyrhizum*
	15	*Salsola collinsa+Stipa krylovii*
	16	*Allium polyrhizum+Stipa klemenzii*

Table 3.2 Descriptive statistics of the ecological parameters for the investigated plant communities.

Grassland type	Field site	AGB [a] (g/m^2)		CCP [a] (%)		CH [a] (cm)		NPS [a] (n)	
		Mean	SD	Mean	SD	Mean	SD	Mean	SD
Meadow steppe	1	656.79	76.81	63.04	11.89	35.56	3.95	14.04	3.17
	2	634.39	175.60	51.85	15.28	32.41	5.34	17.04	0.61
	3	547.63	137.86	63.33	6.19	26.67	3.38	16.63	0.94
	4	481.06	38.31	44.07	1.70	20.22	0.29	14.81	2.68
	5_Fenced	492.97	42.26	40.00	6.96	35.30	3.17	11.96	2.43
	5_Grazed	361.31	35.62	38.92	11.28	21.44	4.73	11.51	3.76
	6_Fenced	419.42	115.55	39.26	4.98	30.85	4.33	15.03	2.07
	6_Grazed	295.59	48.44	31.30	2.80	19.30	2.12	9.67	1.37
	7_Fenced	822.17	63.07	66.48	13.17	44.63	3.53	8.85	1.54
	7_Grazed	258.89	44.94	50.93	12.84	14.89	1.09	8.44	1.20
Typical steppe	8	430.32	38.70	44.44	3.38	23.33	0.96	6.11	0.44
	9	418.58	21.90	43.89	2.78	26.85	0.85	9.22	0.19
	10	390.01	83.13	46.67	11.48	30.19	2.57	7.67	0.40
Desert steppe	11	143.53	9.74	25.56	2.55	12.85	1.98	7.48	0.74
	12	100.13	23.75	23.15	3.78	15.37	0.64	4.78	0.68
	13	106.71	13.13	27.22	2.89	19.44	0.56	5.63	0.71
	14	168.26	27.53	29.07	3.35	13.15	1.16	7.81	0.45
	15	430.58	5.29	40.93	2.31	14.07	1.77	8.00	0.62
	16	167.90	52.39	32.22	10.18	11.30	0.85	7.93	1.12

[a] CCP means canopy cover percentage; CH means canopy height; NPS means number of plant species; and SD means standard deviations of measurements from three subplots at each site.

3.4.2 Canopy Reflectance Curves of the Investigated Plant Communities

Given space limitations, we only showed the spectral reflectance curves and their first-order derivatives for one of the three plots at each site (Fig. 3.2). The spectral reflectance curves of the investigated grassland communities showed clear differences across meadow, typical, and desert steppes. The NIR reflectance generally decreased from meadow to typical and desert steppes. The green peaks and red valleys were distinctive in meadow and typical steppes and less differentiable in desert steppe. The spectral reflectance curves of grassland communities in desert steppe were similar to the reflectance curve of bared soil. The field sampling sites in desert steppe were with low canopy cover percentages (Table 3.2), vegetation-soil spectral mixing is still a challenge in desert steppe. The reflectance curves of grassland communities at site 15 were the outliers in desert steppe (Fig. 3.2e). At this site, the NIR reflectance of grassland communities was higher than the other field sites, and the red valley was also distinctive. This site also had the highest values of ecological variables among the six sites of desert steppe (Table 3.2). The first-order derivatives for all of the grassland communities had two peaks: one was in the green bands, and the other was in the red-edge, and the maximum values of the first-order derivatives were distinctive in the red-edge peaks (Fig. 3.2b, d, and f). Overall, the maximum values of the first-order derivatives generally decreased from meadow to typical and desert steppes. This was consistent with the distinctiveness of red-edges of the spectral reflectance curves.

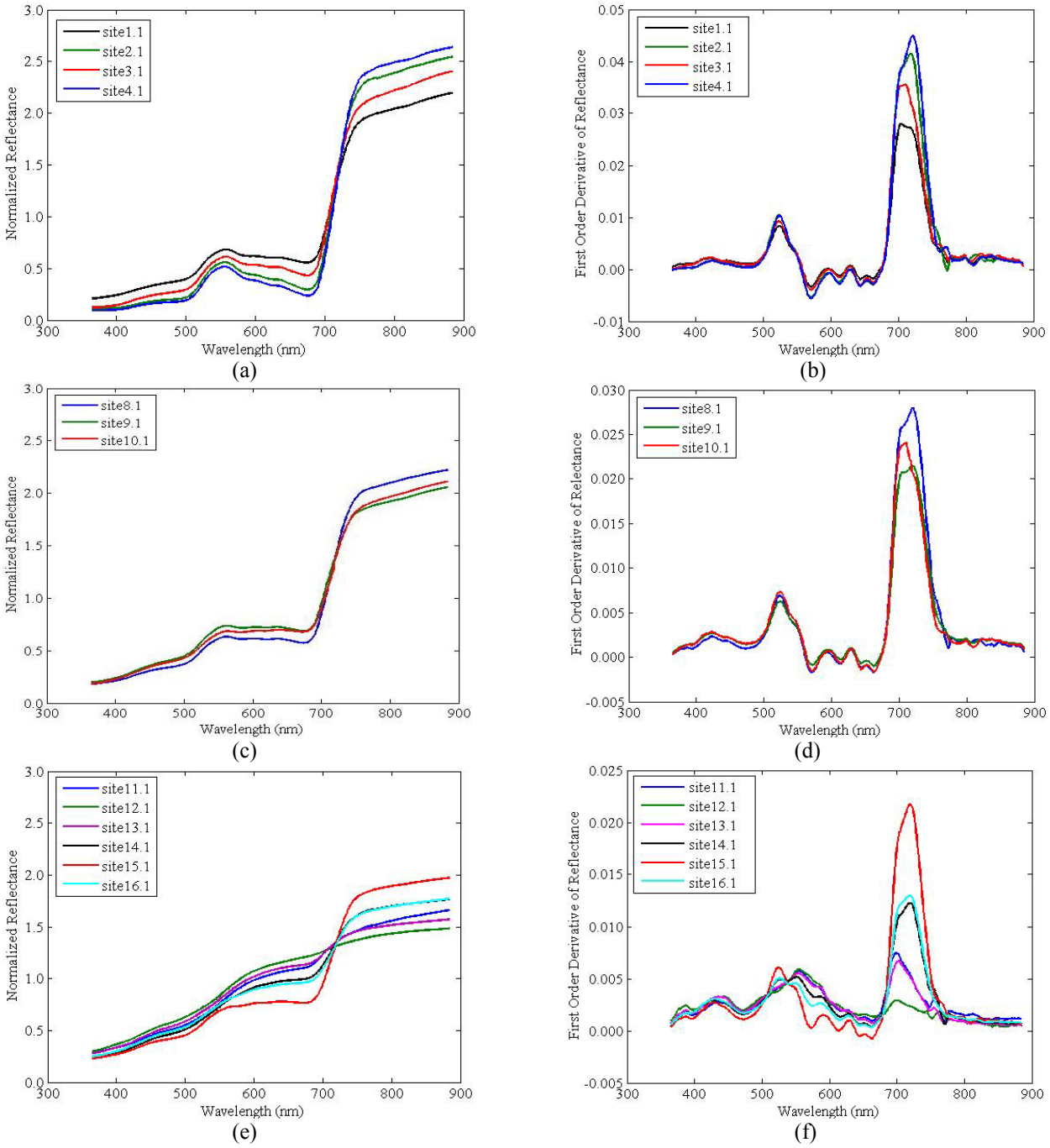

Fig. 3.2 The normalized canopy reflectance curves and their first-order derivatives of the investigated grassland communities: (a), (c), and (e) are the normalized reflectance curves in meadow, typical, and desert steppes; (b), (d), and (f) are the first-order derivatives of (a), (c), and (e). In each plot, there were measurements from at least 12 subplots (120 measurements) used for spectral averaging. In order to make the reflectance curves more readable, standard deviation bars were not added on the plots.

Investigating whether grassland communities under different human disturbance can be spectrally differentiated is important for monitoring and mapping grassland degradation status under human disturbance. Similar to the above analyses, we analyzed the spectral reflectance curves for the three sites with fenced and grazed plot pairs. Given space limitations, we only showed the reflectance curves and their first-order derivatives for one of the three plots at each study site (Fig. 3.3). The sampled grassland communities of the fenced and grazed plots can be differentiated by their normalized spectral reflectance curves and their first-order derivatives. Compared with the grazed plots, the fenced plots had higher values of normalized reflectance in the NIR wavebands and lower values of normalized reflectance in the visible wavebands. The first-order derivatives of spectral reflectance were distinctive in the red-edge (Fig. 3.3b, d, and f). Livestock grazing affected the spectral reflectance characteristics of grassland communities. However, due to lack of detailed data about livestock grazing intensity for the grazed plots, we were not able to explain the variations of the difference in the normalized reflectance between the fenced and grazed plots across the three study sites. The REIP for the plots in the field sites with grazed and fenced plot pairs, calculated by the five methods, are shown in Table 3.3. The REIP in the fenced plots were generally higher than the REIP of the grazed plots. This was the so called “blue-shift” due to livestock grazing. For some fenced and grazed plot pairs, the REIP calculated by the maximum first-order derivative method and the four-point linear interpolation method were the same or counterintuitive (i.e., the REIP of the grazed plots were higher).

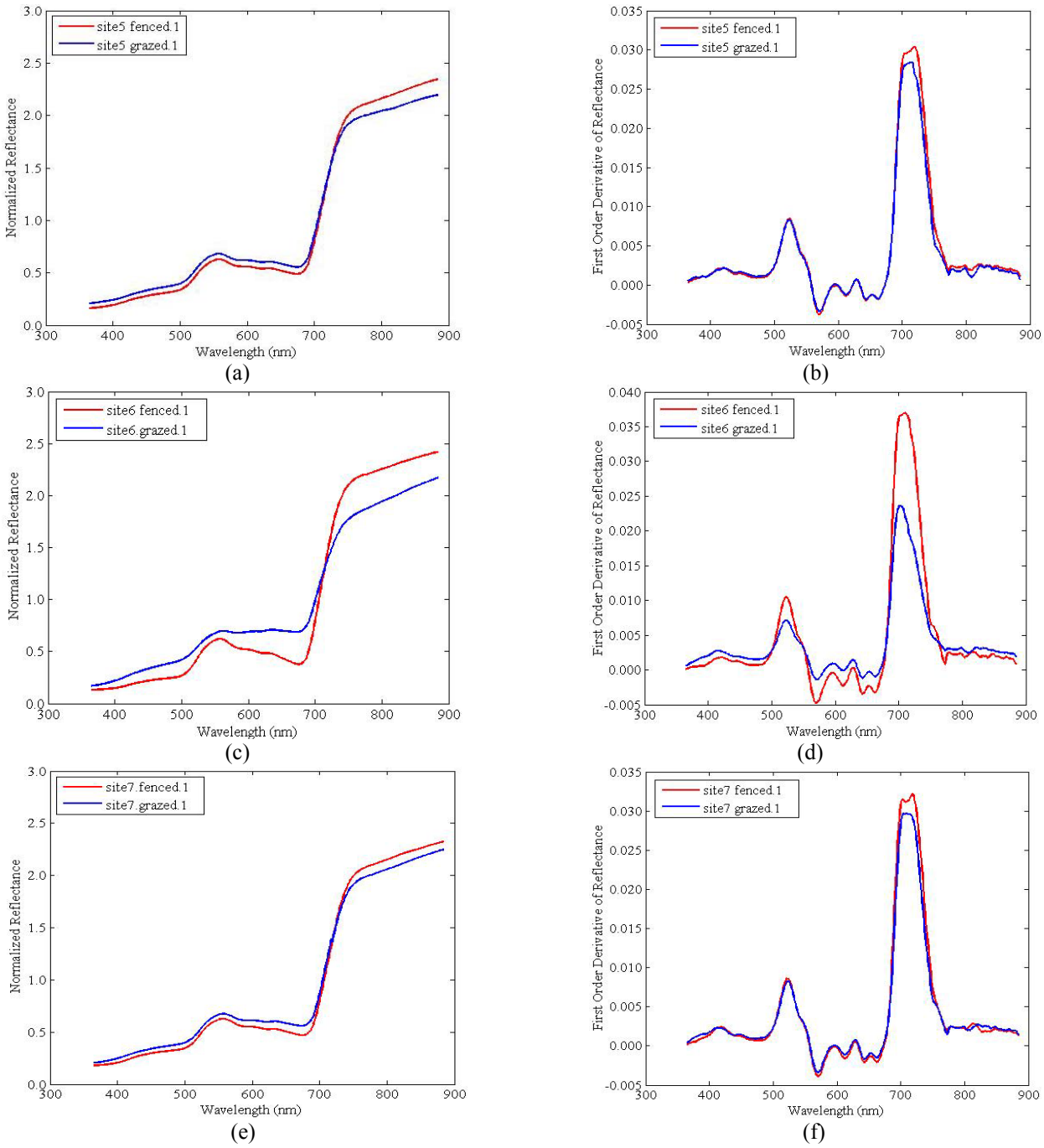

Fig. 3.3 The normalized canopy reflectance curves and their first-order derivatives of the field sites with fenced and grazed plot pairs: (a), (c), and (e) are the normalized reflectance curves; (b), (d), and (f) are the first-order derivatives of (a), (c), and (e). In each plot, there were measurements from at least 12 subplots (120 measurements) used for spectral averaging. In order to make the reflectance curves more readable, standard deviation bars were not added on the plots.

Table 3.3 The REIP of reflectance for the sites in meadow steppe with fenced and grazed plot pairs.

Field site	Field plot	MFD [a]		LFPI [a]		IGM [a]		PCF [a]		LEM [a]	
		Mean	SD	Mean	SD	Mean	SD	Mean	SD	Mean	SD
5	Fenced.1	713	0.59	718	0.60	717	0.58	718	0.48	718	0.53
	Grazed.1	710	0.61	716	0.70	715	0.65	713	0.50	715	0.61
	Fenced.2	714	0.56	717	0.57	716	0.57	716	0.59	717	0.62
	Grazed.2	710	0.55	712	0.42	710	0.60	711	0.63	713	0.38
	Fenced.3	**708**	**0.59**	718	0.56	715	0.48	717	0.70	716	0.72
	Grazed.3	**717**	**0.52**	716	0.39	711	0.54	716	0.54	712	0.60
6	Fenced.1	714	0.74	715	0.77	714	0.69	714	0.73	713	0.68
	Grazed.1	710	0.67	713	0.52	705	0.47	709	0.60	708	0.53
	Fenced.2	**707**	**0.55**	714	0.35	713	0.51	712	0.57	714	0.54
	Grazed.2	**710**	**0.50**	712	0.33	704	0.66	707	0.49	708	0.47
	Fenced.3	712	0.53	715	0.39	713	0.43	714	0.55	715	0.56
	Grazed.3	708	0.42	711	0.28	708	0.21	711	0.29	709	0.31
7	Fenced.1	**709**	**0.56**	**718**	**0.44**	718	0.69	718	0.64	718	0.63
	Grazed.1	**715**	**1.03**	**718**	**0.82**	715	0.88	715	0.93	716	0.85
	Fenced.2	720	0.62	719	0.30	717	0.73	719	0.75	717	0.77
	Grazed.2	719	0.61	717	0.47	709	0.66	715	0.65	714	0.56
	Fenced.3	717	0.55	**717**	**0.58**	716	0.62	716	0.62	716	0.63
	Grazed.3	715	0.53	**718**	**0.61**	714	0.56	713	0.40	714	0.38

[a] MFD means maximum first-order derivative; LFPI means linear four-point interpolation; IGM means the inverted Gaussian method; PCF means polynomial curve fitting; LEM means the linear extrapolation method; and SD means standard deviation of measurements from at least 12 subplots in each plot.

3.4.3 Optimal Narrowband Vegetation Indices

The coefficient of determination (R^2) for the relationships between AGB and three narrowband VI (i.e., SR, NDVI, and SAVI) computed from all two band combinations between red (630−690 nm) and NIR (760−900 nm) reflectance is shown in Fig. 3.4. The meeting point of each pair of wavelengths in the plots corresponds to the R^2 value between AGB and VI calculated from the reflectance values in those two wavebands. The plots showed that the relationships between AGB and VI varied a function of two-band combinations between the red and NIR reflectance. In meadow steppe, the R^2 values produced by NDVI and SAVI showed similar correlation patterns (Fig. 3.4d and g). NDVI produced higher R^2 values than SAVI in typical and desert steppes. SR produced the lowest R^2 values in typical steppe and the highest R^2 values in desert steppe (Fig. 3.4b and c). Overall, the R^2 values decreased from desert to typical and meadow steppes. Moreover, all of the three VI did not show good predictive power for AGB in meadow steppe ($R^2 < 0.2$, $p < 0.05$) and typical steppe ($R^2 < 0.3$, $p < 0.05$). The grassland

communities in meadow and typical steppes had higher values of AGB and canopy cover percentage than the grassland communities in desert steppe (Table 3.2). The narrowband VI used this study still had the “saturation problem” in predicting AGB for the grassland communities with high vegetation densities. The linear relationships between VI and AGB were dependent on the types of grassland ecosystems and un-suitable for application to large geographic areas.

.

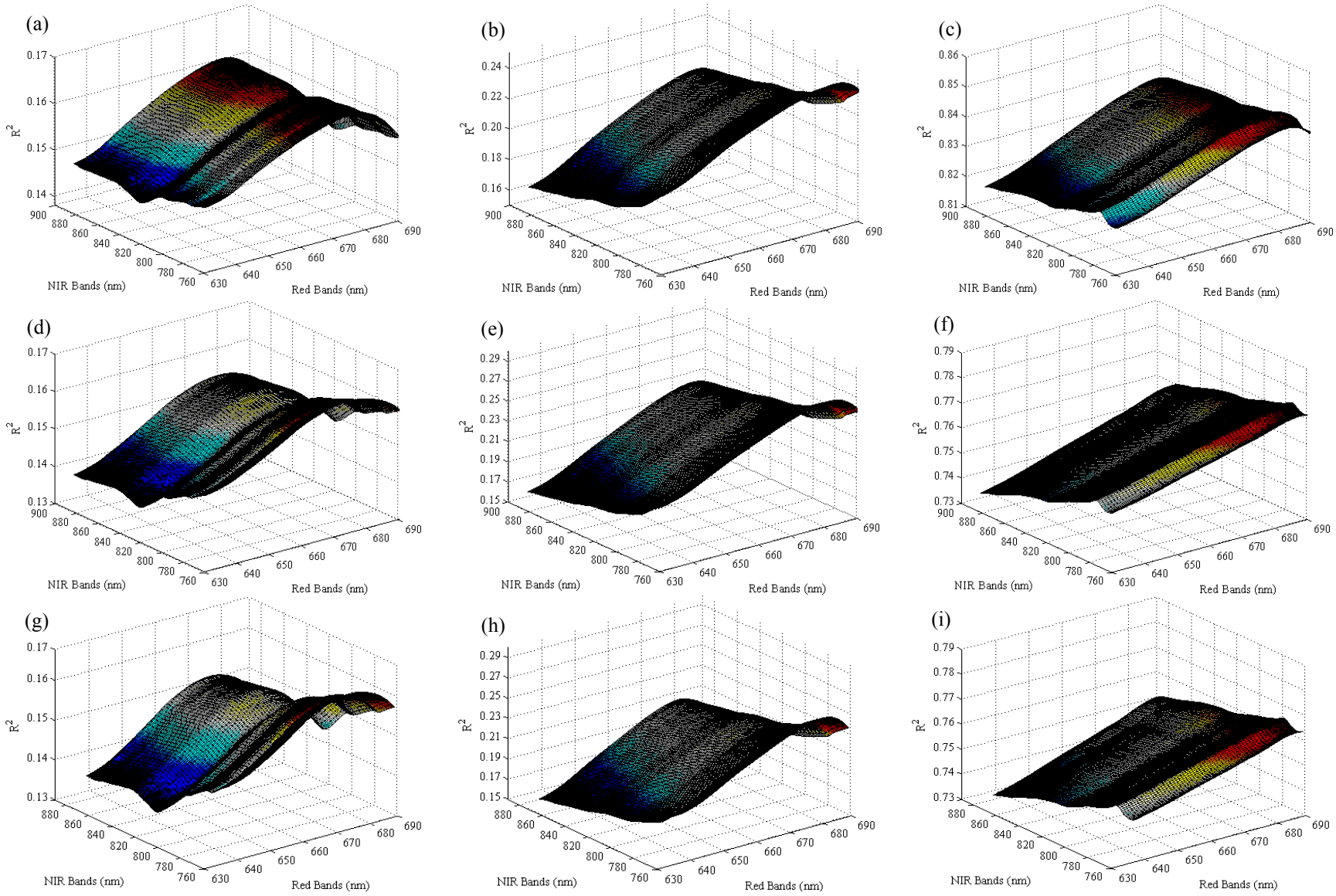
(a)
(b)
(c)
(d)
(e)
(f)
(g)
(h)
(i)
R2
NIR Bands (nm)
Red Bands (nm)

Fig. 3.4 The correlation plots representing the coefficient of determination (R^2) of the linear relationships between VI and AGB, calculated from all possible combinations spread across red and NIR bands: (a), (b), and (c) are the R^2 for the regressions between SR and AGB in meadow, typical, and desert steppes, respectively; (d), (e), and (f) are the R^2 values for the regressions between NDVI and AGB in meadow, typical, and desert steppes, respectively; and (g), (h), and (i) are the R^2 for the regressions between SAVI and AGB in meadow, typical, and desert steppes, respectively.

Narrowband combinations that formed the optimal VI for the three types of grassland ecosystems were determined based on the R^2 values in the plots (Fig. 3.4). The optimal red and NIR band combinations for the three VI are shown in Table 3.4. The optimal narrowbands varied across meadow, typical, and desert steppes. The optimal red wavelengths were generally decreasing from desert to typical and meadow steppes. The optimal NIR wavelengths were the longest in desert steppe, but they were similar in meadow and typical steppes. The linear relationships between VI and AGB were statistically significant at $p < 0.05$, $p < 0.05$, and $p < 0.01$ levels for meadow, typical, and desert steppes, respectively. Together with the REIP and TVI, the three optimal VI were used for predicting AGB of grassland communities for the three types of grassland ecosystems.

Table 3.4 The optimal red and NIR band combinations for predicting AGB in meadow, typical, and desert steppes.

Grassland type	VI	Red band (nm)	NIR band (nm)	R^2	*p*
Meadow steppe	SR	675	760	0.16	< 0.05
	NDVI	677	760	0.16	< 0.05
	SAVI	677	761	0.16	< 0.05
Typical steppe	SR	684	760	0.24	< 0.05
	NDVI	683	761	0.26	< 0.05
	SAVI	684	760	0.25	< 0.05
Desert steppe	SR	687	781	0.84	< 0.01
	NDVI	687	780	0.77	< 0.01
	SAVI	688	780	0.76	< 0.01

3.4.4 Linear Relationships between Hyperspectral Indices and Aboveground Biomass

The performances of linear regression models for predicting AGB using multiple hyperspectral indices are presented in Table 3.5. By stratifying the field spectral and ecological data according to the three types of grassland ecosystems, it was observed that the strength of the linear relationships between hyperspectral predicators and AGB varied across the three types of

grassland ecosystems. The linear regression models with higher R^2 values generally had lower values of the cross-validated root mean square errors ($RMSE_{CV}$). The R^2 values for the linear relationships between VI and AGB decreased from desert to typical and meadow steppes. TVI had the lowest prediction accuracies in meadow and desert steppes. SR had the best prediction accuracies in desert steppe. However, compared with optimal NDVI and SAVI, it had lower prediction accuracies in meadow and typical steppes. SAVI had lower prediction accuracies in typical and desert steppes than NDVI. Compared with VI, the REIP had better prediction accuracies in meadow and typical steppes, but it had lower prediction accuracies in desert steppe. The REIP estimated by the maximum first-order derivative method and the four-point linear interpolation had the lowest performance among the linear regressions using the REIP as the predictor, and the linear regression models based on the REIP extracted by the two methods were also not statistically significant in desert steppe.

Table 3.5 The results of linear regressions between hyperspectral indices and AGB in meadow, typical, and desert steppes.

Hyperspectral Indices	Meadow steppe			Typical steppe			Desert steppe		
	R^2	*p*	$RMSE_{CV}$ [a] (g/m^2)	R^2	*p*	$RMSE_{CV}$ [a] (g/m^2)	R^2	*p*	$RMSE_{CV}$ [a] (g/m^2)
VI									
SR	0.16	< 0.05	96.01	0.24	< 0.05	69.16	0.84	< 0.01	22.33
NDVI	0.16	< 0.05	95.20	0.26	< 0.05	66.33	0.77	< 0.01	24.49
SAVI	0.16	< 0.05	95.66	0.25	< 0.05	67.98	0.76	< 0.01	25.70
TVI	0.15	< 0.05	97.82	0.25	< 0.05	67.50	0.73	< 0.01	23.62
REIP									
MFD	0.32	< 0.05	77.16	0.27	< 0.05	64.41	0.10	> 0.05	50.73
LFPI	0.32	< 0.05	77.82	0.28	< 0.05	63.02	0.08	> 0.05	52.16
IGM	0.35	< 0.05	75.35	0.32	< 0.05	57.40	0.14	< 0.05	43.25
PCF	0.34	< 0.05	76.03	0.30	< 0.05	60.08	0.13	< 0.05	45.81
LEM	0.37	< 0.05	74.28	0.32	< 0.05	56.52	0.15	< 0.05	41.57

[a] $RMSE_{CV}$ means cross-validated root mean square errors for the linear regressions.

3.5 Discussion

We have presented the ecological and spectral characteristics of the representative grassland communities sampled in the field across an ecological gradient of the Inner Mongolian grasslands. The differences in spectral reflectance of grassland communities across the three

major types of grassland communities were resulted from multiple factors, such as dominant plant species, grassland aboveground biomass, canopy cover percentage, and biophysical environment. The dominant plant species for the investigated field sites were mostly different (Table 3.1). This could cause differences in leaf pigments and canopy structures, which consequently caused differences in spectral reflectance given the same aboveground biomass. Second, aboveground biomass of the investigated grassland communities varied from 822.17 g/m^2 in meadow steppe to 100.13 g/m^2 in desert steppe. Differences in biomass density and chlorophyll concentration caused variations in radiation absorption in the red bands and reflectance in the NIR bands. Third, the surveyed field sites were with different percentages of vegetation cover, the spatial variations in soil background (e.g., soil type and water content) and standing litters of vegetation could result in significant differences in spectral reflectance.

Besides the spectral variations across different types of grassland ecosystems, the spectral variations between the fenced and grazed plots were also differentiable. From Tables 3.1 and 3.2 we can see that livestock grazing affected the dominant plant species of grassland communities, aboveground biomass, and other ecological variables, these consequently affected the spectral reflectance of grassland communities. For example, in the grazed plots, the higher reflectance in the visible bands and the lower reflectance in the NIR bands could be caused by the lower vegetation densities and canopy cover percentages. In this study, the maximum first-order derivative method and the four-point linear interpolation method generated some indistinctive and counterintuitive REIP between grazed and fenced plots (Table 3.3). Previous studies also showed that the maximum first-order derivative method has limitations because the maximum derivative values occur within two principal spectral regions around 700 nm and 725 nm (Cho, 2007), and the four-point linear interpolation method can produce REIP estimates biased to longer wavelengths (Cho and Skidmore, 2006).

The spatial variations of the linear relationships between AGB and VI could also be explained by the variations in ecological characteristics of the investigated grassland communities. Among the three optimal narrowband VI, SR and NDVI are determined only by spectral reflectance in the red and NIR bands. They are more sensitive to chlorophyll concentration. High chlorophyll concentration in meadow and typical steppes affected the saturation of radiation absorption in the

red bands, which consequently affected VI calculated from reflectance in the red and NIR bands. Therefore, the R^2 values for the regressions between AGB and VI were lower in meadow and typical steppe. In desert steppe, lower chlorophyll concentration alleviated the saturation effect of red reflectance. Therefore, the R^2 values for the sites in desert steppe were higher. Moreover, compared with NDVI, SAVI did not improve the predictions of AGB. Possible reasons, such as lower variations in soil background and vegetation density in each type of grassland ecosystems, could explain the phenomena. TVI showed the lowest prediction accuracies in meadow and desert steppes. This indicated that TVI was not a good predictor of AGB for the grassland communities with high or low vegetation densities. The REIP calculated by the five methods produced better prediction accuracies than VI in meadow and typical steppes, but it was not a good predictor of AGB in desert steppe. This was mainly caused by the fact that red-edge was mostly indistinctive for the grassland communities in desert steppe (Fig. 3.2e). Other studies have shown that the REIP was a good predictor ($R^2 > 0.6$) of AGB in humid grassland areas (Cho et al., 2007). Our study sites were distributed in semiarid and arid grassland regions. The spectral reflectance of grassland communities in these regions was quite different from the above studies.

3.6 Conclusions

The ecological variables of the investigated grassland communities generally decreased from meadow to typical and desert steppes. In the three sites with permanent exclosures, the grazed plots had higher values of ecological variables than the fenced plots. The spectral reflectance curves of the representative grassland communities and the grassland communities with and without livestock grazing were generally differentiable, and they were distinctive in the red-edge bands of the reflectance spectrum. For the three study sites with grazed and fenced plot pairs, the fenced plots had higher reflectance in the NIR bands and lower reflectance in visible bands than the grazed plots. The REIP of the grazed plots showed “blue-shift.” Over all, the predictive power of optimal narrowband VI for AGB generally decreased from desert to typical and meadow steppes. All narrowband VI tended to saturate at the study sites with high vegetation densities. The REIP was not a good predictor of AGB in desert steppe.

In conclusion, our research results indicated that *in situ* hyperspectral remote sensing is useful for discriminating different grassland communities across an ecological gradient of the Inner Mongolian grasslands and the grassland communities with and without livestock grazing. The results also demonstrated that care must be taken when using regression models for linking spectral and ecological measurements in large geographic scales since they are lack of portability over different types of grassland ecosystems. In the future, we plan to use imaging spectrometers to map grassland types and their qualities in the Inner Mongolian grasslands for reducing the workload and errors of visually interpreting multispectral Landsat images. The *in situ* hyperspectral remote sensing studies provide the foundations for future large-scale efforts of using images derived from imaging spectroradiometers. Considering the large geographic scale and the spatial heterogeneity of the Inner Mongolian grasslands, additional field samplings may be still needed in order to build a rich spectral library for various grassland communities in different biophysical and livestock grazing conditions.

Acknowledgements

This work was conducted with financial support from the NASA Land-Cover and Land-Use Change Program (NNX09AK87G). The authors appreciate the hard work from the students of the Institute of Botany, Chinese Academy of Science (CAS), and Inner Mongolian Agricultural University for field data collection in the summer of 2010. The graduate student Jie Dai from the University of Michigan helped to clean the field data for this work. The authors also would like to acknowledge the Field Spectroscopy Facility group at the University of Edinburgh for their sample MATLAB codes of processing field spectral data.

PART III

INTERPRETATIONS OF GRASSLAND DYNAMICS

Chapter Four

Sustainable Governance of the Mongolian Grasslands: Comparing Ecological and Social-Institutional Changes in Mongolia and Inner Mongolia, China

Abstract

Over the past fifty years, a number of processes have conspired to undermine grassland ecosystem services on the Mongolian plateau. In this chapter, we focus on human dimensions of grassland degradation on the Mongolian plateau since the early 1960s. Mongolia and IMAR share similar ecological gradients of climate, vegetation, and soils, and have undergone significant social-institutional and ecological transformations: from collective to market economies, increasing market integration, and climate variations and change that affect vegetation productivity and human livelihoods. However, the two regions are different in their demographic, ethnic, cultural, economic, and political contexts. Moreover, their governments have different approaches to grassland management. These features of the two regions make comparative analysis interesting and causal inference meaningful for enhancing understanding of sustainable governance and social-ecological dynamics in grassland ecosystems. In the chapter, we first review the literature on models and frameworks for studying grassland dynamics, which were developed by ecologists and institutional analysts. Then, we adopt a hybrid state-market-community framework to analyze the dynamics of social-ecological systems in Mongolian grasslands over the past fifty years based on grassland, socioeconomic, and climate data. We end the chapter with a discussion of strategies for sustainable governance of the Mongolian grasslands in the contexts of climate change and increasing market integration.

Keywords: Grassland degradation; social-institutional changes; climate change; the state-market-community framework; sustainability; Mongolian plateau

---

Wang J., Brown D., and Agrawal A. Sustainable governance of the Mongolian grasslands: comparing ecological and social-institutional changes in the context of climate change in Mongolia and Inner Mongolia, China. In: *Dryland East Asia (DEA): Land Dynamics amid Social and Climate Change*. Edited by Chen J., Wan S., Henebry G., Qi J., Gutman G., Sun G., and Kappas M. HEP-De Gruyter. 2013.

4.1 Introduction

Grasslands occupy about 50% of the earth's terrestrial surface (and 38% of the Asian continent) and are generally characterized by single-stratum vegetation structures dominated by grasses and other herbaceous plants. They provide about 70% of the forage for domestic livestock globally (Brown et al., 2008). The Mongolian grasslands in Mongolia and Inner Mongolia Autonomous Region (IMAR), China constitute the dominant component of the Eurasian grasslands (Angerer et al., 2008). As relatively intact terrestrial ecosystems, they play a significant role in sequestrating carbon dioxide, conserving biodiversity, and providing livelihood benefits to herders. For example, the Mongolian plateau was estimated as a carbon sink of 0.03 Pg C $year^{-1}$ in the 1990s (Lu et al., 2009), compared with the intact tropical forests of 1.33 Pg C $year^{-1}$ in that period (Pan et al., 2011). The numbers of plant species in Mongolia and IMAR are roughly over 3,000 (MNET, 2009) and 2,100 (Xing, 2008). Grassland degradation involves the deterioration of social-ecological performances of these ecosystems, for example for livestock production, and is one of the major environmental problems worldwide. Recent studies show that grasslands in IMAR and Mongolia have degraded to varying degrees; the degradation status in IMAR is more serious than in Mongolia (Angerer et al., 2008; Jiang et al., 2006). Grassland degradation and rural poverty are twin problems; recent studies show that the major income sources for rural households in IMAR and Mongolia are still from livestock production (Olonbayar, 2010; Waldron et al., 2010). Herders in Mongolia rely more heavily on grasslands for their livelihoods than do the herders in IMAR; the livelihood strategies of herders are more diversified in IMAR (Zhen et al., 2010). Both Mongolia and IMAR have been transitioning from a centrally planned economy to a less regulated economy. As a corollary, herders have sought to increase their livelihood benefits by increasing livestock numbers, leading to over-stocking and grassland degradation in many parts of the region.

Scholars from multiple disciplines have contributed to a better understanding of the dynamics of social-ecological systems in the Mongolian grasslands. Increasing populations of humans and livestock, inefficient institutional arrangements for resource governance, distorted market incentives, reclamation of grasslands for grain production, urbanization, changing climate, and the increasing frequencies of climate hazards have all been identified as among the major drivers

of grassland degradation (Angerer et al., 2008; Bijoor et al., 2006; Fernandez-Gimenez, 1997; Humphrey and Sneath, 1999; Jiang et al., 2006; Li et al, 2007; Neupert, 1999; Sneath, 1998; Zhang, 2007). However, most of the existing work tends to focus on one or two factors that cause grassland degradation and poverty, and provides solutions based on their identified factors. There has been little to no systematic analysis of how different factors and their interactions drive the dynamics of grassland social-ecological systems in the Central Asian region. However, the dramatic changes that the grasslands of IMAR and Mongolia have witnessed over the past half century necessitate a systematic investigation of the factors shaping grassland social and ecological dynamics to improve their understanding and sustainability.

In this chapter, we review the models and explanatory frameworks developed by grassland ecologists and institutional analysts and discuss the management and institutional strategies they offer. We bring together different types of evidence on changes of grassland quality and associated social-institutional processes in the context of climate change. We examine the available data in relation to different frameworks, and discuss an explanatory approach that considers state, market and community actors in relation to grassland dynamics and outcomes (Lemos and Agrawal, 2006). We discuss the feasible strategies for addressing grassland degradation, and societal adaptations to environmental change. We adopt an integrated and multiscale state-market-community framework for analyzing environmental problems associated with complex human and environment interactions. Linking historical social-institutional changes and dynamics of grassland productivity allows us to understand the dynamics of Mongolian grassland social-ecological systems over the past fifty years. Our integrated and multi-scalar approach considers as well the feedbacks and interactions between social, institutional, ecological and biophysical aspects of grassland systems, and leads to a more comprehensive consideration of alternative strategies to grassland management. Finally, we draw conclusions about the dynamics and sustainability of grassland social-ecological systems on the Mongolian plateau.

4.2 Explanatory Models of Grassland Dynamics

Broadly speaking, grassland ecologists have distinguished between two models of grassland dynamics: the equilibrium ecosystem model and the non-equilibrium ecosystem model. The equilibrium ecosystem model follows the Clementsian succession theory according to which natural vegetation in a given ecological site reaches a state of equilibrium over time, given climate and soil conditions (Zhang and Li, 2008). In equilibrium grazing systems, climate conditions are relatively constant with low interannual variability, enabling stable seasonal rhythms of vegetation growth across the years. In these zones, grazing intensity has a direct impact on grassland quality, and over-grazing leads to the deterioration of grassland quality. The preferred management recommendation is to stock grasslands at or below carrying capacity. This grazing model is still the dominant model used to make carrying capacity-based grassland management policies in China and Mongolia (Olonbayar, 2010; Zhang, 2007). The goal of these policies is to control the numbers of humans and livestock or ensure long-term exclusion of livestock grazing to allow grassland quality to recover and persist. However, this model has been criticized on the grounds that it ignores and at best simplifies spatial and temporal variability of precipitation and grassland productivity in grasslands. Because it does not take into account the extremely high levels of spatio-temporal variability characteristic of semiarid and arid ecological regions, prescriptions based on its assumptions, particularly those related to sedentarization of herders and animals, have also been viewed as faulty.

Over the past decades, a non-equilibrium approach to ecosystem functioning has been developed to explain grassland dynamics in the semiarid and arid regions. In non-equilibrium ecological landscapes, the high variability of climatic conditions is more important for the quality of grasslands than the livestock grazing intensity (Ellis and Swift, 1988; Oba et al., 2000). Predictions from non-equilibrium theories have been tested in the semi-arid and arid grassland regions of Mongolia and China and shown to better explain grassland dynamics (Fernandez-Gimenez, 1999; Ho, 2001; Zhang, 2007). In these regions, a simple carrying capacity value oversimplifies the dynamics of the environment. Livestock grazing needs to be organized according to variable precipitation patterns and forage availability, and these vary enormously across space and over the years.

Another school of thought for governing grassland resources comes from neo-institutional economists, who focus on analyzing efficient institutional arrangements for sustainable use of natural resources. There are three main institutional frameworks for governing natural resources: privatization, state/public ownership, and community-based resource management. Traditionally, privatization and state control have been recognized as the two major solutions to solve problems of unsustainable harvesting of natural resources (Hardin, 1968). In the past decades, Ostrom and other institutional analysts have demonstrated self-organized collective action as an alternative approach to govern common pool natural resources (Agrawal, 2001; Ostrom, 1990, 2005, 2010). Because mobility is an essential characteristic of traditional herding strategies in semiarid and arid regions, cooperative use of grasslands by mobile herders can reduce the uncertainties caused by variations in precipitation and vegetation productivity in a given location, and reduce overall uncertainty (Agrawal, 2001; Wilson and Thompson, 1993). Studies have shown that large differences in levels of grassland degradation under a traditional, self-organized group property regime (Mongolia) versus national government management (China and Russia) on the Mongolian plateau (Humphrey and Sneath, 1999; Sneath, 1998). Mongolia has allowed pastoralists to continue their traditional group-property institutions, which enable large-scale movements between seasonal pastures. China and Russia imposed agricultural collectives, which involve sedentarization and permanent settlements.

Besides pure state-, market-, or community-based governance strategies, Lemos and Agrawal (2006) proposed a governance framework that recognizes the importance of hybrid arrangements for sustainable environmental governance. Such hybrid arrangements connect the state, market, and community. The Lemos and Agrawal framework is particularly useful for dealing with complex and multiscale environmental problems such as climate change and ecosystem degradation. State, community, and market actors have different strengths, and can play different roles in resource management in terms of institution building and implementation, collective action, and market incentives. Co-management links the state and local communities. Public-private partnerships link the state and markets, and private-social partnerships link markets and communities. For the dynamics of social-ecological systems in the Mongolian grasslands over the past fifty years, the national governments of Mongolia and China, local grazing communities,

and local and international markets all have played significant roles. However, the importance of their roles has changed over-time.

4.3 Analyses and Results

About 66% of the land in IMAR (0.78 million km^2) is classified as grasslands, a quarter of all Chinese grasslands (Zhang, 1992). Nearly 84% of the total territory in Mongolia (1.26 million km^2) is covered by grasslands (Angerer et al., 2008). Mongolia and IMAR share the similar ecological gradient of vegetation, which varies from forests to forest/meadow steppe, typical steppe, desert steppe, and desert (Fig. 4.1). Recent studies from China and Mongolia show that 90% of the total grasslands in IMAR and 78% of the grasslands in Mongolia have degraded to varying degrees (Erdenetuya, 2006; Ministry of Agriculture, China, 2007).

Several large-scale field ecological surveys were conducted to assess grassland quality, measured by dry biomass, over the last fifty years: four in IMAR and three in Mongolia. These field grassland surveys were based mainly on large-scale field samplings, but the latter two times in IMAR were assisted by geospatial technologies. The overall grassland productivity in IMAR is higher than in Mongolia (Fig. 4.2). This is mainly caused by the climate constraints. IMAR is with warmer temperature and has more annual precipitation than Mongolia. In period 2, the average grassland biomass in IMAR and Mongolia decreased to 57.1% and 75.9% of the value in period 1, respectively (Fig. 4.2). By period 3, the average grassland biomass in the two regions decreased to 44.8% and 57.7% of period 1, respectively. The results of the most recent survey (2009–2010) in IMAR show that the average grassland biomass increased slightly to 48.1% of period 1. Moreover, the survey results of Mongolia also show that the average number of grass species per hectare decreased by periods 2 (24) and 3 (18) to 84.6% and 62.3% of period 1 (31), respectively (Olonbayar, 2010).

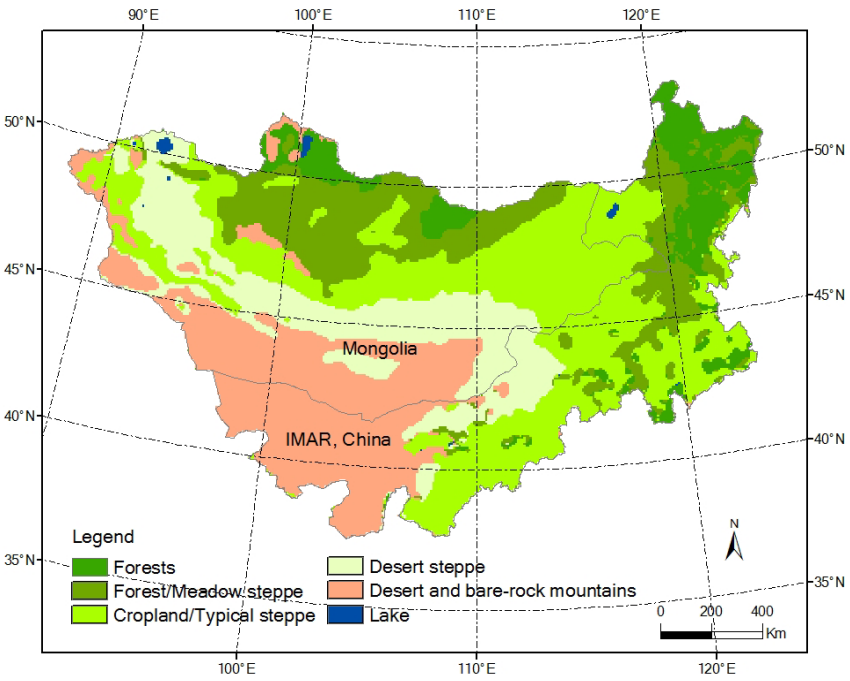

Fig. 4.1 Spatial distributions of the major vegetation types on the Mongolian plateau. Source: vegetation maps of IMAR and Mongolia were respectively provided by the Institute of Botany, China, and the Institute of Botany, Mongolia. They were made respectively in the 1990s and 1980s. The original scale of the two vegetation maps is 1:1,000,000.

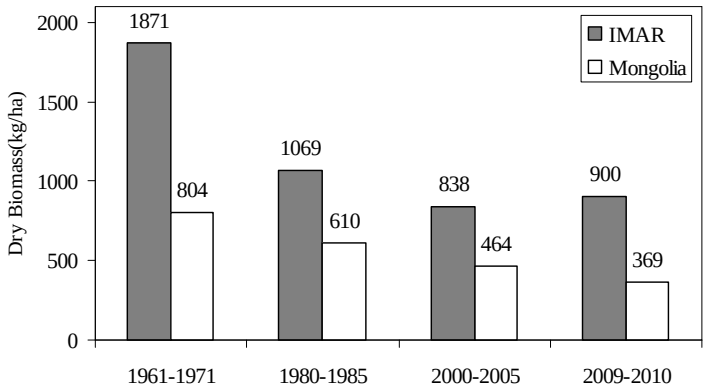

Fig. 4.2 Changes of the average grassland biomass of IMAR and Mongolia over the past fifty years. Source: the data of IMAR was provided by the Inner Mongolian Institute of Grassland Survey and Design (IMIGSD, 2011) and the data of Mongolia was reconstructed from Olonbayar, 2010.

By the early 1960s, both IMAR and Mongolia had completed a dramatic social transformation from the traditional "communal" ownership into collective economies, begun in the late 1950s. They experienced privatization in the middle and late 1980s, respectively. In IMAR after 2000, the Chinese national government has been making and implementing a range of policies to restore grassland quality. These policies are known as "Grain to Green" policies (Liu et al., 2008). Given these broad social-institutional changes, we divide the last fifty years into three

sub-periods: collectivization (1961–1985), privatization (1986–2000), and recentralization (2000–present) periods. The recentralization period applies only to IMAR, China. Parallel with these economic changes, social-institutional changes have influenced the social organizations, culture, land-use behaviors of herders, and populations of human and livestock, which have consequently affected grassland quality and the livelihoods of herders in the two regions.

4.3.1 Collectivization of Pastures and Livestock

In the 1950s, pastures and livestock in IMAR and Mongolia were collectivized by a policy called "state purchase." Herders were responsible for selling livestock products to the state at below-market prices based on planned, rather than actual, numbers of livestock (Fernandez-Gimenez, 1997). In the early 1960s, all herders in IMAR and Mongolia were members of grazing collectives, and most of the livestock and pastures were collectively owned by the local grazing communities. Under the collective institutional arrangements, herders had little incentive to manage livestock well or increase livestock numbers. The total numbers of livestock and the herd compositions by species in Mongolia (1961–1990) and IMAR (1961–1985) were fairly stable in the collective period (Fig. 4.3). In Mongolia, collectives, called *negdel*, played a central role in allocating pastures and campsites and directing seasonal movements that often respected pre-existing customary rights and were regulated and tightly controlled by *soums* (counties) and *Aimags* (provinces).

Pastoral land-use practices remained mobile and herding families were generally supported by deliveries of hay, and thus had little impact on grassland quality (Ojima and Chuluun, 2008). The collectives also engaged in veterinary services, producing livestock products, preventing livestock loss from natural hazards, and improving pasture quality through the development of water points at strategic locations. However, in this period, the overall herding radius decreased and herders were confined to smaller areas, thereby limiting access across broad ecological zones and reducing access to diverse forage resources used traditionally. Moreover, through the building of water facilities, winter shelters, and *soum* centers and the investments in 'scientific' management of livestock, the nomadic pastoral economy was transforming into a sedentary and intensive one (Fernandez-Gimenez, 1997). In Mongolia, the conversion of grasslands for grain

production started in the year 1959 and 1.34 million hectares of grasslands were converted to cropland prior to the early 1990s (Olonbayar, 2010). Although some grazing activities were sedentarized and some grassland was converted into cropland, the overall grassland quality in Mongolia did not degrade rapidly in the collective period (Fig. 4.2).

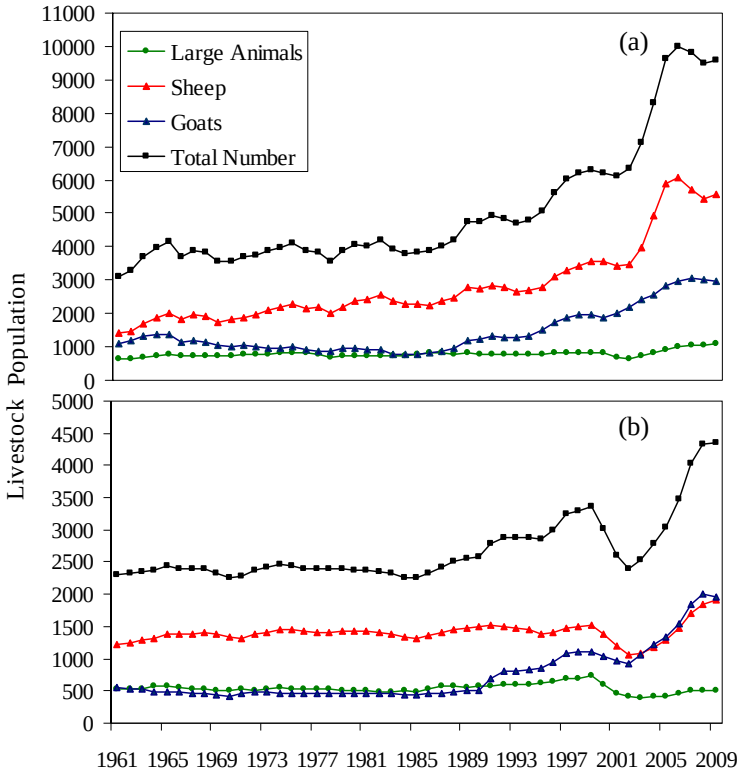

Fig. 4.3 Changes of livestock numbers in IMAR, China, (a) and Mongolia (b) (1961–2009) (Unit: 10,000). Source: Annual census books of IMAR, China, and Mongolia (ACBIMAR, 2005, 2010; ACBM, 1990, 2010).

In IMAR, grazing collectives called *production teams* can migrate within their village boundaries seasonally and to other villages (or *soums*) in the years with natural disasters. Similar to Mongolia, grazing collectives were responsible for managing pastures and livestock production. In the collective period, human population in IMAR increased rapidly from around 12 million to 20 million (Fig. 4.4). The increased population was mainly from the migration of *Han* people from other provinces. The negative consequences of the "Great Leap Forward" (1957–1959) and the consecutive large-scale natural disasters (1960–1961) caused the "Great Famine" in the most of China. Population migration in this period was partially driven by the national policy for solving the starvation problem in China. Fertile grasslands were reclaimed for

food production (Jiang, 2005). The “Grain First” policy implemented in the “Cultural Revolution” period (1966–1976) also caused large areas of grasslands to be converted to cropland (Jiang, 2005; Zhang, 2007). During the period 1949–1985, 9.2 million hectares of fertile grasslands were used for grain production, mainly corn and potatoes (Table 4.1). Conversion from grassland to cropland can easily destroy the thin surface soil layers and destabilizes underlying sandy layers. This can consequently cause desertification, leading to cropland abandonment in a few years. Some of the new migrants worked on grain production, and others migrated into pastoral areas to compete for pasture resources with local herders. Moreover, many coal and metal mining sites were built in IMAR in this period (Neupert, 1999). Due to the loss of fertile grasslands, overstocking and other intensive grassland-use behaviors (e.g. mining and collection of traditional herbal medicines), the average grassland biomass decreased rapidly from 1871 kg/ha to 1069 kg/ha, roughly in the corresponding period (Fig. 4.2).

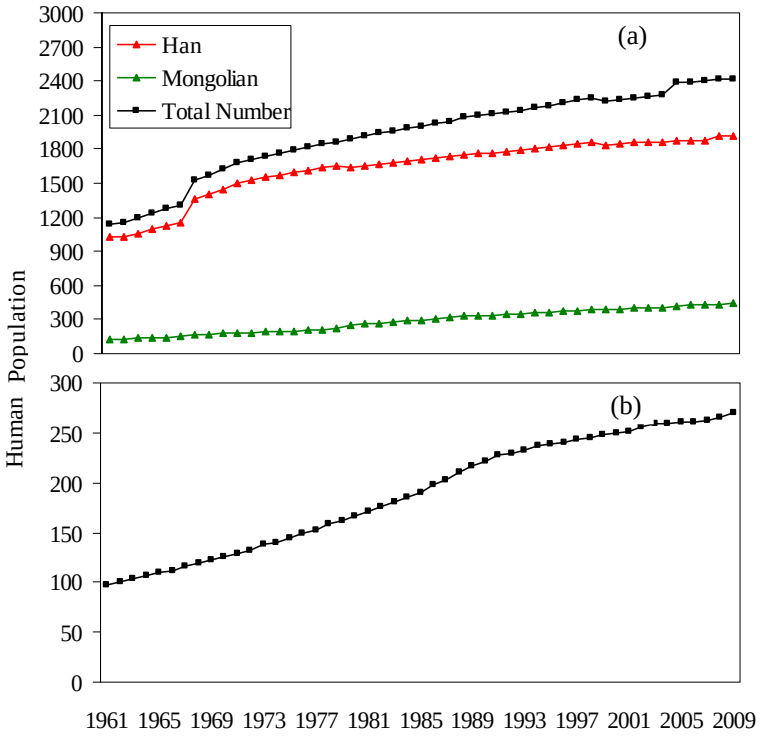

Fig. 4.4 Demographic changes in IMAR, China, (a) and Mongolia (b) (1961–2009) (Unit: 10,000). Source: Annual census books of IMAR, China, and Mongolia (ACBIMAR, 2005, 2010; ACBM, 1990, 2010).

Table 4.1 Amounts of grassland area reclaimed in IMAR (1949–2005) (Unit: 1,000,000 hectares).

Study Period	Grain Production	Fodder Production	Other Uses
1949-1985	9.20	0.00	0.00
1985-2000	6.30	1.40	1.40
2000-2005	0.00	5.60	0.00
Total Area	15.50	7.00	1.40

Source: Inner Mongolian Institute of Grassland Survey and Design (IMIGSD, 2008).

4.3.2 Privatization and Market Incentives

In the middle of 1980s, the Household Production Responsibility System (HPRS), also called the Double-Contract System, was introduced from the agricultural province of China to the pasture areas of IMAR. Livestock production was first contracted to herder households by local governments (1984– 1988). Then, pastures were allocated to individual households (1989–1995). At the same time, China started its transition from the central planned economy to market economy. In Mongolia, the free-market reforms began with the first democratic elections in 1990. Privatization and market incentives stimulated herders to increase their livestock numbers in order to gain more benefits from livestock production. Sharp increases in all prices of livestock products in Mongolia during the latter half of the 2000s have similar trends with the increases of livestock numbers. The similar increasing trends between livestock numbers and the prices of livestock products are also seen in IMAR (Fig. 4.5). Compared with Mongolia, livestock production in IMAR is more connected to local and international markets, since market economy is more developed in China than in Mongolia. Since the late 1980s and the early 1990s, the total number of livestock in IMAR and Mongolia increased rapidly (Fig. 4.3). For example, in 1990, Mongolia had 25.9 million domesticated animals. In 1998, this had grown to 32.9 million an increase of 27%. Other studies also show that the high price of cashmere in international markets triggered the rapid growth of goats (Ojima and Chuluun, 2008). The species composition also changed since the early 1990s, and the number of goats increased more rapidly than other species in both IMAR and Mongolia (Fig. 4.3).

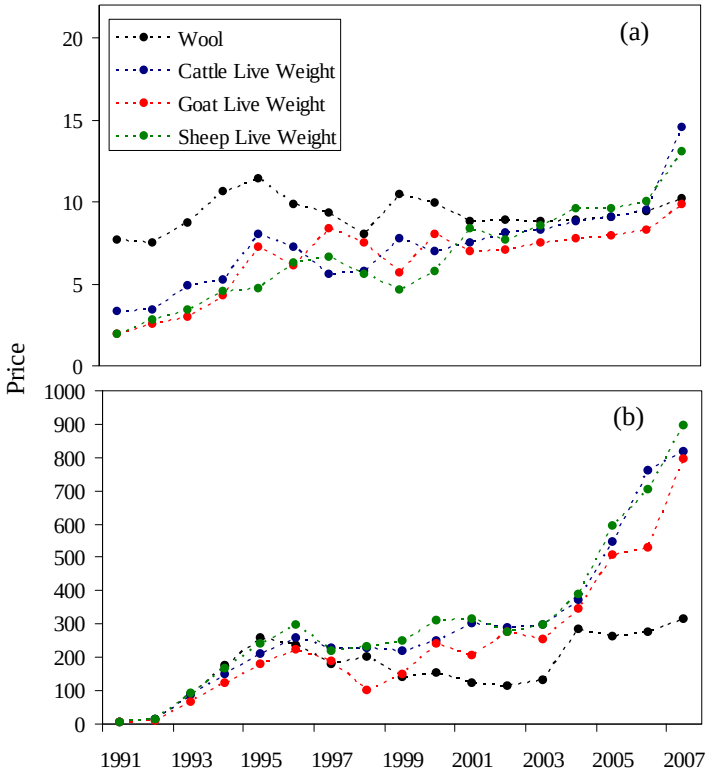

Fig. 4.5 Changes of the prices of livestock products in IMAR (Unit: 1000 Yuan/Tonne) (a) and Mongolia (Unit: 1000 MNT/Tonne) (b) (1991–2007). The historical prices from the Food and Agriculture Organization (FAO) were adjusted to constant 1991 currency. Source: FAO price statistics database (FAO, 2011).

In IMAR, with pastures contracted to individual herder households, herders could not migrate over large areas after privatization. In this period, pastoralists were sedentarized, and migratory grazing was converted to year-round grazing on small pieces of contracted pastures. The leasing term of the contracted pastures was 30 years, and herders did not have the full ownership of the pastures, decreasing incentives to protect pastures (Humphrey and Sneath, 1999; Li et a., 2007). Contracting pastures to individual households destroyed the intact grassland ecosystems and traditional customs for pasture use, and conflicts over pasture use increased (Williams, 2002). The implementation of the HPRS has been recognized as a major reason for grassland degradation in IMAR (Li et al., 2007; Li and Huntsinger, 2011; Sneath, 1998; Zhang, 2007; Zhang and Li, 2008). Increased stocking rates and year-round grazing adversely affects pasture vegetation growth and regeneration and leads to deterioration of grasslands. In addition, the privatization period saw large areas of fertile pastures in IMAR converted for producing grain (6.3 million hectares) and fodder (1.4 million hectares) (Table 4.1). Human population also continued increasing due to immigration and natural growth (Fig. 4.4) and herd sizes steadily

increased during the 1990s along with prices of livestock products. As more mining and other industries continued to compete with local herders for land the grasslands available for grazing decreased and grazing intensity increased. Fencing on contracted lands exacerbated the problem of reduced pasture area. The increases in grazing intensity likely explain the decreases in the average grassland biomass from 1069 kg/ha to 838 kg/ha, roughly corresponding to this study period (Fig. 4.2).

In Mongolia, due to the lack of efficient resource institutions to govern grassland use, most grassland became open-access resources. Levels of conflict over grassland use increased. Traditional grazing customs such as reciprocal use of grasslands in natural disaster years declined (Upton, 2009). Livestock privatization had a tremendous impact on livestock production and the marketing of livestock products. Herders became livestock owners and simultaneously lost the support of collectives (mainly the transportation support for seasonal and interannual migrations). Poor families who could not afford long-distance migrations migrated less frequently or became sedentary grazers around water points or fertile pastures. The numbers of water facilities and pasture reserves also decreased (Olonbayar, 2010). Data from the census books of Mongolia show that the area of cropland decreased 24.3% from 1995 to 2009 (ACBM, 2005, 2010). Cropland abandonment made lands prone to wind erosion. Roughly corresponding to this period, the average grassland biomass decreased from 610 kg/ha to 464 kg/ha (Fig. 4.2).

4.3.3 Recentralization of Grassland Management in IMAR, China

Since the year 2000, grassland management in Inner Mongolia, China, was recentralized to the national government. Therefore, we call this study period the “Recentralization Period.” The national government has implemented several projects for ecological restoration and conservation in the pasture areas of IMAR, such as “Converting Pastures to Grasslands” and “Ecological Restoration of the Sandstorm Sources of Beijing-Tianjin-Tangshan.” Most of the counties in IMAR are involved in these two projects. Under these policies, herders are subsidized in the forms of grain and money for grazing bans (all year round), grazing restrictions (on a seasonal basis), rotational grazing, migration out of pastures, pen-feeding livestock, and importing high value-added livestock. Due to grazing restrictions, pen-feeding of livestock has

become popular in IMAR. This is one of the major reasons for the abrupt increase in total livestock numbers in IMAR after 2002 (Fig. 4.3). In 2011, the national government of China started a new ecological compensation and restoration project. Eight grassland provinces and autonomous regions, including IMAR, are involved in the project. This policy is still based on the equilibrium model of grassland dynamics and emphasizes reducing grazing intensity in order to keep the balance between grassland capacity and stocking rates. The social-ecological outcomes of the new policy are still to be assessed.

In the recentralization period, local herders in IMAR have been marginalized in the policy making and implementation processes, and many of the same problems associated with collectivization have become evident. Conflicts exist between the market-oriented behaviors of local herders and the grassland conservation and restoration goals of the national government. For example, violations to the policies of grazing restrictions and bans commonly exist in IMAR (Bijoor et al., 2006). High monitoring and implementation costs make these policies difficult to implement. Moreover, these polices have ignored the diversity of grassland ecosystems across the ecological gradient. Additionally, due to pen-feeding, 5.6 million hectares of grasslands were reclaimed for fodder production during 2000–2005 (Table 4.1). Recent studies show that the overall grassland degradation status did not get changed, although in some local areas, grassland quality has improved (Ministry of Agriculture, China, 2007).

4.3.4 Changing Roles of the State, Market, and Community for Grassland Management

In the three study periods, state, market, and community actors played significant roles in influencing grassland-use behaviors of herders, and their roles also changed over time. In the collective periods of Mongolia and IMAR, there was little market influence on grassland management and livestock production. The state and local grazing communities governed grassland resources and managed livestock production. After privatization, both Mongolia and IMAR have transformed from central planned economies towards free market economies. Livestock production by herders has become linked to fluctuations in global and local market demands. The roles of the state and local grazing communities have been deemphasized, especially in Mongolia. Traditional grazing customs have also not played a role in coordinating

livestock grazing. In the recentralization period in China, grassland management was recentralized to the national government. Though grassland-use behaviors of herders are still market-oriented, they are restricted by the new rules created by the state. Local communities no longer play important roles in governing grassland resources in the recentralization period.

4.3.5 Climate Variability and Change: History and Future

Over the past fifty years, the overall climate in IMAR and Mongolia became warmer and drier (Fig. 4.6). The increasing trends of annual mean temperature were significant in both IMAR and Mongolia ($r^2_{IMAR} = 0.57$, $p_{IMAR} < 0.01$; $r^2_{Mongolia} = 0.48$, $p_{Mongolia} < 0.01$). However, the decreasing trends of annual total precipitation were not significant in both IMAR and Mongolia ($r^2_{IMAR} = 0.02$, $p_{IMAR} = 0.37$; $r^2_{Mongolia} = 0.07$, $p_{Mongolia} = 0.05$). Other studies also showed that annual mean temperature increased about 2.1 °C in Mongolia and about 2 °C in IMAR; annual precipitation decreased about 7.0% in Mongolia (NCRM, 2009) and about 6.6% in IMAR (Ding and Chen, 2008). Drought increased significantly in Mongolia in the last 60 years, particularly in the last decade (NCRM, 2009). The worst droughts and Dzuds (heavy winter snowstorms) Mongolia experienced recently were in the consecutive summers and winters of 1999, 2000, 2001, and 2002, which affected 50–70% of the territory. The substantial decline of livestock numbers between 1999 and 2002 (Fig. 4.3) was mainly caused by droughts and winter snowstorms in these years. About 35% (12 million) of the total number of livestock perished in the period. Recent studies show that in Mongolia, grassland productivity in areas in which grazing is not allowed has also decreased by 20–30% in the past 40 years (Angerer et al., 2008). By statistical analyses of the climate data collected at national standard stations of Mongolia and IMAR over the past fifty years, we found that the interannual variability of precipitation in the growing season (from April to September) of most stations are over 0.35 (the coefficient of variance). Therefore, most parts of the Mongolian plateau can be seen as non-equilibrium grassland ecosystems.

Future climate scenarios show that in the next 30 years, annual mean temperature will increase 0.4–1.6 °C, especially in summer and autumn (0.8–1.6 °C), and there is no apparent

increase of annual precipitation on most parts of the Mongolian plateau (Tang et al., 2008). IPCC AR4-A1B future climate scenarios of the Mongolia plateau (mean projections of 21 models, Christensen et al., 2007) show that comparing the end of this century (2080–2099) with the end of last century (1980–1999), winter temperature will increase 3–5 °C; summer temperature will increase 2.5–4 °C; winter precipitation will increase 5–30%; summer precipitation in most areas will increase 5–15%, except in some parts of the western Mongolian plateau. Livelihoods of herders on the Mongolian plateau will be more vulnerable to future adverse climate conditions.

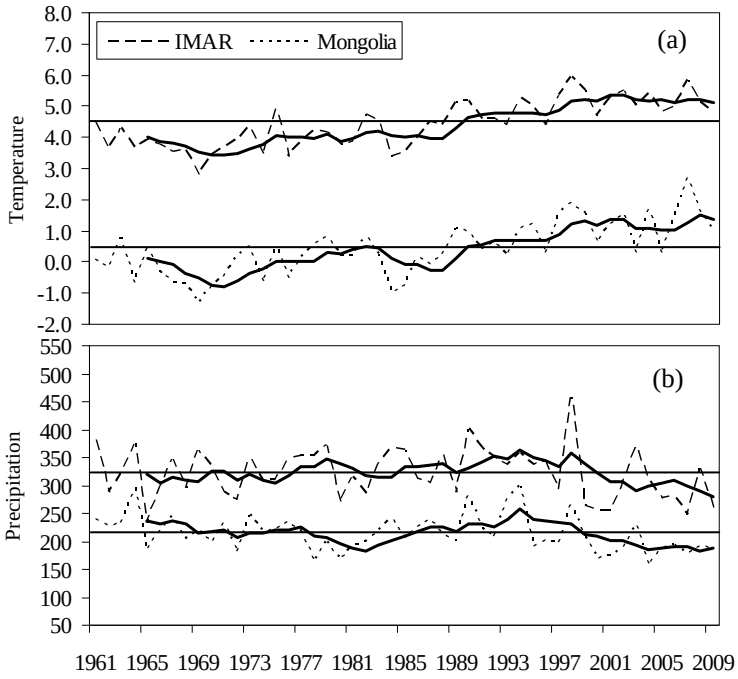

Fig. 4.6 The temporal variability of annual mean temperature (Unit: °C) (a) and annual precipitation (Unit: mm) (b) in IMAR and Mongolia with multi-year means and five-year moving averages (1961–2009). Source: national standard climate stations of IMAR, China, and Mongolia (CIMAR, 2011; CM, 2011).

4.4 Discussion

Over the past fifty years, grassland quality on the Mongolian plateau has been deteriorating, which has endangered the livelihoods of local herders. Future climate change and the increasing integration into world markets have the potential to exacerbate these problems. Therefore, simple solutions like those based on carrying-capacity are not sufficient for solving these complex and multiscale natural resource problems. An interdisciplinary framework that integrates social and

ecological systems is needed to understand the dynamics of social-ecological systems in the Mongolian grasslands over the past fifty years, and to consider strategies for sustainable management in the future (Ostrom, 2009). In the context of warming and drying climate, social-institutional factors played significant roles in changing grassland-use behaviors of herders and grassland quality. These socioeconomic factors also interact with each other. The roles of the state, market, and community in governing grassland resources in Mongolia and IMAR have changed over time. The above analyses show that none of the historical resource institutions implemented in IMAR and Mongolia (collectivization, privatization, and recentralization) was efficient for sustainable governance of grassland resources.

Grassland degradation and the increasing frequencies of climate hazards, such as drought and Dzud (heavy winter snowstorms that interact with summer droughts to endanger livestock), have endangered the livelihoods of herders. Since the middle 1990s, the poverty rate in pastoral areas of IMAR has increased. Grassland degradation, natural disasters, increasing costs of herding, and increasing competition in the livestock product markets were identified as the major reasons (Li et al., 2007; Zhang, 2007). In IMAR, fodder cost is the major household expenditure of herders (Li et al., 2007). Environmental problems have also made the poverty situation worse in Mongolia. For example, in 1998, the national poverty rate of Mongolia was slightly below 35%, and it increased to 36.1% in 2001–2002 as a consequence of the severe natural disasters between 1999 and 2002 (Olonbayar, 2010). Social-institutions also affect the adaptive capacity of herders to climate hazards. For example, studies show that the implementation of HPRS in IMAR, China, decreased the adaptive capacity (the ability to migrate to other places and to get help from other herders and/or the local governments in the natural disaster years) of herders to climate variability and change (Li and Huntsinger, 2011).

The high costs of privatization and the top-down hierarchy of state control render these approaches inefficient for governing grassland resources in the semiarid and arid regions. Grassland productivity and water resources are with high spatial and temporal variability in these regions, which makes demarcation of grassland resources very difficult. High monitoring costs make “command and control” an inefficient way for governing grasslands. The social-ecological performances (overall grassland degradation condition and rural poverty) of policies

implemented in the recentralization period of China have demonstrated that state-control is inefficient. Community-based resource management (CBRM), which has cooperation and collective action at its core, has been recommended by scholars for solving grassland problems in the semiarid and arid regions of Mongolia and China (Angerer et al., 2008; Banks, 2001; 2003; Banks et al., 2003; Bijoor et al., 2006; Fernandez-Gimenez, 1997; Ho, 2001; Humphrey and Sneath, 1999; Li et al., 2007).

Traditionally, herders on the Mongolian Plateau had a culture of reciprocal and exchange use of grasslands in natural disaster years, and the grazing boundaries and movement patterns were also flexible. These informal norms and rules enabled them to adapt to the spatial-temporal variability of climate and grassland productivity. However, social-institutional changes (collectivization and privatization) altered the social organizations and the cooperative culture. For example, in Mongolia, the traditional grazing organizations, called *khot ail* and consisting of several households with clanship and/or kinship camping together, were replaced by grazing specialization groups, for example goat/sheep management groups, which were not family based. After privatization, due to market incentives and the lack of effective resource institutions to coordinate grassland use, the use of grasslands became competitive. The number of conflicts over grassland use increased (Upton, 2009). The broad institutional changes in IMAR were similar. Moreover, in IMAR, contracting grasslands and livestock production to herder households have caused social stratification and further incentivized competitions among herders (Williams, 2002). These changes make it difficult to consider recovering traditional customs in livestock grazing.

In order to avoid the degradation of grasslands due to trampling from daily grazing and to make seasonal and interannual migrations possible, cooperative use of pastures is necessary. Cooperative organizations, such as pasture-use groups and water-facility-use groups, can help herders to improve their livelihoods and better adapt to future adverse climate conditions. The formation of collective action needs external drivers and internal coordination mechanisms (Ostrom, 2005) and effective decentralization requires the support from formal institutions (Ribot and Agrawal, 2006). In Mongolia and IMAR, support from the national governments can help the formation of cooperative organizations. For example, the national government of China

has been providing subsidies for supporting herders to build cooperation organizations in order to increase their profits of livestock production in the market economy. A formal agricultural cooperative law was also implemented in the year 2007 to support the organization of agricultural cooperatives. For areas that are near the major or local markets, market-oriented cooperative organizations can be built, while areas distant from markets but with high frequencies of natural disasters might benefit from subsistence-oriented cooperative organizations. Where disasters happen with relatively high frequency, cooperation can be among neighbors or among villages or counties, since in serious natural disaster years a large geographical area could be affected simultaneously.

Community-based resource management is not a panacea for reversing grassland degradation. High stocking rates caused by the increased human and livestock populations have reduced the feasibility of migration, especially in IMAR, China, and state-control of the overall grazing intensity of a large geographic area is still necessary. State-control policies need to be sensitive to spatial and temporal variations within the grassland ecosystems. Otherwise, those polices will not be effective and will lack the support from local herders. For example, annual precipitation in the eastern part of IMAR is fairly stable. Grazing intensity is the major cause for grassland degradation in those areas. Therefore, state grazing-control or privatization might be more effective than cooperative use in these areas, since cooperation and collective action involves lots of transaction costs, such as searching, negotiation, contracting, monitoring, and sanctions. Moreover, long-distance and frequent seasonal and interannual migrations are also not necessary in regions with stable precipitation and productivity.

Livelihood diversification has been promoted by the state as a major approach to adapt to environmental change. For example, in order to reduce stocking rates, the national government of China has been providing subsidies for herders to leave pastures and find jobs in cities. However, due to the lack of education and training, this policy has not worked well (Bijoor et al., 2006). Therefore, more institutional and government support may be needed in the future for herders to adapt their livelihoods to the changing climate and grassland services. Besides adjusting resource institutions and polices, improving grazing technologies is another solution. Indigenous knowledge (Fernandez-Gimenez, 2000) and recent research on grassland ecology and

grassland use and management provide a broad knowledge base for technical solutions to reduce grassland degradation. Introducing new species with high productivity is an important approach for improving livestock production in the semiarid and arid regions. However, this strategy can increase the natural and economic risks of livestock production. Whether this strategy is feasible also depends on institutional supports, such as markets for livestock products, technology training, livestock insurance, and financial support.

4.5 Conclusions

Most areas of the grassland ecosystems on the Mongolian plateau can be classified as non-equilibrium ecosystems. Institutions that govern grasslands should accommodate the characteristics of grasslands. The traditional nomadism was adapted to local climate conditions, and also preserved ecosystem functions of grasslands. However, in the past fifty years, the social-institutional changes have undermined the traditional resource institutions and replaced them with a series of alternative systems. Sustainability of the Mongolian grassland social-ecological systems has been affected as a result. A warmer and drier climate and the increasing frequencies of climate hazards have increased the vulnerability of the livelihoods of local herders on the Mongolian plateau. Therefore, understanding these changes and providing feasible strategies to cope with the environmental problems are urgent.

Numerous scholars from different disciplinary backgrounds have contributed to these topics. However, a systematic analysis is still missing. In this chapter, we adopt an integrated state-market-community model to analyze the dynamics and sustainability of the Mongolian grassland social-ecological systems. The results indicate that drivers from the human dimensions, such as institutional and policy changes and demographic change, play significant roles in changing grassland quality over the past half century. In this chapter, we propose cooperative use of grasslands to cope with future climate change and market fluctuations. In regions with high environmental variability, cooperation and collective action can pool climate risks over space and increase the predictability of precipitation and grassland productivity. With the increasing integration into the world market, market-oriented cooperative production can increase profits of livestock production. Diverse institutional arrangements and strategies are necessary to

accommodate diverse ecosystem types and social situations across ecological gradients and social-political regions. In all, sustainable governance of grassland social-ecological systems on the Mongolian plateau in the context of climate change need the integration and coordination of forces from the state, market, and local grazing communities.

Acknowledgements

This work was conducted with financial support from the NASA Land-Cover and Land-Use Change Program (NNX09AK87G). The authors would like to thank Professor Qi Xing from the Inner Mongolian Institute of Grassland Survey and Design, China, for data collection of this work.

Chapter Five

Drivers of the Dynamics in Net Primary Productivity across Agro-Ecological Zones of Mongolia and Inner Mongolia, China

Abstract

Understanding the drivers of dynamics in grassland productivity is prerequisite for studying effective resource policies that can be used to govern grassland resources sustainably. We present a diagnostic analysis of the major drivers of the dynamics in net primary productivity (NPP) across agro-ecological zones on the Mongolian plateau. We estimated a spatial panel data model for NPP (1986−2009) as a function of climatic and socioeconomic variables. Static and dynamic spatial panel models were estimated in each of six sub-regions, which were classified based on rural livelihoods and agro-ecological models of grassland dynamics, to identify the major drivers of NPP dynamics. The statistical modeling results indicated that the major drivers of NPP dynamics vary across the six sub-regions. Grain output was the major predictor of NPP dynamics in the farming and farming-grazing zones of Inner Mongolia. Precipitation and livestock populations both had significantly positive relationships with NPP in the two grazing zones of Inner Mongolia. However, in Mongolia, livestock populations was the only significant predictor of NPP in the grazing zone with relatively stable climate, and precipitation was the only significant predictor of NPP in the grazing zone with highly variable climate. Human land-use and livestock management behaviors and the bidirectional causal relationships between livestock populations and NPP could explain the positive relationships between livestock population and NPP. The heterogeneous drivers of NPP dynamics across space indicated the necessity of diverse resource policies and institutions for sustainable governance of grasslands.

Keywords: Grassland ecosystem; net primary productivity; drivers; spatial panel data models; agro-ecological zones; Mongolian plateau

---

Wang, J., Brown, D. G., and Chen, J. Drivers of the dynamics in net primary productivity across ecological zones on the Mongolian plateau. *Landscape Ecology*, 2013, DOI 10.1007/s10980-013-9865-1.

5.1 Introduction

Grassland degradation on the Mongolian plateau, including the country of Mongolia and the Inner Mongolia Autonomous Region (IMAR), China, has undermined ecosystem functions, including carbon sequestration (Lu et al., 2009), and endangered the livelihoods of local herders (Chapter Four; Li et al., 2007) since the early 1960s, especially following the political-economic transitions in IMAR and Mongolia in the mid-1980s and the early 1990s, respectively. Empirical studies have shown that grassland degradation has increased the cost of livestock grazing, and poverty has become prevalent in the grazing communities of Mongolia and IMAR, China (Olonbayar, 2010; Zhang, 2007). Understanding the drivers and mechanisms of grassland productivity dynamics over the past decades on the Mongolian plateau is prerequisite for developing effective resource policies and institutions that can govern grassland resources sustainably. Previous studies have identified that climate change, increasing populations of humans and livestock, inefficient resource institutions, distorted market incentives, and reclamation of grasslands for grain production are the major causes for grassland degradation on the Mongolian plateau (Chapter Four; Fernandez-Gimenez, 1997; Neupert, 1999; Sneath, 1998). However, most of these studies just focused on one or several of these drivers at regional scales, and a systematic analysis of the major drivers across heterogeneous landscapes of the Mongolian grasslands is still needed.

Since the early 1960s, climate on the Mongolian plateau has been getting warmer and drier (Chapter Four). Studies have also shown that in some areas of Mongolia where grazing is not allowed grassland productivity has declined by 20–30% over the past 40 years (Angerer et al., 2008). IMAR and Mongolia have been transforming from centrally planned to market economies since the mid-1980s and the early 1990s, respectively. Grasslands in IMAR have been allocated to individuals through contracts and fenced. Nomadic herding has been replaced by farming and livestock grazing activities. As a result, seasonal and interannual migrations have become less feasible. In Mongolia, due to lack of effective resource institutions, conflicts among herders over grassland use have increased since the early 1990s (Upton 2009). Moreover, livestock privatization and market factors have given herders strong incentive to keep more animals and therefore stimulated the growth of livestock populations. For example, based on annual census

data, livestock populations in IMAR increased from around 40 to 100 million between 1985 and 2009; livestock populations in Mongolia increased from 26 to 33 million between 1990 and 1998 (ACBIMAR, 2010; ACBM, 2010). Livestock populations in Mongolia crashed in the 1999-2002 Dzud, although they rebuilt by 2009. They crashed again (though less extremely) in the 2009-2010 Dzud. The rapid increase of livestock populations following economic transitions caused disastrous impacts on grassland quality. Livestock privatization and grazing sedentarization have been identified as the major reasons for the degradation of the Mongolian grasslands, especially in IMAR (Humphrey and Sneath, 1999; Jiang et al., 2006; Li et al., 2007; Li and Huntsinger, 2011). Studies based on large-scale field samples showed that from the early 1980s to 2010, the average grassland dry biomass productivity in IMAR and Mongolia decreased from 1069 to 900 kg/ha and from 610 to 369 kg/ha, respectively, (IMIGSD 2011; IOB, Mongolia 2011). However, the extent of grassland degradation in Mongolia is still controversial (Addison et al. 2012).

Our understanding of the dynamics in grassland productivity and sustainable governance of grassland resources rests on contributions from both ecologists and institutional economists. Grassland ecologists developed two conceptual explanations of the dynamics in grassland productivity, referred to as the equilibrium and non-equilibrium grassland models, although there are still some controversies about these models (Briske et al., 2003; Ellis and Swift, 1988; Fernandez-Gimenez, 1999; Oba et al., 2000; Wehrden et al. 2012; Zemmrich et al. 2010). In grazing zones with relatively stable climate, vegetation can have stable seasonal growth rhythms across the years. Livestock grazing intensity has a direct impact on grassland quality, and over-grazing leads to the deterioration of grassland quality. However, in grazing zones with highly variable climate, climate has a more important effect on grassland quality than livestock grazing intensity (Ellis and Swift 1988; Oba et al. 2000). Predictions from the non-equilibrium ecosystem model have been tested in grassland areas of Mongolia and China and shown to better explain grassland productivity dynamics in the semi-arid and arid portions of the region (Fernandez-Gimenez, 1999; Ho, 2001; Zhang, 2007).

Institutional economists interested in studying sustainable governance of natural resources focus on analyzing the social-ecological performance of resource institutions. Three institutional solutions studied for solving common-pool natural resources problems include privatization,

state-control, and community-based natural resource management (Agrawal, 2001; Hardin, 1968; Ostrom, 1990, 2005, 2010). In the semiarid and arid grasslands, cooperative use of grasslands, which facilitates seasonal and interannual migrations, can reduce uncertainties caused by the highly variable precipitation and grassland productivity and avoid pasture over-grazing in the years with droughts (Agrawal, 2001; Wilson and Thompson, 1993). Studies have shown that clear differences in levels of grassland degradation were achieved under mobile grazing in Mongolia versus forced grazing sedentarization in China and Russia (Sneath 1998; Humphrey and Sneath, 1999).

The primary objective of this work was to identify the major drivers of the dynamics in grassland net primary productivity (NPP) across agro-ecological zones and between IMAR and Mongolia after economic transitions in these two political regions. Statistical models have commonly been estimated to diagnose the major drivers of land-use and land-cover change (Brown et al., 2004; Seto and Kaufmann, 2003), and we used static and dynamic spatial panel data models (Elhorst, 2010a; Lee and Yu, 2010) to evaluate the major drivers of dynamics in grassland productivity across agro-ecological zones and two political regions of the Mongolian grasslands. To the best of our knowledge, this is the first use of spatial panel data models for modeling land-use and land-cover change. Satellite images provide a strong basis for measuring grassland productivity at a regional scale, as the dependent variable in the spatial panel data models. Time-series satellite images offer the opportunity for studying grassland productivity over time and space. Specifically, we estimated annual grassland NPP using a remote sensing based light-use efficiency (LUE) approach. The independent variables are the biophysical and/or socioeconomic factors that we hypothesized to drive the dynamics of grassland productivity, including demographic and climatic variables. Because we are concerned with a large area, socioeconomic census data are virtually the only source of region-wide data on the socioeconomic factors, like livestock populations.

Most parts of the Mongolian grasslands are semiarid and arid regions with high interannual variations of precipitation and grassland productivity. For thousands of years, pastoralists have adapted to the highly variable and vulnerable physical environment by migrating seasonally and inter-annually, and nomadism also preserved the grassland ecosystems. Over the past half

century, a large amount of the Mongolian grasslands have been reclaimed for grain and fodder production, especially in IMAR, China. In addition, cropland productivity was also included in the analyses of grassland productivity dynamics because we were not able to exclude cropland from the analysis. We hypothesized that the major drivers of the dynamics in grassland NPP vary across agro-ecological zones and two political regions. Specifically, we hypothesized that: grain output is the major determinant of NPP dynamics in the farming and farming-grazing zones; livestock grazing intensity is the major driver of NPP dynamics in the grazing zone with relatively stable climate; precipitation is the major driver of NPP dynamics in the grazing zone with highly variable climate; the major drivers of NPP dynamics vary between IMAR and Mongolia, given that grazing systems in IMAR are likely also affected by external forces, e.g., market incentives and fodder import from farming areas.

To test the hypotheses, we first divided the Mongolian grasslands into several sub-regions, based on the livelihood sources of rural households and amounts and the interannual variability of precipitation, stated in the non-equilibrium grassland models. Then, we diagnosed the major drivers of NPP dynamics in each of these sub-regions by estimating spatial panel data models. Finally, we interpreted the results in light of scholarship on efficient resource institutions that can govern grassland resources sustainably in the context of the causal factors identified by statistical models. The reminder of this chapter is organized as follows. In Section 5.2, we describe the study area and the datasets used. Section 5.3 introduces the methodology for classifying the sub-regions of the Mongolian grasslands and the structures of the static and dynamic spatial panel data models used in this work. In Section 5.4, we present the modeling results and interpretations. In Section 5.5, we summarize the findings and discuss model limitations and policy and institutional implications.

5.2 Study Area and Data

5.2.1 Study Area

The Mongolian plateau is part of the larger central Asian plateau and has an area of approximately 2.6 million km^2. It is occupied by Mongolia in the northwest and IMAR, China, in the southeast. The study area exhibits gradients of topography, climate, soil, and vegetation (Fig. 5.1). Climate on the Mongolian plateau is continental with extremely cold winters and warm summers. The multi-year mean annual precipitation varies from less than 50 mm in the western desert to around 650 mm in the northeastern forests. Grasslands are the dominant ecosystem types, covering about 66% (0.78 million km^2) and 84% (1.26 million km^2) of the total territories in IMAR and Mongolia, respectively (Angerer et al., 2008; Zhang, 1992). Over the past 50 years, some of the grasslands in IMAR and Mongolia have been reclaimed for grain and fodder production, especially in IMAR. During 1985–2005, 20.3% (23.9 million hectares) of the total land in IMAR was reclaimed for grain production, fodder production, and other uses (IMIGSD, 2008). Since the year 2000, the national government of China has implemented a range of policies for grassland restoration in IMAR, including cropland abandonment (Waldron et al., 2010). In Mongolia, 1.34 million hectares of grasslands were converted to cropland from the late 1950s to the early 1990s (Olonbayar, 2010). The total area of cropland in Mongolia decreased 24.3% from 1995 to 2009 (ACBM, 2010). The decreasing trend was mainly driven by the abandonment of state-owned farms following the economic transition in Mongolia (Olonbayar, 2010).

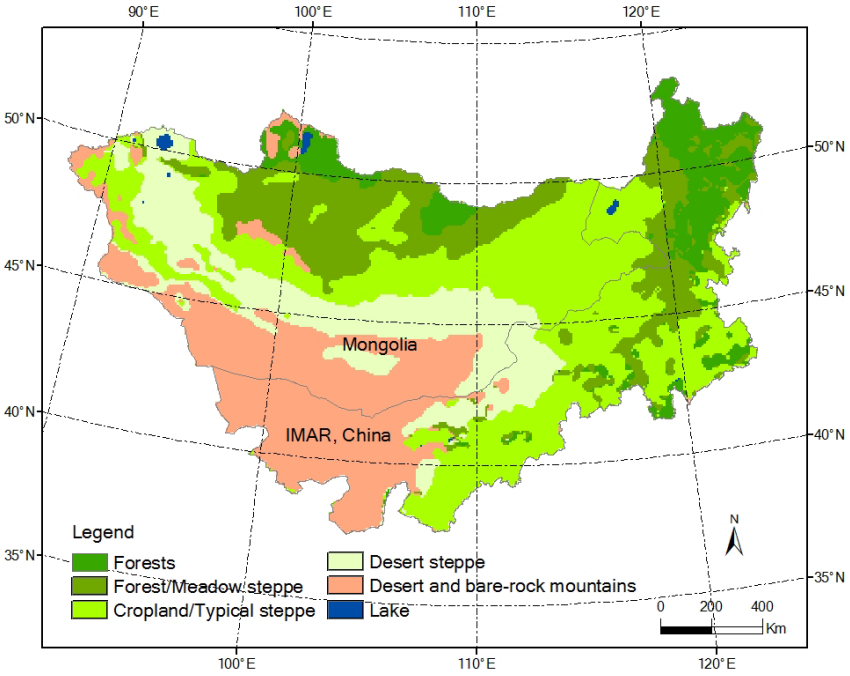

Fig. 5.1 Spatial distributions of the major land-cover types on the Mongolian plateau. Source: vegetation maps of IMAR and Mongolia were respectively provided by the Institute of Botany, China, and the Institute of Botany, Mongolia. They were made in the 1990s and 1980s, respectively. The original scale of the two vegetation maps was 1:1,000,000.

5.2.2 Time-series of Annual NPP

Regional-scale annual NPP (1986−2009) was estimated using a light-use efficiency (LUE) approach based on remotely sensed data. Vegetation NPP ($g \cdot C \cdot m^{-2} \cdot day^{-1}$) represents the total amount of solar energy converted into dry plant matter through photosynthesis, and it is calculated as the total energy used in plant photosynthesis (referred to as gross primary productivity; GPP) subtracted by the energy used for plant respiration for maintenance and growth. In the LUE approach, GPP is assumed to be proportional to the amount of absorbed photosynthetically active radiation (APAR). APAR is the product of incident photosynthetically active radiation (PAR) and the reflectance properties expressed through a vegetation index (Running et al., 1999). Annual NPP is accumulated in the growing season of grasslands. In the Mongolian grasslands, the growing season is roughly from late April to September. Detailed descriptions about the NPP estimation and validation procedures for the annual grassland NPP time-series on the Mongolian plateau are provided in Chapter Two. The spatial resolution of the annual NPP time-series was 8 × 8 km.

5.2.3 Climate and Socioeconomic Data

We compiled climate data from national standard meteorological stations in Mongolia (17 stations) and IMAR (47 stations) (CIMAR 2011; CM 2011). We spatially interpolated monthly total precipitation and monthly mean temperature (1986−2009) using universal kriging. Previous studies using long-term field measurements of aboveground biomass have shown that grassland productivity in IMAR was sensitive to mean temperature and total precipitation between January and July (Bai et al., 2008). The climate variables accumulated between January and July were used as independent variables in the spatial panel data models. County-level annual livestock populations (the year-end value), grain output, and human populations of IMAR (1986–2007) and the province-level annual populations of people and livestock of Mongolia (1995–2009) were compiled from annual census books of IMAR and Mongolia (ACBIMAR, 2010; ACBM, 2010). Based on census data, cropland occupies only a very small portion (less than 0.5%) of Mongolia (ACBM, 2010). Therefore, we did not use data on grain output of Mongolia. To match the scale of the socioeconomic data, we spatially aggregated climate and NPP datasets to county and province levels in IMAR and Mongolia, respectively.

5.3 Methods

5.3.1 Mapping Agro-ecological Zones of the Mongolian Grasslands

Ecological conditions, including climate and vegetation (Fig. 5.1), vary greatly across the Mongolian grasslands. In order to identify the major drivers of the dynamics in grassland NPP over space, we assigned the counties and provinces of IMAR and Mongolia to different agro-ecological zones based on information about sources of rural household income and precipitation criteria associated with non-equilibrium model of grassland dynamics (Ellis and Swift, 1988; Zhang, 2007). Based on census data (ACBIMAR, 2010; ACBM, 2010), if more than 80% of agricultural income of rural households in a jurisdictional unit is from farming or grazing, we assigned the unit as farming or grazing zone, respectively. If farming and grazing income were both in the range 20%–80% of the total agricultural income, we assigned the unit into farming-grazing zone. The annual mean precipitation and the interannual variability of precipitation

(1986−2009) were used to distinguish grazing zones with different climate conditions (Ellis and Swift, 1988; Fernandez-Gimenez, 1997). The grazing zone with relatively stable climate was defined as having a mean annual precipitation of more than 250 mm and the interannual variability of precipitation, represented by the coefficient of variation of annual precipitation, of less than 33%. The grazing zone with highly variable climate was defined as having a mean annual precipitation of less than 250 mm and the coefficient of variation of annual precipitation of more than 33%. Compared to the vegetation map (Fig. 5.1), we can find that most of meadow steppes of IMAR and Mongolia are in the grazing zones with relatively stable climate; and typical and desert steppes are mostly in the grazing zones with highly variable climate (Fig. 5.2).

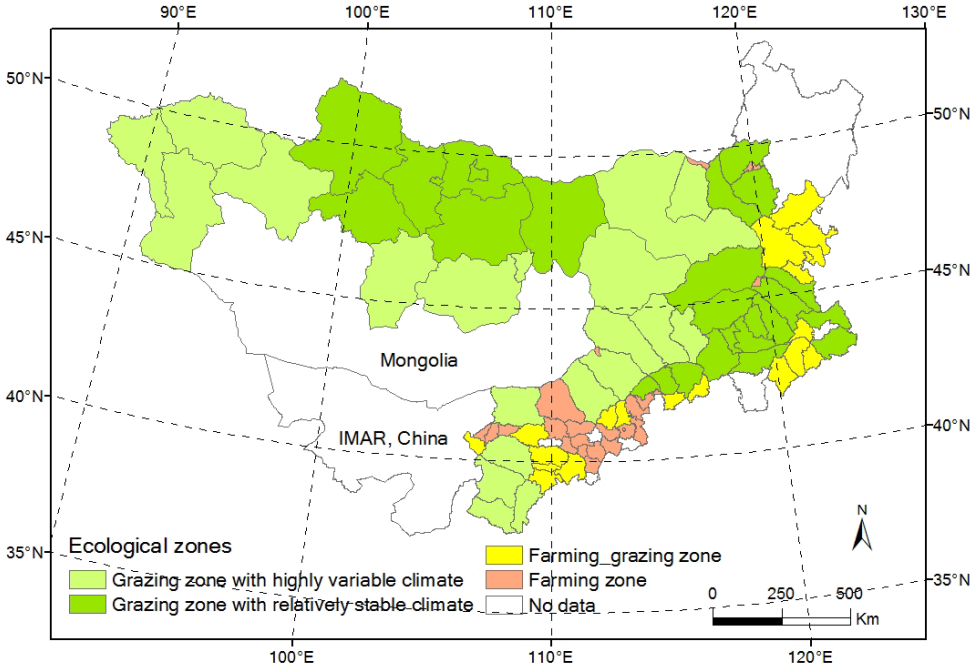

Fig. 5.2 Spatial heterogeneity of grassland social-ecological systems in Mongolia and IMAR, China.

5.3.2 Modeling the Drivers of NPP Dynamics with Spatial Panel Data Models

We began with exploratory analysis of the correlations between annual NPP and explanatory variables across time in each county or province, and we assigned each correlation to one of the four types: significantly positive ($p < 0.05$), positive but not significant ($p > 0.05$), negative but not significant ($p > 0.05$), and significantly negative ($p < 0.05$). We used the false discovery rate (FDR) control procedure to exclude the polygons that may be falsely labeled due to spatial

autocorrelations of these variables (Benjamini and Hochber, 1995). The threshold value of FDR was set equal to 0.05. Next, we built regression models between the time-series of NPP and explanatory variables. A simple cross-sectional regression model that links NPP and socioeconomic and biophysical variables does not allow sufficient degrees of freedom to estimate statistically reliable models (Frees, 2004; Hsiao, 1986). To increase the reliability of modeling results, we used panel data analysis to take advantage of the increased variation and reduced collinearity in data that we collected at the smallest possible administrative unit over time. Panel data models can be used to relax the common assumptions in traditional cross-sectional or time-series data analyses that regression parameters are identical for all individuals or at all time points. Incorporating heterogeneity into panel data models is often motivated by the concern that important explanatory variables have been omitted from panel data models (Frees, 2004). The obvious generalization of the constant-intercept-and-slope model for panel data is to introduce dummy variables to account for the effects of those omitted variables that are specific to individual cross-sectional units but stay constant over-time, and the effects that are specific to each time point but are the same for all cross-sectional units (Elhorst, 2003, 2010a; Hsiao, 1986). Panel data models can be assigned into four types in representing the heterogeneity among individual units: fixed effects, random effects, fixed coefficients, and random coefficients models (Elhorst, 2010a).

Panel data models are promising options for modeling land-use and land-cover change. They allow relationships between the independent variable (drivers of land-use and land-cover change) and the dependent variable (measures of land-use and land-cover) to vary across space and time (Brown et al., 2004; Seto and Kaufmann, 2003). Because we only modeled NPP dynamics following major economic transitions in Mongolian and IMAR, we assumed no time-specific effects and focused only on individual (spatial location) specific effects. The spatial panel data models, used in this work, have heterogeneous intercepts and homogeneous slope. Spatial specific effects may be treated as fixed effects or as random effects. In the fixed effects models, a dummy variable is introduced for each spatial unit; while in random effects models, the effects that are specific to spatial units are treated as a standard Gaussian random variable. When the random effect model is implemented, the units of observation should be representative of a large population, and the number of units should potentially be able to go to infinity (Elhorst, 2010a).

In this work, we have a limited number of observational units in Mongolia and IMAR. Therefore, we chose the spatial fixed effect models.

A simple panel data model with spatial fixed effects is (Frees, 2004)

$$y_{it} = x_{it}\beta + \mu_i + \varepsilon_{it} \tag{5-1}$$

where y_{it} is the dependent variable value at measurement of unit i ($i = 1, 2, \ldots, N$) and time point t ($t = 1, 2, \ldots, T$); x_{it} is vectors of observations for m independent variables ($[N \times T] \times m$); β is a matching vector of fixed but unknown model parameters ($m \times [N \times T]$); ε_{it} is an independently and identically distributed error term with zero mean and variance of σ^2; μ_i denotes a spatial specific effect. The standard reasoning behind spatial specific effects is that they control for all space-specific and time-invariant variables whose omissions could bias the parameter estimates in a typical cross-sectional model (Elhorst, 2010a). In the case of our modeling of grassland NPP dynamics, we may omit some space-specific variables that affect annual NPP dynamics, for example soil fertility. The random variables μ_i and ε_{it} are assumed as independent of each other. For many panel datasets, the number of units is large relative to the number of observations per unit, and these are useful to reveal the relationships among variables and to account for subject-level heterogeneity (Frees, 2004).

Grassland NPP aggregated at jurisdictional levels tends to have spatial and/or spatio-temporal autocorrelations. In order to account for the spatial and/or temporal interactions, we used both static and dynamic spatial panel data models to diagnose the drivers of NPP dynamics across ecological gradients and between IMAR and Mongolia. When the interactions between spatial units of observation are taken into consideration, the panel data model will contain a spatially lagged dependent variable or a spatial autoregressive process in the error term, known as the spatial lag model and the spatial error model, respectively (Elhorst, 2010a). In this study, we chose spatial-lag models to account for the spatial autocorrelations of grassland annual NPP on the Mongolian plateau. This assumes that grassland productivity in one study unit was affected by the productivities of neighboring units. For example, if a study unit was surrounded by neighboring units with high productivities, this unit might have better ground water supply and

be less affected by wind erosion. In addition, the spatial fixed effects included in the panel model could also account for the missing variables (e.g., soil types) which could explain the spatial differences in grassland annual NPP. The spatial lag model posits that the dependent variable value is affected by the value of the dependent variable in neighboring units

$$y_{it} = \delta \sum_{j=1}^{N} w_{ij} y_{jt} + x_{it}\beta + \mu_i + \varepsilon_{it} \tag{5-2}$$

where $i = 1, 2, \ldots, N$, $j = 1, 2, \ldots, N$, $t = 2, 3, \ldots, T$, δ is called the spatial autoregressive coefficient, representing the influence from neighboring units. w_{ij} is an element of the spatial weights matrix, and it describes the proximity of two observational units. It is assumed that the spatial weights matrix is a pre-specified non-negative matrix. We assumed a constant spatial weight matrix over time, based on the inverse distance method to calculate spatial weights between spatial units in the software package ArcGIS (ESRI, Redlands, CA, USA).

An important advantage of panel data is the opportunity to model the dynamic patterns in the data. Incorporating the correlation structure of the data over time is important for achieving efficient parameter estimates, especially for datasets with many observations over time (Elhorst, 2010a; Frees, 2004). If temporal autocorrelation of the dependent variable is taken into consideration, the spatial panel data model becomes a dynamic spatial panel data model.

$$y_{it} = \delta \sum_{j=1}^{N} w_{ij} y_{jt} + \gamma y_{i,t-1} + \rho \sum_{j=1}^{N} w_{ij} y_{j,t-1} + x_{it}\beta + \mu_i + \varepsilon_{it} \tag{5-3}$$

where $i = 1, 2, \ldots, N$, $j = 1, 2, \ldots, N$, $t = 2, 3, \ldots, T$. The parameters γ and ρ are measures of the relationship between $y_{i,t-1}$ and $y_{i,t}$, which are called the temporal and spatio-temporal autoregressive parameters, respectively. In this study, grassland annual NPP tended to be temporally auto-correlated. Grassland NPP in one specific year was affected by productivities in the previous years (e.g., livestock overgrazing tends to cause the degradation in grassland productivity). Therefore, in addition to static spatial panel data models, we also ran the dynamic spatial panel data models in this study.

Given space limitations, the parameter estimation procedures for static and dynamic spatial panel data models are not detailed here. Readers are referred to Elhorst (2010b), Lee and Yu

(2010), and Yu et al. (2008) for detailed discussions about using the maximum likelihood method to estimate the parameters of the spatial panel data models. The t-test was used to assess whether the estimated regression coefficients were significantly different from zero. We calculated the goodness of fit (pseudo-R^2) to measure the explanatory power of the spatial panel data models. In order to test the contribution of each of the independent variables to both static and dynamic spatial panel data models, we iteratively removed the independent variables and ran the spatial panel data models to calculate the values of pseudo-R^2. The static and dynamic spatial panel data models used in this study were coded by the authors in MATLAB (Mathworks Inc., Natick, Massachusetts, USA), based on the sample MATLAB codes provided in Elhorst (2010b) and Lee and Yu (2010). The biophysical and socioeconomic data used for fitting the static and dynamic spatial panel data models (Table 5.1) were normalized to 0−1.

Table 5.1 Variables for the static and dynamic spatial panel data models.

Name	Description	Definition
NPP	Net primary productivity	Annual NPP accumulated in the growing season from late April to September
PRECIP	Precipitation	Total monthly precipitation from January to July
TEMP	Temperature	Mean monthly temperature from January to July
LIVE	Livestock population	Year end livestock population
GRAIN	Grain output	Annual grain output
POP	Human population	Annual human population
DELTA (δ)	Spatial autoregression	Spatially lagged dependent variable in Equations 5-2 and 5-3
RHO (ρ)	Spatio-temporal autoregression	Spatio-temporally lagged dependent variable in Equation 5-3
GAMMA (γ)	Temporal autoregression	Temporally lagged dependent variable in Equation 5-3

5.4 Results

5.4.1 Correlations between NPP and Explanatory Variables

Temperature was positively correlated with NPP in most parts of Mongolia and IMAR, but most of the correlations were not statistically significant (Fig. 5.3a and e). The relationships between NPP and precipitation were only significant in two provinces of Mongolia (Fig. 5.3b); both of which are in the grazing zone with highly variable climate (Fig. 5.2). In most semiarid and arid counties of IMAR, precipitation was significantly correlated with annual NPP (Fig. 5.3f). In Mongolia, livestock populations were positively correlated with NPP in the grazing zone with

relatively stable climate, although the correlation relationships were not statistically significant for most provinces; in Mongolia, the correlations between livestock populations and NPP were not significant for most provinces in the grazing zone with high variable climate (Fig. 5.3c). The correlations between NPP and human populations were not significant for all provinces. The correlations were positive for most provinces in the grazing zone with highly variable climate and negative in most provinces in the grazing zone with relatively stable climate (Fig. 5.3d). Livestock populations were positively correlated with NPP in most of the grazing counties of IMAR (Fig. 5.3g). Annual grain output was significantly correlated with NPP in most of the farming and farming-grazing counties of IMAR (Fig. 5.3h). Human populations were significantly correlated with NPP in some of the farming counties of IMAR (Fig. 5.3i).

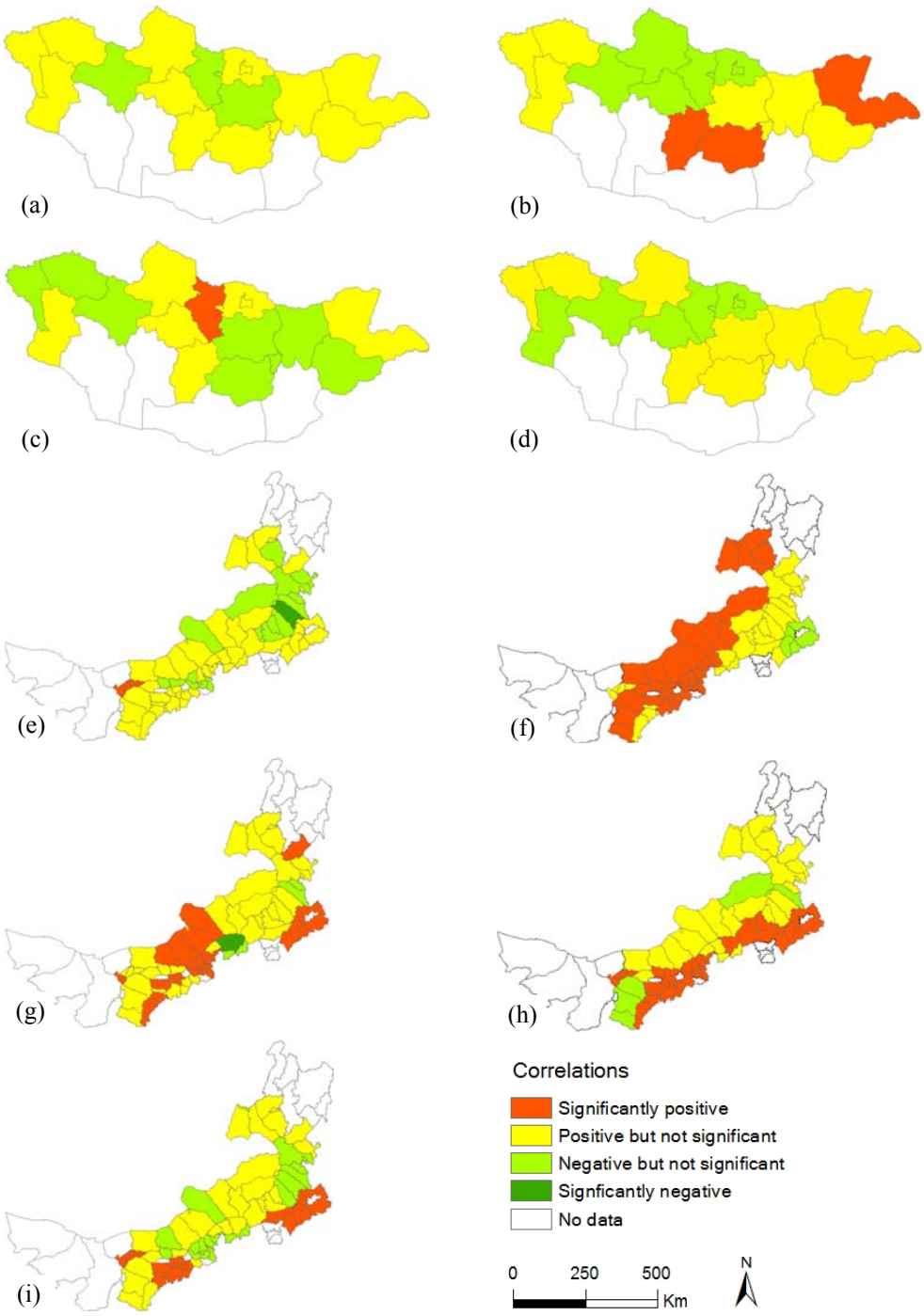

Fig. 5.3 Temporal correlations between NPP and explanatory variables in counties of IMAR (1986−2007) and provinces of Mongolia (1995−2009): (a) NPP–temperature in Mongolia; (b) NPP–precipitation in Mongolia; (c) NPP–livestock populations in Mongolia; (d) NPP–human populations in Mongolia; (e) NPP–temperature in IMAR; (f) NPP–precipitation in IMAR; (g) NPP–livestock populations in IMAR; (h) NPP–grain output in IMAR; (i) NPP–human populations in IMAR.

5.4.2 Drivers of NPP Dynamics across Agro-ecological Zones

In the farming and farming-grazing zones of IMAR, precipitation and grain output had significantly positive relationships with NPP (Table 5.2). In these two regions, grain production was the major human land-use activity, and grain output played a dominant role in influencing NPP dynamics. In the two grazing zones of IMAR, precipitation and livestock populations had significantly positive relationships with NPP. In IMAR, precipitation played a dominant role in influencing annual NPP dynamics in the grazing zone with highly variable climate, and its influence relative to livestock populations was lower in the grazing zone with relatively stable climate. In Mongolia, precipitation was the only factor that had a significantly positive relationship with NPP in the grazing zone with highly variable climate. In this zone, livestock populations were negatively correlated with NPP, although the linear relationship was not significant. In Mongolia, livestock population was the only factor that was significantly correlated with NPP in the grazing zone with relatively stable climate. This zone is mainly distributed in the northern mountainous regions with cold and wet climate (Fig. 5.2), and precipitation was less important in influencing NPP dynamics. For most of the agro-ecological zones, human populations did not have a significant linear relationship with NPP. Temperature did not have significant linear relationships with NPP in any zone; the observed relationships were negative for most zones.

The relationships between NPP and explanatory variables identified by the spatial panel data model were consistent with results of the exploratory correlation analyses (Fig. 5.3). For all of the agro-ecological zones, the spatially lagged NPP had significant linear relationships with the dynamics of NPP (Table 5.2). The values of the spatial fixed effects of the spatial panel data models for IMAR and Mongolia show clear spatial patterns (Fig. 5.4). As a result, the spatial fixed effects in the models could account for some of the missing explanatory variables of the dynamics of annual NPP.

Table 5.2 Static spatial panel data models for NPP dynamics using normalized variables.

Variable	IMAR, China				Mongolia	
	Farming	Farming_grazing	Grazing zone_H	Grazing zone_S	Grazing zone_H	Grazing zone_S
PRECIP	0.1826***	0.0275**	0.2568***	0.1684***	0.0927**	-0.0304
TEMP	0.0054	-0.0264	-0.0157	-0.0909	-0.0149	0.0410
LIVE	0.0431	0.0084	0.1381**	0.1281**	-0.0353	0.1053**
GRAIN	0.2579***	0.0468**				
POP	0.1842*	0.0944	0.0962	0.4042*	0.0060	-0.3106
DELTA	0.1361**	0.6690***	0.1361**	0.1361**	0.3285***	0.5107***
Pseudo-R^2	0.8935	0.8709	0.8640	0.8082	0.8613	0.8894

*** $p < 0.001$; ** $p < 0.01$; * $p < 0.05$

Note: Grazing zone_H means the grazing zone with highly variable climate; and Grazing zone_S means the grazing zone with relatively stable climate.

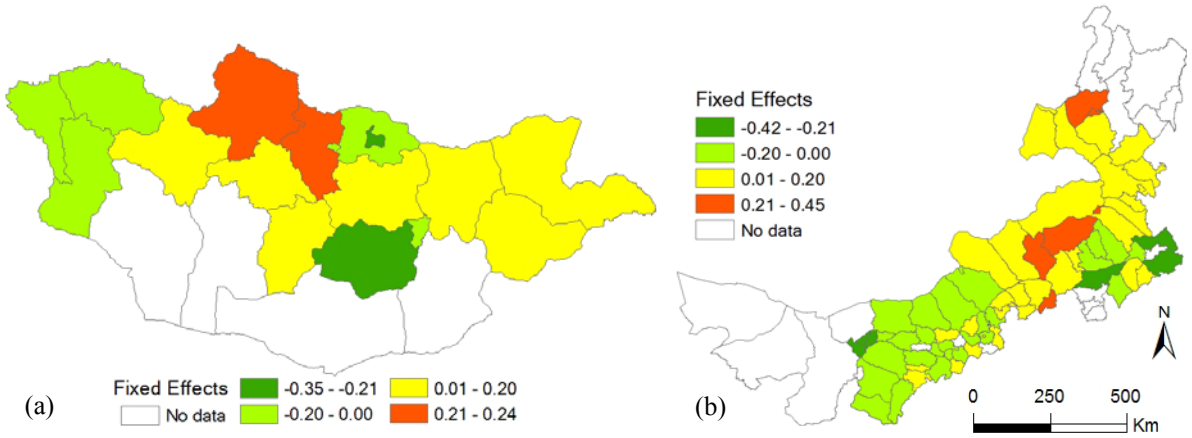

Fig. 5.4 Values of the spatial fixed effects for the static spatial panel data models of NPP dynamics: (a) Mongolia; (b) IMAR.

Adding the temporally lagged dependent variable and the spatio-temporally lagged dependent variable into the models did not change the relationships among the variables much. The relative importance of the causal factors in all of the sub-regions did not change in any of the models, although the temporally lagged dependent variable was significantly correlated with NPP in the farming-grazing zone and the grazing zone with relatively stable climate of IMAR (Table 5.3). This suggested that the models can provide the basis for constructing unbiased estimators when the dynamic aspects of the dependent variable are ignored. The values of the overall goodness of fit (pseudo-R^2) for the spatial panel data models show that all of the models have high explanatory power for the dynamics of NPP (pseudo-$R^2 > 0.8$). The results of testing the relative influence of each variable on the model's ability to predict NPP indicated that the spatially lagged NPP had the highest explanatory power for all panel data models. Grain output had high explanatory power in farming and farming-grazing zones of IMAR. Precipitation and livestock

populations had high explanatory power in the two grazing zones of IMAR. In Mongolia, precipitation was the only variable that had high explanatory power in the grazing zone with highly variable climate, and livestock populations was the only variable that had high explanatory power in the grazing zone with relatively stable climate (Tables 5.4 and 5.5).

Table 5.3 Dynamic spatial panel data models for NPP dynamics using normalized variables.

Variable	IMAR, China				Mongolia	
	Farming	Farming_grazing	Grazing zone_H	Grazing zone_S	Grazing zone_H	Grazing zone_S
PRECIP	0.0963***	0.0294***	0.1302***	0.0873***	0.0925**	-0.0517
TEMP	-0.0244	-0.0324	-0.0153	-0.0367	-0.0142	0.0360
LIVE	0.0381	0.0070	0.0941**	0.0564*	-0.0370	0.1103**
GRAIN	0.1304***	0.0462**				
POP	0.0749*	0.0803	0.0780	0.1996*	0.0054	-0.2965
DELTA	0.1325***	0.6733***	0.1327***	0.1310***	0.3719***	0.5572***
RHO	0.0025	-0.1571	0.0182	-0.1991	-0.1355	-0.0744
GAMMA	0.0767	0.2077***	0.0231	0.1545*	0.1682	0.0913
Pseudo-R^2	0.9006	0.8825	0.8913	0.8104	0.8692	0.8996

*** $p < 0.001$; ** $p < 0.01$; * $p < 0.05$

Note: Grazing zone_H means the grazing zone with highly variable climate; and Grazing zone_S means the grazing zone with relatively stable climate.

Table 5.4 Pseudo-R^2 values of static spatial panel data models for NPP dynamics: iteratively removing the independent variables to show their explanatory power.

Variable	IMAR, China				Mongolia	
	Farming	Farming_grazing	Grazing zone_H	Grazing zone_S	Grazing zone_H	Grazing zone_S
PRECIP	0.7784	0.7616	0.6343	0.6559	0.6024	0.7093
TEMP	0.8913	0.8657	0.8586	0.8062	0.8370	0.8125
LIVE	0.8394	0.8002	0.7049	0.6346	0.7992	0.6250
GRAIN	0.6123	0.6305				
POP	0.8288	0.7809	0.8086	0.7058	0.8026	0.7338
DELTA	0.4512	0.3086	0.4979	0.4713	0.4377	0.4107
Overall	0.8935	0.8709	0.8640	0.8082	0.8613	0.8894

Note: Grazing zone_H means the grazing zone with highly variable climate; and Grazing zone_S means the grazing zone with relatively stable climate.

Table 5.5 Pseudo-R^2 values of dynamic spatial panel data models for NPP dynamics: iteratively removing the independent variables to show their explanatory power.

Variable	IMAR, China				Mongolia	
	Farming	Farming_grazing	Grazing zone_H	Grazing zone_S	Grazing zone_H	Grazing zone_S
PRECIP	0.7812	0.7488	0.6130	0.6496	0.6003	0.7882
TEMP	0.8981	0.8711	0.8663	0.7993	0.8471	0.8207
LIVE	0.8431	0.8129	0.6992	0.6125	0.7960	0.6190
GRAIN	0.6036	0.6254				
POP	0.8259	0.8092	0.8160	0.6981	0.8015	0.7305
DELTA	0.4225	0.3119	0.4492	0.4637	0.4317	0.4139
RHO	0.8874	0.8794	0.8831	0.8059	0.8572	0.8701
GAMMA	0.8890	0.8633	0.8795	0.7937	0.8490	0.8693
Overall	0.9006	0.8825	0.8913	0.8104	0.8692	0.8996

Note: Grazing zone_H means the grazing zone with highly variable climate; and Grazing zone_S means the grazing zone with relatively stable climate.

5.5 Discussion

We analyzed the drivers of NPP dynamics across the agro-ecological zones in the Mongolian grasslands, using spatial panel data models. Most of the Mongolian grasslands are located in semi-arid and arid regions, and precipitation was significantly correlated with NPP, except in the grazing zone with relative stable climate in Mongolia. Annual grain production was the major reason for NPP dynamics in the farming and farming-grazing zones of IMAR. Livestock populations had significantly positive relationships with NPP in the two grazing zones of IMAR and the grazing zone with relative stable climate in Mongolia. These relationships were counter to the hypotheses generated by the equilibrium grassland model, which postulates that increased grazing intensity results in decreased productivity and grassland degradation in places where climate is stable (Fernandez-Gimenez, 1999; Zhang, 2007). Possible reasons for these counterintuitive results include imports of fodder and hay from other areas (e.g., farming and farming-grazing areas), human land-use (e.g., fertilization and irrigation) and livestock management activities, impacts of climate hazards on livestock populations, and low grazing intensity (i.e., not reaching the carrying capacity of pastures). In addition, there may be some endogeneity, in which herders move over time to areas with high productivity because they are high and abandon areas of low productivity. Such endogenous interactions cannot currently be represented in the spatial panel data models.

A number of challenges limit our ability to interpret causation based on the static and dynamic spatial panel data models of NPP dynamics. The results of the panel data models for IMAR and Mongolia may not be comparable because the data for fitting the spatial panel data models of the two regions were aggregated at different spatial and jurisdictional scales. In this case, we do not have fine resolution census data (at soum level) of Mongolia. One of the challenges in merging remotely sensed data and socioeconomic data is to identify the scale of analysis and modeling. Aggregating the values of remote sensing pixels to the scale of census polygons is a common way to match the two types of data. Because census data are collected at different jurisdictional levels with different sizes, analyzing and modeling the causes of land-use and land-cover change often requires attention to the modifiable area unit problem (MAUP), i.e. the shape and size of data aggregation affects analysis. MAUP can produce analytical artifacts that result from the variations in the sizes and geographic arrangement of geographical units (Brown et al., 2004). The relationships inferred among the variables in the models may change as the sizes of spatial units change.

Inaccuracies and errors associated with data used in this study can be a problem. The estimated NPP included the productivity of cropland, and we were not able to exclude farming activities from the study area. Grassland biomass was not the only food source for livestock, especially in IMAR. Using imported fodder will definitely affect the model-inferred relationships between annual NPP and livestock populations. Compared with Mongolia, the grazing systems in IMAR were more strongly affected by fodder imported from farming regions because of grassland degradation and incentives for keeping more animals, stimulated by market benefits (Li et al., 2007; Zhang, 2007). Further, the data about the populations of people and livestock did not measure exactly the variables of interest. The data on human populations used here included both urban and rural populations, and we were not able to exclude urban population from total population due to lack of detailed data. The data of livestock populations used in the panel data models included both locally grazed and stall-fed livestock populations, and we did not have detailed census data about the proportions of livestock populations that were stall-fed. This data problem was less serious in Mongolia because most animals were locally and seasonally grazed.

Livestock management behaviors of herders also affected the statistical modeling results. Studies have shown that in IMAR, the number of livestock that herder households plan to manage is usually based on two factors: the ability to buy fodder during droughts and the anticipated amount of rainfall in the next year (Zhang, 2007). Herders usually do not want to sell most of their livestock in the years with droughts when livestock prices were fairly low, and they usually want to buy fodder or migrate to greener places to keep their livestock alive and wait for the years with more rainfall. These livestock management behaviors of local herders should affect the inferred relationships among the variables. Moreover, empirical studies indicate that it usually takes four years to recover the livestock populations after severe droughts, due to the breeding cycles of livestock (Zhang, 2007).

Assumptions in the spatial panel data models, such as linear relationships among the variables, no correlations among independent variables, and no autocorrelations of independent variables, also affect the identification the major drivers of NPP dynamics accurately. Panel data modeling methods that account for both spatial and temporal autocorrelations of dependent and independent variables are still under development (Elhorst, 2010a). In the static and dynamic spatial panel data models, the spatial autocorrelation term had significant relationships with NPP. This may be caused by other missing explanatory variables, such as soil fertility and ground water, which caused the spatial autocorrelation of NPP. In addition, we assumed unidirectional causal relationships for the spatial panel data models, i.e., the selected independent variables were the dominant causal factors for NPP dynamics. The endogeneity problem caused by the bidirectional causal relationships between livestock populations and NPP could affect parameter estimations and the interpretations of the modeling results, especially in the grazing zones with relative stable climate in which livestock grazing intensity played a more important role in affecting NPP dynamics. Model misspecification can lead to spurious results. This is especially the case with panel data, where model coefficients can vary both temporally and spatially (Brown et al., 2004). The spatial panel data models that can account for the endogeneity problem are still underdevelopment. Finally, similar to any other statistical methods, spatial panel data models were insufficient to establish causal relationships among variables. However, they can be more useful than purely cross-sectional data models in establishing causality.

Understanding the drivers of NPP dynamics across heterogeneous landscapes is important for providing evidence-based policy recommendations for sustainable governance of grassland resources. The heterogeneous drivers of NPP dynamics indicated the necessity of diverse resource policies and institutions to accommodate the diversity of grassland social-ecological systems and to govern grassland resources sustainably (Ostrom, 2005). In the grazing zones with highly variable climate, cooperative use of grasslands is an effective way to minimize the loss caused by the high interannual variability of precipitation and forage. Studies have shown that in Mongolia, grassland productivity degraded the most in meadow steppe, and this was mainly driven by grazing sedentarization and overgrazing in these areas (Olonbayar 2010). In the grazing zones with relatively stable climate, controlling livestock grazing intensity is important for sustainable use of grasslands.

Acknowledgments

This work was conducted with financial support from the NASA Land-Cover and Land-Use Change Program (NNX09AK87G). The authors would like to thank Dr. Paul Elhorst from University of Groningen and Dr. Jihai Yu from University of Kentucky for their guidance in building spatial panel data models.

PART IV

SOCIAL ADAPTATION TO ENVIRONMENTAL CHANGE

Chapter Six

Climate Adaptation, Local Institutions, and Rural Livelihoods: A Comparative Study of Herder Communities in Mongolia and Inner Mongolia, China

Abstract

The livelihoods of natural resource dependent herders on the Mongolian plateau are vulnerable to climate change and pasture degradation, both of which have threatened the sustainability of their economic activities. Therefore, social adaptation to environmental change is increasingly important for local sustainable development. This chapter applies an analytical framework focused on adaptation, institutions, and livelihoods (AIL) to study climate adaptation and local institutions on the Mongolian plateau. A household survey was designed based on the AIL framework and implemented in each of three grassland community types (meadow, typical and desert steppes) in both Mongolia and China. The analytical results, based on field data from diverse institutional, social, and ecological contexts, revealed prominent differences in the way herders adapted to environmental change between the two countries. Local institutions, including public, private, and civic institutions, played the central role in shaping and facilitating livelihood adaptation practices of herder households. However, they have undermined the adaptive capacity of herder communities in some ways. While mobile grazing was the predominant adaptation strategy for herders in the Mongolian grasslands to cope with uncertainties in precipitation and forage, the storage of fodder and hay represents the second most important strategy. Multilevel statistical models of fodder purchasing behaviors indicated that livestock management behaviors, household financial capital, climate variability, and the status of pasture degradation had statistically significant relationships with the percentage of income spent on fodder and hay.

Keywords: Climate adaptation; local institutions; rural livelihoods; Mongolian grasslands; sustainability

---

Wang, J., Brown, D. G., Agrawal, A., Xing, Q. Climate adaptation, local institutions, and rural livelihoods: A comparative study of herder communities in Mongolia and Inner Mongolia, China. Manuscript submitted for review.

6.1 Introduction

Climate change has been increasing the vulnerability of livelihoods in the natural resource dependent rural populations (Agrawal, 2009; Eakin, 2005; Fernandez-Gimenez et al., 2012). Climate dynamics affect rural communities through changes in both the mean values of key climate variables and their variability (Lemos et al., 2007). Rural communities have constantly adapted to changes in the conditions and dynamics of the climate and natural resources they experience. Social vulnerability, adaptation, and adaptive capacity are interrelated terms in the analysis of the potential effects of environmental change, especially climate change, on local communities and their potential responses to it (Adger, 2006; Smit and Wandel, 2006; Turner II et al., 2003). Adaptation to climate change can happen at multiple scales (Adger, 2005), e.g., resulting from top-down changes in policies and institutions and bottom-up household autonomous responses, and their effectiveness depends on a variety of environmental and social contextual factors that are both internal and external to local communities (Agrawal, 2009).

Institutions, which are the formal laws and policies and informal norms and rules that structure human interactions and govern the interactions between humans and their environment (North, 1990; Ostrom, 1990), can either enhance or undermine the adaptive capacity of rural populations for environmental change (Adger, 2000; Agrawal, 2009; Li and Huntsinger, 2011). Local formal institutions are the instruments of the national-level policies and institutions. Local informal institutions have evolved in response to international, national, and local contexts to structure human interactions. In order to reduce climate-related vulnerability, it is crucially important to understand how local institutions shape climate adaptation and how local institutions can strengthen the adaptive capacity of rural populations.

Local institutions, including public/governmental, private/market, and civic/community institutions, play a key role in livelihood adaptation to environmental change, as reflected in the adaptation, institutions, and livelihoods (AIL) framework, developed by Agrawal (2009) (Fig. 6.1). In the context of climate change as a major stressor on the natural resource dependent rural populations, local institutions can influence rural livelihoods and their adaptation in three major ways: they shape the impact of climate change on rural communities; they shape the ways that

rural communities respond to climate change; they are the intermediaries for external support to local climate adaptation. External interventions that facilitate climate adaptation can work through provision of information, technology, finance, and leadership (Agrawal, 2009). By examining livelihood adaptation strategies historically adopted by rural communities, the role of local institutions in climate adaptation can be observed. Based on such observations, Agrawal (2009) identified five basic livelihood adaptation strategies in the context of environmental risks to livelihoods: *mobility*, which pools risks across space; *storage*, which pools and reduces climate risks over time; *livelihood diversification* reduces risks across assets owned by households or collectives; *common pooling*, which pools risks across households in local communities; and *market exchange*. He argued that all of these livelihood adaptation strategies can only work in certain formal (e.g. property rights) and informal (e.g. trust and reciprocity) institutional arrangements, i.e., adaptation never occurs in an institutional vacuum.

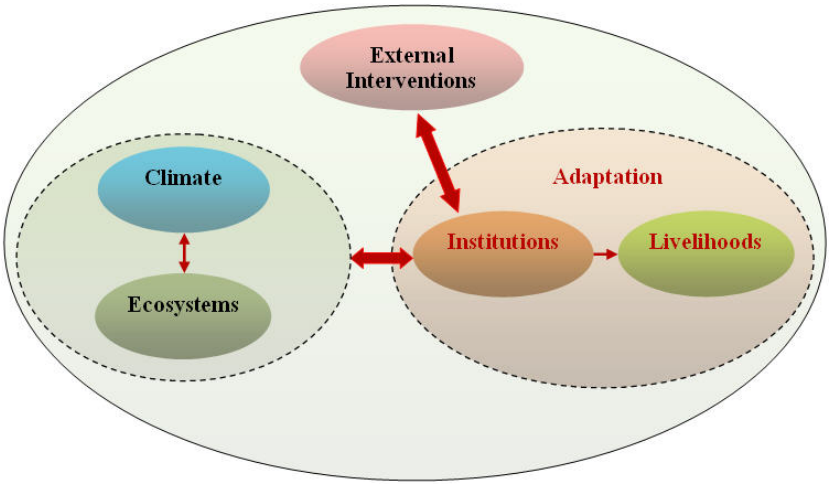

Fig. 6.1 The framework of adaptation, institutions, and livelihoods (adapted from Agrawal, 2009).

In the semiarid and arid grasslands of the world, such as Africa and Inner Asia, migration has been a particularly important livelihood adaptation strategy for pastoralists to live with the highly variable precipitation and forage. Migration over large geographic distances represents a key adaptation strategy to the high spatio-temporal variability of precipitation and grassland productivity. For centuries, institutional arrangements that include flexible property boundaries and reciprocal use of pastures have allowed pastoralists to use grassland resources efficiently and to cope with frequent climate hazards. Those local institutions have evolved over thousands of years and are well fit the biophysical characteristics of local ecological systems. The pastoral

system on the Mongolian plateau, including the country of Mongolia and the Inner Mongolia Autonomous Region (IMAR), China, was a typical example of the traditional grazing systems. Over thousands of years, herders on the Mongolian plateau have adapted to the highly variable climate and forage by altering their mobility patterns, shifting livelihood strategies, varying herd compositions, and undertaking marketing activities (Fernandez-Gimenez, 1997). However, over the past fifty years (1961−2010), climate change and pasture degradation have increased the vulnerability of livelihoods for herders on the Mongolian plateau (Chapter Four). In this context, we analyzed the interactions among climate-related vulnerability, livelihood adaptation, local institutions, and external interventions in the two neighboring countries of Mongolia and China, based on the AIL framework (Agrawal, 2009). Comparative analyses of livelihood adaptation practices under different institutional arrangements in the two countries can help us understand the relationships between local institutions and climate adaptation. This information is meaningful for guiding policy interventions to strengthen the adaptive capacity of herder communities for future climate change.

We designed a household survey based on the AIL framework to study livelihood adaptation of herders on the Mongolian plateau to environmental change. The household survey was implemented to sample herder households from a range of environmental conditions within Mongolia and IMAR, China. Matched sites in each of three ecological zones in the two different countries helped to reduce the differences in underlying ecological variability between the two countries and allowed us to focus on differences in adaptation strategies and local institutions across the border. Our focus was on the following questions: (1) what were the major livelihood adaptation strategies adopted by herders on the Mongolian plateau to cope with climate change and pasture degradation over the past ten years?; (2) what kinds of local institutions were those livelihood adaptation strategies facilitated by?; and (3) what were the determinants of variations in livelihood adaptation choices? For the third question, we focused on identifying the determinants of fodder purchasing behaviors of herders. While mobile grazing was the predominant adaptation strategy for herders in the Mongolian grasslands to cope with uncertainties in precipitation and forage, the storage of fodder and hay represents the second most frequent strategy. This strategy has become increasingly important as opportunities for mobile grazing have decreased and diminished in Mongolia and IMAR (Chapter Four;

Olonbayar, 2010). In addition, we interpreted more fodder purchasing as an indicator that households were experiencing effects from pasture degradation and increased climate variability as the two major environmental stressors that herders in the Mongolian grasslands have had to face to in recent years.

We hypothesized that: (1) livelihood adaptation strategies varied between Mongolia and IMAR and these differences reflected differences in local institutions; and (2) local resource institutions/policies, livestock management strategies, market influences, climate variability, household capital, and the status of pasture degradation were the major determinants associated with purchasing fodder and hay by herder households on the Mongolian plateau. Following the introduction, Section 6.2 provides the descriptions of the study area, survey design, and field data collection. Section 6.3 introduces the methods for analyzing livelihood adaptation practices of herders over the past ten years and diagnosing the determinants of fodder purchasing behaviors of herders. The results are presented in Section 6.4. Finally, we summarize the findings of this work and discuss the implications of the results for building adaptive capacity for environmental change on the Mongolian plateau.

6.2 Study Area and Data

6.2.1 Study Area

The Mongolian plateau exhibits gradients of topology, climate, soils, and vegetation, but vegetation is predominately comprised of grassland ecosystems. About 84% (1.26 million km^2) and 66% (0.78 million km^2) of the total areas of Mongolia and IMAR, are classified as grasslands (Angerer et al., 2008; Zhang, 1992). Climate change and pasture degradation have been evident on the Mongolian plateau over the past half century. Climate there has been warmer and drier since the early 1960s. Between 1961 and 2009, annual mean temperature increased about 2.1 °C in Mongolia and about 2.0 °C in IMAR, and annual precipitation decreased about 7.0% in Mongolia and about 6.6% in IMAR (Chapter Four). The frequencies of climate hazards have also increased. Droughts increased significantly in Mongolia over the past 60 years, particularly in the last decade (NCRM, 2009). The worst droughts and winter snowstorms

(*Dzuds*) that Mongolia experienced recently were in the consecutive summers and winters of 1999, 2000, 2001, and 2002, which affected 50–70% of the total territory. About 12 million livestock perished in that period (Chapter Four). The 2010 *Dzud* was the worst ever, resulting in the death of about 8.5 million livestock or 20% of the 2009 national livestock populations in Mongolia (Vernooy, 2011). Future climate scenarios for this region indicated that climate will continue to become warmer and drier in the next few decades (Christensen et al., 2007). Large-scale field ecological surveys also indicated that pastures have degraded, and the average grassland biomass productivity in IMAR and Mongolia decreased from 1871 to 900 kg/ha and from 804 to 369 kg/ha, respectively, between 1961 and 2010 (IMIGSD, 2011; IOB, Mongolia, 2011).

IMAR and Mongolia have also undergone dramatic social-institutional changes over the past five decades. By the early 1960s, IMAR and Mongolia had completed a dramatic social transformation from the traditional "communal" ownership into collective economies, which happened in the late 1950s and the early 1960s, respectively. They both experienced privatization in the mid-1980s and early 1990s, respectively. In IMAR, pastures were allocated to individual households and fenced, which is known as "household production responsibility systems (HPRS)." Mobile grazing in most parts of IMAR has been sedentarized, characterized by farming, stall-feeding, and local grazing. The implementation of HPRS has been recognized as the major cause of pasture degradation in IMAR (Humphrey and Sneath, 1999; Li et al., 2007; Sneath, 1998; Zhang, 2007). Herder households are trapped in a self-reinforcing cycle of a declining resource base and low incomes. This cycle is a result of intense pressures imposed on the grasslands by humans and their livestock. Since the early 2000s, the Chinese national government has been making and implementing a range of policies to break the self-reinforcing cycle of a declining resource base and poverty (Waldron et al., 2010). One of these policies is known as "Grain to Green," which involves converting pastures and farmland to grasslands in IMAR (Liu et al., 2008). In Mongolia, animals have been privatized and pastures are under state ownership but have become open-access resources, due to the lack of effective resource institutions needed for cooperative management. Migration distances and frequencies have decreased, especially in the areas with fertile pastures and water resources (Olonbayar, 2010). Since the economic reforms of the early 1990s, herders in Mongolia have lost transportation

support from the government for migrations and the supplies of hay and fodder in harsh winter and spring seasons. Herders with limited household endowments tend to migrate less frequently or to be sedentary grazing. Moreover, in Mongolia, the collapse of the collective economy and livestock privatization has led to an increase in the domestic subsistence orientation (Humphrey and Sneath, 1999). In contrast, the market economy in IMAR is growing rapidly, and herders benefit from livelihood opportunities generated by the thriving economy and strong governmental investments.

6.2.2. Household Survey

We selected six case study sites across ecological gradients of the Mongolian grasslands with three distributed in each IMAR, China, and Mongolia (Fig. 6.2). Field sites with different social-institutional and ecological contexts were selected to ensure the surveyed households can sufficiently cover many empirical cases of livelihood adaptation practices adopted by different social groups.

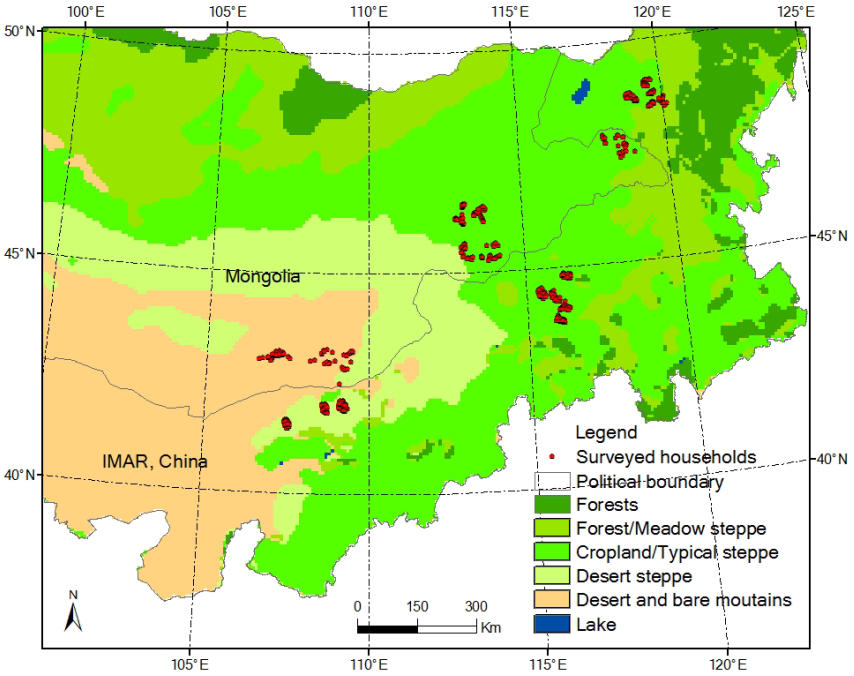

Fig. 6.2 The major vegetation types on the Mongolian plateau (shaded colors) and the locations of surveyed herder households (red dots). The vegetation maps of Mongolia and IMAR were made by the Institute of Botany, Mongolia (1980s), and the Institute of Botany, China (1990s), respectively. The original scale of the two vegetation maps was 1:1,000,000.

Based on the local social, institutional and ecological contexts, and consultations with our collaborators in Mongolia and IMAR, we identified 51 household livelihood adaptation strategies, of which we asked local herders to select the others they had undertaken over the last ten years. Based on the characteristics of the 51 adaptation strategies, they were categorized into the five major livelihood adaptation types in the AIL framework: mobility, storage, communal pooling, livelihood diversification, and market exchange. In addition to mobile herding activities, mobility in this study also included urban-rural and rural-urban migrations of herder households. Besides climate-driven decision making, these adaptation strategies can also result from pasture degradation and non-climate related socioeconomic changes, for example fluctuations in the prices of livestock products. We also asked the respondents to identify local institutions that facilitated each livelihood adaptation strategy. According to the AIL framework, local institutions related to climate adaptation were assigned into three major types: public/governmental, private/market, and civic/community.

Local resource institutions/policies (property rights, environmental policies, and governmental subsidies), livestock management strategies (stall-feeding, local-grazing, and migratory grazing), market influences (accessibility to markets, percentage of sold livestock last year, and effects of price fluctuations for livestock products), climate variability (numbers of droughts and snowstorms over the last ten years), and household capital, including human (labor availability, education, and grazing experience), materials (grazing, farming, and living facilities and instruments), natural (livestock population, areas of owned pastures, and accessibility of water resources), financial (income sources and expenditures), and social capital (help from relatives, neighbors, friends, and local institutions), that were hypothesized to be associated with livelihood adaptation practices of herders were all assessed through questions asked of households in the questionnaire. Our questionnaire was pretested and revised iteratively on the basis of qualitative interviews with local herders, governmental officials, and grassland scientists.

The household survey was implemented in IMAR and Mongolia, in autumn 2010 and spring 2011, respectively. For each of the six case study sites, villages in IMAR and soums (towns) in Mongolia were stratified based on the following variables: distances to major markets/towns, population density, livestock grazing intensity, and the average number of livestock owned by

each household. Villages and soums in different categories were selected. In each village and soum, all of the herder households in that administrative unit were first numbered in order. Then, a random sample was selected from each village/soum with a random number generator. At least 30 herder households were surveyed in each village/soum. If the surveyed units had fewer than 60 households, we surveyed all of them. In total, 15 villages in IMAR, including 541 herder households, and seven soums in Mongolia, including 210 herder households, were surveyed. Local grassland survey experts from the two countries assisted us in implementing the household surveys.

6.3 Methods

6.3.1 Descriptive Analyses of Livelihood Adaptation Strategies

To understand the differences in livelihood adaptation choices across the two countries and ecological gradients, we first counted the frequencies of the 51 livelihood adaptation strategies adopted by the surveyed herder households, and labeled the associated local resource institutions that facilitated those livelihood adaptation choices. By doing this, we were able to compare the differences in livelihood adaptation strategies of herder households in the two countries, and the local resource institutions that facilitated those livelihood adaptation strategies of herders. In addition, we also calculated summary statistics to describe the income and expenditure structures of the herder households across three broad vegetation types (meadow, typical, and desert steppes) in the two neighboring countries. These descriptive statistics were intended to reveal the variations in the livelihoods of the respondents between the two neighboring countries.

6.3.2 Modeling Fodder Purchasing Behaviors of Herders

As the storage of fodder and hay is the strategy to cope with uncertainties in precipitation and forage that herders cited with the second highest frequency, we aimed to diagnose the determinants of fodder purchasing behaviors of herders. Understanding the determinants and constraints of livelihood adaptation practices is important for making evidence-based policies for

building adaptive capacity for future environmental change. For example, policies related to whether sedentary grazing is superior to mobile grazing. In this study, field data collected at household and village levels were fitted into a series of random-intercept multilevel linear models to diagnose the determinants associated with the percentage of income spent on fodder and hay. Multilevel statistical models are designed for dealing with nested data, i.e., lower level observations that are members of several groups at the higher levels (Gelman and Hill, 2007). The dependent variable is affected by independent variables measured at both individual and group levels. In this case, the percentage of income spent on fodder and hay at the household-level was affected by both household-level and village/soum-level variables. Multilevel statistical models can be assigned into fixed-effects and random-effects models (Gelman and Hill, 2007). Fixed-effects models are used when the samples of interest are assumed to not be randomly selected and no generalizations are going to be made. Otherwise, random-effects models, in which the variance that exists between groups is modeled explicitly by adding random terms, may be used. In addition, introducing random terms to models can also prevent model residuals from being heteroskedastic (Overmars and Verburg, 2006).

Based on the correlation structure of the household-level variables collected by our surveys, we selected only a few of these variables for the subsequent inclusion in the multilevel statistical models (Table 6.1). The two variables indicating the livestock management behaviors (stall-feeding or migratory grazing) of the respondents were included in the models. The percentage of sold livestock was included as an indicator of livestock commercialization and market influences. Years of grazing experience and total annual income were included in the models to indicate human and financial capital, respectively. Income was calculated in Chinese RMB, assuming an exchange rate of 225 Mongolian tugrik per RMB. Number of livestock and ownership of living and grazing facilities and instruments were included into the models as indicators of household material capital. Because the property rights of pastures in Mongolia and IMAR were different, the areas of pastures owned by the surveyed households were not comparable. Only winter reserves of pastures were reported as the owned pastures of the surveyed households in Mongolia, whereas all of the pastures in the surveyed sites of IMAR have been contracted to herder households. Therefore, we excluded this variable. We used the accessibility of water resources represented by using pump irrigation as an indicator of natural capital of the surveyed herder

households. We were not able to collected high quality data related to social capital. Therefore, variables related to this category were not included into the models.

Besides the household-level variables, the status of pasture degradation is another hypothesized determinant associated with fodder purchasing behaviors. Pasture degradation was recorded by the percentages of degraded pastures in each village/soum and measured by the Institute of Botany, Mongolia (IOB, Mongolia, 2011), and the Inner Mongolian Grassland Institute of Survey and Design, China (IMIGSD, 2011), respectively. Because pasture degradation may be correlated with others independent variables that are also related to the percent of income spent on fodder and hay, we modeled its influence in a two-stage process. First, we diagnosed the correlates of pasture degradation at the village/soum-level. Then, the independent variables that were diagnosed as not statistically significant in the resulting model were added together with the variable of the percentage of degraded pastures into the multilevel statistical models as the village/soum-level variables. We hypothesized that the interannual variability of precipitation, livestock grazing intensity, population density, and the percentage of herder households with migratory grazing within a village or soum were correlated with the status of pasture degradation (Table 6.1). Most of the variables were measured for the year 2009, except the interannual variability of precipitation, which was calculated using climate data observed at nearby climate stations over the past 30 years. All variables included in the statistical models were normalized to 0−1, based on their observed minimum and maximum values.

Table 6.1 The socioeconomic and biophysical variables measured at the household and village/soum levels.

Hypothesized Factors	Data Collection Items	Measurement Unit
Household-level		
Livestock management	Percentage of stall-fed livestock last year	%
	Percentage of seasonally grazed livestock last year	%
Market influence	Percentage of sold livestock last year	%
Human capital	Grazing experience	Years
Material capital	Living, grazing, and farming facilities and instruments	RMB
Natural capital	Livestock population	SFU
	Accessibility of water resources (using pump irrigation)	Yes/No
Financial capital	Total annual income	RMB
Village/soum-level		
Climate variability	Interannual variability of precipitation	N/A
Human impact	Grazing intensity	SFU/hectare
	Population density	Person/hectare
Livestock management	Percentage of households with seasonal grazing	%
Resource condition	Percentage of degraded pastures	%

Note: SFU means sheep forage unit. The SFUs for sheep, cow, cameral, horse, goat are 1, 5, 6, 7, and 0.5, respectively (Fernandez-Gimenez et al., 2012).

A simple multiple linear regression (MLR) was first used to diagnose the correlates of the status of pasture degradation.

$$y_i = \beta_0 + \beta_i x_i + r_i \tag{6-1}$$

where y_i is the percentage of degraded pastures within the villages/soums, x_i are the explanatory variables, r_i is the random error term. The ordinary least squares (OLS) method was used to estimate model parameters. The MLR model was performed in the SPSS software package (IBM, New York, USA, 2012).

We built five multilevel statistical models with different levels of complexity to model fodder purchasing behaviors of herders. Model 1 was a random-intercept model without any explanatory variables. The village/soum-level effects were added in the model as the random component (Equation 6-2). For this model, the variance of the dependent variable was parsed into two parts: one part was due to the household-level variance, and the other part was due to the village/soum-level variance.

$$y_{i,j} = \gamma_{00} + U_{0j} \tag{6-2}$$

where $y_{i,j}$ is the livelihood adaptation strategy for household i in village/soum j. In this case, it is the percentage of income spent on fodder and hay for herder households, which is a continuous variable ranging from 0 to 1. r_{00} is the intercept, U_{0j} is the random error term for village/soum j. Model 1 was used as the baseline model to estimate if the village/soum-level variance in the dependent variable was statistically significant. Different groups of independent variables were added in the subsequent models to detect their influences on the variance.

In Model 2, a group of independent variables, related to livestock management and market influences at the household-level, was first included. We assumed that these were the most important variables for predicting fodder purchasing behaviors of herders.

$$y_{i,j} = \gamma_{00} + \gamma_{10}x_{1i,j} + \cdots + \gamma_{q0}x_{qi,j} + U_{0j} \quad (6\text{-}3)$$

where $\gamma_{00} + \gamma_{10}x_{1i,j} + \cdots + \gamma_{q0}x_{qi,j}$ is called the fixed part of the model, where γ_{q0} is the regression coefficient, $x_{qi,j}$ is the explanatory variable for household i in village/soum j, U_{0j} is the random term for village/soum j. In Model 3, a group of independent variables related to household capital were added in. The variables included in Models 2 and 3 were measured at the household-level. These two groups of variables were added into the models separately because we wanted to explore whether including variables related to household capital can significantly increase the predictability of the model. The increased model predictability was measured by the reduced variance at the village/soum-level.

The household-level variables can explain part of variability at both individual and group levels in the case where the values of the household-level variables are consistently higher or lower than the general mean for a given village. For example, the total annual income can be consistently higher in some of the villages/soums and lower in others. Besides the household-level variables, we also included the village/soum-level variables in Models 4 and 5 (which differ in their treatments of endogenous grassland degradation, described below). As stated above, the second-level variables were selected based on the statistical analyses of the correlates of pasture degradation within villages/soums.

$$y_{i,j} = \gamma_{00} + \gamma_{10}x_{1i,j} + \cdots + \gamma_{q0}x_{qi,j} + \gamma_{01}z_{1j} + \cdots + \gamma_{0r}z_{rj} + U_{0j} \quad (6\text{-}4)$$

where $\gamma_{01}z_{1j} + \cdots + \gamma_{0r}z_{rj}$ is the fixed effect of the village/soum-level independent variables, where γ_{0r} is the regression coefficient, z_{rj} is the explanatory variable for village/soum j. The proportion of variance of the independent variables that was accounted for by the village/soum-level independent variables ($\rho(U_0)$) was calculated by dividing the variances at the village/soum-level ($\text{var}(U_0)$) by the total variance of the models. The multilevel statistical models were performed with the HLM software package (HLM 6.08; Raudenbush et al., 2012). All of the multilevel statistical models were estimated using the restricted maximum likelihood (REML) method.

6.4 Results

6.4.1 Local Institutions and Climate Adaptation

Differences in livelihood adaptation strategies were much larger between the two countries than across ecological settings. For this reason, we focus on describing country-level differences and the institutional facilitators of the adaptation strategies. Mobility and storage were the two most frequent types of livelihood adaptation strategies for herders to adapt to the highly variable precipitation and forage (Table 6.2). Stopping migration was the most frequently cited livelihood adaptation strategy in IMAR. Other sedentarization related livelihood adaptation strategies, such as building permanent houses and winter shelters and improving the storage of fodder and hay, also ranked among the most common. These adaptation strategies were mainly facilitated by the national environmental policies for recovering grassland quality in IMAR. Local public institutions are the instruments for the implementation of the national environmental policies (e.g. "Grain to Green" policies). Only a few of the storage and mobility related livelihood strategies in IMAR were facilitated by civic/communal institutions, such as using pump irrigation and changing the time of hay cutting (Table 6.2). These were bottom-up livelihood adaptation strategies, which were mainly implemented through decentralized decision making. In Mongolia, mobility-related livelihood adaptation strategies were still the dominant strategies to cope with uncertainties in precipitation and forage. However, we can also see indicators of sedentarization in livestock grazing in Mongolia, indicated by the storage-related strategies, such as building

winter shelters and using pump irrigation. These livelihood adaptation strategies were mostly facilitated by civic/community institutions (Table 6.2).

Communal pooling was a frequently used strategy for herders in both IMAR and Mongolia. In IMAR, communal pooling was mostly market-oriented taking the form of organized agricultural cooperatives for increasing their benefits of livestock production. In contrast to IMAR, communal pooling in Mongolia was mostly subsistence-oriented in the form of pooling pastures together for migratory grazing. These two communal-pooling strategies were mainly facilitated by different types of local institutions. Agricultural cooperatives were mainly promoted by governmental and private institutions; more than 90% of the agricultural cooperatives mentioned by IMAR respondents were led by local governmental officials (e.g. village leaders). Pooling pastures for communal use in Mongolia was a form of self-organized cooperation for pooling climate risks across space and improving the efficiency of pasture-use. This kind of community-based natural resource management in Mongolia was mainly facilitated by traditional social norms and rules for mobile grazing, such as flexible pasture boundaries and reciprocal use of pastures in the years with climate disasters. In addition, in order to adapt to an increasingly warmer and drier climate, digging wells together was a fairly common livelihood adaptation practice for the respondents in the two countries (Table 6.2).

Livelihood diversification was mentioned as a strategy that herder communities used to adapt to climate change and pasture degradation, and it includes both subsistence-oriented activities (e.g. harvesting wild plants) and off-farming incomes (e.g. starting home-based business). The rapidly growing Chinese economy has increased off-farm work opportunities for herders in IMAR. For example, about one third of the surveyed herder households in IMAR started home-based private businesses. The income structure was more diversified overall in IMAR than in Mongolia (Fig. 6.3). Moreover, market incentives have stimulated herders to feed more animals and to introduce new animal species with higher productivity (Table 6.2). In addition, pasture rental markets have been emerging and are under development in IMAR. Herders can sublease their contracted pastures to others to gain benefits. This can increase pasture-use efficiency and decrease climate related vulnerability of herders. The less developed market economy in Mongolia created fewer opportunities for herders to have off-farm jobs. Governmental support

was important for herder livelihoods in the two countries. Half of the surveyed households in IMAR and one third of the surveyed households in Mongolia took loans from their governments. Governmental subsidies were also important income sources for herder households in the two countries (Fig. 6.3).

Market incentives influenced livestock management behaviors of herders through the prices of livestock products. All of the surveyed households were asked what they would do in response to rises in the prices of livestock and livestock products. More than 80% of the respondents in the two countries thought they would increase their livestock population or change herd compositions to gain more profits. Selling more livestock and livestock products were important strategies to improve the living conditions of herder households in both IMAR and Mongolia (Table 6.2). Improving breed quality and productivity by introducing the "improved" foreign breeds was also an important strategy for the two countries, especially in IMAR, China.

Table 6.2 The livelihood adaptation strategies of the surveyed herder households in Mongolia, and IMAR, China (2000−2009).

Adaptation Type	Livelihood Adaptation Items	Mongolia			IMAR, China		
		Frequency*	Rank†	Institutions‡	Frequency*	Rank†	Institutions‡
Mobility	Alter the beginning of Migration	54	7	C	33	29	C
	Alter the period/duration of migration	59	5	C	31	30	C
	Alter the end dates of migration	60	4	C	24	31	C
	Alter distance of migration	40	16	C	24	32	C
	Migrate more frequently	48	12	C	18	37	C
	Migrate less frequently	35	21	C	19	34	G
	Stop migration	0	32		470	1	G
	Move all the time	36	18	C	71	20	C
	Migrate to different locations	42	15	C	19	35	G
	Temporary migration to urban areas or abroad	36	19	C	5	48	C
	Temporary migration to other rural areas	40	17	C	2	51	C
	Permanent migration to urban areas	36	20	C & G	4	49	G
Storage	Improve storage of fodder and hay	51	10	C	353	8	C
	Stall-feed more livestock	0	33		237	16	G & M
	Start hay cutting earlier or later	0	34		59	24	C
	Stop hay cutting	0	35		18	38	C
	Use manure of family herd on the field	0	38		37	28	C
	Reduce expenses by consuming less	47	13	C	366	6	C
	Reduce livestock, surpluses or savings	2	30	C	333	9	C
	Use irrigation	0	39		19	36	C
	Mini dams	0	40		11	42	C
	Use pump or manual irrigation	76	2	C	46	25	C
	Improve management of water points	26	22	C	66	23	C
	Build permanent house	0	41		417	2	G
	Build a new or improve winter shelter	15	23	C	379	4	G
	Begin new veterinary practices	0	42		301	12	G

Table 6.2 The livelihood adaptation strategies of the surveyed herder households in Mongolia, and IMAR, China (2000−2009) (Continued).

Adaptation Type	Livelihood Adaptation Items	Mongolia			IMAR, China		
		Frequency*	Rank†	Institutions‡	Frequency*	Rank†	Institutions‡
Communal Pooling	Dig wells together with other people	52	9	C	83	19	C & G
	Start communal water harvesting	0	43		9	44	C
	Pool contracted pastures together	210	1	C	23	33	C & G
	Join agricultural cooperatives	0	44		135	18	M & G & C
Livelihood Diversification	Increase the time of off-farm working	6	26	C & M	4	50	C & M
	Apply different feed to animals	4	27	C	366	7	C & G
	Adopt new animal species	0	45		318	10	G & M
	Start home-garden agriculture	4	28	C	38	27	C
	Change kind of crops being cultivated	0	46		12	40	C & M
	Change use of plots for grazing or agriculture	0	37		9	43	C
	Sell handicrafts	0	47		12	41	C
	Start tree nursery	0	48		16	39	C & M
	Sublease land	0	49		252	15	G & M
	Eat different foods	49	11	C	77	21	C
	Start a business	0	50		201	17	C & M
	Collect traditional herb medicine	1	31	C	6	45	C
	Start harvesting wild plants	53	8	C	6	46	C
	Plant fruit trees	0	51		6	47	C & M
	Take loans from banks/government	72	3	G	380	3	G
Market Exchange	Buy animals to increase herd size	45	14	M	265	14	M
	Buy animals to improve breed productivity	14	25	M	313	11	M & G
	Sell more animals	55	6	M	376	5	M & G
	Change the herd composition	3	29	M	266	13	M & G
	Sell more agricultural or animal products	15	24	M	81	20	M
	Start early animal breeding	0	36		39	26	G & M

Note: The numbers of surveyed households in Mongolia and IMAR, China, were 210 and 541, respectively. G represented governmental institutions; M represented market institutions; and C represented community institutions.

* The selected frequency of the livelihood adaptation items.

† The order for the selected frequency of the livelihood adaptation items.

‡ The type of local institutions that facilitated the livelihood adaptation items.

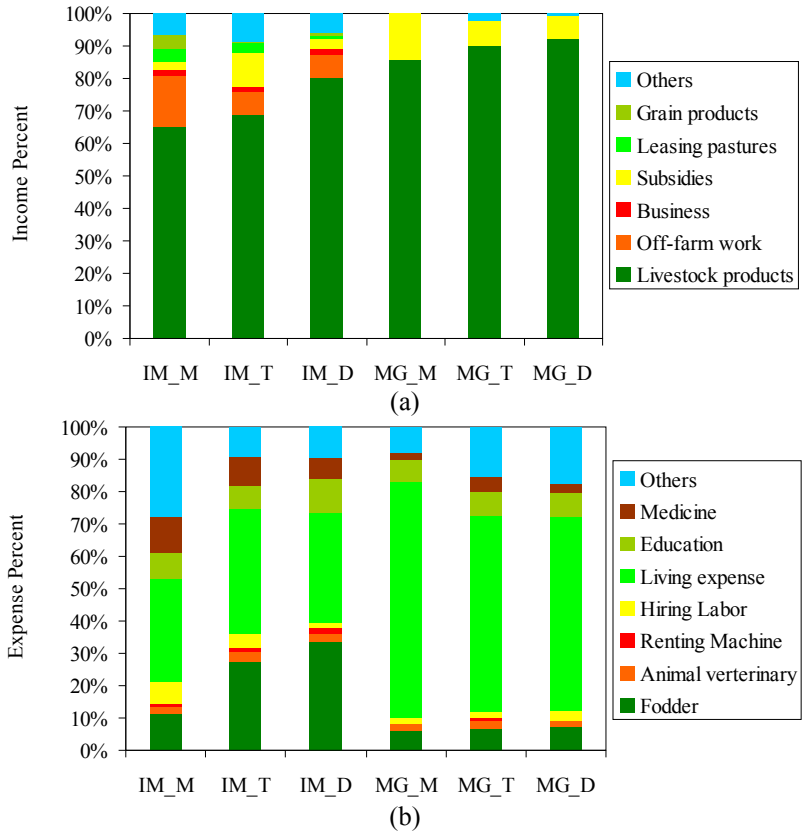

Fig. 6.3 Income (a) and expenditure (b) structures of IMAR and Mongolia. IM_M, IM_T, IM_D, MG_M, MG_T, and MG_D means the study sites in meadow, typical, and desert steppes of IMAR and Mongolia, respectively.

6.4.2 Determinants of Fodder Purchasing Behaviors

The percentage of households undertaking seasonal migrations in each village/soum was the only variable that had a statistically significant relationship with the percentage of degraded pastures within the surveyed villages/soums for the six case study sites (Table 6.3). Grazing intensity was a poor guide to the status of pasture degradation. It was the way pastures were used, not only the populations of humans and livestock that was the most important factor in analyzing the causes of pasture degradation. The highest levels of pasture degradation were found in the sites with the lowest livestock mobility. The status of pasture degradation in the three sites of Mongolia was much less serious than the three sites of IMAR. A possible reason for the phenomena was that livestock grazing in Mongolia was always managed in such a way that it allowed virtually full reproduction of grass productivity. The ecological outcomes of pasture-use under different resource institutions, implemented in Mongolian and IMAR, can be illustrated

with a striking Landsat-5 satellite image, taken on June 28, 2010 (Fig. 6.4). The location of the international border, despite not being added explicitly to the image, is indicative of the different grazing systems in operation in the neighboring region of the two countries.

Table 6.3 The estimates of the effects of biophysical and socioeconomic variables on the percentage of degraded pastures within the surveyed villages/soums.

Independent Variables	Parameters	SE
Intercept	0.803	0.415
Interannual variability of precipitation	0.476	1.332
Percentage of households with seasonal migrations	−0.766*	0.106
Livestock grazing intensity	0.040	0.221
Population density	0.216	0.184
R^2	0.840	

Note: The number of surveyed villages/soums was 22. SE means standard error.
* $p \leq 0.001$.

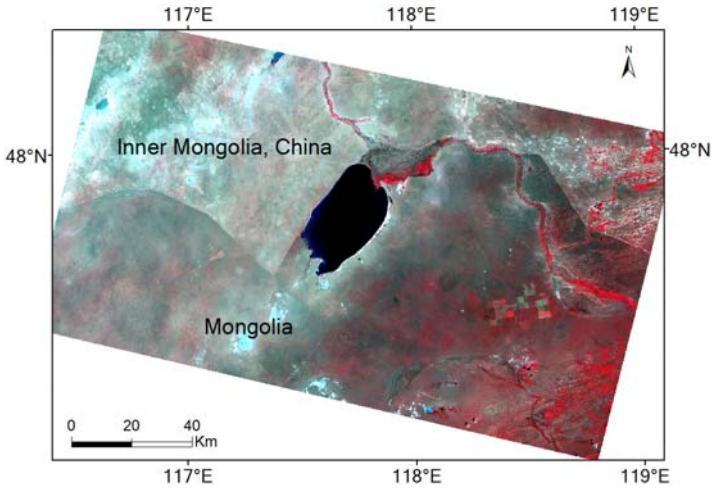

Fig. 6.4 A Landsat-5 satellite image covering the border between China and Mongolia. The area covers one of the six case study sites for the household surveys (the site in northeastern Mongolia; Fig. 6.2). Lakes are black and dark blue. Areas with the most vegetation are red. Greens and grays indicate intermediate amount of vegetation, and pale and white areas are sandy and bare earth.

The results of the multilevel statistical analyses indicated that adding the three explanatory variables in Model 2 reduced the variance of the random component at the village/soum-level (Table 6.4). The percentage of stall-fed livestock and the percentage of seasonally grazed livestock had positive and negative relationships with the percent income spent on forage, respectively. These two variables were indicators of livestock management behaviors. The percentage of stall-fed livestock affected the independent variable more strongly than the

percentage of seasonally grazed. Our survey data indicated that around 12% of the herder households in IMAR had seasonal migrations, and the rest of them had combined livestock management behaviors of stall feeding and local grazing. In Mongolia, all of the animals were managed by combinations of local grazing and migratory grazing. The percentage of sold livestock did not have a statistically significant relationship with the percentage of income spent on fodder and hay.

Adding the explanatory variables about household capital in Model 3 only slightly reduced the variance of the random component at the village/soum-level. This indicated that household capital did not provide good predictability of fodder purchasing behaviors. The total annual income, as an indicator of financial capital, was the only form of household capital that had a statistically significant relationship with the percentage of income spent on forage. Our survey data indicated that the average annual income for the respondents in Mongolia was only about 28% of the average income values for the respondents in IMAR. Herder households with higher total income were more capable of purchasing fodder to cope with precipitation uncertainty. Grazing experience had a negative and insignificant relationship with the percentage of income spent on forage. Livestock populations and grazing and living facilities had positive and insignificant relationships with the percentage of income spent on forage. The accessibility of pump irrigation, which was also an indicator of sedentarization, had a positive and insignificant relationship with the percentage of income spent on forage.

After including the variables of grazing intensity and the interannual variability of precipitation, measured at the village/soum-level, into Model 4, the variance of the random component at the village/soum-level decreased substantially. Apparently the variance was captured by the included explanatory variables at the village/soum-level. The interannual variability of precipitation had a significant and positive relationship with the percentage of income spent on forage. In the study area, the interannual variability of precipitation increased from meadow to typical and desert steppes. The similar trend can be found in the percentage of income spent on forage in IMAR (Fig. 6.3). Grazing intensity in this model did not have a statistically significant relationship with the percentage of income spent on forage.

In Model 5, we replaced mobile grazing at the household-level with pasture degradation at the village/soum-level, since mobility was the only statistically significant variable for the status of pasture degradation (Table 6.3). The percentage of degraded pastures within villages/soums had significant and positive relationships with the percentage of income spent on fodder and hay (Table 6.4). After adding the variable of pasture degradation, the significance level of the household-level financial capital decreased. The interannual variability of precipitation still had a significant relationship with the percentage of income spent on forage. The proportion of the village/soum-level variance to the total variance only decreased slightly after including the variable of pasture degradation.

Table 6.4 The estimations of the determinants for the livelihood adaptation behaviors of purchasing fodder and hay.

Independent Variables	Model 1		Model 2		Model 3		Model 4		Model 5	
	Parameters	SE	Parameters	SE	Parameters	SE	Parameters	SE	Parameters	SE
Fixed effects										
Household-level										
Intercept	0.212*	0.032	0.206*	0.032	0.216*	0.044	0.082‡	0.037	0.006	0.037
Percentage of stall-fed livestock			0.226*	0.023	0.229*	0.023	0.234*	0.023	0.231*	0.023
Percentage of seasonally grazed livestock			−0.037‡	0.023	−0.043‡	0.022	−0.041‡	0.022		
Percentage of sold livestock			−0.020	0.021	−0.023	0.021	−0.024	0.021	−0.026	0.021
Grazing experience					−0.062	0.071	−0.059	0.072	−0.059	0.072
Total annual income					0.140†	0.045	0.146†	0.049	0.137‡	0.049
Number of livestock					0.013	0.039	0.010	0.041	0.020	0.042
Grazing and living facilities and instruments					0.003	0.034	0.004	0.034	0.020	0.033
Pump irrigation					0.012	0.012	0.003	0.013	0.006	0.013
Village/soum-level										
Interannual variability of precipitation							0.331*	0.070	0.266*	0.069
Grazing intensity							0.056	0.065	0.009	0.045
Percentage of degraded pastures									0.179*	0.052
Random effects										
var(U0)	0.022*		0.017*		0.016*		0.006*		0.005*	
ρ(U0)	0.461		0.424		0.407		0.216		0.182	

Note: The number of surveyed herder households was 751; the number of surveyed villages/soums was 22. SE means standard error. var(U0) is the variance component at the village/soum-level. ρ(U0) is the proportion of variance at the village/soum-level to the total variance.

* $p \leq 0.001$.

† $p \leq 0.01$.

‡ $p \leq 0.05$.

6.5 Discussion

Most of the Mongolian grasslands experience high interannual variability of precipitation and forage. Seasonal and interannual migrations used to be the dominant strategies of herders to cope with precipitation uncertainty. Traditional mobile grazing was assisted by only small amount of fodder and hay input for winter and spring seasons. There has been a decrease in grazing mobility for both IMAR and Mongolia over the past century (Chapter Four). The striking difference between Mongolia and IMAR is that pasture in IMAR has been allocated to individual households. In contrast, Mongolia still has a more flexible and mobile grazing system, although the frequencies of migrations have decreased (Olonbayar, 2010). Climate change and pasture degradation have increased livelihood vulnerability of herders on the Mongolian plateau. Social adaptation, in the forms of adjustments to policies, institutions, and livelihood strategies, are important for local sustainable development. Our survey data show that herder households in the two neighboring countries have taken divergent paths in adapting to environmental change. Their livelihood adaptation choices have been shaped by local public, private, and civic institutions. The roles of local institutions in facilitating and undermining adaptive capacity of herder communities for environmental change were illustrated in our comparisons of the survey responses in the two countries.

Livelihood adaptation strategies of the respondents in IMAR were mostly facilitated by strong governmental interventions and market incentives created by the rapid growing Chinese economy (Table 6.2). These have increased the adaptive capacity of local herders in terms of finance, technology, information, and leadership. However, they have undermined the adaptive capacity of local herders by changing social structures of herder communities and making mobile grazing less feasible. Stopping migration was the top livelihood adaptation choice for the respondents in IMAR (Table 6.2). Grazing sedentarization is the major goal of the current environmental policies, including “Grain to Green,” implemented in IMAR. Herders have been subsidized to stall-feed livestock and to reduce herd size (Chapter Four). However, sedentary grazing has increased the cost of livestock production (Li et al., 2007). Based on responses to survey questions about income and expenses, about 40% of the respondents in IMAR had negative household incomes for the year 2009.

In addition, herders in IMAR are encouraged by local governments to feed "introduced" high-productivity livestock species. Our data show that about 58% of the respondents in IMAR selected this livelihood adaptation choice. However, the introduced breeds are usually not adapted to local climate conditions. Therefore, special requirements, such as warm winter shelters and large inputs of fodder and hay, are usually required. The introduction of foreign livestock breeds to the Mongolian grasslands, especially in IMAR, seems to have contributed to the reduction in mobility over the past half century (Humphrey and Sneath, 1999). Empirical studies also showed that this kind of technology innovation also undermined the adaptive capacity of local herders for climate hazards (Li and Li, 2012).

In contrast to IMAR, livelihood adaptation strategies of the respondents in Mongolia were mainly facilitated by civic/communal institutions in terms of traditional norms of mobile grazing (Table 6.2). Governmental policies and institutions were much less influential in Mongolia than in IMAR. This was related to the retreat of governmental investments in Mongolia after the economic reform in the early 1990s. For example, our survey data show that the death rates of livestock species were much higher in Mongolia than in IMAR for the year 2009. Most animals died due to the lack of forage supplies and migrations in the harsh climate conditions of winters and early springs. Herders in Mongolia received less governmental support than herders in IMAR. Moreover, the incomes sources of herder households were also less diversified in Mongolia than in IMAR (Fig. 6.3). In Mongolia, most herder households produce the same livestock products, which cause a lowering of prices and few guaranteed purchasers. The high transportation cost due to distant markets also increases the cost of producing livestock products (Humphrey and Sneath, 1999).

In addition, governments in Mongolia and IMAR responded differently to the negative consequences of market incentives. Take the cashmere as an example. Goats were previously less important, in part because they are not as well adapted to the climate conditions in the Mongolian grasslands. The rapid increase of goat populations was mainly stimulated by the cashmere price in the international markets (Ojima and Chuluun, 2008). The eating habit of goats causes damage to the vulnerable grassland environment on the Mongolian plateau (Neupert,

1999). In IMAR, herders have been forbidden to graze goats since the early 2000s. Changing herd compositions in IMAR was mainly forced by the governmental policies. However, there have been no effective policy interventions to reduce goat populations in Mongolia.

With grazing sedentarization and pasture degradation, the storage of fodder has become one of the major livelihood strategies to cope with precipitation uncertainty in the Mongolian grasslands, especially in IMAR, China. The cost of fodder and hay also became one of the major household expenditures for herders on the Mongolian plateau (Fig. 6.3b). This has increased the livelihood vulnerability of herders to climate variability, especially in IMAR, China. The results of our statistical analysis indicate that livestock management practices (stall-feeding and migratory grazing), household financial capital, the interannual variability of precipitation, and the percentage of degraded pastures within villages/soums had statistically significant relationships with the percentage of income spent on fodder and hay (Table 6.4). As discussed above, livestock management behaviors in the two political regions were mainly shaped by local resource institutions. Herder households in IMAR with more financial capital were more capable of purchasing fodder to cope with precipitation uncertainty. With grazing sedentarization, poor herders who cannot afford buying fodder to feed their livestock were more vulnerable to climate variability.

The percentage of income spent on fodder and hay decreased from desert to typical and meadow steppe. The pattern was more apparent in IMAR than in Mongolia (Fig. 6.3). The spatial variation of climate variability, which has the same trend along the same ecological gradient, may be the major reason for the phenomena. The percentage of degraded pastures within villages/soums had positive relationships with the percentage of income spent on fodder and hay (Table 6.4). For all of the six study sites, the status of pasture degradation was less serious in Mongolia than in IMAR. Our research results also showed that the level of mobile grazing was the only variable that had statistically significant relationship with the status of pasture degradation (Table 6.3). Because of the effect of livestock management practices on pasture degradation and the effect of pasture degradation on fodder purchasing behaviors, we concluded that livestock management practices were an underlying determinant for fodder purchasing behaviors of herders on the Mongolian plateau.

Grazing sedentarization has increased the livelihood vulnerability of herders on the Mongolian plateau to environmental change, especially in IMAR. Therefore, the traditional strategies of mobile grazing, flexible property boundaries, and reciprocal use of pastures continue to be as the key strategies for herders on the Mongolian plateau to adapt to climate change and pasture degradation. With the sedentarization trend of livestock grazing over the past decades, fodder storage became another key strategy to cope with uncertainties in precipitation and forage, especially in IMAR, China. The results of multilevel statistical modeling of fodder purchasing behaviors of herders implied that, besides adjusting local resource institutions, grassland restoration and increasing household capital are also significant approaches to building adaptive capacity of herder communities for environmental change, although household financial capital was the only statistically significant variable among all of the household variables. Recovering grassland quality can improve the resilience of grassland ecosystems to climate change. Increasing human capital in terms of education and health, social capital in terms of trust and reciprocity, natural capital in terms of the accessibility of grassland and water resources, material capital in terms of grazing facilities and instruments, and financial capital in terms of governmental low interest loans and subsidies are also important ways for building adaptive capacity.

Acknowledgements

This work was conducted with financial support from the NASA Land-Cover and Land-Use Change Program (NNX09AK87G). We thank the Inner Mongolian Institute of Survey and Design, and the Institute of Botany, Mongolian Academy of Sciences, Mongolia, for their helpful assistance in implementing the household surveys in the two countries. The graduate student Jie Dai from the University of Michigan helped us clean the original survey data.

Chapter Seven

Exploring the Role of Local Institutions in Adaptation to Environmental Change in the Semiarid and Arid Mongolian Grasslands: An Agent-Based Modeling Approach

Abstract

Communal pastures in the traditional grazing societies like Inner Mongolia, China, have been privatizing to herder households over the past decades. Migration, which used to be the major strategy for local herders to adapt to the highly variable environmental condition, has become less feasible. As a result, the livelihoods of local herders have become more vulnerable to climate variability and change. This paper presents an agent-based modeling approach to explore efficient resource institutions in adaptation to climate change and grassland degradation in the semiarid and arid Mongolian grasslands. Based on an agent-based model informed by empirical studies, we analyzed the social-ecological performance of alternative resource institutions (i.e. sedentary grazing, pasture rental markets, and reciprocal use of pastures) and their combinations. We also explored effective social mechanisms for promoting and maintaining cooperation among herders. The modeling results showed that under certain conditions resource institutions that can facilitate cooperative use of pastures (i.e. pasture rental markets and reciprocal use of pastures) generated better social-ecological performance (i.e. average net benefit of agent and grassland quality) than the performance of sedentary grazing. Agent diversity and social norms were important for promoting cooperation among herders. Social structures (i.e. the density of kinship connections) and governmental regulations were important for solving the free-rider problem and maintaining cooperation.

Keywords: Social adaptation; climate change; grassland degradation; local institutions; agent-based modeling; Mongolian grasslands

---

Wang, J., Brown, D. G., Riolo, R., Page, S., and Agrawal, A. Exploring the role of local institutions in adaptation to environmental change in the semiarid and arid Mongolian grasslands: An agent-based modeling approach. Manuscript submitted for review.

7.1 Introduction

In the semiarid and arid grasslands of the world, such as Africa and Inner Asia (i.e., Southern Russia, Mongolia, and Northern China), herders used to have the tradition of migrating in large geographic distances to adapt to the highly variable precipitation and grassland productivity. Flexible property boundaries, reciprocal use of pastures, and underlying social networks allowed herders to use grassland resources efficiently and to survive in the regions with frequent climate hazards (Fernandez-Gimenez, 1997; Humphrey and Sneath, 1999; Mwangi, 2007). Those local institutions have evolved over thousands of years and can well fit the biophysical characteristics of local environment. However, in some countries like China, communal pastures in those traditional grazing societies have been privatizing to individuals over the past half century (Humphrey and Sneath, 1999; Mwangi, 2007). Local governments in those societies anticipated that private ownership could create incentives for herders to adopt better pasture-use practices, which could consequently increase pasture-use efficiency and livelihood benefits to herders (Mwangi, 2007; Williams, 2002; Zhang, 2007).

The two political regions on the Mongolian plateau, including Mongolia and the Inner Mongolia Autonomous Region, China, have been transforming from centrally planned to market economies since the mid-1980s and the early 1990s, respectively. Pastures in Inner Mongolia have been privatizing to individual households since then, and livestock was privatized at the beginning of their economic transformations. Most pastures have been contracted to individual households and fenced. In Mongolia, pastures there have become open-access resources due to lack of effective resource institutions. The process of grazing sedentarization has been almost completed in Inner Mongolia. In Mongolia, poor families, who could not afford long-distance migrations, migrated less frequently or became sedentary grazers around water points or fertile pastures (Olonbayar, 2010). Along with grazing sedentarization, the social norms of reciprocal use of pastures that the traditional nomadism was relied on have been disappearing (Li and Huntsinger, 2011; Upton, 2009). Migration, which used to be the major adaptation strategy for herders to cope with uncertainties in precipitation and grassland productivity, has become less feasible.

Studies based on large-scale field sampling showed that grassland productivity in Mongolia and Inner Mongolia has degraded seriously since the early 1960s. Between 1961 and 2010, the average grassland biomass productivity in Inner Mongolia and Mongolia had decreased from 1871 to 900 kg/ha and from 804 to 369 kg/ha, respectively (IMIGSD, 2011; IOB, Mongolia, 2011). Grazing sedentarization has been recognized as one of the major reasons for grassland degradation on the Mongolian plateau, especially Inner Mongolia (Humphrey and Sneath, 1999; Li et al., 2007; Sneath, 1998; Williams, 2002; Zhang, 2007). Besides grassland degradation, climate on the Mongolian plateau has been getting warmer and drier, and the frequencies of climate hazards have increased over the past half century (Chapter Four). For example, climate hazards caused disastrous outcomes on the livelihoods of herders in Mongolia between 2000 and 2010. Drought and winter snowstorms between 1999 and 2002 caused the death of 12 million animals (Chapter Four). Winter snowstorms in the spring of 2009 resulted in the death of 8.5 million animals (Vernooy, 2011). Until recently, the major rural income of Mongolia and Inner Mongolia was still from herding (Olonbayar, 2010; Waldron et al., 2010). Grassland degradation and climate change have increased the cost of livestock grazing and endangered the livelihoods of local herders. Poverty has been prevalent in herder communities of Inner Mongolia and Mongolia (Olonbayar, 2010; Zhang, 2007).

In this chapter, we study social adaptation to climate change and grassland degradation in the Mongolian grasslands. Social adaptation to environmental change can result from top-down changes in policies and institutions and bottom-up household-level autonomous responses (Agrawal, 2009). Research based on extensive case studies has shown that local institutions played the central role in shaping and facilitating livelihood adaptation strategies of rural populations for climate change (Agrawal, 2010). Institutions, including formal laws and policies and informal norms and rules, are humanly devised constraints that shape human interactions and reduce social uncertainties (North, 1990; Ostrom, 1990). The institutions for sustainable governance of natural resources have been studied for a long time (Agrawal, 2001; Ostrom, 1990, 2005, 2009; Wilson and Thompson, 1993).

The development of local institutions for adapting to environmental change usually involves collective action of local people. The free-rider problem is an innate problem of collective action.

The existence of free-riders affects the maintenance of cooperation. For example, in a pasture-use group that herders pool their pastures for communal grazing, some herders may overgraze communal pastures to increases their own benefits, and some herders may not let other herders access their pastures. The free-rider problem can cause the collapse of collective action. Over the past decades, several social mechanisms have been identified for solving the free-rider problem and maintaining cooperation. The first mechanism is to keep the size of the cooperation group small, which is also known as "small-scale collective action (Olson, 1965)." The organization cost of cooperation increases with increases in the size of a cooperation group. Communication and monitoring become difficult when the size of cooperation group is large. The second mechanism is the rights of free entry and exit, which is also known as "voluntary games (Nowak, 2006)." If agents cannot benefit from being in a cooperation group, and they cannot afford the exit cost of leaving a cooperation group, then free-riding will be the dominant strategy for the agents. Otherwise, the rights of free entry and exit create "threats" for members in a cooperation group who plan to play free-ride. Kinship is another important mechanism for maintaining cooperation (Nowak, 2006). Kinship can lower the organization cost of cooperation by making communication and trust easier. In addition, punishing free-riders, also known as negative selective incentives (Nowak, 2006; Olson, 1982), is also an important social mechanism for maintaining cooperation. Punishment creates a cost to an agent who plays free-ride. The above four social mechanisms are complementary for maintaining cooperation.

My primary goal was to study efficient resource institutions for social adaptation to climate change and grassland degradation in the semiarid and arid Mongolian grasslands with high environmental variability. We aimed to answer the following question: what are the efficient resource institutions that can improve social-ecological outcomes of pasture-use in the semiarid and arid Mongolian grasslands in the context of climate change? We hypothesized resource institutions that can facilitate cooperative use of pastures can generate better social-ecological performance than the performance of sedentary grazing without cooperation. Based on an agent-based model informed by empirical studies in Inner Mongolia, we tested this hypothesis and explored effective social mechanisms for promoting and maintaining cooperation among herders. Agent-based modeling is a useful tool to dynamically examine the social mechanisms for promoting and maintaining cooperation.

Agent-based modeling is a promising quantitative methodology for social science research (Axerold, 1997; Epstein, 2007; Epstein and Axtell, 1997; Miller and Page, 2007). Agent-based models are process-based models that can be used to explain empirical phenomena, to help design and choose institutions, and to generate alternative scenarios of agent actions and interactions. Agent heterogeneity, learning and adaptation, and social interactions can be easily included in the computational models. In the field of sustainability in social-ecological systems, agent-based models have been used in modeling urban sprawl and ecological effects (Brown et al., 2008), deforestation and reforestation (Manson and Evans, 2007), pasture dynamics and management (Bell, 2011), and environmental migrations (Kniveton et al., 2011). The decision-making process of agents (e.g., land users and managers) and their social interactions can be explicitly included in the models. Agent-based models also have been used for studying institutions for sustainable governance of common-pool natural resources (Bravo, 2011; Deadman et al., 2000; Janssen and Ostrom, 2006a). Although agent-based models are effective tools for exploring alternative scenarios of human-environment interactions, they should be built on social theories that can explain agent actions and interactions. If these models are expected to have real-world policy implications, they should be informed by empirical studies (Janssen and Ostrom, 2006b).

Following the introduction, we introduce the empirical background of the agent-based model of resource institutions in Section 7.2. Section 7.3 presents the conceptual agent-based model of resource institutions. Section 7.4 illustrates the designed computational experiments. Section 7.5 provides the modeling results. Finally, we discuss the real-world implications of the modeling results and possible model extensions.

7.2 Empirical Background

We developed our agent-based model of resource institutions using information derived from empirical studies in the Mongolian grasslands. Over the past decades, self-organized resource institutions (i.e., pasture rental markets and reciprocal pasture-use groups) have been emerging in the Mongolian grasslands for adapting to climate change and grassland degradation. Pasture rental markets have been emerging in Inner Mongolia since the mid-1990s (Li and Huntsinger,

2011; Zhang, 2007), through which herders can rent pastures from others to minimize the loss caused by climate hazards. Herders leasing pastures to others also gain benefits from pasture rental fees. Therefore, the emergence of pasture rental markets can increase pasture-use efficiency when drought happens. However, there are barriers to the development of pasture rental markets. Most herders are only willing to lease pastures to their relatives and friends because strangers may overgraze their rented pastures and/or destroy water facilities. Moreover, the transportation cost of migration and the pasture rental fee are usually too expensive for local herders. Therefore, most herders do not migrate, except when they may lose most of their animals in climate hazards (Zhang, 2007). Besides pasture rental markets, reciprocal pasture-use groups also have been emerging in both Inner Mongolia and Mongolia over the past decades. These cooperation groups were mostly self-organized by relatives, friends, and neighbors for improving pasture-use efficiency and adapting to climate change (Bijoor et al., 2006; Vernooy, 2011).

Besides empirical studies in literature, we also designed a household survey and implemented it in both Inner Mongolia and Mongolia to understand the interactions among climate adaptation, local institutions, and rural livelihoods of herder communities in the Mongolian grasslands. We surveyed 541 herder households in 15 villages of Inner Mongolia and 210 households in seven soums/towns of Mongolia, which were distributed across the major vegetation types of the Mongolian plateau, in autumn 2010 and spring 2011, respectively (Fig. 7.1). The content of the household survey included herders' demographic and socioeconomic attributes, pasture-use and livestock management behaviors, and livelihood adaptation strategies to changes in climate, grassland productivity, policies, and market prices of livestock products over the past ten years. Our household survey results showed that pasture rental markets emerged in our sampled villages in Inner Mongolia, and the pasture rental fee was one of the major household income sources for herders there. Reciprocal pasture-use groups emerged in our household survey sites of Inner Mongolia and Mongolia. The results of our household survey also showed that local institutions, including local public/state, private/market, and communal/civic institutions, played the central role in shaping and facilitating livelihood adaptation strategies of herders. The developments of pasture rental markets and pasture-use groups in Inner Mongolia were mainly facilitated by local public/state and private/market institutions. The emerged pasture-use groups

in Mongolia were mainly facilitated by local communal/civic institutions. Empirical studies about grassland social-ecological systems on the Mongolian plateau from literature and our household survey informed our design of social mechanisms included in the agent-based model of resource institutions. Moreover, empirical data also helped to calibrate the values of model parameters.

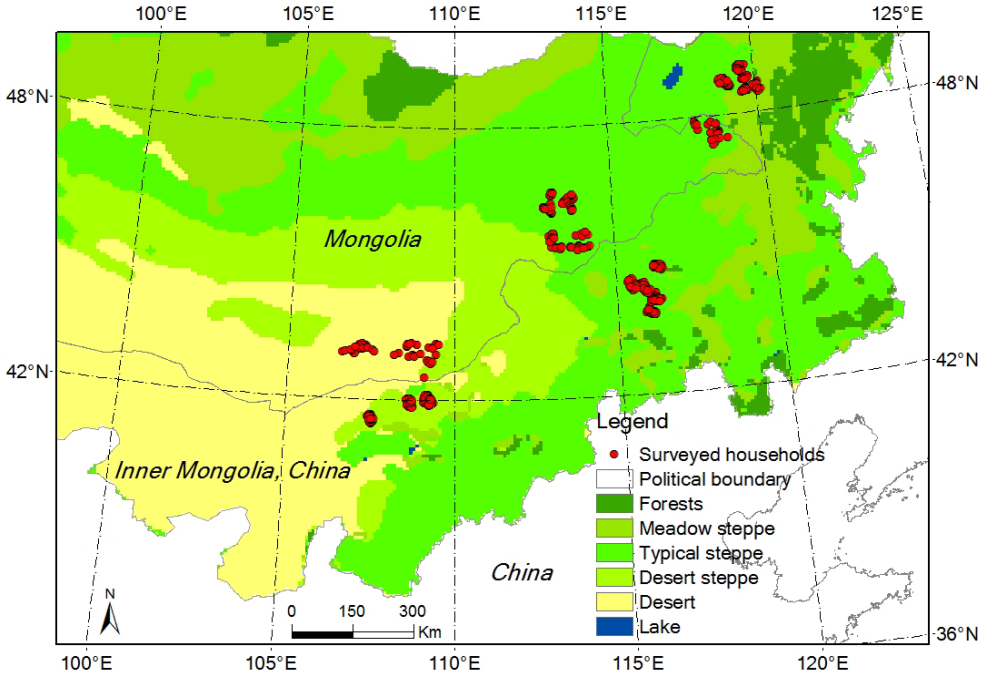

Fig. 7.1 Major vegetation types (shaded color) and the surveyed herder households (red dots) in the Mongolian grasslands. Vegetation maps of Mongolia and Inner Mongolia were made by the Institutes of Botany, Mongolia (1980s) and China (1990s), respectively.

7.3 The Conceptual Agent-Based Model

7.3.1 The Agent Landscape and Agents

The agent-based model includes an agent landscape, represented by equally divided pasture parcels. Pastures and sheep were owned privately by agents. In the spring, grass grew to certain heights. The grass growth rates were drawn from a normal distribution, with a mean and a standard deviation. Drought was the exogenous driver that caused changes in grass productivity. In the summer, drought hit the parcels of the agent world randomly with a probability, and each parcel had the same probability to be hit. The productivities of grass on the parcels hit by drought

and their neighborhood parcels (i.e., within a radius) were influenced by drought. If the agents, who owned the parcels influenced by drought, could not find available parcels to migrate to, they would overgraze their pastures. This would consequently cause decreased grass growth rates (i.e., grassland degradation). We assumed that if the biomass left after grazing was less than 10% of the initial grown biomass, this parcel would have decreased grass growth rates for the subsequent model step (Table 7.1). This was to represent damage to plants and roots that can occur when pastures are overgrazed. The parcels with decreased grass growth rates were counted as degraded pasture parcels. Biomass for each parcel was set to zero at the end of each model step, and grass grew from zero at the beginning of the next step. This was to represent the seasonal nature of biomass production.

The model included two types of agents: herder agents and the village manager agent. Agents with the same last name were connected as relatives. Otherwise, they were strangers. Agents with the same last name were distributed randomly in the agent world. Herder agents were assigned into rich and poor agents based on the number of sheep they owned. At the end of each model step, agents sold their sheep to the market to gain benefits. The influence of market incentives on livestock management behaviors of herders was simplified in the model. We assumed that the number of sheep owned by each agent was stable over time, and the number of sheep owned by each agent produced the same number of sheep for the next model step. During drought, agents would lose some proportions of their sheep and grass productivity. They had to buy sheep and fodder from markets to make up for the loss of sheep and fodder caused by drought. The sheep prices in normal and drought years were set as different (Table 7.1). Agents would lose more benefits if they sold all of their sheep during drought. This was caused by the decreased sheep price in drought years.

In this work, we first built the resource institutions of sedentary grazing into the model. Then, we added the cooperation mechanisms of pasture rental markets and reciprocal use of pastures into the model, separately and together, to analyze social-ecological outcomes of pasture use under alternative resource institutional scenarios (Fig. 7.2). The social outcome of pasture-use was measured by the average net benefit of agents, and the ecological outcome of pasture-use was measured by the number of undegraded parcels in the agent world.

Table 7.1 The values of the major parameters of the agent-based model.

ID	Parameter name	Value	Source
1	pasture size per parcel	100 ha	Assumed
2	drought probability in the agent world	10%	This study
3	consumption rate of grass per sheep	1 tonne/year	This study
4	grassland productivity in a normal year	1.5 tonne/ha (SD: 0.3)	IMGSD, 2011
5	grassland productivity for the next year after over-grazing	1.0 tonne/ha (SD: 0.2)	IMGSD, 2011
6	drought radius (number of parcels impacted by drought)	1 (9 parcels)	Assumed
7	percentage of productivity loss: the parcel hit by drought	80%	Assumed
8	percentage of productivity loss in drought: neighborhood parcels	50%	Assumed
9	percentage of agents willing to share pastures to strangers	100%	Assumed
10	searching radius of a rich agent	2	Assumed
11	searching radius of a poor agent	1	Assumed
12	maximum trials for searching available pastures	3	Assumed
13	percentage of rich agents in the agent world	20%	This study
14	number of sheep owned by a rich agent	50	This study
15	number of sheep owned by a poor agent	30	This study
16	sheep price in a normal year	1/sheep	This study
17	sheep price in a drought year	0.5/sheep	This study
18	fodder price	0.25/tonne	This study
19	percentage of sheep loss caused by drought without migration	50%	Zhang, 2007
20	transportation cost per distance	1/parcel distance	Zhang, 2007
21	price willingness to ask for leasing pastures	10 (SD: 2)	Zhang, 2007
22	price willingness to pay relative to the percentage of total benefit	25% (SD: 5%)	Zhang, 2007
23	organization cost of cooperation for strangers	0.1/person	Assumed
24	organization cost of cooperation for relatives	0.01/person	Assumed
25	increasing rate of cooperation benefit with each additional agent	1%/person	Assumed
26	exit cost of leaving a cooperation group	1	Assumed
27	punishment cost of being found as a free-rider	20	Assumed

Note: The numbers of sheep owned by rich and poor agents, percentages of rich and poor agents, sheep prices in normal and drought years, and fodder price were calibrated using our household survey data of this study. These values were set proportional to the original values for the convenience of calculation. SD means standard deviation.

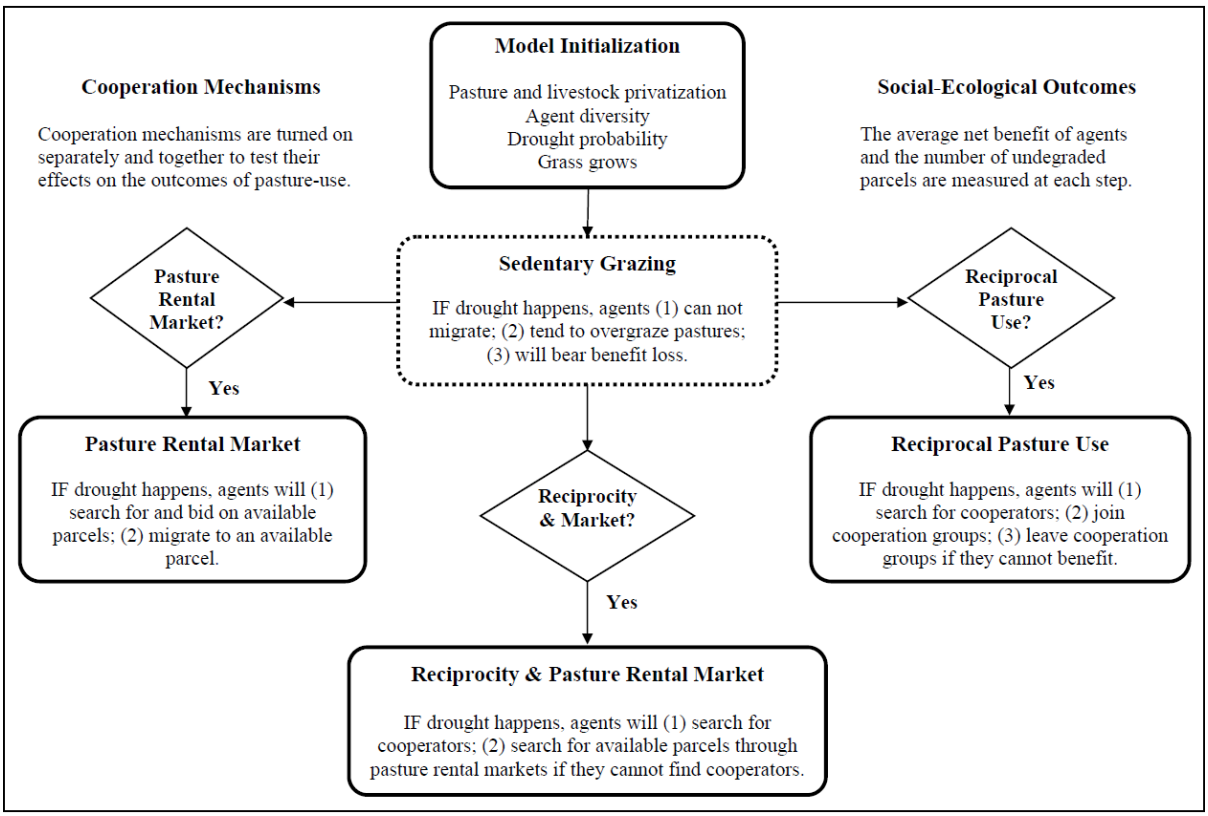

Fig. 7.2 The conceptual agent-based model of resource institutions.

7.3.2 Sedentary Grazing

Each step, agents grazed their sheep on their own parcels. During drought, agents could not migrate to other parcels. The net benefit of agents under the institutional scenario of sedentary grazing was calculated by

$$U_{1i}(n_i) = n_i \cdot B_i - C_i \tag{7-1}$$

where U_{1i} is the net benefit of agent i; n_i is the number of sheep owned by the agent i; B_i is the benefit from selling one sheep; and C_i is the cost of buying sheep and fodder when drought happens. The average net benefit of agents and the number of undegraded parcels in the agent world were measured at each model step.

7.3.3 Pasture Rental Markets

When the mechanism of pasture rental markets was included in the model, agents, who owned the parcels hit by drought, would search in their neighborhoods for available parcels to migrate to. The available parcels were defined as the parcels that had enough left biomass to support migrants. The number of migrants one agent could support was based on how much biomass they had left on the basis of without causing grassland degradation in the subsequent model step. We assumed poor agents had a smaller searching radius than rich agents (Table 7.1). The searching agents bid on available pastures in their neighborhoods. The price that an agent was willingness to pay was based on the budget of the agent and a random component, which was drawn from the standard normal distribution. The budget for each agent was based on the number of sheep they had. The price that an agent was willing to ask was drawn from a normal distribution with a mean and a standard deviation (Table 7.1).

As one way to represent the bounded rationality of agents, we assumed that a searching agent could bid on at most three parcels. The agents, who offered the highest prices for the available parcels, could put those parcels on their final selection list. Finally, these agents calculated whether they could benefit from migrating to the nearest parcel in their selection list. If they could benefit from migration, they paid pasture rental fees and the transportation cost of migration. Otherwise, they stayed on their own pastures. Moreover, not all agents were willing to lease pastures to strangers, and this was a parameter set in the model (Table 7.1). The agents, who were willing to lease pastures to strangers, were distributed randomly in the agent world. At the end of each model step, all migrant agents moved back to their parcels. The net benefit of agents under the institutional scenario of pasture rental markets was calculated by

$$U_{2i}(n_i) = n_i \cdot B_i + B_{0i} - C_{0i} - C_{1i} - C_{2i} \quad (7\text{-}2)$$

where U_{2i} is the net benefit of agent i; n_i is the number of sheep owned by the agent i; B_i is the benefit from selling one sheep; B_{0i} is the benefit from leasing pastures to others; C_{0i} is the cost of renting pastures; C_{1i} is the cost of leasing pastures; and C_{2i} is the transportation cost of migration. If agents could not find available parcels to migrate to, they had to bear the loss caused by drought. They calculated their net benefits by Equation 7-1. Besides the average net benefit of

agents and the number of undegraded parcels, the numbers of agents who found or did not find pastures to migrate to through pasture rental markets were also measured at each model step.

7.3.4 Reciprocal Use of Pastures

When the mechanism of reciprocal use of pastures was included in the model, agents, who owned the parcels hit by drought, would have incentives to search for cooperators in their neighborhoods. To cooperate means that they would share pastures with each other during drought. If agents found cooperators who had enough biomass to support migrants, they would migrate to the pastures of their cooperators without paying pasture rental fees or taking the risk of no available pastures could be found in pasture rental markets. Reciprocity reduced the risk of no parcels being available in pasture rental markets. The searching radii for rich and poor agents were defined as the same as in pasture rental markets. The benefits of cooperators increased as increases in the size of a cooperation group because of the economies of scale. The economies of scale were defined as the increasing bargaining power and the resulting higher livestock sale prices with increases in the size of a cooperation group. Agents in a cooperation group had to pay the organization cost of cooperation. The organization cost of cooperation increased with increases in the size of a cooperation group. This mechanism was contradictory to the mechanism of the economies of scale in the development of reciprocal pasture-use groups. Agents in a cooperation group also had to pay the transportation cost of migration if they migrated to other parcels. The migration distance of cooperators was expected to decrease as more agents joined the cooperation group.

The net benefit of agents under the institutional scenario of reciprocal use of pastures was calculated by

$$U_{3i}(n_i) = n_i \cdot B_i \cdot (1+\lambda_i) - C_{1i} - C_{2i} \cdot (1+\beta_i) - C_{3i} \cdot (1+\gamma_i) - C_{4i} \quad (7\text{-}3)$$

where U_{3i} is the net benefit of agent i; n_i is the number of sheep owned by the agent i; B_i is the benefit from selling one sheep; C_{1i} is the cost of sharing pastures; C_{2i} is the transportation cost of migration; C_{3i} is the organization cost of cooperation; C_{4i} is the exit cost of leaving a

cooperation group; λ_i is the increased proportion of cooperation benefit because of the economies of scale; β_i is the decreased proportion of transportation cost with increases in the number of cooperators; γ_i is the increased proportion of the organization cost with increases in the size of a cooperation group; and λ_i, β_i, and γ_i are functions of the number of agents in a cooperation group. At each model step, agents made decisions about whether to stay in or leave a cooperation group based on whether they could benefit from being a cooperation group. Besides the average net benefit of agents and the number of undegraded parcels, the numbers of cooperators and cooperation groups were also measured at each model step.

7.3.5 The Free-Rider Problem in Cooperation

If cooperators could not benefit from being in a cooperation group, and they could not afford the exit cost of leaving the cooperation group, these cooperators would turn into free-riders. Being free-riders means these agents did not share their own pastures with others, but they would migrate to pastures of other cooperators when drought hit their pastures. Free-riders still had to pay the organization cost of cooperation. The existence of free-riders increased the cost of sharing pastures for other cooperators in a cooperation group. The net benefit of agents in a cooperation group with free-riders was calculated by

$$U_{4i}(n_i) = n_i \cdot B_i \cdot (1+\lambda_i) - C_{1i} \cdot (1+\alpha_i) - C_{2i} \cdot (1+\beta_i) - C_{3i} \cdot (1+\gamma_i) - C_{4i} - C_{5i} \quad (7\text{-}4)$$

where U_{4i} is the net benefit of agent i; α_i is the increased proportion of pasture-sharing cost, and α_i is the function of the number of free-riders in a cooperation group; C_{5i} is the cost of being found as a free-rider; and other parameters in Equation 4 have the same meaning with the parameters in Equation 3. Besides the average net benefit of agents and the number of undegraded parcels, the numbers of cooperators, free-riders, and cooperation groups were also measured at each model step.

7.4 Computational Experiments

7.4.1. The Social-Ecological Performance of Alternative Resource Institutions

In the first set of experiments, we analyzed the social-ecological performance of four institutional scenarios: sedentary grazing, pasture rental markets, reciprocal use of pasture, and the combined institutions of reciprocity and pasture rental markets. We changed the drought probability in the agent world to analyze social-ecological outcomes of pasture-use under alternative climate and institutional scenarios. When the cooperation mechanisms of pasture rental markets and reciprocal use of pastures were both added into the model, agents, who owned the parcels hit by drought, would search available parcels to migrate to through pasture rental markets if they could not find reciprocal pasture-use groups to join. If agents could not find available parcels from either pasture rental markets or reciprocal pasture-use groups, they had to bear the loss caused by drought. We set the price of one sheep in a normal year as one unit, and the values of other parameters were set relative to the sheep price (Table 7.1). In this set of experiments, all agents were willing to lease pastures to strangers. The organization cost of cooperation (i.e., 0.1 per person for strangers) and the increasing rate of cooperation benefit (i.e., 0.1 per ten people) were assumed values (Table 7.1). The values of the two parameters were set such that the organization cost of cooperation for each cooperator increased 0.1 with each new agent in the cooperation group, and the cooperation benefit to each cooperator increased 1% with each additional agent in the cooperation group.

In this set of experiments, we also ran verification experiments of model mechanisms and did sensitivity analyses of model parameters. First, we ran experiments to verify the mechanism of pasture rental markets included in the model. We varied the percentage of agents, who were willing to lease pastures to strangers, from 100% to 50% and 0% to test whether the percentage of agents who could find pastures to migrate to was increased. Second, we analyzed the sensitivity of the performance of reciprocal use of pastures to the organization cost of cooperation and the increasing rate of cooperation benefit because these two parameters were set without empirical data. The organization cost of cooperation was varied from zero per person to 0.5 per person in equal increment of 0.05, and the increasing rate of cooperation benefit was

varied from 1% per person to 5% per person in equal increment of 1%. The values of these two parameters were varied separately. For the verification experiments and sensitivity analyses, we set a constant drought probability (i.e. 10%) in the agent world.

7.4.2. Social Mechanisms for Promoting Cooperation

In the second set of experiments, we explored two social mechanisms for promoting cooperation among herders under the institutional scenario of reciprocal use of pastures. For the baseline scenario, no other social mechanisms were included in the model other than reciprocal use of pastures. Then, we added agent diversity into the model. In this set of experiments, we set 20% agents in the agent world had the same last name, and the other 80% agents had random last names. This is a key cooperation mechanism for herder communities of the Mongolian grasslands because kinship networks are important for herders to pool climate risks across space and social groups. When this mechanism was included in the model, the organization cost of cooperation was lower for relatives than for strangers (Table 7.1). We assumed that the organization cost for relatives was 10% of the organization cost for strangers. The organization cost was calculated based on the number of relatives and strangers in a cooperation group. The organization cost of cooperation (i.e. 0.1 per person for strangers; 0.01 per person for relatives) and the increasing rate of cooperation benefit (i.e. 1% per person) were assumed values. We also did sensitivity analyses of the two parameters. The value ranges of these two parameters were set the same as in the first set of experiments.

The second social mechanism added into the model was neighborhood effects through the formation of social norms. Agent diversity was turned off when this mechanism was turned on. When neighborhood effects were included in the model, agents would copy the behaviors of their neighbors if they could benefit from changing their behaviors. The neighboring eight parcels of a parcel were defined as the neighbors of that parcel. The number of neighborhood agents with the same behavior for an agent to change its behavior was also set as a model parameter. The value of the parameter was varied from 75% to 50% and 25%. In this process, the criterion for an agent to change its behavior based on the conformity of its neighbors' behaviors was decreased. Moreover, we set a constant drought probability (i.e. 10%) in the agent world.

7.4.3. Social Mechanisms for Maintaining Cooperation

In the third set of experiments, we explored two social mechanisms for solving the free-rider problem and maintaining cooperation. When the kinship mechanism was included in the model, free-riders would only free-ride on strangers, and the organization cost of cooperation for relatives was lower than for strangers. In this experiment, we varied the density of kinship connections. The number of agents with the same last name was increased in 10% increments from 10% (i.e., other 90% agents had random last names) to 100%. The second social mechanism added into the model was the punishment mechanism. The kinship mechanism was turned off when the punishment mechanism was turned on. When this mechanism was included in the model, agents in a cooperation group would not play free-ride if they could not afford the punishment cost of being found as free-riders. If the punishment cost was higher than the net benefit of an agent, the agent would not play free-ride. In this set of experiments, the punishment cost on free-riders was increased in 10% increments from 10% to 100% of the gross benefit of a poor agent. The village manager agent operated the behavior of punishing free-riders, and this was to avoid the second or higher order free-rider problem in cooperation (Boyd et al., 2000). The two social mechanisms were added into the model separately in a sequence. In this experiment, we also set a constant drought probability (i.e. 10%) in the agent world.

The agent-based model was coded in Eclipse using Java and RepastJ 3.1 libraries (North et al., 2007). In order to make the social-ecological performance of alternative resource institutions comparable, we set the values of the basic model parameters as the same for all computational experiments. The basic model parameters included the number of sheep owned by rich and poor agents, percentages of rich and poor agents, the number of sheep owned by rich and poor agents, growth rates of grass at normal and degradation status, the consumption rate of grass per sheep, and prices of fodder and sheep. Moreover, for the institutional scenarios of pasture rental markets and reciprocal use of pastures, the transportation cost per distance was set as a constant (Table 7.1). Most of the above parameters were set using empirical data from literature and our household survey. The complexity of the agent-based model of resource institutions was represented by the social mechanisms included in the model. Although the size of the agent world was scalable, we used a small agent world with the size of 10 × 10 to diagnose the

interactions of the social mechanisms and the social-ecological performance of different resource institutions. For each experiment, we ran the model 20 steps to represent 20 years. In order to account for the random parts in the model, we ran each experiment 30 times and averaged social-ecological outcomes of pasture-use over 30 time runs.

7.5 Results

7.5.1 The Importance of Cooperation in Climate Adaptation

The three different institutional scenarios produced different patterns of agent activity (Fig. 7.3). During drought, some of the agents could not find available parcels to migrate to through pasture rental markets (Fig. 7.3b). Reciprocal pasture-use groups emerged after a few model steps (Fig. 7.3c). For the experiments of verifying the mechanism of pasture rental markets included in the model, the modeling results showed that with decreases in the percentage of agents who were willing to lease pastures to strangers, the percentage of agents could find available parcels to migrate to decreased from around 70% to 50% and 10%. These modeling results verified that fewer agents could find parcels to migrate to when fewer agents were willing to lease pastures to strangers.

The results under the four institutional scenarios and different conditions of drought probability indicated that sedentary grazing without cooperation had the lowest level social-ecological performance (Fig. 7.4). Reciprocal use of pastures had better social-ecological performance than the performance of pasture rental markets. However, when adding both reciprocity and pasture rental markets into the model, the modeling results did not change much. This indicated that reciprocity played stronger role in facilitating cooperation among agents. Reciprocal use of pastures allowed herders to pool climate risks across space and improve social-ecological outcomes of pasture-use. The modeling results also showed that with increases in drought probability, the comparative advantage of cooperative use of pastures, which was facilitated by pasture rental markets and reciprocal use of pastures, became more evident. The results of our sensitivity analyses showed that both ecological and economic performance of reciprocal use of pastures declined with increasing organization costs and decreasing benefits

from cooperation (Fig. 7.5). By comparing the performance of reciprocal use of pastures and the performance of pasture rental markets under the same drought probability, we found that reciprocal use of pasture had better performance than the performance of pasture rental markets only when the organization cost of cooperation for strangers was less than 0.15 per person and the increasing rate of cooperation benefit was more than 1% per person.

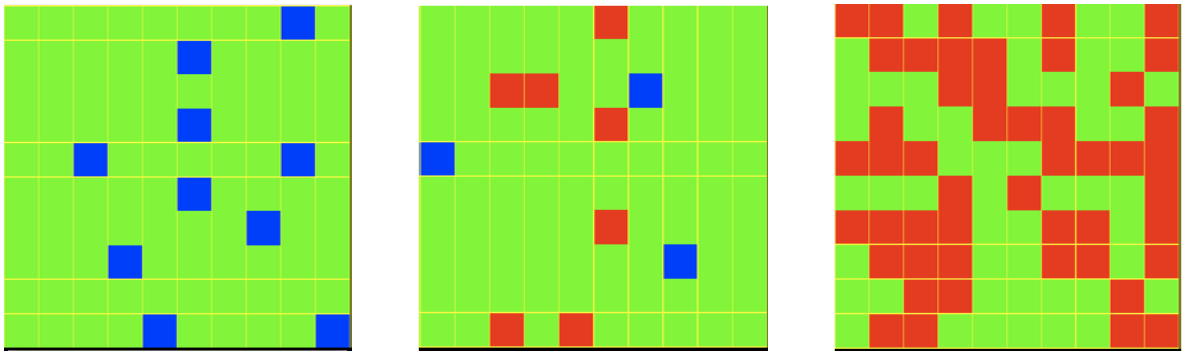

(a) (b) (c)

Fig. 7.3 Snapshots of the experiments for the three institutional scenarios. (a) sedentary grazing. (b) pasture rental markets. (c) reciprocal use of pastures. The green blocks were the parcels not hit by drought; the blue blocks in (a) were the parcels hit by drought; the blue blocks in (b) were the parcels hit by drought, and the agents did not find parcels to migrate to; the red blocks in (b) were the parcels hit by drought, and the agents found parcels to migrate to; the red blocks in (c) were cooperators.

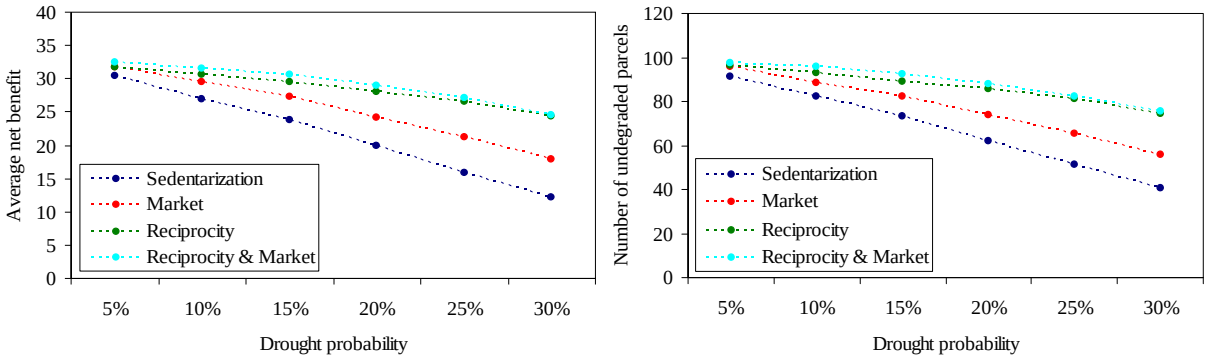

(a) (b)

Fig. 7.4 The social-ecological performance of four institutional scenarios under different conditions of drought probability. (a) the average net benefit of agents. (b) the number of undegraded parcels.

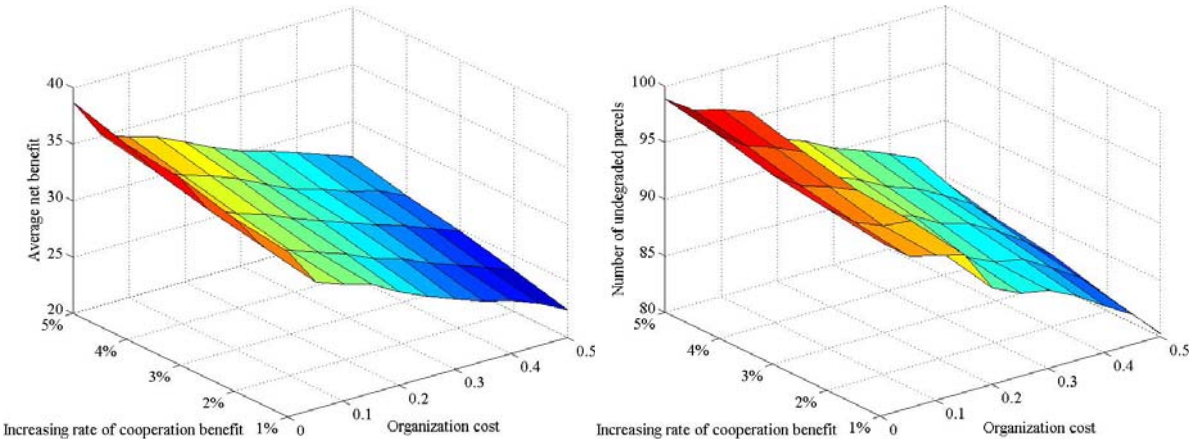

Fig. 7.5 Sensitivity analyses of the parameters related to the organization cost of cooperation and the increasing rate of cooperation benefit for the institutional scenario of reciprocal use of pastures. (a) the average net benefit of agents; and (b) the number of undegraded parcels in the agent world.

7.5.2 Effects of Agent Diversity and Social Norms on Promoting Cooperation

In comparison with the outcomes of the baseline scenario, the average net benefit of agents and the number of undegraded parcels increased significantly after including agent diversity in the model (Fig. 7.6). The number of strangers in cooperation groups also increased when agent diversity was included in the model. This indicated that adding agent diversity into the model also facilitated cooperation among strangers. The organization cost of cooperation increased with increases in the sizes of cooperation groups. This constrained the sizes of cooperation groups. However, adding agent diversity into the model relaxed the constraint. The sensitivity analyses of model parameters showed that the average net benefit of agents and the percentage of undegraded parcels decreased with increases in the organization cost of cooperation (Fig. 7.7). However, the decreasing rates of the two measurements were lower than their decreasing rates in the first set of experiments (Fig. 7.5). By comparing the performance of reciprocal use of pastures and the performance of pasture rental markets under the same drought probability, we found that reciprocal use of pasture had better performance than the performance of pasture rental markets only when the organization cost of cooperation for strangers was less than 0.25 per person and the increasing rate of cooperation benefit was more than 1% per person. Adding neighborhood effects (i.e. social norms) into the model also promoted cooperation among agents. The social-ecological outcomes of pasture-use increased gradually as the percentage of

neighbors with the same behavior required for an agent to change its behavior varied from 75% to 50% and 25% (Fig. 7.6). Overall, the results of this set of experiments indicated that agent diversity and the prevalence of social norms were important in promoting cooperation among herder agents.

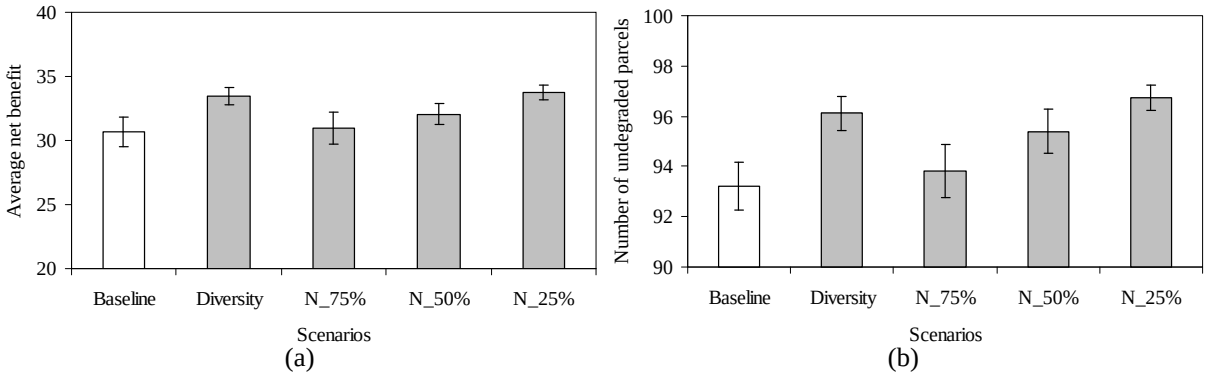

(a) (b)

Fig. 7.6 The social-ecological performance of reciprocal use of pastures with agent diversity and neighborhood effects included in the model. (a) the average net benefit of agents. (b) the number of undegraded parcels. Baseline means the baseline scenario; Diversity means the scenario of agent diversity; and for the scenarios related to neighborhood effects, the neighborhood parameter was changed from 75% (N_75%) to 50% (N_50%) and 25% (N_25%). The error bars represent one standard deviation.

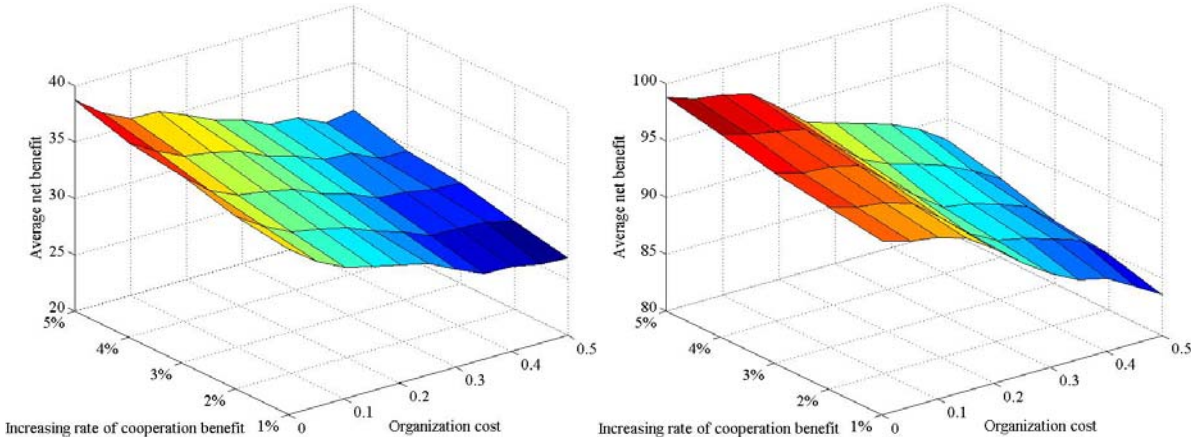

(a) (b)

Fig. 7.7 Sensitivity analyses of the parameters related to the organization cost of cooperation and the increasing rate of cooperation benefit for the institutional scenario of reciprocal use of pastures with the mechanism of agent diversity included in the model. (a) the average net benefit of agents; and (b) the number of undegraded parcels in the agent world.

7.5.3 Solving the Free-Rider Problem in Cooperation

The social-ecological outcomes of pasture-use increased gradually with increases in the density of kinship connections in the agent world. The effects of the kinship mechanism on maintaining cooperation were more prominent when the density of kinship connections was higher than 70% (Fig. 7.8). This was caused by the fact that free-riders would not free-ride on relatives after including the kinship mechanism in the model. Moreover, the organization cost of cooperation decreased with increases in the density of kinship connections. Therefore, adding the kinship mechanism into the model helped to maintain cooperation among herder agents.

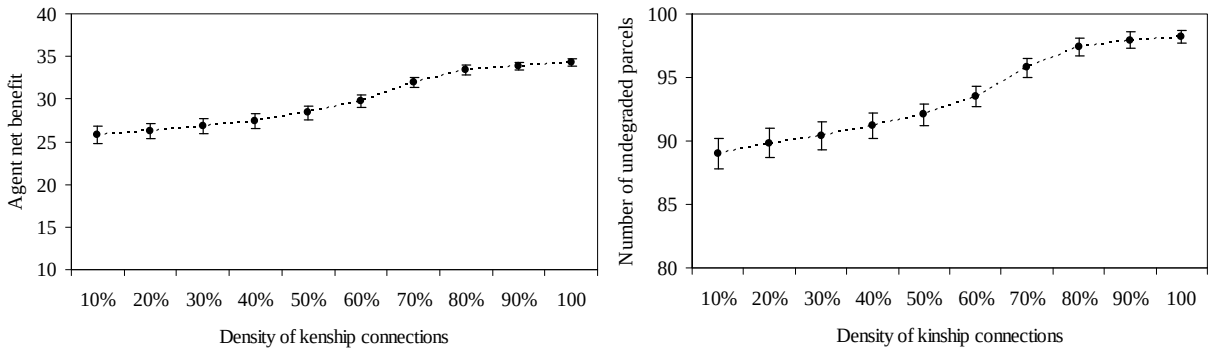

Fig. 7.8 The social-ecological performance of reciprocal use of pasture with the kinship mechanism included in the model. (a) the average net benefit of agents. (b) the number of undegraded parcels. The error bars represent one standard deviation.

The average net benefit of agents first decreased then increased with increases in the punishment cost (Fig. 7.9a). When the punishment cost was low, some of the agents played free-ride because they could take the punishment cost of being found as free-riders. However, when they were found as free-riders, they had to pay the punishment cost. Therefore, the average net benefit of agents decreased at first. However, when the punishment cost was high, fewer agents could take the cost of being found as free-riders. Therefore, the average net benefit of agents increased. Due to the implementation of the punishment mechanism, some agents could not take the cost of being found as free-riders. Therefore, the number of undegraded parcels increased with increases in the punishment cost (Fig. 7.9b).

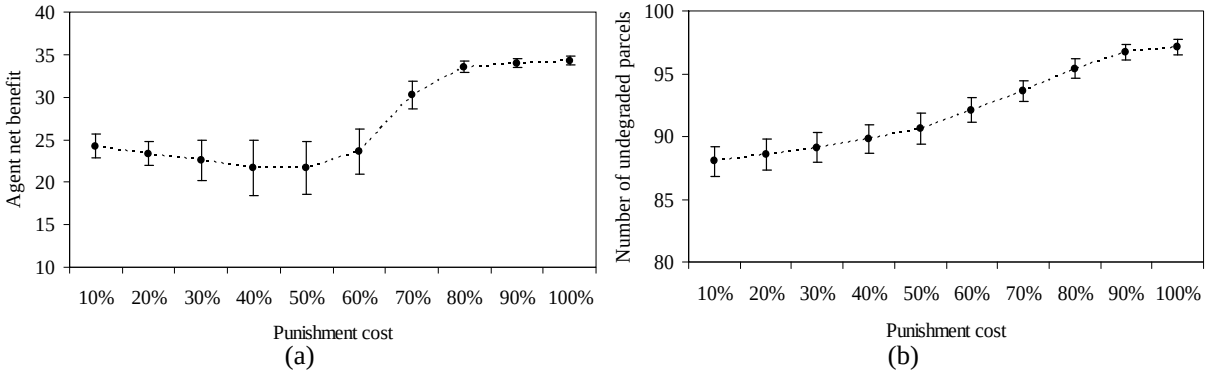

Fig. 7.9 The social-ecological performance of reciprocal use of pasture with the punishment mechanism included in the model. (a) the average net benefit of agents. (b) the number of undegraded parcels. The error bars represent one standard deviation.

7.6 Discussion

We began comparing the social-ecological performance of alternative resource institutions by setting a baseline institutional scenario of sedentary grazing without cooperation. Then, we included the cooperation mechanisms of pasture rental markets and reciprocal use of pastures into the model, separately and together, to compare their performance with the performance of the baseline scenario under different conditions of drought probability. The results showed that sedentary grazing produced the lowest level social-ecological performance among institutional scenarios. Under certain conditions (i.e., the organization cost of cooperation was low), reciprocal use of pastures had better social-ecological performance in comparison with the performance of pasture rental markets; and the advantage of cooperative use of pastures became more evident with increases in drought probability. We also explored effective social mechanisms for promoting and maintaining cooperation among herders. The results showed that agent diversity and social norms played important roles in promoting cooperation; and social structures (i.e., the density of kinship connections) and governmental regulations were important for solving the free-rider problem and maintaining cooperation.

The modeling results implied that relaxing state-control related management strategies and allowing herders to form cooperative arrangements are effective ways to improve social-ecological outcomes of pasture-use in the context of climate change. Grazing sedentarization has been a trend in Mongolia and Inner Mongolia since the late 1950s (Humphrey and Sneath, 1999).

The process of grazing sedentarization has been almost completed in Inner Mongolia. Moreover, state-control related management strategies are the dominant strategies for grassland management in Inner Mongolia. The self-organized resource institutions (i.e., pasture rental markets and reciprocal pasture-use groups) are important ways for herders to improve pasture-use efficiency and minimize the loss caused by climate hazards. Governmental support is also important for promoting and maintaining cooperation by lowering the organization cost of cooperation. For example, local governments can collect information about the demand and supply of pastures and disseminate the information to local herders in drought years. The conflicts of pasture-use in pasture rental markets (e.g., overgrazing rented pastures and disputes over pasture rental fees) can also be solved with the help from local governments. Second, local governments can provide transportation help for poor herders who cannot afford long-distance migrations. Third, governmental incentives (e.g., subsidies and financial supports) can also facilitate the development of self-organized resource institutions. In addition, local governments can also punish herders, who are against the rules of cooperation, for maintaining cooperation among herders.

There are several possible improvements and extensions to the current version of the agent-based model of resource institutions. First, the attributes, actions, interactions of agents in the agent-based model can be further calibrated by empirical data. Second, the relationships between climate and grassland productivity were simplified by setting a hypothetical look-up table. Future work could couple an ecosystem model of grassland dynamics with the agent-based model of resource institutions for an integrated modeling of grassland social-ecological systems. Third, the influence of the fluctuations in livestock prices on livestock management behaviors of herders can be included in the model. Since economic transformations in Mongolia and Inner Mongolia, China, market incentives have been playing an important role in affecting livestock management behaviors of herders. In addition, other social mechanisms for promoting cooperation can also be included in the model. For example, we only used the differences in the organization cost of cooperation for relatives and strangers to represent the role of agent diversity in promoting cooperation. Besides these differences, rich and poor herders usually play different roles in organizing cooperation groups. In this work, this social mechanism was not included in

the model because we did not have enough empirical data to calibrate the roles of rich and poor agents in organizing cooperation groups.

7.7 Conclusions

We analyzed the social-ecological performance of alternative resource institutions in the semiarid and arid Mongolian grasslands in the context of climate change, using an agent-based model informed by empirical studies. Under certain conditions, resource institutions that can facilitate cooperative use of pastures generated better social-ecological outcomes of pasture-use than the performance of sedentary grazing without cooperation. Agent diversity and social norms played important roles in promoting cooperation. Social structures (i.e. the density of kinship connections) and governmental regulations were important for maintaining cooperation. As discussed in the beginning, social-institutions of the traditional grazing societies of Inner Asia and Africa have changed dramatically over the past decades. They have undermined the adaptive capacity of local herder communities for climate change by making mobile grazing less feasible. Although the development of the agent-based model of resource institutions was informed by empirical studies in the Mongolian grasslands, it has important policy and institutional implications for social adaptation to climate change in other semiarid and arid grassland regions of the world with high environmental variability.

Acknowledgements

This work was conducted with financial support from the NASA Land-Cover and Land-Use Change Program (NNX09AK87G). We thank the Inner Mongolian Institute of Survey and Design, and the Institute of Botany, Mongolian Academy of Sciences, Mongolia, for their helpful assistance in implementing the household surveys in the two countries.

PART V

CONCLUSIONS

Chapter Eight

Synthesis

Previous studies have provided general information about the drivers of grassland dynamics on the Mongolian plateau (e.g., Humphrey and Sneath, 1999; Neupert, 1999), social vulnerability and adaptation to climate variability and change for herder communities in Mongolia (e.g., Fernandez-Gimenez et al., 2012; Vernooy, 2011), and the role of local institutions in adaptation to climate change for rural populations (e.g., Agrawal, 2009, 2010). A systematic study about the drivers of grassland dynamics across the heterogeneous Mongolian grasslands is still needed. Moreover, comparative studies of livelihood adaptation practices of herders under different institutional arrangements in the two political regions on the Mongolian plateau can help us understand the relationships between local institutions and climate adaptation. This is also meaningful for guiding policy interventions to strengthen the adaptive capacity of herder communities for climate change. In this research, I contributed new knowledge about: (1) the relative importance of natural and human drives of grassland dynamics across agro-ecological zones and the two political regions on the Mongolian plateau; (2) the major livelihood adaptation strategies of herders in Mongolia and Inner Mongolia, China, and the associated local institutions that facilitated those livelihood adaptation strategies; (3) the efficient resource institutions that can facilitate social adaptation to climate change in the semiarid and arid Mongolian grasslands with high environmental variability.

I used an interdisciplinary approach to understand environmental and social dynamics as well as their interactions. I drew on multiple theoretical frameworks for analyzing social-ecological systems, which were developed by Ostrom (2005, 2009), Lemos and Agrawal (2006), and Agrawal (2009), multiple theories from grassland ecology (Ellis and Swift, 1988) and institutional economics (North, 1990, 2005; Ostrom, 1990, 2005), and methods from remote sensing, household survey, statistical modeling, and agent-based modeling. Grassland ecosystems on the Mongolian plateau were measured using the remote sensing techniques at

both regional and local scales (Chapters two and three). The dynamics of grassland productivity over the past several decades in the region were analyzed qualitatively and quantitatively (Chapters four and five). Social adaptation to environmental change was studied at both household and community levels by extensive household surveys and exploratory agent-based modeling (Chapters six and seven).

The series of studies in this dissertation advanced our understanding of the dynamics in grassland social-ecological systems and social adaptation to climate change and grassland degradation on the Mongolian plateau. Taken as a whole, my dissertation provides knowledge that can support the development of policy and management strategies within the Mongolian plateau to produce more sustainable use of the grassland resources in the context of climate change. In the following, I will draw conclusions for each of the three research objectives listed in Chapter one and discuss the caveats, challenges, and future improvements of the work.

8.1 Conclusions

8.1.1 Remote Sensing of the Mongolian Grasslands

In this part, I focused on mapping and analyzing the dynamics of grassland NPP. This was because the spatial and temporal variations in annual grassland NPP provides important information about the multiple drivers (i.e., natural and human drivers) that contribute to the availability of the key natural resources (i.e., grass biomass) for herder communities on the Mongolian plateau. While using remote sensing techniques for mapping grassland productivity are generally well known, I was able to prolong the available record on the dynamics of grassland NPP, and test the possibility of using hyperspectral data to measure grassland productivity that could be developed in the future.

The long-term analyses of grassland NPP showed that the interannual variability of NPP increased over the study period (1982−2009), especially in desert steppe. Despite the rapid increases of livestock populations in IMAR and Mongolia, NPP only showed significant decrease in some parts of Mongolia during the study period. Spring NPP increased in northern

Mongolia, where climate was cold and humid, and decreased in desert steppe of Mongolia and eastern Inner Mongolia. Summer NPP increased in southern Inner Mongolia, mainly covered by cropland, and decreased in central Mongolia. Annual NPP increased significantly in northern Mongolia and southern Inner Mongolia, and decreased in some parts of desert and typical steppes of the Mongolian grasslands. The interannual variability of NPP decreased with increases in precipitation (January-July), and the interannual variability of NPP increased with increases in the interannual variability of precipitation (January-July). Based on correlation analyses between NPP and climate, NPP was more strongly associated with precipitation than with temperature, especially in desert and typical steppes. These findings suggest that climatic variability and change is an important underlying cause of variability in grassland productivity, though it is not the whole story.

The results of field hyperspectral remote sensing of grassland communities showed that the spectral reflectance curves of different types of grassland communities were generally differentiable. In the three sites with fenced and grazed plot pairs, the fenced plots had lower reflectance in the visible bands and higher reflectance in the near infrared bands. The grazed plots showed a shift of the red-edge inflection points toward shorter wavelengths (i.e., "blue-shift"). The predictive power of vegetation indices (VI) for aboveground biomass generally decreased from desert to typical and meadow steppes. All narrowband VI tended to saturate at the study sites with high vegetation densities. The REIP produced better prediction accuracies than VI in meadow and typical steppes, but it was not a good predictor of aboveground biomass in desert steppe. The field hyperspectral remote sensing studies provide the foundations for future large-scale efforts of using images derived from imaging spectroradiometers.

8.1.2 Interpretations of Grassland Dynamics

For thousands of years, nomadism allowed local herders in the Mongolian grasslands to adapt the highly variable precipitation and vegetation productivity and preserved the vulnerable grassland ecosystems. Over the past fifty years (1961−2010), social-institutions have changed dramatically in both IMAR and Mongolia, i.e., from communal pastures to collective ownership to privatization. Those social-institutional changes have undermined the traditional resource

institutions and replaced them with a series of alternative systems. Consequently, the sustainability of the Mongolian grassland social-ecological systems was affected. Moreover, climate change and grassland degradation have been evident on the Mongolian plateau over the past five decades, and they have increased the vulnerability of livelihoods for local herders. Socioeconomic factors, such as changes in resource institutions and policies, demographic change, and economic development, played significant roles in changing grassland quality over the past five decades. The roles of state, market, and community in governing grassland resources on the Mongolian plateau also changed over the study period. Sustainable governance of the Mongolian grasslands needs the integration and coordination of the forces from the state, market, and local grazing communities.

In order to analyze the drivers of the dynamics in grassland productivity across heterogeneous landscapes, I further diagnosed the drivers of NPP dynamics across ecological zones in IMAR and Mongolia, using a spatial panel data modeling approach. The statistical modeling results indicated that the major drivers of NPP dynamics vary across the six sub-regions. Grain output was the major predictor of NPP dynamics in the farming and farming-grazing zones of Inner Mongolia. Precipitation and livestock populations both had significantly positive relationships with NPP in the two grazing zones of Inner Mongolia. However, in Mongolia, livestock populations was the only significant predictor of NPP in the grazing zone with relatively stable climate, and precipitation was the only significant predictor of NPP in the grazing zone with highly variable climate. Human land-use and livestock management behaviors and the bidirectional causal relationships between livestock populations and NPP could explain the positive relationships between livestock population and NPP. The heterogeneous drivers of NPP dynamics across space indicated that communities in different ecological and institutional settings face different kinds of challenges in their attempts to produce their livelihoods in these grassland systems. As such, a diversity of resource policies and institutions that are sensitive to these different settings is necessary for sustainable governance of grassland resources.

8.1.3 Social Adaptation to Climate Change and Grassland Degradation

While analyses in the above section provides important information about the drivers of grassland dynamics, understanding how herder households adapt to changes in grassland quality and climate is important for the sustainability of grassland social-ecological systems. In this part, I focused on studying social adaptation, in terms of changes in livelihood and land-use behaviors and changes in resource institutions and policies, to environmental change. I used a household survey to study how herders have adapted to environmental change over the past ten years. Informed by empirical studies in the Mongolian grasslands, I developed an agent-based model of resource institutions to understand how local institutions might best be structured to help herders adapt to environmental change in the future.

The results of my analysis of livelihood adaptation behaviors of herders using household surveys indicated that the differences in livelihood adaptation strategies were prominent between the two countries. Mobility and communal pooling were the two most frequent livelihood adaptation strategies for herders in Mongolia. Storage, livelihood diversification, and market exchange were the three most frequent livelihood adaptation strategies for herders in Inner Mongolia. Livelihood adaptation strategies in Mongolia were mainly shaped and facilitated by local communal institutions. Livelihood adaptation strategies in Inner Mongolia were mainly shaped and facilitated by local public and private institutions. Sedentary grazing and grassland degradation have increased livelihood vulnerability of herders to climate change, especially in Inner Mongolia. Multilevel statistical models of fodder purchasing behaviors of herders indicated that livestock management behaviors, household financial capital, climate variability, and the status of grassland degradation had statistically significant relationships with the percentage of income spent on fodder and hay. The results implied that besides adjusting local institutions, recovering grassland quality and increasing household capital are also important ways for building adaptive capacity of herder communities for future climate change.

The modeling results of the agent-based model of resource institutions showed that under certain conditions resource institutions that can facilitate cooperative use of pastures (i.e. pasture rental markets and reciprocal use of pastures) generated better social-ecological performance (i.e. average net benefit of agent and grassland quality) than the performance of sedentary grazing.

Agent diversity and social norms were important for promoting cooperation among herders. Social structures (i.e. the density of kinship connections) and governmental regulations were important for solving the free-rider problem and maintaining cooperation. The results implied that relaxing state-control related management strategies and allowing herders to form cooperative arrangements are effective ways to improve social-ecological outcomes of pasture-use; and governmental support is also important for promoting and maintaining self-organized resource institutions.

8.2 Research Limitations and Future Directions

8.2.1 Remote Sensing of Grassland Ecosystems

Long-term coarse resolution AVHRR and MODIS NDVI images were integrated to study grassland productivity dynamics between 1982 and 2009. These coarse resolution data are useful for studying vegetation dynamics at regional and global scales. However, the detailed spatial and spectral information may be averaged by these coarse resolution data. For example, in Chapter two, I was not able to exclude cropland from the Mongolian plateau, which could cause ambiguous results about the temporal trends of grassland NPP. Cropland productivity was included in the analysis of grassland NPP. The problem can be serious in IMAR since large amounts of grasslands in IMAR have been plowed for grain and fodder production over the past decades (Chapter Four). Accurate assessment of grassland productivity still needs to exclude cropland from the total study area. Differentiating cropland from grasslands is a challenge since they have similar spectral reflectance characteristics. Object-based image classification using moderate or fine resolution images is one possible method to solve the problem, because cropland parcels are usually with regular shapes. However, high-resolution images are usually needed in order to make objective-based classifications more effective. In addition, NDVI derived from AVHRR and MODIS sensors may be insufficient to monitoring grassland degradation. One of the reasons is that the values of NDVI will saturate at high canopy densities. The other major reason is that grasslands with different biophysical characteristics (e.g. species composition) may produce similar values of vegetation indices if they have similar biomass (Yamano et al., 2003).

Hyperspectral images with hundreds of spectral bands have the potential to accurately map plant communities and their degradation status. In Chapter three, I explored the potential of using hyperspectral remote sensing data to differentiate plant communities and predict ecological variables across ecological gradients of IMAR. However, only a few field sites were investigated, considering the large geographic coverage of the study area. More extensive field spectral and ecological samplings are still needed in order to get reliable and convincing results. This work provides the foundation for future large-scale efforts for monitoring grassland status using hyperspectral remote sensing. Hyperspectral images can be combined and fused with high-resolution images to extract more detailed information of vegetation (Walsh et al., 2008). One major challenge of using hyperspectral images is the data volume. Various algorithms have been developed to handle the data redundancy problem and extract useful information from hyperspectral image cubes (Thenkabail et al., 2012). However, large-scale mapping of grassland communities and extracting the information of grassland degradation from hyperspectral images will still be a challenge.

8.2.2 Climate Adaptation, Local Institutions, and Rural Livelihoods

Understanding the interactions between climate adaptation, local institutions, and rural livelihoods is important for building adaptive capacity of herder communities for future climate change. In my doctoral research, livelihood adaptation behaviors of herders to environmental change were generally investigated. In the future, I hope to revisit the sites included in my dissertation and to do follow-up surveys and in-depth interviews about the livelihoods of herders for the years with climate hazards, such as droughts and snowstorms. Besides a warmer and drier climate, the increased frequencies of climate hazards have caused disastrous effects on livestock grazing in the Mongolian grasslands over the past half century. The results of this work lead me to an interest in studying the impacts of the spatial-temporal variability of droughts and snowstorms on the livelihoods of herders over the past three decades. Satellite data derived from multispectral and radar sensors can be used for studying historical climate hazards. Ultimately, I hope to help policy makers and grassland users design and implement evidence-based policies for building adaptive capacity of local herder communities for future climate change.

The results of my survey analyses showed that local institutions played the central role in shaping and facilitating livelihood adaptation behaviors of herders. The self-organization and evolution of local institutions for governing grassland resources are interesting and meaningful topics. I plan to study the interactions between local institutions, resource behaviors, and changes in grassland quality. The major challenge of this work is to collect accurate information about long-term changes in ecological variables and local resource institutions. I will continue to adopt the approach that links remote sensing, local institutions, and socioeconomic data to study human-environment interactions. Time-series of Landsat images from the mid-1980s to now can be acquired and interpreted to track the changes in grassland quality. Building on the comprehensive household survey data collected in this research, further follow-up surveys and in-depth interviews can be conducted to investigate changes in local resource institutions over the past 30 years. This study can further our understanding of the process of land-use change and the role of local institutions in shaping human-environment interactions.

8.2.3 Modeling Sustainability of Social-Ecological Systems

The agent-based model in this work has a focus on the modeling the social-ecological performance of local resource institutions under different climate scenarios. Other sub-systems of grassland social-ecological systems were simplified. Those simplifications could lower the reliability of the agent-based model to have real world policy and institutional implications. For example, market incentives on the livestock management behaviors of herders were simplified in the model. I assumed that the number of livestock in each herder household was constant overtime. In the real world, the rapid increase of livestock population stimulated by market incentives is one of the major reasons for grassland degradation on the Mongolian plateau, especially in IMAR. Therefore, in the future, modeling the role of local institutions in adaptation to climate change and grassland degradation needs to incorporate the market sub-model. Second, the mechanisms of the dynamics in grassland productivity driven by climate variability were simplified by using a hypothetical look-up table. This simplification can be improved by coupling a simple ecosystem model with the agent-based model.

Moreover, resource institutional change was not explicitly modeled. This is another potential improvement for the model. Endogenous intuitional change, or self-organized resource institutions, is the core part of studying intuitions for governing common-pool natural resources sustainably (Ostrom, 1990). The interactions between macro-level institutional changes and micro-level changes in knowledge, beliefs, and information constraints of actors have been studied by North (2005) and Ostrom (2005). The institutional framework is an external manifestation of the belief systems of individuals. Institutional change is strongly depends on changes occurring in belief systems. At the same time, the institutional structure constraints choices and actions and influences the beliefs of individuals (North, 2005). Agent-based models have been used to model endogenous resource intuitional change (Bravo, 2011). In the future, the interactions between agent beliefs and resource institutions will be further explored. Compared with abstract analytical models (e.g., game theoretical models), agent-based models can generate more realistic scenarios. Besides the above simplifications of the economic, ecological, institutional mechanisms, another limitation of the current version of the model is that some of the model parameters were not empirically calibrated, although the social mechanisms of agent actions and interactions under alternative institutional scenarios were informed by empirical studies in the Mongolian grasslands. Further calibrations of the model parameters using empirical data is still needed if the modeling results are expected have real-world policy and institutional implications.

8.2.4 Scale, Uncertainty, and Error Propagations

Scale is one of the most studied topics in remote sensing, more broadly speaking geographical information science (GIScience) (Liang, 2004; Quattrochi and Goodchild, 1997). Uncertainty and error propagations in spatial analysis and modeling are the emerging topics in GIScience (Burnicki, 2008; Zhang and Goodchild, 2002). In this dissertation, I applied geostatistical inverse modeling (GIM) to produce both the best predictions of a target image at finer resolutions (downscaling) and prediction uncertainties, based on one or more other images with different resolutions, while honoring the original measurements. GIM can also be used for image up-scaling. These have been discussed in Appendix A. For the traditional image re-sampling algorithms, such as nearest neighbor, bilinear interpolation, and cubic convolution, the

uncertainty of the re-sampled results are not provided. Therefore, the analyst does not know the actual uncertainty of the data with changed spatial resolutions. Geostatistical models for image scaling regard the measurements as random fields and produce both spatial predictions and associate prediction uncertainties. Second, in this work, the Gaussian random field model was used in both synthetic and real data modeling experiments. However, lots of measurements do not follow the Gaussian distribution. Therefore, GIM needs to be modified to fit the non-Gaussian data, and this set of models is known as generalized linear mixed models.

In addition, measurement errors can also be accounted by the GIM framework, although I did not run experiments with data associated measurement errors. Measurement errors and errors in spatial analysis and modeling procedures will propagate to lower-stream procedures and final results. In classic geospatial analysis and modeling, these problems are usually ignored or less studied (Heuvelink, 1998). In the future, I plan to generate hundreds of images with different covariance parameters, measurement errors, non-normality, and non-stationarity and explore the problem of error propagations in depth. These synthetic images will be aggregated to different coarser resolutions and downscaled back to the original resolution. The restricted maximum likelihood (REML) method will still be used for covariance parameter estimation from the aggregated synthetic images. The prediction accuracies and associated uncertainties will be assessed in order to understand error propagations in spatial predictions made by GIM.

Appendix A

Geostatistical Inverse Modeling for Super-Resolution Mapping of Continuous Spatial Processes

Abstract

We present a geostatistical inverse modeling (GIM) approach for merging coarse-resolution images with variable resolutions and for super-resolution (i.e. predictions at the sub-pixel level) mapping of continuous spatial processes. We used GIM to produce both spatial predictions of a target image and prediction uncertainties, while preserving the values of original measurements. GIM is totally data driven, and covariance parameters for the target resolution can be directly derived from measurements. We also developed a moving-window GIM approach to accommodate spatial nonstationarity and reduce computational burden associated with large image datasets. First, we demonstrated GIM and moving-window GIM on synthetic images. Aggregated synthetic images with variable resolutions were merged to produce a single resolution image. The modeling results showed that the two approaches can produce accurate spatial predictions and correct prediction uncertainties. Second, we applied moving-window GIM for merging aerosol optical depth (AOD) data with variable resolutions, which were derived from two sensors. The results showed that moving-window GIM can be used for merging complementary AOD data from the two sensors and for super-resolution mapping of global AOD distributions. Therefore, we can conclude that GIM is a practical solution for merging complementary coarse-resolution images and for super-resolution mapping of continuous spatial processes.

Keywords: Multi-resolution data fusion; super-resolution mapping; change-of-support; spatial nonstationarity; geostatistical inverse modeling; spatial prediction; uncertainty

---

Wang, J., Brown, D. G., Hammerling, D. Geostatistical inverse modeling for super-resolution mapping of continuous spatial processes. Manuscript submitted for review.

A.1 Introduction

Synthesizing complementary information derived from multiple sensors prompts the need to study rigorous data fusion algorithms. Data fusion is a process that integrates information derived from different sensors or different spectral bands of the same sensor and produces a single image that contains complementary information from multiple sources, while minimizing loss or distortion of the original data (Hall, 2004; Pohl and Van Genderen, 1998). In this work, we focus on statistical algorithms for merging measurements derived from multiple coarse-resolution sensors. Statistical data fusion combines statistically heterogeneous samples from marginal distributions to make statistical inference about the unobserved joint distributions or functions of them (Braverman, 2008). Statistical data fusion, including those based on geostatistics, can produce spatial predictions of pixel values (Atkinson et al., 2008). Recently, several geostatistical algorithms, including fixed ranking kriging (Cressie and Johannesson, 2008), fixed ranking filtering (Cressie et al., 2010; Kang et al., 2010), spatial statistical data fusion (Nguyen, 2012), space-time data fusion (Braverman et al., 2011), and moving-window kriging (Hammerling et al., 2012), have been developed for mapping global distributions of environmental variables, such as aerosol optical depth (AOD) and carbon dioxide (CO_2), with sparsely distributed remotely sensed data. The numerous algorithms for merging measurements from different spectral bands (e.g. pan-sharpening) are beyond the scope of this chapter.

Measurements from remote sensing sensors are constantly influenced by factors like atmospheric conditions, electronic noise of sensors, and changes in illumination. In order to build geostatistical models of sensor measurements contaminated with measurement errors, we took a stochastic perspective of remote sensing images. We regarded the true spatial process of interest (i.e. spectral radiance) as a random field, i.e., a spatial random process with a set of random variables that have certain probability distributions. Then, a remote sensing image covering an area can be conceived as a realization of the random field. In this work, we adopted the Gaussian random field model, which involves a set of Gaussian probability density functions for random variables. For remote sensing measurements, the values of continuous spatial processes of interest are regularized to discrete pixels by a weighted average process, with the spatial weights determined by point spread functions (PSFs) of sensors (Jupp et al., 1988). The effective

instantaneous field of view (EIFOV) of the sensor is an area over which measurements are averaged. EIFOV defines the spatial support of sensor measurements. Spatial support is a geostatistical concept that means the shape, size, and orientation of measurements (Gotway and Young, 2002, 2005). The value assigned to a pixel represents the average radiance arriving at the sensor from the EIFOV (Jupp et al., 1988). Sensors with different sizes of pixels have different EIFOVs. Therefore, measurements from these sensors have different spatial supports.

Merging remote sensing images with variable resolutions usually involves the change-of-support problem (Curran and Atkinson, 1999; Gotway and Young, 2002, 2005). Several geostatistical algorithms have been developed to solve the change-of-support problem. Area-to-point kriging was developed for downscaling areal data to point support (Kyriakidis, 2004; Kyriakidis and Yoo, 2005). Goovaerts (2008) developed a practical semivariogram deconvolution algorithm to derive point support variogram parameters from areal data. This algorithm solved one of the key problems in the practical application of area-to-point kriging. Moreover, a parallel computing algorithm has been developed for speeding-up the computation involved in the practical application of area-to-point kriging (Guan et al., 2011). Area-to-point kriging has the potential for downscaling remote sensing data. Nguyen et al. (2012) developed a spatial statistical data fusion approach, which incorporated a change-of-support model into fixed rank kriging. It was applied for merging variable-resolution AOD images derived from the Multi-angle Imaging Spectroradiometer (MISR) and the Moderate Resolution Imaging Spectroradiometer (MODIS) sensors.

The spatially varying dependence structure of random variables (i.e. spatial nonstationarity) is another major problem to be dealt with when working with remote sensing images covering large geographic areas. In classical geostatistics, a fundamental assumption of most models is that random fields are second-order stationary, i.e., in a relatively small region the mean values of random variables are constant and the covariance between the values of random variables only depends on the distance between them (Chilès and Delfiner, 2012). However, for spatial data covering large geographic areas, this assumption may not be true because spatial heterogeneity is a typical characteristic for remote sensing images covering large geographic areas. In this work, we differentiated two types of spatial nonstationarity: one is spatial nonstationarity in the mean

values of regionalized variables, and the other is spatial nonstationarity in the covariance structure. The need to address spatial nonstationarity has been discussed in the field of geostatistics over the past decades. Universal kriging is one way to address spatial nonstationarity in the mean values of regionalized variables. Hass (1990) applied a moving-window kriging approach to model acid depositions. For this method, measurements in local-windows are used for parameter estimations and spatial predictions. This approach is simple to be implemented, and it alleviates the problem of spatial nonstationarity. Due to local fitting and computing, moving-window kriging is also computationally efficient. One caveat of the local-window approach is that there is no consistent covariance function over the whole study domain. Higdon et al. (1999) convolved spatially varying kernels to give a nonstationary version of the squared exponential stationary covariance function. This approach has been applied in modeling remote sensing images (D'Hondt et al., 2007). Although this method can produce a consistent covariance function over the whole prediction domain, the Gaussian kernel applied in this method was too smooth for real spatial processes.

Besides spatial nonstationarity, the problem of computational burden also needs to be solved when applying geostatistical models to deal with large spatial data. The local-window approach is one way to solve the problem of computational burden. Data dimension reduction is another way to reduce computational burden associated with large spatial data (Wikle, 2010). Cressie and Johannesson (2008) developed a spatial mixed effects model, called fixed rank kriging, with a flexible family of nonstationary covariance functions. For this approach, kriging can be done exactly, and the computational complexity is linear to the size of the data. Moreover, Cressie et al. (2010) developed a spatial-temporal random effect model, called fixed rank filtering, which integrates fixed rank kriging and Kalman filter for dealing with large spatial-temporal data. Fixed rank kriging and fixed rank filtering are both approaches of data dimension reduction. These methods eliminate or reduce some components of spatial variability to improve computational efficiency.

In this work, we present a geostatistical inverse modeling approach for merging coarse-resolution remote sensing images with variable spatial supports. Geostatistical inverse modeling was designed to be statistically principled, and it was designed to preserve the information of

original measurements, i.e., honoring the original data. In the geostatistical inverse modeling framework, the restricted maximum likelihood method was used for estimating covariance parameters related to the change-of-support problem. Moreover, we contributed a moving-window geostatistical inverse modeling approach to accommodate spatial nonstationarity and reduce computational burden associated with large image datasets. Following the introduction, we introduce the geostatistical inverse modeling methodology in Section A.2. In Section A.3, we illustrate the modeling experiments on synthetic and real images. The modeling results are presented in Section A.4. Finally, we discuss possible model improvements and summarize the major findings of this work.

A.2 Methodology

A.2.1 Geostatistical Inverse Modeling

Geostatistical inverse modeling (GIM) follows a Bayesian approach, and it is based on the principle of combining prior information (i.e. spatial and/or temporal autocorrelation) with information from available measurements (Michalak et al., 2004). Spatial and/or temporal autocorrelation can provide information about the structure of the data that can be used to reduce prediction uncertainty. GIM has been applied in ground water systems (Kitanidis, 1995), contaminant sources identification (Snodgrass and Kitanidis, 1997), estimating surface fluxes of atmospheric trace gases (Gourdji et al., 2008; Michalak et al., 2004), characterizing attribute distributions in water sediments (Zhou and Michalak, 2009), and merging remote sensing images with variable resolutions (Erickson and Michalak, 2006). There remain unrealized opportunities for using GIM for image scaling (i.e. downscaling and up-scaling) and multi-resolution data fusion. In comparison with area-to-point kriging, which also deals with predicting point values from available areal data, the covariance parameters in the GIM framework can be inferred directly from measurements by the restricted maximum likelihood algorithm. Multiple measurements with different spatial supports can also be explicitly accounted in the GIM framework.

The spatial prediction problem of GIM can be expressed as

$$z = \mathrm{h}(s, r) + v \tag{A-1}$$

where z is an $n \times 1$ vector of measurements; s is an $m \times 1$ vector of predictions; and the vector r contains other parameters in the transformation function $\mathrm{h}(s, r)$. This function can be expressed as a linear transformation of predictions, which is represented by the relationships between measurements and predictions. For remote sensing applications, the transformation function can be defined as point spread functions (PSFs) of sensors. PSFs for many electro-optical sensors follow a two-dimensional Gaussian distribution (Huang et al., 2002). The vector v describes the model-data mismatch, which means the mismatch between underlying true spatial processes and measurements. The vector v represents measurement errors of remote sensing images. In the GIM framework, the prior and posterior probability density functions are with respect to the measurements z.

$$p(s, \beta \mid z) \propto p(s, \beta) \cdot p(z \mid s) \tag{A-2}$$

where $p(s, \beta)$ is the prior probability density function; $p(z \mid s)$ is the likelihood of measurements; and $p(s, \beta \mid z)$ is the posterior probability density function. The prior probability density function represents the assumed spatial structure of the unknown surface (i.e. prediction field), which is described by a covariance function. The multivariate Gaussian distribution model is used in the GIM framework.

$$p(s, \beta) \propto |Q|^{-1/2} \exp\left[-\frac{1}{2} (s - X\beta)^T Q^{-1} (s - X\beta) \right] \tag{A-3}$$

where X is an $m \times t$ matrix of auxiliary variables related to the distribution of predictions; t is the number of auxiliary variables; β is a $t \times 1$ vector of drift coefficients on X; $X\beta$ is the model of the trend; and Q is an $m \times m$ matrix representing the spatial autocorrelation of residuals that are not explained by the model of the trend. The likelihood of the measurements represents the degree to which a prediction of the unknown function s reproduces the measurements z (Kitanidis, 1995; Michalak et al., 2004)

$$p(z \mid s) \propto |R|^{-1/2} \exp\left[-\frac{1}{2} (z - Hs)^T R^{-1} (z - Hs) \right] \tag{A-4}$$

where H is an $n \times m$ matrix representing relationships between measurements and predictions; and R is an $n \times n$ matrix representing the model-data mismatch. Then, the posterior probability density function of the unknown surface distribution s becomes

$$p(s,\beta \mid z) \propto |R|^{-1/2} |Q|^{-1/2} \exp\left[-\frac{1}{2}(z-Hs)^T R^{-1}(z-Hs) - \frac{1}{2}(s-X\beta)^T Q^{-1}(s-X\beta) \right] \quad \text{(A-5)}$$

By taking the negative logarithm of the above formula, we can get the objective function of GIM

$$L_{s,\beta} = (z-Hs)^T R^{-1}(z-Hs) + (s-X\beta)^T Q^{-1}(s-X\beta) \quad \text{(A-6)}$$

The best predictions (i.e. minimizing the squared errors between spatial predictions and measurements) are obtained by minimizing the above objective function with respect to s and β. By taking the first order derivative of the above objective function with respect to s and β and expressing the resulting in the matrix form, we can get the solution of the geostatistical inverse model

$$\begin{bmatrix} HQH^T + R & HX \\ (HX)^T & 0 \end{bmatrix} \begin{bmatrix} \lambda^T \\ M \end{bmatrix} = \begin{bmatrix} HQ \\ X^T \end{bmatrix} \quad \text{(A-7)}$$

where λ is an $m \times n$ matrix of estimated weights assigned to related observations; and M is a $p \times m$ matrix of Langrange multipliers. By solving λ and M, the best predictions and their variances are produced by

$$\hat{s} = \lambda z \quad \text{(A-8)}$$

$$V_{\hat{s}} = -XM + Q - QH^T\lambda \quad \text{(A-9)}$$

where $\hat{s}$ are the best predictions of pixel values at m locations of the prediction field; and the diagonal elements of $V_{\hat{s}}$ represent the predicted error variance of individual elements in $\hat{s}$. An overview of the GIM methodology for synthesizing information of multiple images with variable resolutions is shown in Fig. A.1.

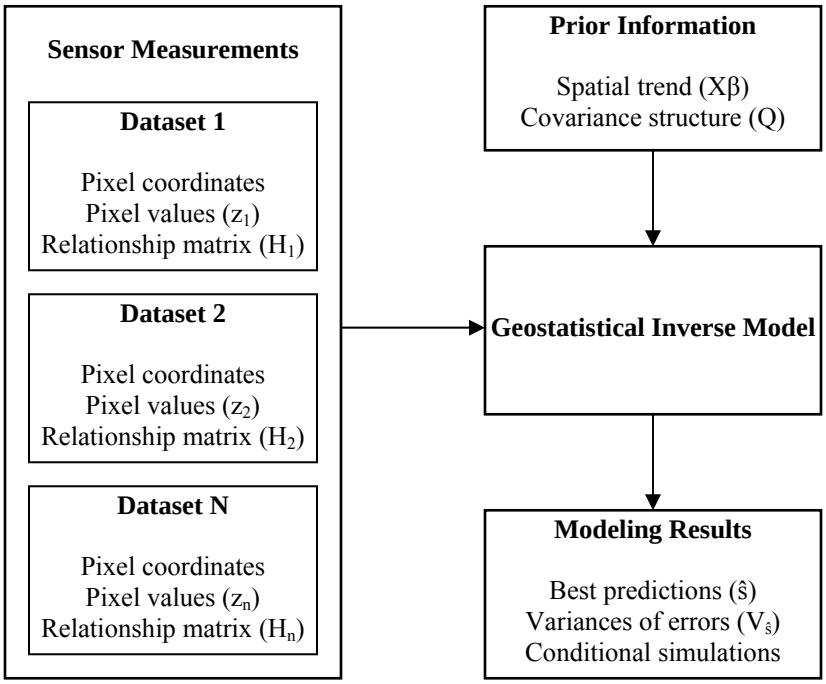

Fig. A.1 A flowchart of the geostatistical inverse modeling methodology for merging remotely sensed data with variable resolutions to produce a single resolution image. Multiple datasets ($z_1, z_2, \ldots, z_n$) can be merged to produce one single resolution image with different relationships matrices ($H_1, H_2, \ldots, H_n$). The prior information on the covariance structure of the prediction field (Q) was also estimated from the measurements (see the following section).

In order to accommodate spatial nonstationarity and reduce computational burden associated with large spatial data, we developed a moving-window GIM approach, which is an integration of GIM and the moving-window approach. The general idea of moving-window GIM is that instead of using all available measurements to predict the value at a prediction location, only measurements within local-windows are used. Local-windows are centered at prediction locations. The rationale behind this approach is that measurements distant from a prediction location may contribute very little to the prediction, except the situation that the correlation length is long. In most remote sensing applications, this is particularly true because images usually cover everywhere in the study domain, except the missing pixels caused by measurement errors or clouds. Moreover, the point spread functions (PSFs) of optical sensors also have a blurring effect because pixel values are calculated using data from neighboring pixels (Huang et al., 2002). In this work, the size of local-windows was chosen based on pre-calculations of covariance parameters over the prediction domain in order to guarantee the size of local-

windows meets both computational requirements and the accuracy of approximation. We used measurements in local-windows for both parameter estimations and spatial predictions.

A.2.2 Covariance Parameter Estimations

Parameter estimations refer to the statistical inference of covariance parameters for a stochastic model of measurements. There are several approaches for estimating covariance parameters of geostatistical models, such as ordinary least square (OLS; Bogaert and Russo, 1999), weighted least square (WLS; Cressie, 1985), and restricted maximum likelihood (REML; Kitanidis, 1995; Michalak et al., 2004). In this work, we applied REML for optimizing covariance parameters by maximizing the likelihood of measurements. REML is a variant of the maximum likelihood (ML) algorithm. REML leads to less biased estimates of covariance parameters when the sample size is small (Diggle and Ribeiro Jr., 2007). Image scaling and multi-resolution data fusion involve two types of parameter estimations. The differentiation is based on whether measurements are available at the prediction resolution. If there are available measurements at the prediction resolution, we can directly estimate covariance parameters using the measurements. Otherwise, we have to infer covariance parameters at the prediction resolution using data measured at another spatial resolution. REML can be used for both types of parameter estimations.

First, when measurements are available at the prediction resolution, the REML approach for parameter estimations is referred to as "REML-Kriging (Gourdji et a., 2010; Nagle et al., 2011)." The objective function of "REML-Kriging" is defined as

$$L_{\Psi} = \frac{1}{2}\ln|Q| + \frac{1}{2}\ln\left|X^T Q^{-1} X\right| + \frac{1}{2}\left[s^T (Q^{-1} - Q^{-1} X (X^T Q^{-1} X)^{-1} X^T Q^{-1}) s\right] \quad \text{(A-10)}$$

In this case, the gradient-based searching routine can be used for parameter optimization because the number of measurements is usually quite large for remote sensing applications. Uncertainties of covariance parameters (i.e. sill, range, and nugget) can also be calculated by the Hessian computation.

Second, when no measurements are available at the prediction resolution, the REML approach for parameter estimations is referred to as "REML-Inverse Modeling (Kitanidis, 1995; Michalak et al., 2004)." The objective function of "REML-Inverse Modeling" is defined as

$$L = \frac{1}{2}\ln|\Psi| + \frac{1}{2}\left|X^T H^T \Psi^{-1} HX\right| + \frac{1}{2} z^T \Xi z \tag{A-11}$$

$$\Psi = HQH^T + R \tag{A-12}$$

$$\Xi = \Psi^{-1} - \Psi^{-1} HX (X^T H^T \Psi^{-1} HX)^{-1} X^T H^T \Psi^{-1} \tag{A-13}$$

If the number of measurements is small, we can use the unconstrained nonlinear optimization routine for parameter optimization. Otherwise, the gradient-based searching routine can be applied for parameter optimization. The two optimization algorithms are both provided in the software package MATLAB (Mathworks Inc., Natick, Massachusetts, USA). In the moving-window GIM framework, we used "REML-Inverse Modeling" for parameter estimations in local-windows. This was because "REML-Inverse Modeling" leads to less biased estimates of covariance parameters when the sample size is small (Diggle and Ribeiro Jr., 2007). The unconstrained nonlinear optimization routine was applied for optimizing covariance parameters in local-windows.

In this work, we applied the exponential covariance function for all geostatistical models. The form of the exponential covariance function and the corresponding semivariogram model are defined as

$$Q(h \mid \sigma^2, l) = \sigma^2 \exp(-\frac{h}{l}) \tag{A-14}$$

$$\gamma(h \mid \sigma^2, l) = \sigma^2 \left[1 - \exp(-\frac{h}{l})\right] \tag{A-15}$$

where σ^2 is the variance; l is the integral scale; and h is the distance between two data. The straight-line distance (i.e. Euclidian distance) and the great-circle distance were both used in this study for different types of problems. The great-circle distance between x_i and x_j is defined as (Diggle and Ribeiro Jr., 2007)

$$h(x_i, x_j) = \theta \cos^{-1}(\sin\varphi_i \sin\varphi_j + \cos\varphi_i \cos\varphi_j \cos(\phi_i - \phi_j)) \tag{A-16}$$

where θ is the radius of the Earth; φ_i and ϕ_i are the latitude and longitude of x_i, respectively; and φ_j and ϕ_j are the latitude and longitude of x_j, respectively.

A.2.3 Unconditional and Conditional Simulations

Unconditional and conditional simulations are spatially consistent Monte Carlo simulations. They are geostatistical approaches for describing spatial variability of random fields. Conditional simulations generate realizations of a random field that possess the same structural characteristics as measurements. It can also reproduce measurements. Conditional simulations are equally likely realizations that have the same spatial structure defined by the covariance function. Unconditional simulations also follow the same spatial dependence structure defined by measurements, but they cannot reproduce measurements (Chilès and Delfiner, 2012; Diggle and Ribeiro Jr., 2007). Unconditional and conditional simulations can generate multiple outcomes, and each of which is an equally likely realization. When modeling a stationary Gaussian random field over an area that is much larger than the range, a single simulation can give a view of a variety of possible local situations (Chilès and Delfiner, 2012).

In order to demonstrate the application of GIM for image downscaling and multi-resolution data fusion on synthetic images with spatially stationary characteristics, we used unconditional simulations to generate such synthetic data. In this case, the Gaussian random field model was used in modeling the spatial random process. The Gaussian models are widely used because they are simple, and they can capture a wide range of spatial behaviors according to the specification of their correlation structures (Diggle and Ribeiro Jr., 2007). The random field is spatially stationary (i.e. second-order stationary) if the mean values of regionalized variables are constant, and the covariance is only determined by the distance between two measurements (Chilès and Delfiner, 2012). The generation of synthetic images proceeded as follows. The user-specified covariance function was first decomposed by the Cholesky decomposition

$$Q = CC^T \tag{A-17}$$

where Q is the covariance function. The unconditional simulations were generated by

$$s_{ui} = X\beta + Cu_i \tag{A-18}$$

where $X\beta$ is the model of spatial trend and can be set as zero; and u_i is a vector of normally distributed random numbers with zero-mean and unit-variance. In the case of generating synthetic images, the model of spatial trend was set as zero.

The conditional simulations of the geostatistical inverse model were defined as (Kitanidis, 1995; Michalak et al., 2004)

$$s_{ci} = s_{ui} + \lambda\left(z + v - Hs_{ui}\right) \tag{A-19}$$

where v is a normally distributed random number, which is sampled from the model-data mismatch error covariance R with zero-mean and variance σ_R^2; and s_{ui} is the unconditional simulation of GIM (Equation A-18).

A.2.4 Fixed Rank Kriging

In order to demonstrate the application of moving-window GIM for image downscaling and multi-resolution data fusion on synthetic data with spatially nonstationary characteristics, we used fixed ranking kriging (FRK; Cressie and Johannesson, 2008) to generate such synthetic data. FRK is a low-rank representation of spatial continuous random processes, and it eliminates or reduces some components of spatial variability to improve computational efficiency. This data dimension reduction approach was developed for dealing with the spatial prediction problem associated with large spatial data. Moreover, remote sensing images covering large geographic areas usually have spatially nonstationary characteristics. FRK can accommodate spatial nonstationarity by using a set of multi-scale basis functions. Readers are referred to Cressie et al. (2010), Cressie and Johannesson (2008), and Kang et al. (2010) for detailed discussions about FRK. Only brief descriptions are provided here because we only used FRK to generate synthetic images. Here, our goal was to make statistical inferences about a spatial process $\{Y(s): s \in D \subset \mathbb{R}^d\}$ based on measurements with errors.

The measurements are given by the data model

$$Z(s) = Y(s) + \varepsilon(s) \tag{A-20}$$

where $\{\varepsilon(s) : s \in D\}$ is a white-noise Gaussian process with mean zero and variance $\sigma_\varepsilon^2 > 0$. We assumed that $Y(s)$ has the following structure

$$Y(s) = \mu(s) + \upsilon(s) \tag{A-21}$$

where $\mu(\cdot)$ is a deterministic trend function representing the large-scale variability(e.g., $\mu(\cdot) = X\beta$). The small-scale variability is modeled as a Gaussian process. $\upsilon(\cdot)$ is assumed as with zero-mean and follows a spatial random effect model. The unknown random variables to be predicted are fixed at a number, which is equal to the number of spatial basis functions. It can be expressed as

$$\upsilon(s) = S(s)'\eta + \xi(s) \tag{A-22}$$

where $S(\cdot) \equiv (S_1(\cdot), ..., S_r(\cdot))'$ is a set of basis-functions, which can capture different scales of spatial dependence. The basis-functions are not necessarily orthogonal, but they should represent information at multiple resolutions. The multi-resolution wavelet basis function (Cressie et al., 2010; Kang et al., 2010) and the bi-square basis function (Cressie and Johannesson, 2008; Nguyen, 2012) have been used in the previous studies. In this work, we chose the bi-square basis function considering its simplicity and computational efficiency (Cressie and Johannesson, 2008).

$$S_{j(l)}(u) = \begin{cases} \left\{1 - (\left\|u - v_{j(l)}\right\| / r_l)^2\right\}^2, & \left\|u - v_{j(l)}\right\| \le r_l \\ 0, & \textit{otherwise} \end{cases} \tag{A-23}$$

where $v_{j(l)}$ is one of the center points of the l_{th} resolution ($l = 1, 2, 3, \cdots N$); and r_l=1.5 (i.e. the shortest arc distance between center points of the l_{th} resolution). The generated synthetic images can have more spatial variability by increasing the number of resolutions in the model. However, this will increase computational requirements for generating such synthetic data. The spatially nonstationary covariance function is modeled as

$$C(u, v) = S(u)'\mathrm{K}S(v), \qquad u, v \in \mathbb{R}^d \tag{A-24}$$

where K is a positive definite $r \times r$ unknown matrix; $\eta = (\eta_1, ..., \eta_r)'$ is a zero-mean Gaussian random vector with $\mathrm{cov}(\eta) \equiv \mathrm{K}$; and $\xi(\cdot)$ captures the fine-scale spatial variability. The fraction of

the fine-scale spatial variability to the total spatial variability and the signal to noise ratio of the generated synthetic image can also be defined in the FRK model (Cressie et al., 2010).

A.3 Computer Experiments

In this work, the overall geostatistical modeling experiments proceeded as follows. First, in order to isolate various problems associated with real images (e.g. measurement errors), we demonstrated the applications of GIM and moving-window GIM for image downscaling and multi-resolution data fusion on synthetic images. Second, we applied moving-window GIM for merging AOD measurements derived from two sensors and for super-resolution mapping of global AOD distributions. For all experiments on synthetic and real data, we used REML for estimating covariance parameters. In order to assess prediction accuracies and the correctness of prediction uncertainties, we calculated the root mean square error (RMSE) between spatial predictions and measurements, and the percentage of pixels in original images with their values falling within two standard deviations of the best predictions. We called the first measure the "RMSE index" and the second measure the "percentage index." In addition, image registration is a major step prior to pixel-level data fusion. We assumed that the images used for multi-resolution data fusion have been registered correctly. Analyzing the influence of image mis-registration on the accuracy of spatial predictions was beyond the scope of this work. All of the geostatistical models discussed in the chapter (Section A.2) and the following experiments were coded in MATLAB by the authors.

A.3.1 Generating Synthetic Images

We applied unconditional simulations with user specified covariance parameters to generate synthetic images with spatially stationary characteristics. The synthetic images with and without the nugget effect were generated and used in the modeling experiments. The simulated reference pixel values were distributed on a 120 × 120 regular grid (of unit cell size). In this work, we differentiated the fine-scale spatial variability of images and the measurement errors of images, and we defined the nugget effect as the fine-scale spatial variability (Cressie et al., 2010).

Moreover, we did not introduce simulated measurement errors into the synthetic images. The covariance functions used for generating synthetic images are

$$C(h) = 0.01 \times (1 - \frac{h}{10}) \quad \text{(A-25)}$$

$$C(h) = 0.005 + 0.02 \times (1 - \frac{h}{5}) \quad \text{(A-26)}$$

where $C(h)$ is the covariance function; and h is the straight-line distance (i.e. Euclidian distance) between two locations. Equation 25 is the exponential covariance function, and the sill and range values are 0.01 and 30, respectively. Equation 26 is a combination of the exponential covariance function and the nugget effect, and the sill and range values are 0.025 and 15, respectively.

We used FRK to generate a synthetic image with spatially nonstationary characteristics. The values of sill and range for the exponential covariance function in the FRK framework were set as 0.05 and 30, respectively. The specified covariance function was used to parameterize the κ matrix in the spatially nonstationary covariance function (Equation 24). In order to simulate spatial variability of real remote sensing images, we used a large number of basis-functions for characterizing multi-scale spatial variability. In this experiment, we set the resolution number (l) as five. The number of bi-square basis-functions used for generating the synthetic image was 1364, which was the sum of basis-functions in each of the five lower resolutions: 4 (1 × 4), 16 (4 × 4), 64 (16 × 4), 256 (64 × 4), and 1024 (256 × 4). We set the fraction of the fine-scale spatial variability to the total spatial variabiltiy as 0.05. We did not introduce measurement errors into the synthetic image. Therefore, the value of the signal-to-noise ratio was set as one. The simulated pixels were distributed on a 320 × 320 regular grid (of unit size).

A.3.2 Merging Synthetic Images with Variable Resolutions

We designed four experiments for demonstrating the application of GIM for image downscaling and multi-resolution data fusion on the synthetic images with spatially stationary characteristics: two were on the synthetic image without the nugget effect, and the other two were on the synthetic image with the nugget effect. The modeling experiments proceeded as follows. Given space limitations, we only used the experiment on the synthetic image without the

nugget effect as an example. First, we averaged the synthetic image to two coarser resolutions using a non-overlapping moving-window. The first aggregated image was with the spatial support of 64 (i.e. the size of the local-window was 8 × 8), and the second aggregated image was with the spatial support of four (i.e., the size of the local-window was 2 × 2). We only used the diagonal part of the second aggregated image for the experiment. We set two relationship matrices (i.e. the H matrix in the GIM framework) for the two aggregated images because they had different spatial supports. We used the uniform distribution function to represent the relationships between coarse-resolution measurements and fine-resolution predictions, and we assumed sub-pixels within a coarse-resolution pixel had the same contribution to the value of the coarse-resolution pixel. The size of the prediction field was set as the same size of the original simulated image. We also generated conditional simulations to show spatial uncertainties of the predictions. In the second experiment, the aggregated image with the spatial support of 64 was merged with the diagonal part of the aggregated image with the spatial support of 16 (i.e. the size of the local-window was 4 × 4). We also ran two similar experiments on the synthetic image with the nugget effect.

We demonstrated the application of moving-window GIM for multi-resolution data fusion on the synthetic image with spatially nonstationary characteristics. Similar to the above experiments, the synthetic image generated by FRK was averaged using non-overlapping moving windows to two coarser resolutions: one aggregated image was with the spatial support of 16 (i.e. the size of the local-window was 4 × 4), and the other aggregated image was with the spatial support of four (i.e. the size of the local-window was 2 × 2). Only the diagonal part of the second aggregated image was used in the experiment. We also set two relationship matrices for the two aggregated images with different spatial supports. The uniform distribution function was also used for representing the relationships between coarse-resolution measurements and fine-resolution predictions. In order to assess the modeling results, the size of the prediction field was also set as the same size of the original simulated image.

A.3.3 Merging AOD Measurements with Variable Resolutions

We applied moving-window GIM for merging Level-3 AOD data derived from the MISR and the Terra-MODIS sensors and for super-resolution mapping of global AOD distributions in short time-intervals. The spatial resolutions of Level-3 MISR AOD and Terra-MODIS AOD are 0.5° × 0.5° and 1° × 1°, respectively. MISR and Terra-MODIS are both carried by the Terra satellite but with different sensor characteristics, such as the size of swath and the instantaneous field of view. Second, the algorithms for retrieving AOD from original MISR and Terra-MODIS data are different. MODIS land retrieval algorithm does not operate over desert (e.g. northern Africa and Middle East) or other bright land surfaces, and MODIS has difficulties in computing AOD in part of its swath over dark water due to sun glint. MISR can measure AOD in the above conditions (Kahn et al., 2009). Moreover, MODIS has much wider spatial coverage than MISR does due to its wider swath. However, MISR has measurements in some areas where MODIS does not have. Given the differences in instrumental designs and retrieval algorithms, AOD measurements from the MISR and MODIS sensors were used in conjunction with one another to exploit their complementary strengths, especially for the middle and low latitudes (Kahn et al., 2009). In addition, AOD is changing quickly in space and time, measurements from one sensor in a short time-interval may not be enough to capture the functional features of the continuous AOD process. The complementary coverage makes the two AOD datasets suitable for data fusion.

However, there were several difficulties in merging AOD measurements from the MISR and MODIS sensors. We have discussed spatially nonstationarity and computational burden associated with large spatial data. In the real-data modeling experiments, we had both of the problems. In this part, we ran two experiments: one experiment was merging one-day AOD measurements derived from the two sensors (i.e. August 1, 2008), and the other experiment was merging eight-day AOD measurements derived from the two sensors (i.e. from July 28, 2008 to August 4, 2008). These data were selected randomly with no specific reasons. For the one-day AOD measurements, the numbers of pixels for MISR AOD and MODIS AOD measurements were 15,612 and 23,253, respectively. For the eight-day AOD measurements, the numbers of AOD measurements from the two sensors were 129,664 and 40,766, respectively. Most of the

AOD measurements from the two sensors were made between 70° N and 50° S, and between 180° W and 180° E. For the two real-data modeling experiments, MISR AOD and MODIS AOD were merged and downscaled to 0.25° × 0.25° for super-resolution mapping of global AOD distributions. Similar to the experiments on synthetic data, we also used two relationship matrices for the two AOD measurements with different spatial supports. The uniform distribution function was also used to calculate the relationship matrices in the GIM framework. We applied moving-window GIM to accommodate spatial nonstationarity and reduce computational burden associated with large spatial data. By pre-calculations and analyses, we set a local-window with the size of 2000-km for both parameter estimations and spatial predictions. Even for the areas with AOD measurements from both MODIS and MISR, merging them through the moving-window GIM approach can provide more accurate and robust predictions of the true AOD process. We also calculated prediction uncertainties for the two real-data experiments.

A.4 Results

A.4.1 Results of Synthetic Image Modeling

The three synthetic images were generated as realizations of Gaussian random fields, and the histograms of pixel values for the three images were normally distributed (Fig. A.2d-f). For the synthetic images generated by unconditional simulations, the image without the nugget effect and with a longer correlation length and a lower sill (Fig. A.2a) showed less spatial variability than the other image (Fig. A.2b). The synthetic image generated by FRK is shown in Fig. A.2c.

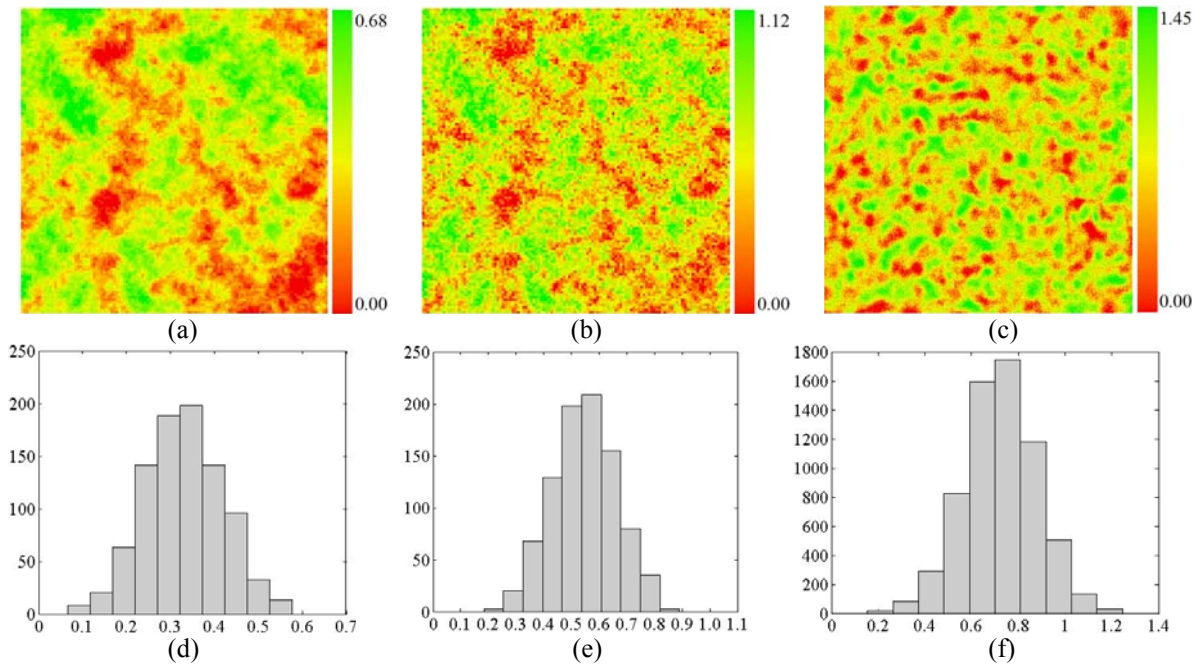

Fig. A.2 Synthetic images: (a) and (b) are the images without and with nugget effect, respectively. These two images were generated by unconditional simulations. (c) is the image with nugget effect, generated by FRK. (d), (e), and (f) are the histograms for the images (a), (b), and (c), respectively.

The modeling results of the five synthetic data modeling experiments are shown in Table A.1. The values of the RMSE index and the percentage index showed that the spatial predictions were all accurate and the prediction uncertainties were all correct. The values of the RMSE index for the five experiments were lower than 10% of the original measurements. Theoretically, for realizations of Gaussian random fields, 95% of the pixel values of the original images should fall within the two standard deviation bounds of the best spatial predictions. The prediction accuracies for the experiments using the images without the nugget effect (Experiments 1 and 2) were better than the results of the experiments using the images with the nugget effect (Experiments 3 and 4). The prediction accuracies for the experiments using fine-resolution aggregated images (Experiments 1 and 3) were better than the results of the experiments using coarse-resolution aggregated images (Experiments 2 and 4). The prediction accuracy for Experiment 5 was better than the results of the first four experiments, and the percentage index for this experiment was also higher than the results of the first four experiments. These may be caused by the fact that the synthetic image generated by FRK was smoother than the synthetic images generated by unconditional simulations.

Given space limitations, we only showed the figures of modeling results of Experiments 1, 3, and 5 (Fig. A.3). The spatial predictions showed more spatial details for the diagonal parts with fine-resolution aggregated data added in (Fig. A.3b, f, and j). The diagonal parts also had lower prediction uncertainties (Fig. A.3c, g, and k). These results were reasonable because all spatial predictions benefit from the presence of nearby measurements. Spatial predictions made in the densely measured regions should have lower errors than those made in the sparsely measured regions. The conditional simulations (Fig. A.3d, h, and l) looked more realistic as the original simulated data (Fig. A.2a, b, and c) and showed less smoothing effect than spatial predictions (Fig. A.3b, f, and j). From Fig. A.3k we can see that the values of prediction uncertainties (i.e. standard errors) varied across the domain. This demonstrated that moving-window GIM accommodated spatial nonstationarity of the synthetic image generated by FRK. This implied that using spatially stationary covariance functions for realizations of nonstationary random fields may introduce more prediction errors and generate incorrect prediction uncertainties.

Table A.1 Results of merging multi-resolution synthetic images.

Experiments with aggregated images	RMSE Index	Prediction uncertainty		Percentage index
		Lower_bound	Upper_bound	
Images with spatially stationary characteristics				
Images without the nugget effect				
Experiment 1: 15 × 15 and part of 60 × 60	0.0395	0.0237	0.0663	95.60%
Experiment 2: 15 × 15 and part of 30 × 30	0.0427	0.0305	0.0667	95.72%
Images with the nugget effect				
Experiment 3: 15 × 15 and part of 60 × 60	0.1008	0.0781	0.1361	95.61%
Experiment 4: 15 × 15 and part of 30 × 30	0.1074	0.0917	0.1369	95.65%
Images with spatially nonstationary characteristics				
Experiment 5: 160 × 160 and part of 80 × 80	0.0361	0.0209	0.0816	98.27%

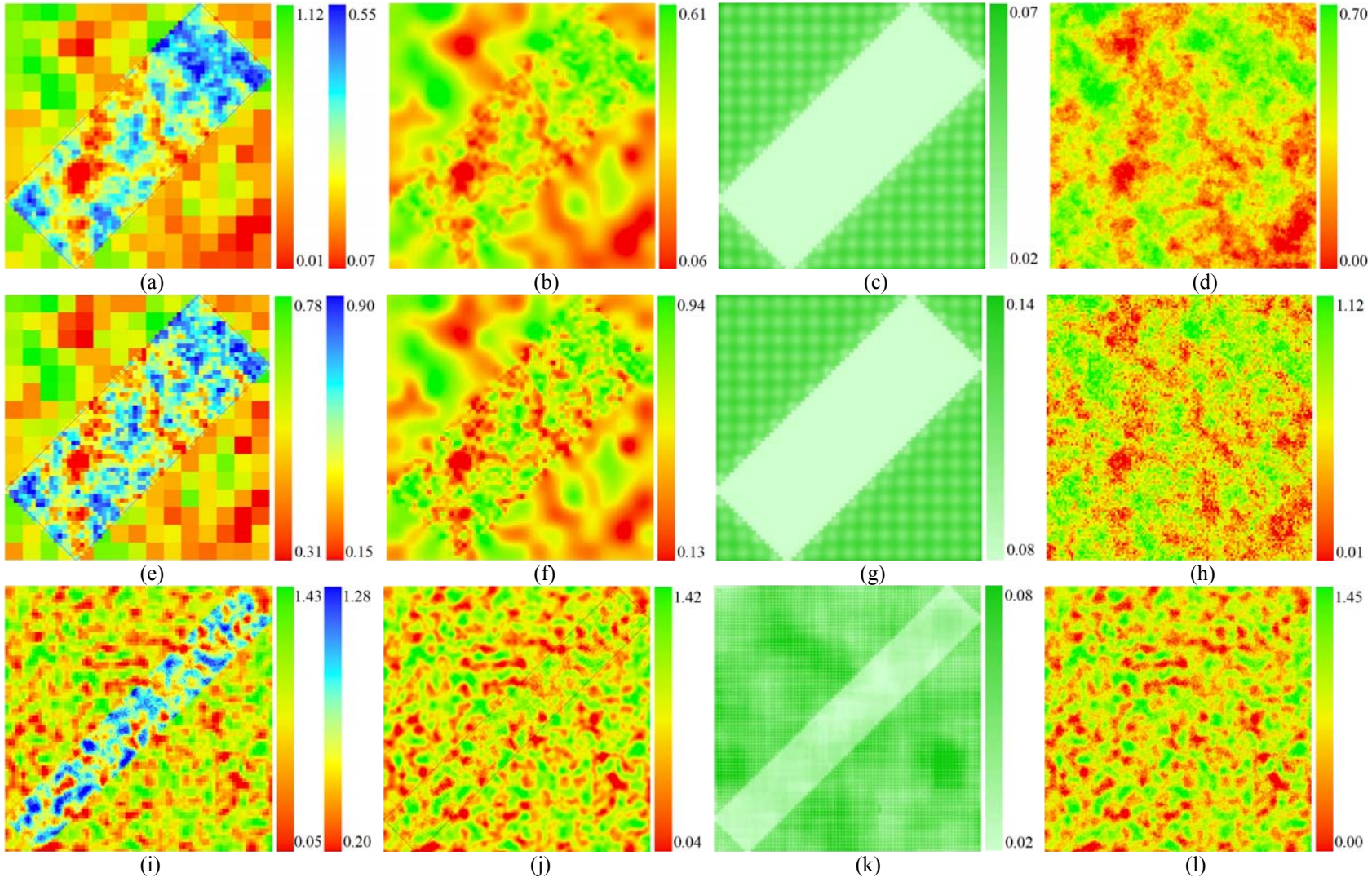
1.12
0.55
0.01
0.07
(a)
0.61
0.06
(b)
0.07
0.02
(c)
0.70
0.00
(d)
0.78
0.90
0.31
0.15
(e)
0.94
0.13
(f)
0.14
0.08
(g)
1.12
0.01
(h)
1.43
1.28
0.05
0.20
(i)
1.42
0.04
(j)
0.08
0.02
(k)
1.45
0.00
(l)

Fig. A.3 Results of merging synthetic images with variable resolutions: (a), (e), and (i) are the overlays of synthetic images with different resolutions for Experiments 1, 3, and 5, respectively; (b), (f), (j) are the spatial predictions with data from (a), (e), and (i), respectively; (c), (g),and (k) are the prediction uncertainties for (b), (f), and (j), respectively; and (d), (h), (l) are the conditional simulations for (b), (f), and (j), respectively.

A.4.2 Super-Resolution Mapping of Global AOD Distributions

From the one-day AOD measurements derived from the MISR and MODIS sensors (Fig. A.4a and c), we can see that MODIS had more complete spatial coverage than MISR did. MODIS AOD was missing in some of the low and middle latitudes (Fig. A.4a). MISR had measurements in those regions, but the field of view of MISR was narrow (Fig. A.4c). The eight-day MODIS AOD measurements had more complete coverage than the one-day MODIS AOD measurements. However, there were still gaps in the low and middle latitudes (i.e. North Africa and Middle East) (Fig. A.4b). The eight-day MISR AOD measurements had much better coverage than the one-day AOD measurements, but they still did not cover the whole globe (Fig. A.4d). Visually, the data gaps of the eight-day MODIS AOD can be mostly covered by the eight-day MISR AOD. Merging the two datasets can produce a more complete picture of global AOD distributions.

By comparing the spatial predictions using the one-day and eight-day AOD measurements (Fig. A.4e and f), we can find that although the general patterns of the two images were similar, there were still apparent differences between the two figures, especially in North Eurasia and North America. This indicated that aerosol concentrations were shifting quickly over space and time. Therefore, mapping AOD distributions over short time-intervals may be important. Studies showed that the high concentrations of AOD were from different sources: high AOD values in North Africa and Middle East, Central Africa, and East Asia (e.g. China) and North America were mainly from dust, smoke, and pollution, respectively (Ichoku et al., 2004). The standard errors of spatial predictions showed that the errors of the experiment using the eight-day measurements (Fig. A.4g) were apparently lower than the errors of the experiment using the one-day measurements (Fig. A.4h). In addition, the prediction uncertainties in some of the low and middle latitudes with fewer measurements were much higher than the prediction uncertainties in the regions with dense measurements. These were reasonable because there were few measurements to constrain spatial predictions in the low and middle latitudes.

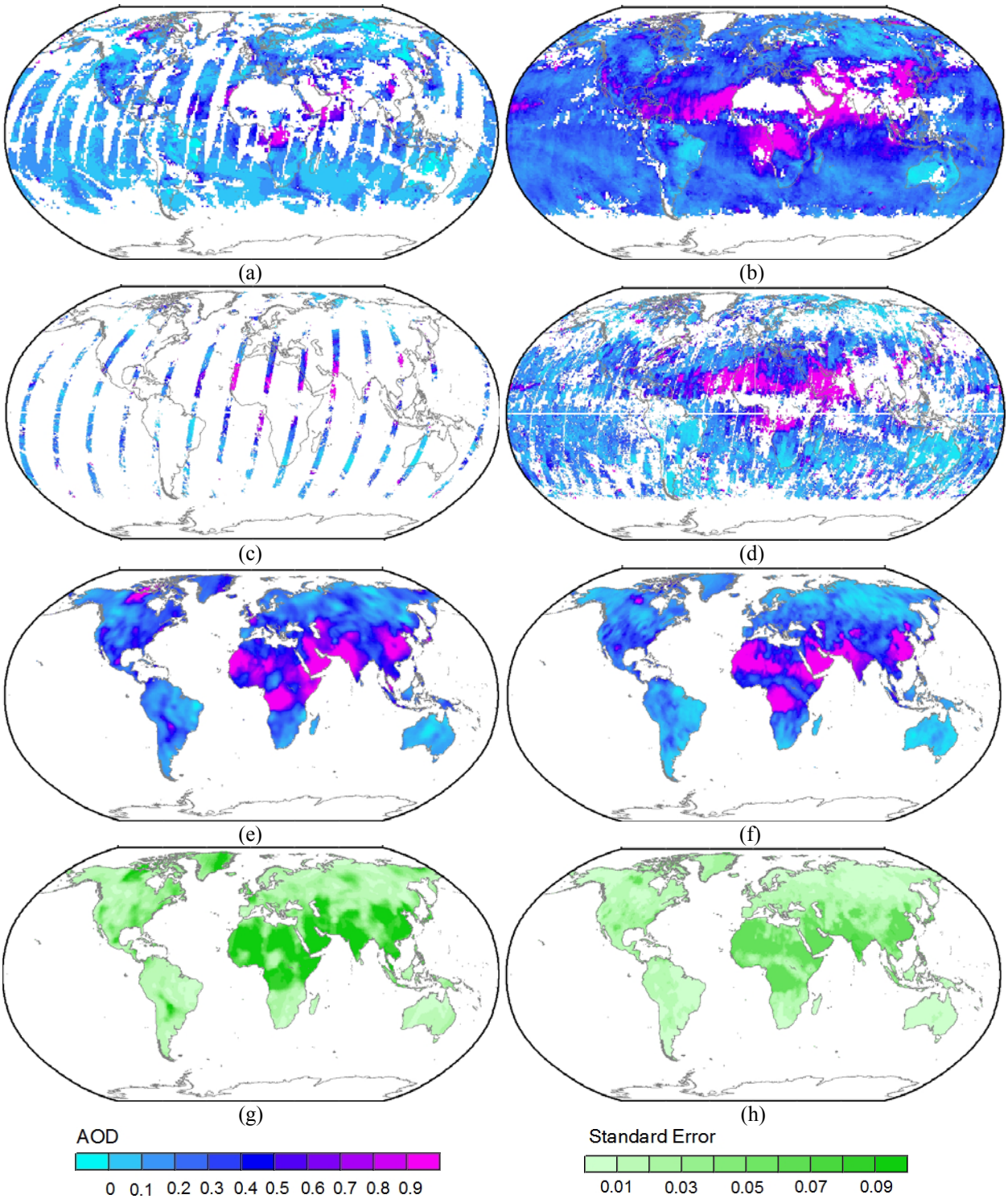

Fig. A.4 Results of multi-resolution real data fusion: (a) and (c) are the one-day measurements of AOD derived from the MODIS and MISR sensors , respectively; (b) and (d) are the eight-day measurements of AOD derived from the MODIS and MISR sensors, respectively; (e) is the spatial predictions with measurements from (a) and (c); (f) is the spatial predictions with measurements from (b) and (d); and (g) and (h) are the prediction uncertainties associated with (e) and (f), respectively. Only modeling results covering the continents are shown in the maps.

A.4.3. Moving-Window GIM versus Spatial Statistical Data Fusion

In order to gain insights into the relative performance and computational efficiency of moving-window GIM, we compared this approach with spatial statistical data fusion (SSDF; Nguyen et al., 2012). SSDF is a recently developed geostatistical approach for merging large spatial data with variable resolutions. SSDF was developed based on FRK, and it uses a data dimension reduction approach to improve computational efficiency. For this experiment, we selected subsets of the eight-day AOD measurements from the MISR and MODIS sensors within the latitudes 20°N – 60°N and the longitudes 70°E – 120°E. The numbers of pixels for AOD measurements from the MISR and MODIS sensors within the subsets were 4412 and 1477, respectively. We randomly selected 10% of the AOD measurements and treated them as testing data. The remaining 90% of the data were used for spatial predictions. In this experiment, the spatial predictions were made at the resolution of 0.25° × 0.25°. For SSDF, the number of bi-square basis functions used was 340 (i.e. the resolution number was four). The spatial predictions were averaged back to the resolutions of AOD measurements for cross-validations. The values of RMSE for moving-window GIM and SSDF were 0.3519 and 0.8106, respectively. However, SSDF was more computationally efficient than moving-window GIM. For this experiment, SSDF took about 117 seconds on a 2.8 GHz machine with an Intel Core Processor, and moving-window GIM took about 6 minutes on a 16-processor work station (i.e. the computing process was parallelized). These were reasonable because SSDF eliminates some components of spatial variability to improve computational efficiency.

A.5 Discussion and Conclusion

We have demonstrated GIM and moving-window GIM for image downscaling and multi-resolution data fusion on synthetic and real images. There were several limitations in the above experiments. First, we did not deal with measurement errors of remote sensing images. For the experiments on synthetic and real images, we treated the nugget effect as the fine-scale variability of images, and we built geostatistical models to model it. However, real remote sensing images are always contaminated with measurement errors. Future work needs to examine the influence of measurement errors. Fortunately, GIM can account for measurement

errors by the model-data mismatch matrix (i.e. the R matrix in the GIM framework). Second, we applied the Gaussian random field model for both synthetic and real images. In some cases, measurements may have non-Gaussian characteristics. In those occasions we need to extend the geostatistical inverse model to accommodate non-Gaussian spatial data by using a set of models known as generalized linear mixed models. The actual probability distributions of measurements need to be explored in order to define the link function of generalized linear mixed models. Third, we did not use auxiliary information for spatial predictions, although GIM can include auxiliary variables (i.e. the spatial trend part of the GIM framework) to improve prediction accuracies. Other studies showed that including auxiliary variables in the GIM framework can improve prediction accuracy (Gourdji et al., 2008). However, adding inappropriate auxiliary information may bias the model. Usually, a statistical test of the contributions of auxiliary variables is needed (Gourdji et al., 2008).

We used REML for estimating covariance parameters related to the change-of-support problem. The estimated covariance parameters are always associated with errors, and these errors can consequently propagate to spatial predictions. Therefore, analyzing error propagations is very important for understanding the accuracy of spatial predictions. By running modeling experiments, we found that the errors associated with the estimated covariance parameters increased with increases in the resolution gap between measurements and spatial predictions. More in-depth analyses about error propagations in spatial predictions using GIM are still needed. Moreover, we only applied GIM for merging coarse-resolution satellite images. However, when applying GIM on fine-resolution images with tens or hundreds of millions of pixels, computations will still be a problem. This is similar to many other geostatistical models for dealing with large spatial data. We developed a moving-window GIM approach to reduce computational burden associated with large spatial data. When parallelizing the computations of moving-windows, spatial predictions can be made very fast. Besides parallel computing, low-rank representations (Wikle, 2010) and covariance tapering (Fuentes and Smith, 2001) are also possible solutions to the problem of computational burden. Furthermore, although we used the uniform distribution function to simulate the relationships between coarse-resolution measurements and fine-resolution predictions, real point spread functions (e.g. two-dimensional Gaussian distribution) of sensors can be used to calculate the relationship matrix (i.e. the H

matrix in the GIM framework). Finally, we only applied GIM for image downscaling. GIM can also be used for image up-scaling with one or more measurements, if we set-up a coarse prediction grid and define the relationship matrix between fine-resolution measurements and coarse-resolution predictions.

We have presented an introduction of the GIM methodology for merging coarse-resolution images with variable resolutions and for super-resolution mapping of continuous spatial processes. The results of synthetic data modeling experiments showed that GIM and moving-window GIM can produce accurate spatial predictions and correct prediction uncertainties. The results of real data modeling experiments showed that moving-window GIM can be used for merging complementary MISR AOD and MODIS AOD data and for super-resolution mapping of global AOD distributions. To the best of our knowledge, this is the first introduction of the moving-window GIM approach for solving the scale and data fusion related problems in remote sensing.

Acknowledgements

The work was conducted with financial support from NASA Land-Cover and Land-Use Change Program (NNX09AK87G). The authors would like to thank the science teams for producing and sharing the products of MODIS AOD and MISR AOD. The authors also would like to thank Dr. Hai Nguyen from Jet Propulsion Laboratory, California Institute of Technology, and Dr. Emily Kang from University of Cincinnati for providing the sample codes related to fixed rank kriging and spatial statistical data fusion.

References

ACBIMAR (Annual Census Book of Inner Mongolia Autonomous Region). (2005, 2010). Hohhot, Inner Mongolia, China.

ACBM (Annual Census Book of Mongolia). (1990, 2010). Ulaanbaatar, Mongolia.

Adam, E., and Mutanga, O. (2009). Spectral discrimination of papyrus vegetation (Cyperus papyrus L.) in swamp wetlands using field spectrometry. *ISPRS Journal of Photogrammetry and Remote Sensing*, 64: 612−620.

Addison, J., Friedel, M., Brown, C., Davies, J., and Waldon, S. (2012). A critical review of degradation assumptions applied to Mongolia's Gobi Desert. *The Rangeland Journal*, 34: 125–137.

Adger, W. N. (2000). Institutional adaptation to environmental risk under the transition in Vienam. *Annals of the Association of American Geographers*, 90: 738–758.

Adger, W. N. (2006). Vulnerability. *Global Environmental Change*, 16: 268–281.

Adger, W. N., Arnell, N. W., and Tomplins, E. L. (2005). Successful adaptation to climate change across scales. *Global Environmental Change*, 15: 77–86.

Agrawal, A. (2001). Common property institutions and sustainable governance of resources. *World Development*, 29: 1649–1672.

Agrawal, A. (2009). Climate adaptation, local institutions, and rural livelihoods. In: *Adapting to Climate Change: Thresholds, Values, Governance*. Edited by Adger, W. N., Lorenzoni, I., and O'Brien, K. L. Cambridge University Press, New York, USA.

Agrawal, A. (2010). The role of local institutions in adaptation to climate change. In: *Social Dimensions of Climate Change: Equity and Vulnerability in a Warming World*. Edited by Mearns, R., and Norton, A. World Bank, Washington, DC, USA.

Anderies, J. M., Janssen, M. A., and Ostrom E. (2004). A framework to analyze the robustness of social-ecological systems from an institutional perspective. *Ecology and Society*, 9: 18.

Angerer, B. J., Han, G., Fujisaki, I., and Havstad, K. (2008). Climate change and ecosystems of Asia with emphasis on Inner Mongolia and Mongolia. *Rangelands*, 6: 46–51.

Asner, G. P., Elmore, A. J., Olander, L. P., Martin, R. E., and Harris, A. T. (2004). Grazing systems, ecosystem responses, and global change. *Annual Review of Environment and Resources*, 29: 261−299.

Atkinson, P. M., Pardo-Iguzquiza, E., and Chico-Olmo, M. (2008). Downscaling cokriging for super-resolution mapping of reflectance. *IEEE Transactions on Geoscience and Remote Sensing*, 46: 573−580.

Axerold, R. (1997). *The complexity of cooperation: Agent-based models of competition and collaboration*. Princeton University Press. Princeton, USA.

Bai, Y., Wu, J., Xing, Q., Pan, Q, Huang, J., Yang, D., and Han, X. (2008). Primary production and rain use efficiency across a precipitation gradient on the Mongolian plateau. *Ecology*, 89: 2140–2153.

Banks, T. (2001). Property rights and the environment in pastoral China: evidence from the field. *Development and Change*, 32: 717–740.

Banks, T. (2003). Property rights reform in rangeland China: dilemmas on the road to the household ranch. *World Development*, 31: 2129–2142.

Banks, T., Richard, C., Ping, L., and Yan, Z. (2003). Community-based grassland management in western China. *Mountain Research and Development*, 23: 132–140.

Bell, A. (2011). Environmental licensing and land aggregation: an agent-based approach to understanding ranching and land use in rural Rondõnia. *Ecology and Society,* 16: 31.

Benjamini, Y., and Hochber, Y. (1995). Controlling the false discovery rate: a practical and powerful approach to multiple testing. *Journal of the Royal Statistical Society: Series B*, 57: 289–300.

Berterretche, M., Hudak, A. T., Cohen, W. B., Maiersperger, T. K., Gower, S. T., and Dungan, J. (2005). Comparison of regression and geostatistical methods for mapping Leaf Area Index (LAI) with Landsat ETM+ data over a boreal forest. *Remote Sensing of Environment*, 96: 49–61.

Bijoor, N., Li, W., Zhang, Q., and Huang, G. (2006). Small-scale co-management for the sustainable use of Xilingol Biosphere reserve, Inner Mongolia. *Ambio*, 35: 25–29.

Blackburn, G. A. (1998). Quantifying chlorophylls and caroteniods at leaf and canopy scales: An evaluation of some hyperspectral approaches. *Remote Sensing of Environment*, 66: 273−285.

Bogaert, P., and Russo, D. (1999). Optimal spatial sampling design for the estimation of variogram based on a least squares approach. *Water Resources Research*, 35: 1275−1289.

Bonham-Carter, G. F. (1988). Numerical procedures and computer program for fitting an inverted Gaussian model to vegetation reflectance data. *Computers and Geoscience*, 14: 339−356.

Boyd, R., Gintis, H., and Bowles, S. (2010). Coordinated punishment of defectors sustains cooperation and can proliferate when rare. *Science,* 328: 617−620.

Braverman, A. (2008). Data fusion. In *Encyclopedia of quantitative risk analysis and assessment*. Edited by Melnick, E. L., and Everitt, B. S. pp. 125−139. John Wiley & Sons, Inc. New York, USA.

Braverman, A., Nguyen, H., and Cressie, N. (2011). Space-time data fusion for remote sensing applications. Working paper. California Institute of Technology, CA.

Bravo, G. 2011. Agent beliefs and the evolution of institutions for common-pool resource management. *Rationality and society,* 23: 117−152.

Briske, D. D., Fuhlendorf, S. D., and Smeins, F. E. (2003). Vegetation dynamics on rangelands: a critique of the current paradigms. *Journal of Applied Ecology*, 40: 604–614.

Brogaard, S., Runnstrom, M., and Seaquist, J. (2005). Primary production of Inner Mongolia, China, between 1982 and 1999 estimated by a satellite data-driven light use efficiency model. *Global and Planetary Change*, 45: 313–332.

Broge, N. H., and Leblane, E. (2000). Comparing prediction power and stability of broadband and hyperspectral vegetation indices for estimation of green leaf area index and canopy chlorophyll density. *Remote Sensing of Environment*, 76: 156−172.

Brown, D. G., Robinson, D. T., An, L., Nassauer, J. I., Zellner, M., Rand, W., Riolo, R., Page, S. E., Low, B., and Wang, Z. (2008). Exurbia from the bottom-up: Confronting empirical challenges to characterizing a complex system. *Geoforum*, 39: 805−818.

Brown, D. G., Walker, R., Manson, S., and Seto, K. C. (2004). Modeling land cover and land use change. In: *Land Change Science: Observing, Monitoring, and Understanding Trajectories of Change on the Earth's Surface*. Edited by Gutman, G.. Janetos, A. C., Justice, C. O., Moran, E. F., Mustard, J. F., Rindfuss, R. R., Skole, D., Turner II, B. L., and Cocharne, M. A. pp. 395–409. Kluwer Academic Publishers. Norwell, USA.

Brown, M. E., Pinzón, J. E., Didan, K., Morisette, J. T., and Tucker, C. J. (2006). Evaluation of the consistency of long-term NDVI time-series derived from AVHRR, SPOT-Vegetation, SeaWiFS, MODIS, and Landsat ETM+ sensors. *IEEE Transactions on Geoscience and Remote Sensing*, 44: 1787–1793.

Brown, J. R., and Thorpe, J. (2008). Climate change and rangelands: responding rationality to uncertainty. *Rangelands*, 6: 3–6.

Burnicki, A. C. (2008). *Spatial and temporal patterns of errors in land cover change analyses: identifying and propagating uncertainty for ecological monitoring and modeling*. Ph.D. Dissertation. University of Michigan, Ann Arbor.

Chatterjee, A., Michalak, A. M., Kahn, R. A., Paradis, S. R., Braveman, A. J., and Miller, C. E. (2010). A geostatistical data fusion technique for merging remote sensing and ground-based observations of aerosol optical thickness. *Journal of Geophysical Research*, 115, D20207, doi: 10.1029/2009JD013765.

Chilès, J., and Delfiner, P. (2012). *Geostatistics: modeling spatial uncertainty*. John Wiley & Sons, Inc. Hoboken, USA.

Cho, M. A. (2007). *Hyperspectral remote sensing of biochemical and biophysical parameters: The derivative red-edge "double-peak feature", a nuisance or an opportunity*? Ph.D. Dissertation. Wageningen University, The Netherlands.

Cho, M. A., and Skidmore, A. K. (2006). A new technique for extracting the red-edge position from hyperspectral data: the linear interpolation method. *Remote Sensing of Environment*, 101: 181−193.

Cho, M. A., Skidmore, A. K., Corsi, F., Van Wieren, S. E., and Sobhan, I. (2007). Estimation of green grass/herb biomass from airborne hyperspectral imagery using spectral indices and partial least squares regression. *International Journal of Applied Earth Observation and Geoinformation*, 9: 414−424.

Christensen, J. H., Hewitson, B., Bucuioc, A., et al. (2007). Regional climate projections. In: *Climate Change 2007: IPCC Report, Chapter 11*. pp. 847–887. Cambridge University Press. New York, USA.

CIMAR (Climate dataset of Inner Mongolia Autonomous Region) (196–2009). (2011). Monthly mean climate dataset of Inner Mongolia. Inner Mongolia Meteorology Bureau. Hohhot, Inner Mongolia, China.

CM (Climate dataset of Mongolia) (1961–2009). (2011). Monthly mean climate dataset of Mongolia. Mongolia Meteorology Bureau. Ulaanbaatar, Mongolia.

Cressie, N. (1985). Fitting variogram models by weighted least squares. *Mathematical Geology*, 17: 563−586.

Cressie, N., and Johannesson, G. (2008). Fixed rank kriging for very large spatial data sets. *Journal of Royal Statistical Society B*, 70: 209–266.

Cressie, N., Shi, T., and Kang, E. (2010). Fixed rank filtering for spatial-temporal data. *Journal of Computational and Graphical Statistics*, 19: 724–745.

Curran, P. J., and Atkinson, P. M. (1999). Issues of scale and optimal pixel size. In: *Spatial Statistics for Remote Sensing*, Springer Press. Enschede. The Netherlands.

Darvishzadeh, R. (2008). *Hyperspectral remote sensing of vegetation parameters using statistical and physical models*. Ph.D. Dissertation. Wageningen University, The Netherlands.

Darvishzadeh, R., Skidmore, A., Schlerf, M., and Atzberger, C. (2008). Inversion of a radiative transfer model for estimating vegetation LAI and chlorophyll in a heterogeneous grassland. *Remote Sensing of Environment*, 112: 2592−2604.

Dawson, T. P., and Curran, P. J. (1998). A new technique for interpolating the reflectance red-edge position. *International Journal of Remote Sensing*, 19: 2133−2139.

Deadman, P., Schlager, E., and Gimblett, R. (2000). Simulating common pool resource management experiments with adaptive agents employing alternate communication routines. *Journal of Artificial Societies and Social Simulation*, 3: 2.

D'Hondt, O., López-Martínez, C., Ferro-Famil, L., and Pottier, E. (2007). Spatially nonstationary anisotropic texture analysis in SAR images. *IEEE Transactions on Geoscience and Remote Sensing*, 45: 3905–3918.

Diggle, P., and Ribeiro Jr., P. J. (2007). *Model-based geostatistics*. Springer Press. New York, USA.

Ding, X., and Chen T. (2008). The annual variation characteristics of temperature and precipitation in Inner Mongolia in recent 50 years. *Inner Mongolia Meteorology*, 2: 17–19.

Dungan, J. (1998). Spatial prediction of vegetation quantities using ground and image data. *International Journal of Remote Sensing*, 19: 267–285.

Eakin, H. (2005). Institutional change, climate risk, and rural vulnerability: cases from central Mexico. *World Development*, 33: 1923–1938.

Elhorst, J. P. (2003). Specification and estimation of spatial panel data models. *International Regional Science Review*, 26: 244–268.

Elhorst, J. P. (2010a). Spatial panel data models. In: *Handbook of applied spatial analysis*. Edited by Fisher, M. M., and Getis, A. pp. 377–407. Springer Press. New York, USA.

Elhorst, J. P. (2010b). MATLAB software for spatial panels. Presented at the IVth world conference of the spatial econometrics association (SEA), Chicago, USA.

Ellis, J., and Swift, D. (1988). Stability of African pastoral ecosystems: Alternate paradigms and implications for development. *Journal of Range Management*, 41: 450–459.

Epstein, J. (2007). *Generative social science: studies in agent-based computational modeling*. Princeton University Press. Princeton, USA.

Epstein, J., and Axtell, R. (1997). *Growing artificial societies: social science from the bottom up*. Brookings Institute Press. Washington, DC, USA.

Erdenetuya, D. (2006). Assessment of pasture land condition by NDVI. In: *Proceedings of 'theoretical and practical conference on issues and challenges of pasture management'*, Ulaanbaatar, Mongolia.

Erickson, T., and Michalak, A. M. (2006). Merging of variable-resolution imagery using geostatistics and sensor PSFs. In: *Proceedings of ASPRS Annual Conference*, Reno, USA.

Fang, J., Piao, S., Field, C., Pan, Y., Guo, Q., Zhou, L., Peng, C., and Tao, S. (2003). Increasing net primary production in China from 1982 to 1999. *Frontiers in Ecology and Environment*, 1: 293–297.

FAO (Food and Agriculture Organization). Price statistics database (FAOSTAT, PriceSTAT). (Accessed October 20, 2011, http://faostat.fao.org/site/570/default.aspx#ancor).

Fernandez-Gimenez, M. (1997). *Landscapes, livestock, and livelihoods: social, ecological, and land-use change among the nomadic pastoralists of Mongolia*. Ph.D. Dissertation. University of California, Berkeley.

Fernandez-Gimenez, M., and Allen-Diaz, B. (1999). Testing a non-equilibrium model of rangeland vegetation dynamics in Mongolia. *Journal of Applied Ecology*, 36: 871–885.

Fernandez-Gimenez, M. (2000). The role of Mongolian nomadic pastoralists' ecological knowledge in rangeland management. *Ecological Applications*, 10: 1318–1326.

Fernandez-Gimenez, M., Batkhishig, B., and Barbuyan, B. (2012). Cross-boundary and cross-level dynamics increase vulnerability to severe disasters (dzud) in Mongolia. *Global Environmental Change*, 22: 836–851.

Frees, E. W. (2004). *Longitudinal and panel data: analysis and applications in the social sciences*. Cambridge University Press. New York, USA.

Fuentes, M., and Smith, R. L. (2001). A new class of nonstationary spatial models. *Technical Report*, North Carolina State University, Institute of Statistics Mimeo Series #2534, Raleigh, USA.

Gao, B. (2000). A practical method for simulating AVHRR-consistent NDVI data series using narrow MODIS channels in the 0.5–1.0 μm spectral range. *IEEE Transactions on Geoscience and Remote Sensing*, 38: 1969–1975.

Gao, J., Chen, Y., Lu, S., Feng, C., Chang, X., Ye, S., and Liu, J. (2012). A ground spectral model for estimating biomass at peak of the growing season in Hulunbeier grassland, Inner Mongolia, China. *International Journal of Remote Sensing*, 33: 4029−4043.

Gao, X., Huete, A. R., Ni, W., and Miura, T. (2000). Optical-biophysical relationships of vegetation spectra without background contamination. *Remote Sensing of Environment*, 74: 609−620.

Gelman, A., and Hill, J. (2007). *Data analysis using regression and multilevel/hierarchical models*. Cambridge University Press. New York, USA.

Geotz, S. J., Prince, S. D., Goward, S. N., Thawley, M. M., and Small, J. (1999). Satellite remote sensing of primary production: an improved production efficiency modeling approach. *Ecological Modelling*, 122: 239–255.

Gong, P., Pu, R., and Yu, B. (2001). Conifer species recognition: effects of data transformation. *International Journal of Remote Sensing*, 22: 3471−3481.

Goovaerts, P. (2008). Kriging and semivariogram deconvolution in the presence of irregular geographical units. *Mathematical Geology*, 40: 101–128.

Gotway, C. A., and Young, L. J. (2002). Combing incompatible spatial data. *Journal of American Statistical Association*, 97: 632–648.

Gotway, C. A., and Young, L. J. (2005). Change of support: an interdisciplinary challenge. In: *Geostatistics for environmental applications*. Springer Press. Enschede, The Netherlands:

Gourdji, S. M., Hirsch, A. I., Mueller, K. L., Yadav, V., Andrews, A. E., and Michalak, A. M. (2010). Regional-scale geostatistical inverse modeling of North American CO_2 fluxes: a synthetic study. *Atmospheric Chemistry and Physics*, 10: 6151–6171.

Gourdji, S. M., Mueller, K. L., Schaefer, K., and Michalak, A. M. (2008). Global monthly averaged CO_2 fluxes recovered using a geostatistical inverse modeling approach: 2. Results including auxiliary environmental data. *Journal of Geophysical Research*, 113: D21115, doi: 10.1029/2007/JD009733.

Guan, Q., Kyriakidis, P. C., and Goodchild, M. F. (2011). A parallel computing approach to fast geostatistical areal interpolation. *International Journal of Geographical Information Science*, 25(8), 1241–1267.

Hall, D. L. (2004). *Mathematical techniques in multisensor data fusion*. Artech House Inc. Norwood, USA.

Hammerling, D., Michalak, A. M., and Kawa, S. R. (2012). Mapping of CO_2 at high spatiotemporal resolution using satellite observations: Global distributions from OCO-2. *Journal of Geophysical Research*, 117: D06306, doi: 10.1029/2011JD017015.

Hansen, P. M., and Schjoerring, J. K. (2003). Reflectance measurements of canopy biomass and nitrogen status in wheat crops using normalized difference vegetation indices and partial least squares regression. *Remote Sensing of Environment*, 86: 542−553.

Hardin, G. (1968). The tragedy of commons. *Science*, 162: 1243–1248.

Hass, T. C. (1990). Lognormal and moving window methods of estimating acid deposition. *Journal of American Statistical Association*, 85: 950–963.

Heinsch, F. A., Reeves, M., Cotava, P., Kang, S., Milesi, C., Zhao, M., Glassy, J., Jolly, W. M., Lochman, R., Bowker, C. F., Kimball, J. S., Nemani, R. R., and Running, S. (2003). User's guide: GPP and NPP products NASA MODIS land algorithm. http://datamirror.csdb.cn/modis/resource/doc/MOD17_UsersGuide.pdf (last date accessed: 01/07/2012)

Heuvelink, G. B. M. (1998). *Error propagation in environmental modeling with GIS*. Taylor and Francis Inc. Bristol, USA.

Hicke, J. A., Asner, G. P., Randerson, J. T., Tucker, C., Los, S., Birdsey, R., Jenkins, J. C., Field, C., and Holland, E. (2002). Satellite-derived increase in net primary productivity across North America, 1982–1998. *Geophysics Research Letters*, 29: 10.1029/2001GL013578.

Higdon, D. M., Swall, J., and Kern, J. (1999). Non-stationary spatial modeling. In: *Bayesian Statistics 6*. Oxford University Press. Oxford, UK.

Ho, P. (2001). Rangeland degradation in north China revisited? A preliminary statistical analysis to validate non-equilibrium range ecology. *The Journal of Development Studies*, 37: 99–133.

Hsiao, C. (1986). *Analysis of panel data*. Cambridge University Press. New York, USA.

Huang, C., Townshend, J. R. G., Liang, S., Kalluri, S. N. V., and DeFries, R. S. (2002). Impact of sensor's spread function on land cover characterization: assessment and deconvolution. *Remote Sensing of Environment*, 80: 203–212.

Huete, A. R. (1988). A soil-adjusted vegetation index (SAVI). *Remote Sensing of Environment*, 25: 295−309.

Humphrey, C., and Sneath, D. (1999). *The end of nomadism? Society, state and the environment in Inner Asia*. Duke University Press, Durham, USA.

Hurcom, S. J., and Harrison, A. R. (1998). The NDVI and spectral decomposition for semiarid vegetation abundance estimation. *International Journal of Remote Sensing*, 19: 3109−3125.

IMIGSD (Inner Mongolian Institute of Grassland Survey and Design). (2008). *Statistics of the areas of reclaimed grasslands in Inner Mongolia, China*. Hohhot, Inner Mongolia, China.

IMIGSD (Inner Mongolian Institute of Grassland Survey and Design). (2011). *Statistics of grassland quality change in Inner Mongolia, China*. Hohhot, Inner Mongolia, China.

Ichoku, C., Kaufman, Y. J., Remer, L. A., and Levy, R. (2004). Global aerosol remote sensing from MODIS. *Advances in Space Research*, 34: 820–827.

IOB (Institute of Botany), Mongolia. (2011). *Statistics of grassland quality in Mongolia*. Ulaanbaatar, Mongolia.

Jacquemound, S., Bacour, C., Poilve, H., and Frangi, J. P. (2000). Comparisons of four radiative transfer models to simulate plant canopies reflectance: direct and inverse model. *Remote Sensing of Environment*, 74: 471−481.

Jacquemoud, S., Verhoef, W., Baret, F., Bacour, C., Zarco-Tejada, P. J., Asner, G. P., Francois, C., and Ustin, S. L. (2009). POSPECT + SAIL models: a review of use for vegetation characteristics. *Remote Sensing of Environment*, 113: s56−s66.

Janssen, M., and Ostrom, E. (2006a). Adoption of a new regulation for the governance of common-pool resources by a heterogeneous population. In: *Inequality, cooperation and environmental sustainability*. Edited by Baland J-M, Bardhan P and Bowles S. pp. 60−96. Princeton University Press. Princeton, USA.

Janssen, M., and Ostrom, E. (2006b). Empirically based, agent-based models. *Ecology and Society,* 11: 37.

Ji, L., Gallo, K., Eidenshink, J. C., and Dwyer, J. (2008). Agreement evaluation of AVHRR and MODIS 16-day composite NDVI data sets. *International Journal of Remote Sensing*, 29: 4839–4861.

Jiang, H. (2005). Grassland management and views of natures in China since 1949: regional policies and local changes in Uxin Ju, Inner Mongolia. *Geoforum*, 36: 641–653.

Jiang, G., Han, X., and Wu, J. (2006). Restoration and management of the Inner Mongolia grassland require a sustainable strategy. *Ambio*, 35: 269–270.

John, R., Chen, J., Lu, N., and Wilske, B. (2009), Land Cover /land use change and their ecological consequences. *Environmental Research Letters*, 4: 045010. doi: 10.1088/1748-9326/4/4/045010

Jordan, C. F. (1969). Derivation of leaf-area index from quality of light on the forest floor. *Ecology*, 50: 663–669.

Jupp, D. L. B., Strahler, A. H., and Woodcock, C. E. (1988). Autocorrelation and regularization in digital images I. basic theory. *IEEE Transactions on Geoscience and Remote Sensing*, 26: 463–473.

Kahn, R. A., Nelson, D. L., Garay, M. J., Levy, R. C., Bull, M. A., Diner, D. J., Martonchik, J. V., Paradise, S. R., Hansen, E. G., and Remer, L. A. (2009). MISR aerosol product attributes and statistical comparisons with MODIS. *IEEE Transactions on Geoscience and Remote Sensing*, 47: 4095–4114.

Kang, E., Cressie, N., and Shi, T. (2010). Using temporal variability to improve spatial mapping with application to satellite data. *Canadian Journal of Statistics*, 38: 271–289.

Kitanidis, P. K. (1995). Quasi-linear geostatistical theory for inversing. *Water Resources Research,* 31: 2411–2419.

Kniveton, D., Smith, C., Wood, S. (2011). Agent-based model simulations of future changes in migration flows for Burkina Faso. *Global Environmental Change*, 21s: s34−s40.

Knyazikhin, Y., Glassy, J., Privette, J. L., Tian, Y., Lotsch, A., Zhang, Y., Wang, Y., Morisette, J. T., Votava, P., Myneni, R. B., Nemani, R. R., and Running, S. W. (1999). MODIS leaf area index (LAI) and fraction of photosynthetically action radiation absorbed by

vegetation (FPAR) product (MOD15) algorithm theoretical basis document. http://modis.gsfc.nasa.gov/data/atbd/atbd_mod15.pdf (last date accessed: 01/07/2012)

Kyriakidis, P. C. (2004). A geostatistical framework for area-to-point spatial interpolation. *Geographic Analysis*, 36: 259–289.

Kyriakidis, P. C., and Yoo, E. (2005). Geostatistical prediction and simulation of point values from areal data. *Geographic Analysis*, 37: 124–151.

Le Ravalec, M., Noetinger, B., and Hu, L. (2000). The FFT moving average (FFT-MA) generator: an efficient numerical method for generating and conditioning Gaussian simulations. *Mathematical Geology*, 32: 701–723.

Lee, L., and Yu, J. (2010). A spatial dynamic panel data model with both time and individual fixed effects. *Econometric Theory*, 26: 564–597.

Lemos, M. C., and Agrawal, A. (2006). Environmental governance. *Annual Review of Environment and Resources*, 31: 297–235.

Lemos, M. C., Boyd, E., Tompkins, E. L., Osbahr, H., and Liverman, D. (2007). Developing adaptation and adapting development. *Ecology and Society*, 12: 26.

Li, W., Ali, S., and Zhang, Q. (2007). Property rights and grassland degradation: A study of the Xilingol Pasture, Inner Mongolia, China. *Journal of Environmental Management*, 85: 461–470.

Li, W., and Huntsinger, L. (2011). China's grassland contract policy and its impacts on herder ability to benefit in Inner Mongolia: Tragic Feedbacks. *Ecology and Society*, 16: 1.

Li, W., and Li, Y. (2012). Managing rangeland as a complex system: how government interventions decouple social systems from ecological systems. *Ecology and Society*, 17: 9.

Liang, S. (2004). *Quantitative remote sensing of land surfaces*. John Wiley & Sons, Inc. Hoboken, USA.

Lieth, H., and Whittaker, R. H. (1975). *Primary productivity of the biosphere*. Springer Press, New York, USA.

Liu, J., Li, S., Ouyang, Z., Tam, C., and Chen, X. (2008). Ecological and socioeconomic effects of China's policies for ecosystem services. *Proceedings of the National Academy of Sciences USA*, 105: 9477–9482.

Lu, Y., Zhuang, Q., Zhou, G., Sirlin, A., Mellio, J., and Kicklighter, D. (2009). Possible decline of the carbon sink in the Mongolian plateau during the 21st century. *Environmental Research Letters*, doi: 10.1088/1748-9326/4/4/045023.

Ma, W., Liu, Z., Wang, Z., Wang, W., Liang, C., Tang, Y., He, J., and Fang, J. (2010). Climate change alters interannual variation of grassland aboveground productivity: evidence from a 22-year measurement series in the Inner Mongolia grassland. *Journal or Plant Research*, 123: 509–517.

Ma, W., Yang, Y., He, J., Zeng, H., and Fang, J. (2008). Above- and belowground biomass in relation to environmental factors in temperate grasslands, Inner Mongolia. *Science in China Series C: Life Sciences*, 51: 263–270.

Manson, S., and Evans, T. (2007). Agent-based modeling of deforestation in southern Yucatan, Mexico, and reforestation in the Midwest United States. *Proceedings of the National Academy of Science USA,* 104: 20678−20683.

Michalak, A. M., Bruhwiler, L., and Tans, P. P. (2004). A geostatistical approach to surface flux estimation of atmospheric trace gases. *Journal of Geophysical Research*, 109: D14109, doi: 10.1029/2003JD004422.

Miller, J., and Page, S. (2007). *Complex adaptive systems: An introduction to computational models of social life*. Princeton University Press. Princeton, USA.

Ministry of Agriculture, China. (2007). *National rangeland monitoring report 2006*. Beijing, China.

MNET (Ministry of Nature, Environment, and Tourism). (2009). *Mongolia's fourth national report on implementation of convention on biological diversity*. Government of Mongolia: Ulaanbaatar, Mongolia.

Mokany, K., Rasison, R. J., and Prokushkin, A. S. (2006). Critical analysis of root: shoot ratios in terrestrial biomes, *Global Change Ecology*, 12: 84–96.

Monteith, J. L. (1972). Solar radiation and productivity in tropical ecosystems. *Journal of Applied Ecology*, 9: 747–766.

Monteith, J. L. (1977). Climate and the efficiency of crop production in Britain. *Philosophical Transactions of the Royal Society of London Series B*, 281: 277–294.

Mutanga, O. (2004). *Hyperspectral remote sensing of tropical grass quality and quantity*. Ph.D. Dissertation. Wageningen University, The Netherlands.

Mwangi, E. (2007). *Socialeconomic change and land use in Africa: The transformation of property rights in Kenya's Maasailand*. Palgrave MacMillan. New York, USA.

NCRM (National Climate Risk Management): Strategy and Action Plan of Mongolia. (2009). Ulaanbaatar, Mongolia.

Nagle, N. N., Sweeney, S. H., and Kyriakidis, P. C. (2011). A geostatistical linear regression model for small area data. *Geographical Analysis*, 43, 38–60.

Neupert, R. (1999). Population, nomadic-pastoralism and the environment in the Mongolian plateau. *Population and Environment*, 20: 413–441.

Nguyen, H., Cressie, N., & Braverman, A. (2012). Spatial Statistical Data Fusion for Remote Sensing Applications. *Journal of the American Statistical Association*, 107(499), 1004–1018.

North, D. (1990). *Institutions, institutional change and economic performance*. Cambridge University Press. New York, USA.

North, M. J., Howe, T. R., Collier, N. T., and Vos, J. R. (2007). A declarative model assembly infrastructure for verification and validation. In: *Advancing Social Simulation: The First World Congress*. Edited by Takahashi, S., Sallach, D. L., and Rouchier, J. Springer, Heidelberg, FRG.

Nowak, M. (2006). Five rules for the evolution of cooperation. *Science,* 314: 1560−1563.

Oba, G., Stenseth, N. C., and Lusigi, W. J. (2000). New perspectives on sustainable grazing management in arid zones of Sub-Saharan Africa. *Bioscience*, 50: 35–51.

Ojima, D., and Chuluun, T. (2008). Policy changes in Mongolia: implications for land use and landscapes. In: *Fragmentation in semi-arid and arid landscapes: consequences for human and natural systems*. Edited by Galvin, K. A., Reid, R. S., Behnke, Jr., R. H., and Hobbs, N. T. pp: 179–193. Springer Press. Dordrecht, The Netherlands.

Olonbayar, M. (2010). *Livelihood study of herders in Mongolia. Mongolian society for range management*. Ulaanbaatar. Research Report.

Olson, M. (1965). *The logic of collective action: Public goods and the theory of groups*. Harvard University Press. Cambridge, USA.

Olson, M. (1982). *The rise and decline of nations: Economic growth, stagnation, and social rigidities*. Yale University Press. Newhaven, USA.

Ostrom, E. (1990). *Governing the commons: The evolution of institutions for collective action*. Cambridge University Press. New York, USA.

Ostrom, E. (2005). *Understanding institutional diversity*. Princeton University Press. Princeton, USA.

Ostrom, E. (2009). A general framework for analyzing sustainability of socio-ecological systems. *Science*, 325: 419–422.

Ostrom, E. (2010). Beyond markets and states: polycentric governance of complex economic systems. *American Economic Review*, 100: 641–672.

Ostrom, E., and Nagendra, H. (2006). Insights on linking forests, trees, and people from the air, on the ground, and in the laboratory. *Proceedings of National Academy of Sciences USA*, 103: 19224–19231.

Overmars, K. P., and Verburg, P. H. (2006). Multilevel modeling of land use from field to village level in the Philippines. *Agricultural Systems*, 89: 435–456.

Pan, Y., Birdsey, R. A., Fang, J., Houghton, R., Kauppi, P. E., Kurz, W. A., Phillips, O. L., Shvidenko, A., Lewis, S. L., Canadell, J. G., Ciais, P., Jackson, R. B., Pacala, S. W., McGuire, A. D., Piao, S., Rautiainen, A., Sitich, S., and Hayes, D. (2011). A large and persistent carbon sink in the world's forests. *Science*, 333: 988–993.

Piao, S., Fang, J., Ciais, P., Peylin, P., Huang, Y., Sitch, S., and Wang, T. (2009). The carbon balance of terrestrial ecosystems in China. *Nature*, 458: 1009–1014.

Pohl, C., and Van Genderen, J. L. (1998). Multisensor image fusion in remote sensing: concepts, methods, and applications. *International Journal of Remote Sensing*, 19: 823–854.

Potter, C. S., Klooster, S., and Brooks, V. (1999). Interannual variability in terrestrial net primary production: Exploration of trends and controls on regional to global scales. *Ecosystems*, 2: 36–48.

Prince, S. D., and Goward, S. N. (1995). Global primary production: a remote sensing approach. *Journal of Biogeography*, 22: 815–835.

Pu, R. (2012). Detecting and mapping invasive plant species by using hyperspectral data. In: *Hyperspectral remote sensing of vegetation*. Edited by Thenkabail, P. S., Lyon, J. G., and Huete, A. CRC Press. Taylor and Francis Group. pp. 447−465. Boca Raton, USA.

Pu, R., Gong, P., Biging, G. S., and Larrieu, M. R. (2003). Extraction of red-edge optical parameters from Hyperion data for estimation of forest leaf area index. *IEEE Transactions on Geoscience and Remote Sensing*, 41: 916−921.

Qi, J., Chehbouni, A., Huete, A. R., Kerr, Y. H., and Sorooshian, S. (1994). A modified soil adjusted vegetation index. *Remote Sensing of Environment*, 48: 119−126.

Quattrochi, D. A., and Goodchild, M. F. (1997). *Scale in Remote Sensing and GIS*. Lewis Publishers. Bocan Raton, USA.

Raudenbush, S., Bryk, A., and Congdon, K. (2012). HLM6. Hierarchical linear and non-linear modeling. SSI, Scientific Software International.

Ren, H., Zhou, G., and Zhang, X. (2011). Estimation of green aboveground biomass of desert steppe in Inner Mongolia based on red-edge reflectance curve area method. *Biosystem Engineering*, 109: 385−395.

Ribot, J. C., and Agrawal, A. (2006). Recentralizing while decentralizing: how national governments reappropriate forest resources. *World Development*, 34: 1864–1886.

Rouse, J. W., Hass, R. H., Schell, J. A., and Deering, D. W. (1974). Monitoring vegetation systems in the Great Plains with ERTS, third ERTS symposium. NASA SP-351, 1, 309351.

Running, S. W., Nemani, R., Glassy, J. M., and Thornton, P. E. (1999). MODIS daily photosynthesis (PSN) and annual net primary production (NPP) product (MOD17): Algorithm theoretical basis document.

Running, S. W., Nemani, R. R., Heinsch, F. A., Zhao, M., Reeves, M., and Hashimoto, H. (2004). A continuous satellite-derived measure of global terrestrial primary production. *Bioscience*, 54: 547–560.

Sales, M. H., Souza Jr., C. M., Kyriakidis, P. C., Roberts, D. A., and Vidal, E. (2007). Improving spatial distribution estimation of forest biomass with geostatistics: A case study for Rondônia, Brazil. *Ecological Modelling*, 205: 221–230.

Schlerf, M., Atzberger, C., and Hill, J. (2005). Remote sensing of forest biophysical variables using HyMap imaging spectrometer data. *Remote Sensing of Environment*, 95: 177−194.

Schmidt, K. S., and Skidmore, A. K. (2001). Exploring spectral discrimination of grass species in African rangelands. *International Journal of Remote Sensing*, 22: 3421−3434.

Seaquist, J. W., Olsson, L., and Ardö, J. (2003). A remote sensing-based primary production model for grassland biomes. *Ecological Modelling*, 169: 131–155.

Selige, T., Bohner, J., and Schmidhalter, U. (2006). High resolution topsoil mapping using hyperspectral image and field data in multivariate regression modeling procedures. *Geoderma*, 136: 235−244.

Seto, K. C., and Kaufmann, R. K. (2003). Modeling the drivers of urban land use change in the Pearl River Delta, China: integrating remote sensing with socioeconomic data. *Land Economics*, 79: 106–121.

Shen, M., Tang, Y., Klein, J., Zhang, P., Gu, S., Shimono, A., and Chen, J. (2008). Estimation of aboveground biomass using in situ hyperspectral measurements in five major grassland ecosystems on the Tibetan plateau. *Journal of Plant Ecology*, 1: 247−257.

Slayback, D. A., Pinzon, J. E., Los, S. O., and Tucker, C. J. (2003). Northern hemisphere photosynthesis trends 1982–1999. *Global Change Biology*, 9: 1–15.

Smit, B., and Wandel, J. (2006). Adaptation, adaptive capacity, and vulnerability. *Global Environmental Change*, 16: 282–292.

Sneath, D. (1998). State policy and pasture degradation in Inner Asia. *Science*, 281: 1147–1148.

Snodgrass, M. F., and Kitanidis, P. K. (1997). A geostatistical approach to contaminant source identification. *Water Resources Research*, 33: 537–546.

Tang, J., Chen, X., Zhao, M., and Su, B. (2008). Numerical simulations of regional climate change under IPCC A2 scenario in China. *Acta Meteorological Sinica*, 66: 13–25.

Tarnavsky, E., Garrigues, S., and Brown, M. E. (2008). Multiscale geostatistical analysis of AVHRR, SPOT-VGT, and MODIS global NDVI products. *Remote Sensing of Environment*, 112: 535–549.

Thenkabail, P. S., Enclona, E. A., Ashton, M. S., and Der Meer, B. V. (2004). Accuracy assessment of hyperspectral waveband performance for vegetation analysis applications. *Remote Sensing of Environment*, 91: 354−376.

Thenkabail, P. S., Smith, R. B., and De Pauw, E. (2000). Hyperspectral vegetation indices and their relationships with agricultural crop characteristics. *Remote Sensing of Environment*, 71: 158−182.

Titlyanova, A. A., Romanova, I. P., Kosykh, N. P., and Mironycheva-Tokareva, N. P. (1999). Pattern and process in above-ground and below-ground components of grassland ecosystems. *Journal of Vegetation Science*, 10: 307–320.

Todd, D., Hoffer, R. M., and Milchunas. (1998). Biomass estimation on grazed and ungrazed rangelands using spectral indices. *International Journal of Remote Sensing*, 19: 427−438.

Treitz, P. M., and Howarth, P. J. (1999). Hyperspectral remote sensing for estimating biophysical parameters of forest ecosystems. *Progress in Physical Geography*, 23: 359−390.

Tsai, F., and Philpot, W. (1998). Derivative analysis of hyperspectral data. *Remote Sensing of Environment*, 66: 41−51.

Tucker, C. J. (1977). Asymptotic nature of grass canopy spectral reflectance. *Applied Optics*, 16: 1151−1156.

Tucker, C. J., Slaback, D. A., Pinzon, J. E., Los, S. O., Myneni, R. B., and Taylor, M. G. (2001). Higher northern latitude normalized difference vegetation index and growing season trends from 1982 to 1999. *International Journal of Biometeorology*, 45: 184–190.

Turner, D., Gower, S. T., Cohen, W. B., Gregory, M., and Maiersperger, T. K. (2002). Effects of spatial variability in light use efficiency on satellite-based NPP monitoring. *Remote Sensing of Environment*, 80: 397–405.

Turner, D., Urbanski, S., Bremer, D., Wofsy, S. C., Meyers, T., Gower, S. T., and Gregory, M. (2003). A cross-biome comparison of daily light use efficiency for gross primary production. *Global Change Biology*, 9: 383–395.

Turner II, B. L., Kasperson, R. E., Matson, P. A., McCarthy, J. J., Corell, R. W., Christensen L., Eckley, N., Kasperson, J. X., Luers, A., Martello, M. L., Polsky, C., Pulsipher, A., and Schiller, A. (2003). A framework for vulnerability analysis in sustainability science. *Proceedings of National Academy of Sciences USA*, 100: 8074–8079.

Upton, C. (2009). "Custom" and contestation: land reform in post-socialist Mongolia. *World Development*, 37: 1400–1410.

Vernooy, R. (2011). How Mongolian herders are transforming nomadic pastoralism. *Solutions*, 2: 82−87.

Waldron, S., Brown, C., and Longworth, J. (2010). Grassland degradation and livelihoods in China's western pastoral region: A framework for understanding and refining China's recent policy responses. China. *Agricultural Economic Review*, 2: 298–318.

Walsh, S. J., McCleary, A. L., Mena, C. E., Shao, Y., Tuttle, J. P., González, A., and Atkinson, R. (2008). Quickbird and Hyperion data analysis of an invasive plant species in the Galapagos Islands of Ecuador: Implications for control and land use management. *Remote Sensing of Environment*, 112: 1927−1941.

Wehrden, H. V., Hanspach, J., Kaczensky, P., Fischer, J., and Wesche, K. (2012). Global assessment of the non-equilibrium concept in rangelands. *Ecological Applications*, 22: 393–399.

Wikle, C. K. (2010). Low-rank representation for spatial processes. In: *Handbook of Spatial Statistics*. CRC Press. Taylor and Francis Group. New York, USA.

Williams, D. (2002). *Beyond great walls: environment, identity, and development on the Chinese grasslands of Inner Mongolia*. Stanford University Press, Stanford, USA.

Wilson, P. N., and Thompson, G. D. (1993). Common property and uncertainty: compensating coalitions by Mexico's pastoral Ejidatarios. *Economic Development and Cultural Change*, 41: 299–318.

Xing, Q., Wang, Q., and Zhang, D. (2008). *An illustrated handbook on habitual plant of Inner Mongolia grassland.* Inner Mongolia People's Press. Hohhot, Inner Mongolia, China.

Xing, X., Xu, X., Zhang, X., Zhou, C., Song, M., Shao, B., and Ouyang, H. (2010). Simulating net primary production of grasslands in northern Asia using MODIS data from 2000 to 2005. *Journal of Geographical Sciences*, 20(2): 193–204.

Yamano, H., Chen, J., and Tamura, M. (2003). Hyperspectral identification of grassland vegetation in Xilinhot, Inner Mongolia, China. *International Journal of Remote Sensing*, 24: 3171−3178.

Yu, J., De Jong, R., and Lee, L. (2008). Quasi-maximum likelihood estimators for spatial dynamic panel data with fixed effects when both n and T are large. *Journal of Econometrics*, 146: 118–134.

Zemmrich, A., Manthey, M., Zerbe, S., and Oyunchimeg, D. (2010). Driving environmental factors and the role of grazing in grassland communities: A comparative study along an altitudinal gradient in Western Mongolia. *Journal of Arid Environment*, 74: 1271–1280.

Zhang, J., and Goodchild, M. (2002). *Uncertainty in geographic information*. Taylor and Francis Inc., New York, NY.

Zhang, Q. (2007). *Impacts of double-contract responsibility system on rangeland and animal husbandry: a perspective of natural resource heterogeneity*. Ph.D. Dissertation. Beijing University, Beijing.

Zhang, Q., and Li, W. (2008). Policy analysis in grassland management of Xilingol prefecture, Inner Mongolia. In: *The Future of Drylands*. Edited by Lee, C. and Schaaf, T. pp. 493–505. Published joint by UNESO and Spring Press.

Zhang, X. (1992). Northern China. In: *Grasslands and Grassland Science in Northern China*. Edited by National Research Council. pp. 39–54. National Academy Press. Washington, DC, USA.

Zhao, T., Brown, D. G., and Bergen, K. M. (2007). Increasing gross primary production (GPP) in the urbanizing landscapes of Southeastern Michigan. *Photogrammetric Engineering and Remote Sensing*, 73: 1159–1167.

Zhen, L., Ochirbat, B., Lv, Y., Wei, Y., Liu, X., Chen, J., Yao, Z., and Li, F. (2010). Comparing patterns of ecosystem service consumption and perceptions of range management between ethnic herders in Inner Mongolia and Mongolia. *Environmental Research Letters*, 5: 015001, 1–11.

Zhou, Y., and Michalak, A. M. (2009). Characterizing attribute distributions in water sediments by geostatistical downscaling. *Environmental Science and Technology*, 43: 9267–9273.